School of Civil and Mechanical Engineering
Department of Civil Engineering

Mechanical Properties for Buton Asphalt - Aggregates Mixes

Muhammad Karami

This thesis is presented for the Degree of
Doctor of Philosophy
of
Curtin University

April 2016

DECLARATION

To the best of my knowledge and belief this thesis contains no material previously published by any other person except where due acknowledgement has been made.

This thesis contains no material which has been accepted for award of any other degree or diploma in any university.

Signature:

Muhammad Karami
Date: 4/04/2016

ABSTRACT

The objectives of this research are to study the effect on the permanent deformation resistance and the resistant to fatigue cracking of asphalt mixtures using granular Buton Rock Asphalt (BRA) modifier binder. The brand of granular BRA modifier binder is *Retona Pellets*, a commercial products manufactured by PT. Olahbumi Mandiri in Jakarta, Indonesia. The raw materials of this product are obtained from Buton Island in Indonesia. In this study the granular BRA modifier binder consisted of 70% mineral and 30% natural binder. One type of base binder Class-170 (penetration 60/80), crushed granite aggregate, and dense graded aggregate at 10 mm were used in this study. The BRA modified binder was formed by replacing 10, 20, and 30% of the Class-170 with BRA natural binder (by total weight of asphalt binder). In order to meet the research objectives, five laboratory tests were conducted, including indirect tensile stiffness modulus, dynamic creep, wheel tracking, repeated flexural bending and asphalt mixture performance tests. The results of this study show that BRA modified asphalt mixtures performed better than unmodified asphalt mixtures with regard to permanent deformation and fatigue cracking.

ACKNOWLEDGEMENTS

I would like to express my sincere thanks and appreciation to my advisor Professor Hamid Nikraz for his support, thoughtful guidance, motivation and encouragement.

I would like to acknowledge the Directorate of Higher Education (DIKTI) – Indonesian Ministry of Education for financial support within the scholarship programme, and for the support received in undertaking this research from the University of Lampung in Indonesia as my current employer. Thank you to Mr. Andi Salim and Dr. Hasan Hariri of BLN DIKTI Unila supporting team for their support for me and my family during my study in Perth.

A special thanks goes to Mr. Arief Santoso, Mr. Hari Wibowo Purwanto, and Mr. Jimmy Djayawinata for their kind cooperation and support in providing the granular BRA modifier (retona pellets) materials used in this study.

I would like to thank all staff members in pavement and geomechanics laboratory at school of Mechanical and Civil Engineering at Curtin University: Mr. Mark Whittaker and Mr. Darren Isaac for their endless, valuable assistance during the laboratory testing program, and all needed research facilities.

I am very grateful to friends in pavement research group who always help and give me ideas throughout my research work and analysis. Thank you very much to Dr. Hossein Asadi, Dr. Gunawan Wibisono, Mr. Ainalem Nega, Mr. Hassan Malekzehtab, Mr. Sarayoot Kumlai, Mr. Korakod Nusit, Mr. Hyuk Lee, and Mr. Penglow Chow.

A special thanks to my family. I thank my wife, Etyka Handayani Agung, for all of sacrifice, your patience and your prayer that you have made on my behalf. I also have to acknowledge my three lovely kids, Muhammad Fawwaz Rasyad, Najwaa Shafina Aqiila, and Felizya Adzkaa Zhafira Azzaryne for filling my life with joy and happy moments. I would like to express my deepest love to my parents: H. Abdul Kohar and Hj. Tabrizah, and my parents in law: H. Johny Kasim Mochtar and Hj. Hartati Bachtiar for their pray for my success.

LIST OF PUBLICATIONS

During my PhD research, the following publications have been produced:

Conference Papers

(1) Karami, M. and H. Nikraz. "*The effect of granular BRA modifier binder on the stiffness modulus of modified asphalt*". in *Advances in Civil Engineering and Building Materials IV*. 2015, CRC Press. p.345-349. Proceeding of the 4th International Conference on Civil Engineering and Building Materials (CEBM 2014), 23-24 November 2014, Hongkong.
http://dx.doi.org/10.1201/b18415-79

(2) Karami, M. and H. Nikraz, "*Using advanced materials of granular BRA modifier binder to improve the flexural fatigue performance of asphalt mixtures*". In *Procedia Engineering*, 2015. 125: p. 452-460. Proceeding of the 5th International Conference of Euro Asia Civil Engineering Forum (EACEF-5), 15-18 September 2015, The University of PETRA Surabaya, Indonesia.
http://dx.doi.org/10.1016/j.proeng.2015.11.120

Journal Papers

(1) Karami, M. and H. Nikraz. "*Laboratory experiment on resilient modulus of BRA modified asphalt mixtures*". International Journal of Technology – The University of Indonesia (UI), Indonesia. (Under review)

(2) Karami, M., A. Nega, A. Mosadegh, and H. Nikraz. "*Evaluation of Permanent Deformation of BRA Modified Asphalt Paving Mixtures Based on Dynamic Creep Test Analysis*". Journal of Advanced Engineering. 2016; 16:69-81.
DOI:10.4028/www.scientific.net/AEF.16.69

TABLE OF CONTENTS

LIST OF TABLES

LIST OF FIGURES

LIST OF SYMBOLS

a, b,	: constant coefficients of model
$a(T)$	: shift factor as a function of temperature
d	: loading duration
dD/dN	: damage rate
dE^*/dN	: slope of the fitted straight line of phase-2
DS	: dynamic stability
d_{45}, d_{60}	: rutting depths measured at 45 and 60 min
d_{120}, d_{105}	: rut depth after 120 and 105 minute respectively
e	: exponential
E_{00}	: y-axis intercept of the fitted straight line
E^*	: complex modulus
$\|E^*\|$	: dynamic modulus
f	: loading frequency at desired temperature
FN_{Slope}	: rate of deformation (slope of secondary flow)
f_r	: reduced frequency of loading at reference temperature
i	: imaginary component of the complex modulus
k_1, k_2	: variables of the fatigue prediction model
Mr	: resilient modulus
N	: number of load applications that produced ε_p
N	: number of wheel loading cycles per minute
NE	: normalized error
N_f	: number of cycles to failure
N_i	: load cycle value at cycle-i
$R_{rd\text{-}105/120}$	: rate of deformation
S	: resilient modulus
S_f	: flexural stiffness in a given fatigue failure
S_i	: initial flexural stiffness at cycle-i
S_0	: initial flexural stiffness
$S_{master\ curve}$	: resilient modulus obtained from a master curve
S_{Lab}	: resilient modulus obtained from a laboratory test
t	: time
T	: temperature of interest
t_{120}, t_{105}	: time the rut depth is measured at 120th and 105th minute.

β, γ : parameter describing the shape of sigmoidal function

ε_0 : peak (maximum) strain

ε_p : accumulated permanent strain due to dynamic vertical loading

ε_r : resilient deformation at a certain number of load application

ε_t : recoverable strain

$\varepsilon(t)$: total deformation, including elastic, viscoelastic, plastic and visco-plastic deformation

(δ) : phase angle

δ : minimum value of |E*| or |S|

$\delta + \alpha$: maximum value of |E*|

σ_0 : peak (maximum) stress

σ_d : deviator stress or the axial stress

ω : angular velocity

$\mu\varepsilon$: micro strain

LIST OF ABBREVIATIONS

AASHTO : American Association of State Highway Transportation Officials
AS : Australian Standard
BRA : Buton Rock Asphalt
CV : Coefficient of Variation
DER : Dissipated Energy Ratio
ER : Energy Ratio
FN : Flow Number
HMA : Hot Mix Asphalt
Hz : Hertz
IDT : Indirect Tensile
ITSM : Indirect Tensile Stiffness Modulus
LT : Loading Time
MPa : Mega Pascal
ms : mili second
RDEC : Rate Dissipated Energy Change
R/L : Rest period/Loading time
SD : Standard Deviation

CHAPTER 1
INTRODUCTION

1.1 Background

The primary function of asphalt mixture as the top layer of a flexible pavement structure is to withstand the applied traffic loadings during its design life and under different environmental conditions, and to transmit the load to the lower level of the structure including the base, subbase and subgrade without deforming excessively and cracking. However, in recent years, increased traffic load, traffic volume, axle configuration and tyre pressure appear to have added to the demands of the load on the road. Asphalt mixtures, however, are expected to remain strong and durable enough for the length of their design life. Hence, today's challenge is to increase the surface life of asphalt structures.

In order for asphalt mixture to perform adequately, it is well understood that it must be designed properly and be composed of good quality materials, because the properties of the individual components influence the behaviour of asphalt mixtures. According to Newcomb *et al.*[1], three factors affect the distress resistance of asphalt mixtures, including material selection, mix design and performance testing. It is well known that the mechanical properties of asphalt mixtures come from friction and cohesion of the materials in the mixture. Fordyce and O'Donnell[2] - and Choi[3] explained that the friction comes from the interlocking of the aggregates and is affected by the maximum aggregate fraction size and the grading of the aggregates fraction which is blended together, whereas cohesion comes from asphalt binder.

Asphalt binder is a key component that strongly affects and controls the behaviour of asphalt mixtures. The performance of asphalt mixtures is closely related to the performance of asphalt binder. According to Corte[4], the asphalt binder is necessary for providing technical solutions to problems such as the mitigation of rutting and to increase the rigidity of asphalt mixtures. Therefore, to understand the behaviour of asphalt mixtures, it is essential to accurately represent the characteristics of bitumen. For example, a behaviour of asphalt binder such as accumulated deformation strongly contributes to the rutting in asphalt mixtures.

In contrast according to Mallick and El-Korchi[5], the base asphalt binder derived from crude oil distillation is altered several times through the distillation process. This process causes the loss of substances so that the performance of the binder or a mixture of base asphalt binder with aggregates is unfavourable and it is insensitive to changes in temperature, affecting pavement performance[6, 7]. In addition, attention to and awareness of environmental impact and the reduction of emissions has been growing in recent years. As a result, the hot-mix asphalt industry is constantly improving its technology to enhance material performance and construction efficiency, conserve resources and advance environmental stewardship.

Under the circumstances mentioned above, as well as the increase in the cost of materials, especially oil products, studies on the applications of high quality asphalt mixtures are urgently needed in order to improve the resistance to permanent deformation and fatigue cracking of asphalt mixtures. This study deals with the benefit of using granular Buton Rock Asphalt (BRA) modifier binder with the aim of increasing the mechanical performance of asphalt mixtures and to make more effective and efficient use of pavement materials. The raw materials of granular BRA modifier binder are found on Buton Island, Indonesia, and are traditionally known as Buton asphalt (*asbuton*).

A number of research studies on mechanical properties have been carried out to investigate the possibility of using *asbuton* or materials derived from *asbuton* as a partial material substitute/addition in asphalt mixtures[8-15]. Subagio *et al.*[8] reported that the use of *asbuton* filler in Hot Rolled Asphalt (HRA) improved the resilient modulus and resistance to plastic deformation. Further, a study on the feasibility of using *asbuton* filler for fatigue performance found that the number of cycles to failure (N_f) for HRA mixtures containing *asbuton* filler were higher compared with unmodified HRA mixtures at all levels of stress[9]. The test results for Hot Rolled Sheet (HRS) with *asbuton* filler conducted by Subagio *et al.*[10] revealed that the resilient modulus of HRS modified mixtures at a test temperature of 25°C were lower when compared with unmodified HRS mixtures. By comparison, at a test temperature of 45°C the resilient modulus of modified HRS was greater than that of the unmodified HRS mixtures. For wheel tracking tests, unmodified HRS mixtures had the lowest dynamic stability tested at 45°C and the highest dynamic stability at a test temperature of 60°C. However, a more recent study conducted by Hadiwardoyo

and Fikri[14] has shown that the rut depths of Buton Asphalt Modified at test temperatures of 30°C and 60°C were lower when compared with unmodified hot mix asphalt (HMA). Ali[13] investigated the resistance of asphalt mixture with *butonic* bitumen (ACR) to water saturation. The results indicated that ACR mixtures were more durable compared to unmodified asphalt mixtures. In another experiment, the influence of granular and extracted BRA asphalt binder in asphalt mixtures was investigated by Zamhari *et al.*[15]. They used the indirect tensile stiffness modulus (ITSM) test and dynamic creep test. The results indicated that using granular and extracted asphalt binder in asphalt mixtures increased the stiffness modulus and creep stiffness and decreased the rate of permanent deformation.

Despite the progress of research into the use of *asbuton/asbuton* materials, there are still significant gaps in the research into the mechanical properties of BRA modified asphalt mixtures. This is largely due to the complexities of testing magnitude in order to express the response of materials where the temperature and loading time have a substantial impact on the behavior of asphalt mixtures. For example, it is still not known how rest period, traffic volume, and loading time affect the resilient modulus of BRA modified asphalt mixtures. Furthermore, more sophisticated testing equipment and complex parameters are necessary to better understand the response of the BRA modified asphalt mixtures. For example, the Mechanistic - Empirical Pavement Design Guide (MEPDG) has recently recommended determining the dynamic modulus of asphalt mixtures to analyze and predict the performance of asphalt mixtures[16].

With the recent developments in processing technologies, granular BRA modifier binder is now produced as a commercial product. The developments have aimed to enhance the characteristics of granular BRA modifier binder to meet the requirements for use in asphalt mixtures, such as increased rutting resistance and fatigue life. Therefore, a fundamental study on the mechanical properties of BRA modified asphalt mixtures is of great importance to improving understanding on the above issues. The following stages are proposed for achieving the objectives of this thesis.

1.2 Research Objectives and Significance

Two major types of loading affect the performance of asphalt mixtures, including (1) mechanical loading caused by traffic, especially traffic involving heavy

vehicles, and (2) climate effects caused by thermal variation. These two main types of degradation result in permanent deformation (rutting) and fatigue cracking, two of the main failure modes in pavement structural subjected to mechanical loading. The ride quality of the asphalt pavement is ultimately influenced by the deterioration of the asphalt mixtures as a result of these failures. Permanent deformation and fatigue cracking are crucial in asphalt mixtures and must be correctly understood to ensure the quality of the asphalt mixtures.

This study aims to provide a fundamental understanding of the mechanical characteristics of BRA modified asphalt mixtures relating to permanent deformation and fatigue cracking. The objectives and significance of the study are as follows:

1. Permanent deformation happens at high temperatures and/or under a slow loading rate, resulting in the asphalt binder becoming too soft to carry the load. Hence, the first objective was to study the potential use of granular BRA modifier binder in asphalt mixtures to increase the resistance of asphalt mixtures to permanent deformation.
2. In addition, fatigue cracking of asphalt can be caused by mechanical loading from repetitive traffic and/or thermal loading from changes in temperature. Accordingly, the second objective was to study the potential use of granular BRA modifier binder to increase the resistance of asphalt mixtures to fatigue cracking.

1.3 Scope of Work

The scope of work required to achieve the research objectives is as follows:

1. Indirect tensile stiffness modulus (ITSM) test to determine the resilient modulus of unmodified and BRA modified asphalt mixtures;
2. Dynamic creep test to determine the permanent compressive strain characteristics of unmodified and BRA modified asphalt mixtures;
3. Wheel tracking test to determine the rutting performance of unmodified and BRA modified asphalt mixtures;
4. Repeated flexural bending test to determine fatigue life of unmodified and BRA modified asphalt mixtures; and
5. Asphalt mixture performance test (AMPT) to determine the dynamic modulus of unmodified and BRA modified asphalt mixtures.

1.4 Thesis Outline

This thesis is organized into eight chapters with the structure of the thesis shown in Figure 1.1. Each chapter is outlined as follows:

Chapter 1 introduces the background of this study, research objectives, scope of work and thesis outline.

Chapter 2 presents a review of the literature supporting this thesis. This chapter outlines the previous research on asphalt binder and asphalt mixtures with particular reference to modified asphalt binder and modified asphalt mixtures. The chapter also presents the theories on the stiffness and viscoelasticity of asphalt binder and the performance of asphalt mixtures such as the resilient modulus, dynamic modulus, permanent deformation (rutting) and fatigue cracking.

Chapter 3 describes the experimental program, including the stage required to achieve the research objectives along with the methodology for studying the mechanical performance of BRA modified asphalt mixtures. This chapter describes the materials, the mixture design process and the procedures for laboratory testing of asphalt mixtures in order to fully characterize the unmodified and BRA modified asphalt mixtures.

Five tests were conducted with the purpose of studying the mechanical properties of the BRA modified asphalt mixtures presented in Chapters 4 to 7.

Chapter 4 evaluates the effect of granular BRA modifier binder on the resilient modulus of asphalt mixtures based on the results of ITSM tests.

Chapter 5 evaluates the effect of granular BRA modifier binder on the permanent deformation resistance of asphalt mixtures based on the results of the dynamic creep test and wheel tracking test.

Chapter 6 evaluates the effect of granular BRA modifier binder on the fatigue life of asphalt mixtures based on the results of the repeated flexural bending test.

Chapter 7 evaluates the effect of granular BRA modifier binder on the dynamic modulus of asphalt mixtures, based on the results of the dynamic modulus test.

Finally, Chapter 8 presents a summary of the study along with conclusions and recommendations.

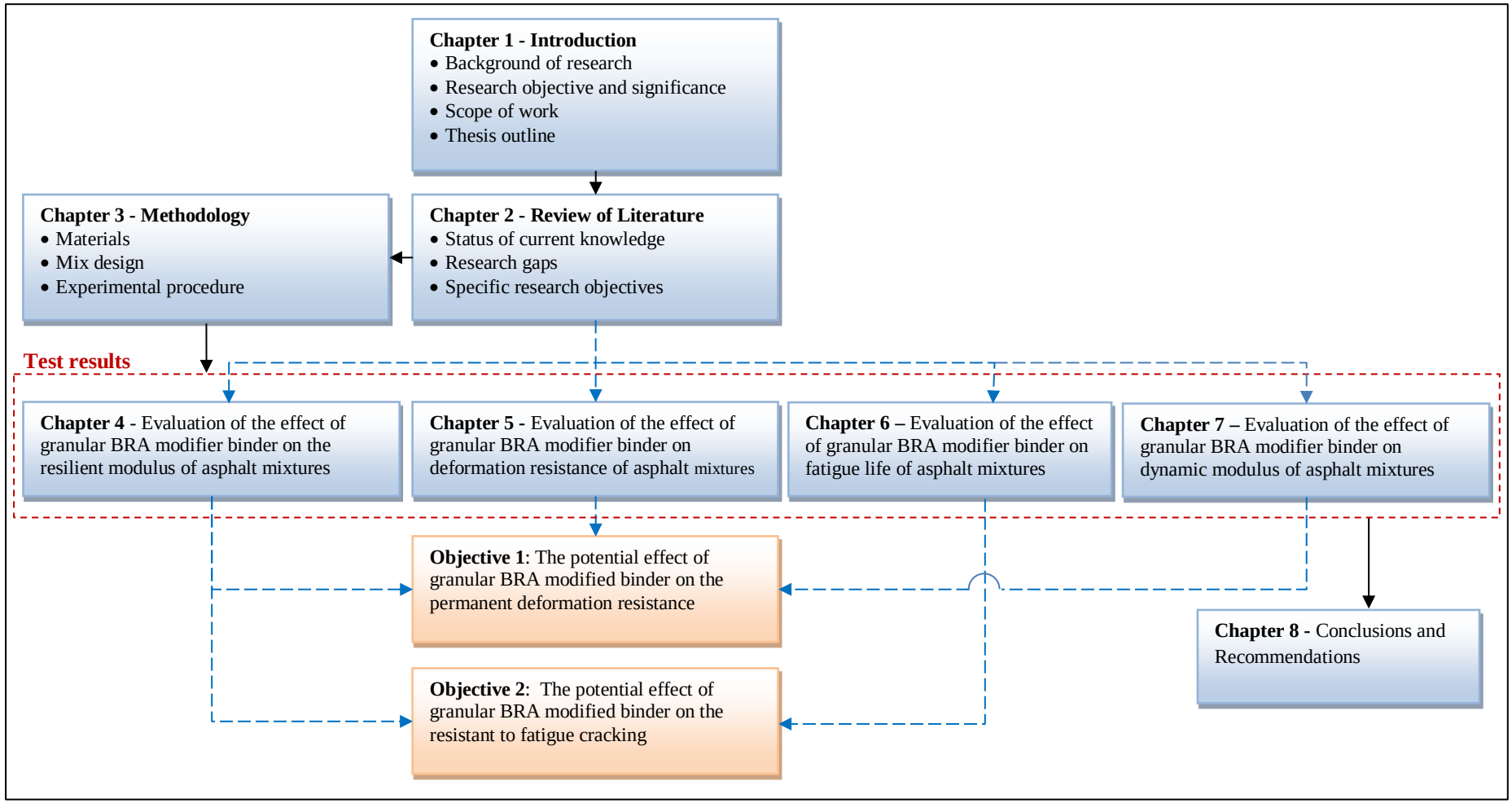

Figure 1-1. The structure of the thesis

CHAPTER 2
REVIEW OF LITERATURE

2.1 Introduction to Literature Review

The mechanical properties of asphalt mixtures are strongly affected by the nature of the asphalt binder. Essentially, the satisfactory performance of an asphalt mixture during its design life can be ensured by controlling its characteristics with regard to the use of asphalt binder as a viscoelastic material. Generally, the main traffic and environment-related performance criteria for asphalt mixtures are permanent deformation and fatigue cracking.

This chapter presents an overview of the stress conditions of asphalt mixture layers on the pavement system, and the necessary mechanical properties of asphalt mixtures related to the concept of mechanistic pavement design. Five fundamental parameters were discussed in order to understand the mechanical characteristics of asphalt mixtures: resilient modulus, dynamic modulus, permanent deformation, rut depth and fatigue life. Since asphalt binder is a key issue in this study, the asphalt binder and BRA modifier binder are explained in terms of the nature, determination of stiffness and characterization.

2.2 Asphalt Mixtures and Stress Conditions

In general, the structural layers of a flexible pavement consist of (from the bottom): subgrade, subbase, road base and surfacing (asphalt mixtures). The last three layers combined must have the ability to spread the traffic load to the subgrade. The mechanisms for the spreading of load in road pavement are presented in Figure 2-1.

As the asphalt mixtures is the first layer to have a contact with traffic, there must be appropriate circumstances for that contact to safe and comfortable under traffic loading and environmental conditions. According to Brown[17], the key characteristics necessary in asphalt mixtures to ensure an ideal pavement are: high stiffness, resistance to cracking and resistance to deformation. The Shell Bitumen Handbooks advise that in order to meet the needs of traffic, asphalt mixtures must have qualities such as resistance to permanent deformation, resistance to fatigue cracking, durability, workability and should contribute to the strength of pavement[18]. As a consequence, asphalt mixtures are essentially required to provide mechanical

properties in the pavement structure such as high elastic stiffness to ensure good load spreading ability, high resistance to fatigue to eliminate crack initiation and propagation from repeated traffic loading and high resistance to permanent deformation to prevent rutting.

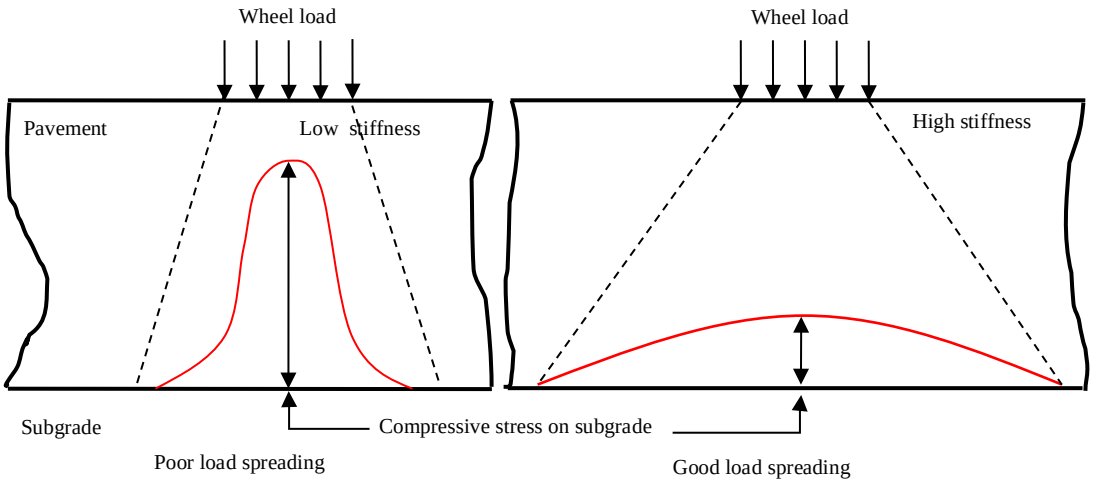

Figure 2-1. Spreading of load in road pavement [17]

The stress on pavement due to the movement of wheel load is illustrated in Figure 2-2. It can be seen that the stress on pavement elements changes with the time as the wheel passes over. Further, variations in vertical, horizontal and shear stress are shown in Figure 2-3. This pattern is repeated for every wheel. Brown[19] explains that the magnitudes of the stress on asphalt mixtures is a function of wheel load and contact pressure along with the geometry and mechanical characteristics of the asphalt mixtures. The response of asphalt mixtures materials in the pavement structure to the type of loading regime shown in Figure 2-3 is then used in the analytical approach to pavement design.

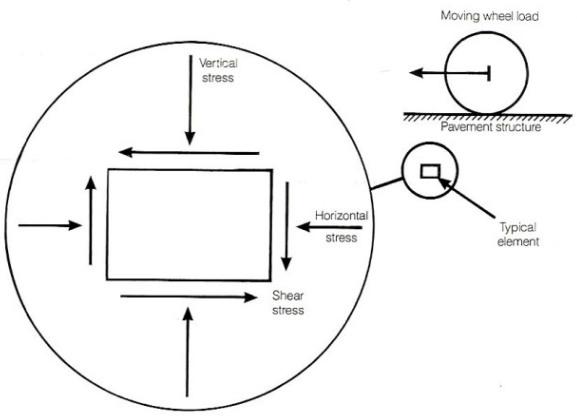

Figure 2-2. Stresses on an element in pavement [18]

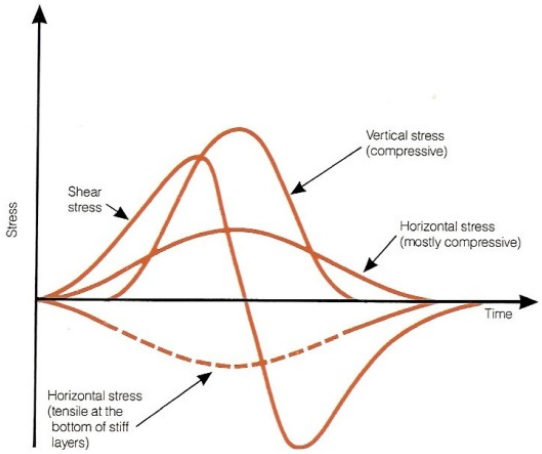

Figure 2-3. Stresses induced by a moving wheel load [18]

2.3 Mechanistic Design

The concept of a mechanistic approach to pavement design was developed and implemented in the 1980s and 1990s when work was proceeding on the development of a new mechanistically-based *AASHTO Pavement Design Guide*. In this concept, physics principles are used to determine the reaction of pavement due to loading.

An analytical approach to pavement design is based on knowledge about the various materials used in pavement structure. The materials and layer thicknesses used in pavement structures are chosen to obtain a critical point at which the pavement can be designed to resist certain types of failure or distress. Peattie[20] explains that analytical design methods are related to selecting the composition and thickness of the layers such that they have the capability to resist stress, strain and deformation greater than that produced by design traffic loading. There are some features of an analytical design system for flexible pavement including: (a) elastic or viscoelastic model to represent the pavement structures, (b) equations for stress, strains, and deformations in the model, (c) the characterization of the mechanical properties of the materials under variations in climate and loading conditions, (d) the criteria for design and performance in term of stress, strain and deformation, and (e) the design system appropriate for use by highway engineers.

Information about the mechanical properties of asphalt mixture materials is necessary for the application of the analytical design method. According to Brown[19] and the Shell Bitumen Handbook[18], two aspects are required from a laboratory test to provide the necessary data for an analytical approach to pavement design relating to the asphalt mixtures: firstly, the elastic response of the materials expressed in term of

a stress-elastic strain relationship and, secondly, the failure conditions in terms of stress or elastic strain relating to the mode of failure that is likely to occur in the road.

2.4 Mechanical Characteristic of Asphalt Mixtures

The mechanical characteristics of asphalt mixtures are closely influenced by the performance of asphalt binder. As described in Section 2.5 of this chapter, asphalt binders have two rheological properties which are thermoplastic and viscoelastic. Therefore, various factors such as time (including: rate of loading, loading time, rest period), temperature, stress state, mode of loading, aging, and moisture affect the mechanical performance of asphalt mixtures. Apeagyei *et al.*[21] stated that the stress-strain behaviour of asphalt mixtures (modulus) depends on temperature and loading rate because asphalt mixtures are considered to be viscoelastic materials. According to Venudharan and Biligiri[22], asphalt mixtures show a linier viscoelastic behaviour instead of illustrating purely elastic and/or viscous behaviour during traffic loading. Consequently, asphalt mixtures produce irrecoverable (plastic) strains and permanent deformation.

Generally, the main performance criteria for asphalt mixtures are permanent deformation and fatigue cracking. These two failure situations possible with asphalt mixtures are associated with traffic. Hence, the asphalt mixtures used in pavement would need to provide enough stiffness to avoid permanent deformation (rutting) and enough flexibility to resist fatigue cracking. The stiffness of asphalt mixtures needs to be optimized to resist rutting and fatigue cracking. Rutting occurs when a slow loading rate is applied at high temperatures, resulting in the asphalt binder becoming too soft and weak to carry the load. Moreover, mechanical loading from repetitive traffic and/or thermal loading from changes in temperature cause the cracking of asphalt mixtures.

To produce anticipated in situ conditions as closely as possible, simplified tests have been introduced which may reproduce certain aspects of in situ behaviour. The determination of the mechanical properties of asphalt mixtures in the laboratory can be divided into three major groups of tests: (1) empirical tests, (2) simulation tests, and (3) fundamental or rheological tests[18, 23].

Empirical tests, such as the Marshall test, are tests to failure under continuous loading. These tests give an appreciation of the materials unrelated to the actual

pavement conditions under traffic loading. The Marshall test cannot give basic information on the stress-strain characteristics of asphalt mixtures. Further, simulation tests such as the wheel tracking test are used to assess the performance of asphalt mixtures in terms of characterizing a distress property by measuring the rut depth after a given number of passes. The results show that a good correlation exists between plastic deformation on roads and performance in the laboratory wheel tracking test[18]. In addition, fundamental or rheological tests generate stress conditions in the asphalt mixtures leading to the development of measurable vertical and horizontal strains produced by the stress imposed on the asphalt mixture specimens. The repeated load triaxial test, uniaxial creep compression test, repeated load indirect tensile test, dynamic stiffness test and fatigue test are among the group of fundamental tests.

2.4.1 Resilient modulus

Many recent studies have used several parameters including resilient modulus, dynamic modulus, stress and strains, deformations, dissipated energy and others to describe the viscoelastic behaviour of asphalt mixtures. Stiffness modulus, however, is an essential parameter for characterizing the performance of asphalt mixtures. Stiffness modulus is a major input in the flexible pavement design methodology regarding the prediction and understanding of the behaviour of asphalt mixtures. Zoorob and Suparma[24] explain that resilient modulus is a criterion of the asphalt mixture's ability to spread the load and also to control the level of traffic. It is well known that traffic creates a tensile strain on the underside of the asphalt mixture layers which are subjected to fatigue cracking, together with compression strain in the subgrade that can lead to permanent deformation. This mechanism has also been described in Section 2.2. As Pourtahmasb *et al.* [25] said, the resilient modulus test can be used to represent conditions in asphalt mixtures subjected to traffic loading and offers the ability of comparing the behaviour of asphalt mixture under various conditions and stress states.

In recent years, the mechanistic approach based on the elastic theory has been used in the philosophy of asphalt pavement design with the aim of changing the previous empirical approach. In this theory, the resilient modulus, as the elastic modulus, is required as input for the elastic properties of pavement materials[22]. In mechanistic pavement design, the multilayer elastic theory or a finite element model

needs resilient modulus data as an input to obtain the response of a pavement under traffic loading in order to design the optimum thickness for a new pavement or to estimate the remaining life of an existing pavement[26]. According to studies, obtaining the resilient modulus of asphalt mixtures using the ITSM test is a means of studying the potential elastic properties of asphalt mixtures in the form of stress-strain measurement[27-31]. Lavasani *et al.*[32] state that the material is considered to be relatively elastic when the material attains a resilient state after a certain critical number of applied loadings. For that reason, the uniaxial strains and displacement in the resilient state can be calculated by using *Mr* as shown in Equation 2-1.

Resilient modulus has been used in a number of studies evaluating and analyzing asphalt mixtures because this test is simple to perform and effective in characterizing the fundamental properties of asphalt mixtures. Resilient modulus is obtained by dividing the applied stress by the recoverable strain at a particular temperature and frequency under repeated load[31, 33] as presented in Equation 2-1.

$$M_r = \frac{\sigma_d}{\varepsilon_t} \qquad (2\text{-}1)$$

where: σ_d : the deviator stress (axial stress in an unconfined compression test or the axial stress)

ε_t : recoverable strain

According to Shafabakhsh and Tanakizadeh[31] and Fakhri and Ghanizadeh[34], the deformation of asphalt mixtures under each load cycle is recoverable and the material is considered to be elastic when a repeated load for a large number of times is small compared to the strength of the materials. Shafabakhsh and Tanakizadeh also state that the resilient modulus is influenced by factors such as test temperature, loading time or loading frequency, rest period and loading pulse waveforms. However, the test temperature has the greatest influence on the resilient modulus[31]. At a typical temperature and traffic speed, asphalt binder behaves in an almost elastic manner. As a consequence, the resilient modulus is a measure of an asphalt mixture's resistance to bending and hence of its load spreading ability[27]. According to Tayfur *et al.*, the asphalt binder and volumetric proportion of the mixtures influence the stiffness modulus[30].

2.4.2 Permanent deformation

Permanent deformation is considered to be one of the common forms of distress associated with load and affects the pavement performance of asphalt mixtures. Generally, permanent deformation consists of a longitudinal settlement in the wheel paths of an asphalt pavement surface, as illustrated in Figure 2-4. It is believed that permanent deformation, commonly referred to as rutting, is caused by short term loading when vehicles pass over the surface, and results from the accumulation of unrecoverable deformation to the asphalt pavement under repetitive traffic loading over a period of time[23, 30, 35, 36].

Figure 2-4. Typical permanent deformation in asphalt pavement [37]

The quality of the asphalt mixture and the mechanical properties of the other layers significantly affect the degree of depression[29]. The internal frictions in the asphalt mixtures provided by aggregates and the cohesion provided by the asphalt binder have a direct effect on permanent deformation. The characteristics of materials such as aggregate maximum size, shape, surface structure and binder stiffness can help to minimize the rutting. According to Vazquez *et al.*[38], gradation characteristics, asphalt binder content and compaction effort affects permanent deformation. Brown[17] states that permanent deformation is influenced by aggregate grading and particle characteristic, while according to Choi[3], an asphalt binder with a higher shear resistance provides better rutting resistance. A study by Little *et al*. cited in Wang[39] showed that some parameters such as the stiffness of asphalt mixtures, mixture volumetrics, and the bonding interaction between asphalt binder and aggregates have an impact on resistance to the permanent deformation of asphalt mixtures. Accordingly, aggregate, binder and air voids are considered to be the components which influence the rutting performance of asphalt mixtures. Therefore,

the design of the asphalt mixtures is directly linked to plastic deformation, so that improving the material properties and mix characteristics is essential for improving the rutting resistance of asphalt mixtures.

In addition, Vazquez *et al.*[38] explain that mix properties, temperature, number of load applications, load frequency and state of stress are primary factors affecting the permanent deformation. Some studies have found that temperature has a significant effect on rutting. Asphalt binder tends to flow more easily at high temperatures, with this condition leading to the pavement becoming softer and more liable to rutting. Apeagyei[40] states that temperature and loading effects have the greatest effect on rutting. Elevated temperature and lower load frequencies (slow moving traffic) are described as critical conditions for asphalt mixtures. At high temperatures and under long periods of loading, the asphalt binder behaves in a viscous manner, leading to viscous flow and plastic deformation in asphalt mixtures. Plastic deformation occurs when aggregate particles move past each other followed by viscous flow in the asphalt binder[41]. The viscous response of asphalt mixtures at high temperature is also stated by Brown[19] to make a substantial contribution to rutting in asphalt mixtures.

Additionally, the impact of changes in air voids in the asphalt layer on rut depth is also important to note. A decrease in air void content to below 2-3% due to densification by traffic load involves the lubricant effect between the aggregates and the reduction of contact points between them. This causes permanent deformation either in the form of volume or shear, depending on whether high temperature or heavy loads are involved[42].

2.4.2.1 Mechanism of rutting

According to studies[35, 36, 43], permanent deformation in asphalt pavement involves two different mechanisms. The first mechanism is known as initial rutting (compactive deformation). The densification of asphalt mixtures during the first year of pavement life is believed to be the main factor in causing the initial rutting, which is then followed by the second mechanism, secondary rutting, also known as shear flow deformation (plastic deformation). Shear flow deformation happens in well-compacted asphalt mixtures as a primary mechanism of rutting for the greater part of the life time of the pavement. Normally, shear flow is caused by the shear strength being insufficient to support the stress.

In the first mechanism, the wheel paths appear in the surface of an asphalt pavement, where the level of the surface is lower than the initial level of the pavement. In the second mechanism, the asphalt mixture materials under the wheel path move to between and outside the wheel path causing upheaval to the side[35, 43]. The volume decrease under the wheel path is approximately equal to the volume increase in the upheaval zone. This indicates that most of the compaction from the first mechanism is complete and further rutting is caused essentially by the second mechanism.

2.4.2.2 Characterization of rutting

Several different kind of laboratory tests are used to characterize the potential for pavement deformation of asphalt mixtures such as the creep test, repeated load test, dynamic tests, diametral tests, simple shear tests and wheel tracking[44]. However, the indirect tensile stiffness modulus test, the dynamic creep test, wheel tracking test and dynamic modulus test were selected for use in this research to determine the mechanical performance of asphalt mixtures and find out the potential for granular BRA modifier binder to increase the deformation resistance of asphalt mixtures.

a. Dynamic creep test

The dynamic creep test is a commonly employed method for studying the mechanism of rutting[35, 36] and has been used to observe the permanent deformation/ rutting resistance of asphalt mixtures[28, 45, 46]. Brown[43] states that the dynamic creep test can be used to assess important characteristic of asphalt mixtures and characterize their long term deformation behaviour. According to Kalyoncuoglu and Tigdemir[43] the creep test is able to provide a good correlation between the measured rut depth and the estimated rutting potential of the asphalt layer. Rutting on creep failure is a function of time. As for viscoelastic materials, the permanent strain component (ε_p) follows a simple power model as a function of the number of loading cycles as shown in Equation 2-2 [47].

$$\varepsilon_p = a\ x\ N^b \tag{2-2}$$

where: ε_p : accumulated permanent strain due to dynamic vertical loading

a,b : regression constants

N : number of load applications that produced ε_p

The curve yielded by the total permanent strain versus the number of loading cycles is the most important output of the dynamic creep test. As described in a number of studies[29, 35, 48, 49], the curve is divided into three distinct zones: the primary, secondary and tertiary zones as illustrated in Figure 2-5. This figure shows that the accumulated strain increases rapidly in the primary zone due to the rearrangement of the structure of the asphalt mixture, with the volume of the asphalt mixture decreasing due to the densification. Zhou and Scullion state that defects occur in asphalt mixtures, such as air voids and dislocations in the aggregates and asphalt binder, which dominate during the primary stage. Under repeated loading, the asphalt mixture hardens with the accumulation of pavement strain, leading to the initiation and growth of microcracks[49]. In the secondary zone, the relationship between the number of loading cycles and accumulated strain is linear (constant). The occurrence of microcracking leads to the development of dislocation between the aggregates, bringing about further softening of the asphalt mixtures to become less hard[49]. The secondary zone is also known as the transition zone between the primary and tertiary zone.

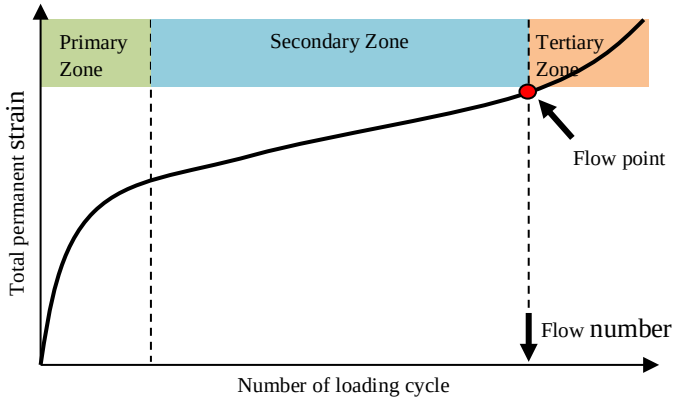

Figure 2-5. The curve for total permanent strain versus number of loading cycles

In the tertiary zone, the accumulated strain starts to increase again. The second mechanism of rutting seems to appear in which shear deformation begins, with the rate of deformation (rutting) increasing with each loading repetition until failure is reached.

Zhou and Scullion state that the propagation of microcracks is gradual in this stage and the cracks coalesce to form macrocracks under continued loading[49]. According to Alavi *et al.*[35], the point where the tertiary zone begins in the creep curve is called the flow point, where the minimum slope is found. The number of cycles corresponding with the flow point is referred to as the flow number (FN).

The concept of the flow number has been commonly used to determine the characteristics of permanent deformation. Many studies have been performed to analyze the rutting performance of asphalt mixture using the permanent strain curve, and have used the flow number as an indicator for evaluating resistance to permanent deformation. Mokhtari and Nejad[29] performed experiment using the flow number to investigate the service life of six different stone mastic asphalts. Permanent strain and creep modulus have been used to evaluate SBS and other different asphalt mixtures[29, 50]. According to Witczak *et al.*[51], the flow point is very important in determining the rutting performance of asphalt mixtures and regression parameters, related to the constant strain rate in the secondary zone.

Goh and You[48] developed a simple stepwise method that can be used to determine and evaluate the initiation of the tertiary zone (flow point) for asphalt mixtures. The method includes three simple steps to determine the flow number from a curve of permanent strain versus loading cycle, including: (1) reallocating the measured results of permanent deformation to smooth the curve trend of the strain versus loading cycle; (2) determining the strain rate at each loading cycle; (3) establishing the flow number by correlating the minimum point of the strain rate to the number of loading cycles. Based on the stepwise concept, an example determination of the flow number is shown in Figure 2-6.

Goh and You[48] also reported that the rate of deformation (slope of secondary flow) showed a strong correlation with permanent deformation. They indicated that the flow number for an asphalt mixture can be computed using the rate of deformation at various temperatures and air void levels using Equation 2-3.

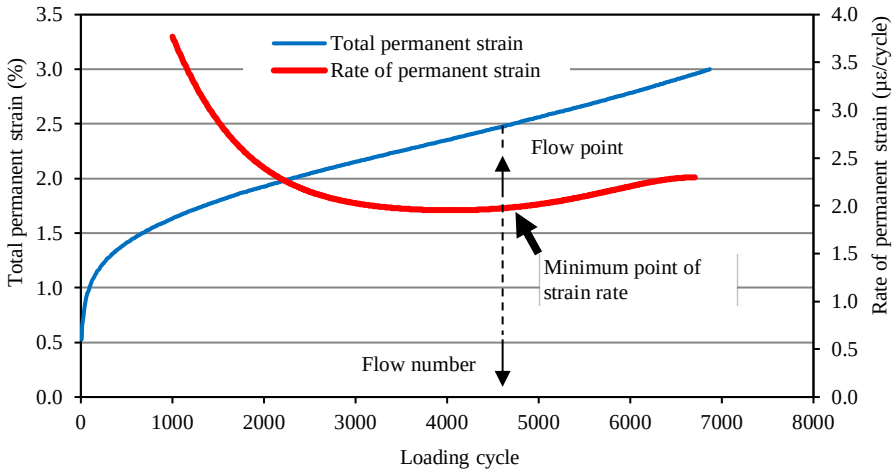

Figure 2-6. Progression curve of total permanent strain and rate of permanent strain

$$Flow\ Number = a \times (FN_{Slope})^{b} \quad (2\text{-}3)$$

where: a, b : regression coefficient

FN_{Slope} : rate of deformation (slope of secondary flow)

In addition, other outputs of the dynamic creep test are the resilient modulus and creep modulus. The resilient modulus and creep modulus are obtained using Equations 2-4 and 2-5[36].

$$M_r = \frac{\sigma_d}{\varepsilon_r} \quad (2\text{-}4)$$

$$M_c = \frac{\sigma_d}{\varepsilon(t)} \quad (2\text{-}5)$$

where: σ_d : deviator stress (kPa)

ε_r : resilient deformation at a certain number of load application (μs)

$\varepsilon(t)$: total deformation, including elastic, visco-elastic, plastic and visco-plastic deformation

b. Wheel tracking test

The wheel tracking test is used to determine the permanent deformation (rutting performance) resistance of asphalt mixtures subject to loaded wheel tracking with the purpose of simulating the effect of traffic at elevated temperatures[42, 52, 53]. Wheel tracking tests are included as an empirical test or simulative test. They directly estimate the rutting depth to describe the internal resistance of asphalt mixtures.

According to the Australian criteria indicated in Austroads AG:PT/T231[54], two parameters, rut depth and tracking rate, are used to determine the performance of asphalt mixtures during wheel tracking tests to evaluate the rut resistance of asphalt mixtures. The rut depth is measured after 10,000 passes and a steady state tracking rate is measured between four and 10 kilo-passes of tracking. In this standard, the tracking rate is used to show the number of loaded passes required to generate a rut depth of 1 mm.

According to Xu *et al.*[55], the rut depth was the primary parameter measured directly during the test as an indicator for rutting resistance, and the rate of deformation was used as a secondary parameter. Xu *et al.*[55] and Chen *et al.*[53] also suggested dynamic stability (DS) as another criterion for studying the permanent deformation resistance of asphalt mixtures as shown in Equation 2-6.

$$DS = \frac{N \text{ x } 15}{d_{60} - d_{45}} = \frac{42 \text{ x } 15}{d_{60} - d_{45}} \quad (2\text{-}6)$$

where: DS : dynamic stability (passes/mm)

N : number of wheel loading cycles per minute (passes)

d_{45}, d_{60} : rutting depths measured at 45 and 60 min, respectively (mm).

Permanent deformation resistance was also evaluated by passing a wheel over the specimen for 120 minutes at a rate of approximately 48 passes per minute, applying a contact stress of 700 kPa at a temperature of 60°C. The total rut depths in the wheel path were evaluated after 120 minutes ($R_{d\text{-}120}$) and the rate of deformation was measured between the 105 and 120th minute of testing ($R_{rd\text{-}150/120}$). Fontes *et al.*[42] and Dias *et al.*[52] presented the rate of deformation in terms of velocity calculated using Equation 2-7.

$$R_{rd\text{-}105/120} = \frac{d_{120} - d_{105}}{t_{120} - t_{105}} \quad (2\text{-}7)$$

where: $R_{rd\text{-}105/120}$: rate of deformation (mm/minute)

d_{120}, d_{105} : rut depth after 120 and 105 minute respectively (mm)

t_{120}, t_{105} : time the rut depth was measured, at 120th and 105th minute.

2.4.3 Dynamic modulus test

Dynamic modulus testing of asphalt mixtures started in 1962, when Papazian (cited in Clyne *et al.*[56]) performed viscoelastic tests on asphalt mixtures by applying sinusoidal stress to cylindrical specimens at a given frequency while measuring the sinusoidal strain response at the same frequency.

Recently, dynamic modulus has been recognized as a performance-related property that can be used to evaluate and characterize the stiffness of asphalt mixtures used for mechanistic-empirical pavement design as a response to various loading and temperature conditions. The development of the *Mechanistic-Empirical Pavement Design Guide* (MEPDG) by the National Cooperative Highway Research Program in 2004 (NCHRP Project 1-37A) for the American State Highway and Transportation Officials (AASHTO) is the most recent and significant effort invested into the mechanistic-empirical (ME) methods. NCHRP Project 1-37A uses dynamic modulus as a design parameter for asphalt mixtures and for the input of HMA characterization at three levels of input (AASHTO 2002).

According to Hu *et al.*[57], dynamic modulus is used to characterize the elastic modulus of asphalt mixtures. Witczak[58] suggests using dynamic modulus as a specification and guideline for controlling the performance of asphalt mixtures. Wang *et al.*[39] used dynamic modulus to evaluate the potential performance of asphalt mixtures. As Flintsch[59] notes, dynamic modulus is used to predict the response parameters for asphalt mixtures that determine their strain and displacement under different loading frequencies and temperatures. Furthermore, the mechanical behaviour of asphalt mixtures can be determined effectively by using the dynamic modulus test[59].

The concept is that the dynamic modulus is used to determine the response of the material under dynamic loading in the range between linier elastic and viscoelastic. Asphalt mixtures are considered to be a linear viscoelastic materials when the strain level is 100 με or lower[60]. According to Yao *et al.*[61], the dynamic modulus is obtained by dividing the loading stress amplitude by the resulting peak to peak recoverable strain.

In the laboratory, the dynamic modulus develops a response under loading conditions of continuous sinusoidal compressive stress at a range of frequencies and temperatures that replicate the actual pavement conditions in the field[57, 62]. The materials respond by developing further strain following a sinusoidal function similar to applied stress. The time lag, however, exists between the applied stress and the response of the materials/strain, as a consequence of the viscoelastic behaviour of the materials. The time lag, usually referred to as the phase angle, is used as a degree of the viscoelastic behaviour of asphalt mixtures with values between 0 (zero) and π/2. The value of 0 (zero) or the small phase lag indicates that the asphalt mixture's behaviour is approximately elastic, while a value of π/2 or a high phase lag indicates that the behaviour of the asphalt mixture is approximately viscous[63].

According to Witczak *et al.*[51] and Kim *et al.*[64], the relationship stress to strain subjected to a continuous sinusoidal loading for linear viscoelastic materials is called the complex modulus, and the dynamic modulus is an absolute value of complex modulus. Daugan *et al.*[65] defined the complex modulus as the ratio of the amplitude of the sinusoidal stress (at various time loadings and loading frequencies) and sinusoidal strain (at the same times and frequencies) resulting in a steady state response. Figure 2-7 shows the time lag due to the dynamic modulus test. The dynamic modulus, referred to as |E*|, is calculated using Equations 2-8 and 2-9[61, 63-66].

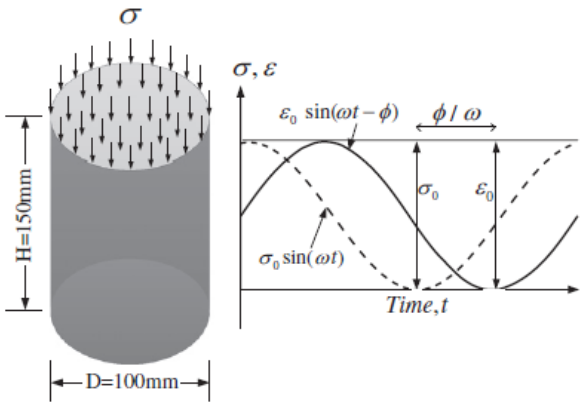

Figure 2-7. Loading pattern for dynamic modulus test [61]

$$E^* = \frac{\sigma}{\varepsilon} = \frac{\sigma_0 e^{i\omega t}}{\varepsilon_0 e^{i(\omega t - \phi)}} = \frac{\sigma_0 \sin \omega t}{\varepsilon_0 \sin(\omega t - \phi)} \quad (2\text{-}8)$$

where: E^* : complex modulus

σ_0 : peak (maximum) stress

ε_0 : peak (maximum) strain

δ : phase angle, degrees

ω : angular velocity

t : time, second

e : exponential

i : imaginary component of the complex modulus

Thus, the dynamic modulus is defined as:

$$|E^*| = \frac{\sigma_0}{\varepsilon_0} \quad (2\text{-}9)$$

The data for the dynamic modulus at a range of test temperature and loading frequencies can be combined to develop a master curve for further analysis. Apeagyei[40] described the reasons for constructing a master curve as follows. Master curves for dynamic modulus can be used for predicting dynamic modulus at temperatures and/or frequencies in the laboratory when there are limitations on equipment and time, modelling the pavements under all possible pavement climates and loading conditions, and also comparing the performance of asphalt mixtures. According to Christensen and Anderson[67], the reaction of asphalt mixtures due to the application of loads at a reference temperature over a range of frequencies or time can be represented by a master curve. Furthermore, a master curve can be used to described the viscoelastic behaviour of asphalt binder and mixtures[68].

Master curves are developed based on the time-temperature superposition principle[21, 62, 68]. According to Kim[64], a master curve is developed using: firstly, the dynamic moduli measured at test temperatures higher than the reference temperature, horizontally shifted to a lower frequency; secondly, the dynamic modulus measured at a test temperature lower than the reference temperature, shifted to a higher frequency. The data are shifted subject to the time until a single smooth function of the curves is constructed. The master curve of the dynamic modulus is modelled by the sigmoidal function described in Equation 2-10[61-63, 66] and the shift factor follows the form presented in Equation 2-11. The procedure for constructing the |E*| can be seen in Apeagyei *et al.*[21]. Figure 2-8 shows a developing master curve in which the dynamic modulus measured at different temperatures was shifted relative to the frequency and then formed a single master curve.

$$\text{Log}\left|E^*\right| = \delta + \frac{\alpha}{1+ e^{\beta+[\gamma(\log f_r)]}} \tag{2-10}$$

where: f_r : reduced frequency of loading at reference temperature

δ : minimum value of E*

$\delta + \alpha$: maximum value of E*

β, γ : parameter describing the shape of the sigmoidal function

Reduced frequency (f_r) is given by the following equation:

$$a(T) = \frac{f}{f_r} \tag{2-11}$$

where: $a(T)$: shift factor as a function of temperature

f : loading frequency at desired temperature

f_r : loading frequency at reference temperature

T : temperature of interest

According to Witczak and Bari[62], a second order regression polynomial can be used to show the relationship between the logarithm of the shift factor and test temperature as shown in Equation 2-12.

$$Log\ a(T_i) = aT_i^2 + bT_i + c \tag{2-12}$$

where: $a(T_i)$: shift factor as a function of temperature T_i

T_i : time of loading at desired temperature

a, b, and c : reduced time of loading at reference temperature

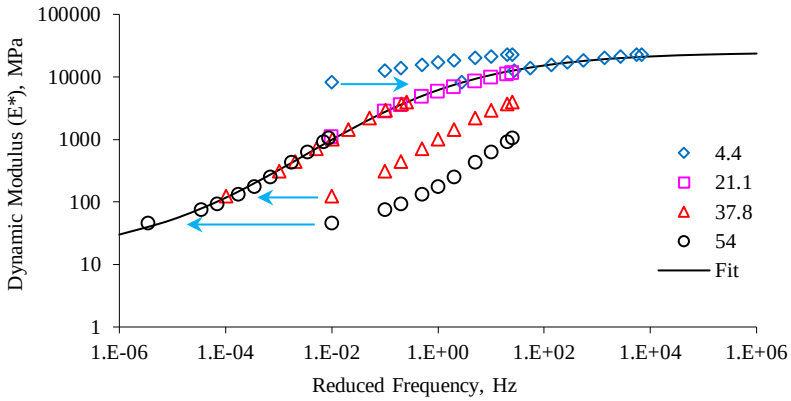

Figure 2-8. Development master curve

Many researchers have discovered that dynamic modulus is affected by asphalt binder stiffness. Zhu *et al.*[69] reported that the addition of polymer changed the dynamic modulus over the range of test temperature and loading frequencies. According to Clyne *et al.*[56] the mixtures with stiffer asphalt binder showed a higher dynamic modulus compared to those with a softer asphalt binder. Wang *et al.*[39] found that SBS modified mixtures showed a trend of higher dynamic modulus tested at temperature of 25 and 58ºC and frequency of 0.1 Hz than the mixtures with virgin binders.

2.4.4 Fatigue Cracking

According to studies, fatigue cracking is a result of fatigue failure due to repetitive stress and strains caused by load and environmental factors, and is considered to be a major form of distress in asphalt mixtures[70-72]. Fatigue cracking occurs when the tensile stress of materials exceeds the tensile strength due to repetitive stress and strain. Cracks form, resulting in the decreased structural capacity of the pavement and increasing the maintenance costs. Cracks also provide pathways for water to penetrate the pavement layer and greatly accelerate the process of deterioration. Hence, the fatigue resistance of asphalt mixes is defined as the capability of the mixes to withstand repetitive loading without any significant failure such as cracking or premature failure, developed under other circumstances such as environmental conditions.

The cracking begins with a microcrack at the points where critical tensile strain/stress occurs, and then grows to form a macrocrack, usually taking an alligator cracking pattern, and finally penetrating the surface of the pavement[73]. According to Di Benedetto *et al.*[74], the process of degradation during fatigue cracking is divided

into two phases. Firstly, there is the initiation and propagation of a microcrack network. The decrease in the modulus occurs in this phase. This phase relates to degradation resulting from damage that is uniformly spread in the asphalt mixtures. The first phase is called the initiation phase. Secondly, a macrocrack appears as a result of the combination of microcracks. Further macrocracks will propagate within the materials. The second phase is called the propagation phase.

As Baburamani[75] notes, the factors influencing fatigue cracking can generally be categorized as follows: loading variables (traffic speed, rest period, axle loads, and axle distribution; environmental factors (temperature, ageing, healing); construction variables; and material characteristics.

2.4.4.1 Studies on asphalt binder to improve fatigue resistance of asphalt mix

The use and development of modified binders in bituminous mixes is important with regard to increasing fatigue performance. Many studies have been carried out on asphalt mixtures to improve resistance to fatigue failure. Some researchers[76-78] have found that polymer-modified binder have a significant effect on improving several properties of asphalt mixtures such as fatigue life. Sibal *et al.*[79] reports that the addition of crumb rubber obtained from waste tires as a fine aggregate increases the fatigue life of asphalt mixtures. Laboratory evaluation of fatigue strength on four-point bending equipment using a flexural bending test was used as described in Section 3.5.4 of Chapter 3. This method has been widely used and has become a standard in many countries[80].

2.4.4.2 Fatigue performance characterization

There are many laboratory test methods used to determine the fatigue strength of asphalt mixtures such as tensile-compression (T/C), two-point bending (2PB), three-point bending (3PB), four-point bending (4PB), and indirect tensile test (ITT). Furthermore, many researchers have developed various concepts for evaluating the fatigue resistance of mixes as shown in Table 2-1[74]. They can be grouped into three types: linear viscoelastic properties E_0 and ϕ_0 (determined at the beginning of each test, N = 100), life duration (number of cycles to specified failure criterion), and fatigue damage characteristics in the crack initiation phase. These three concepts are widely used to study the fatigue failure criteria for asphalt mixtures, including the classical (traditional), the fracture mechanics and the damage-energy approach[81, 82]. According to Baburamani[75], the fracture mechanics and dissipated energy

approaches were included as mechanistic approaches, while the classical criterion was categorized as a phenomenological approach.

Table 2-1. Some of the analyzed output parameter values from fatigue tests

Parameter value	Definition	Type
E_0; ϕ_0	Modulus; phase angle (at 100 cycles)	Linear viscoelastic
N_{f50}	Classical fatigue life at 50% reduction	Life duration
N_t	Fatigue life defined from dissipated energy ratio curve	Life duration
N^*_1; N^*_2	Characteristic number of cycle at sharp changes	Life duration
ε_i	Average strain	Damage
E_{00i}; ϕ_{00i}; W_{00i}	Modulus; phase angle; dissipated energy	Damage
a_{Ti}; a_{wi}; a_{Fi}	Experimental E/E00i slope; normalized energy slope; fatigue damage slope	Damage

In the mechanistic approaches (fracture mechanics and dissipated energy), the damage process in the fatigue occurs in two distinct stages: crack initiation and crack propagation (growth). Generally, fracture mechanics are used to characterize the crack propagation in asphalt mixtures, while the classical and the damage-energy approaches are widely used to develop fatigue prediction models for the crack initiation.

The beam fatigue test is one of the most common methods used to study the fatigue behaviour of bituminous mixes. Beam fatigue can be used to simulate the pattern of flexural stress found in situ where the test results of the beam may reflect the weakness that might occur in the asphalt mixtures. Dondi *et al.*[83] and Khiavi *et al.*[70] state that control stress and control strain are the two loading approaches carried out during the test to simulate the real condition of pavement.

a. Classical approach

In the *classical criterion*, the fatigue life of asphalt mixtures is directly correlated with the initial pavement response (stress/strain). Fatigue testing in this criterion is conducted at various initial stress/strain levels, and the fatigue failure is based on the number of loading cycles to failure in relation to the stress or strain in the asphalt mixtures[72, 84].

In addition, the classical criterion uses the stiffness ratio to analyze the fatigue performance. The stiffness ratio (SR) concept is a traditional fatigue life prediction based on 50% initial stiffness reduction. The SR at the i_{th} loading cycles is defined as the quotient of stiffness at the i_{th} loading cycles to the initial stiffness. Furthermore, the analysis is based on the stiffness ratio curve, where the failure criteria are assumed to be the point in which the number of loading cycles corresponds to the 50% initial stiffness reduction recorded at 50, 200 and 500 cycles[70, 83]. This criterion

was widely modelled by Pell[85], Pronk and Hopman[86], Tayebali *et al.*[87], Abojaradeh *et al.*[88] and Shen and Lu[89]. The Australian standard Austroads AG:PT/T233[90] has also adopted this model as the failure criterion.

A simple form of fatigue model was formulated depending on the mode of loading as follows[75, 91]:

$$N_f = \mathrm{A}\left(\frac{1}{\varepsilon}\right)^{\mathrm{b}} \quad \text{For controlled-strain test} \tag{2-13}$$

$$N_f = \mathrm{C}\left(\frac{1}{\sigma}\right)^{\mathrm{d}} \quad \text{For controlled-stress test} \tag{2-14}$$

where: N_f : number of loading applications to failure

ε, σ : tensile strain or stress repeatedly applied, and

A, b, C, d : material coefficients derived from fitting the data

The magnitude of tensile strain at the bottom of the asphalt layer is used as a criterion where the microcracking, crack initiation and failure have occurred. Accordingly, the relationship between the number of cycles to failure and strain is used as the basis for assessing fatigue performance and enables the determination of the thickness of the asphalt layer in structural pavement design. A study by Pell cited in Shen and Carpenter[91] showed that tensile strain is the more important parameter for fatigue cracking. The results of controlled displacement can be explained with regard to the relationship between initial strain and load repetition, as shown in Equation 2-15 below[75, 92, 93].

$$N_f = \mathrm{k}_1\left(\frac{1}{\varepsilon_0}\right)^{\mathrm{k}_2} \tag{2-15}$$

where: N_f : number of loading applications to failure at a particular level of initial strain

ε_0 : initial tensile strain, and

$\mathrm{k}_1, \mathrm{k}_2$: material coefficients derived from fitting the data

Equation 2-15 represents the relationship between the radial strain at the bottom of the asphalt mixture layer and the number of load applications until the appearance of cracking in the pavement. The fatigue coefficient k_1 and k_2 may vary between models. Usually, the value of k_2 is in a range between 3 and 6, while k_1 is affected by several magnitudes. However, k_1 and k_2 are specific to the asphalt binder

type, asphalt mixture type, volumetric composition, and the test parameters used in the laboratory characterization[75].

A study by Monismith *et al*. cited in Shen and Carpenter[91] stated that the stiffness of asphalt mixtures affects the fatigue life. A modified Equation 2-15 is given as Equation 2-16 to define the mixture's stiffness dependent behaviour.

$$N_f = a\left(\frac{1}{\varepsilon_t}\right)^b . \left(\frac{1}{S_0}\right)^c \qquad (2-16)$$

where: N_f : number of loading application to failure

ε_t : tensile strain

S_0 : mixture stiffness, and

a, b, c : material coefficients, derived from fitting the data

b. Fracture mechanics

Fatigue is considered to be a continuous damage process, and the accumulation of damage is believed to follow a crack propagation law, which begins with the growth of a crack from the initial level (crack initiation) followed by the critical level (failure). A study by Majidzadeh *et al*. cited in Baburamani[75] showed that the Paris law of crack propagation correlates the increase in crack length per load cycle with the stress intensity factor, K_c, in a power law relationship as follows:

$$\frac{dc}{dN} = AK_c{}^n \qquad (2\text{-}17)$$

where: dc/dN : rate of crack propagation

K_c : stress intensity factors, and

A, n : material constant

The *fracture mechanics* approach studies the crack propagation in asphalt mixtures specimens subjected to repetitive loading. Fracture mechanics is the potential energy required to cause cracks and is defined as the area under the stress-strain curve up to peak load[72].

A typical stress-strain relationship obtained from an Indirect Tension Test (IDT) for asphalt mixtures is shown in Figure 2-9. It can be seen from the figure that the fracture energy density (FE_{IDT}) is composed of the total elastic strain energy density (EE_{IDT}) and dissipated creep strain energy density (DE_{IDT}) at failure. The area of

FE_{IDT} is formed by the stress-strain curve up to failure and EE_{IDT} is formed by the failure strain, the resilient modulus (M_r) and the IDT strength (σ_{IDT}).

c. Damage – energy

The *damage-energy approach* may be analyzed with the dissipated energy concept. The dissipated energy (DE) concept states that fatigue life is a function of the accumulation of dissipated energy on each loading cycles where the dissipated energy in a cycle is affected by the energy dissipated in the previous cycles.

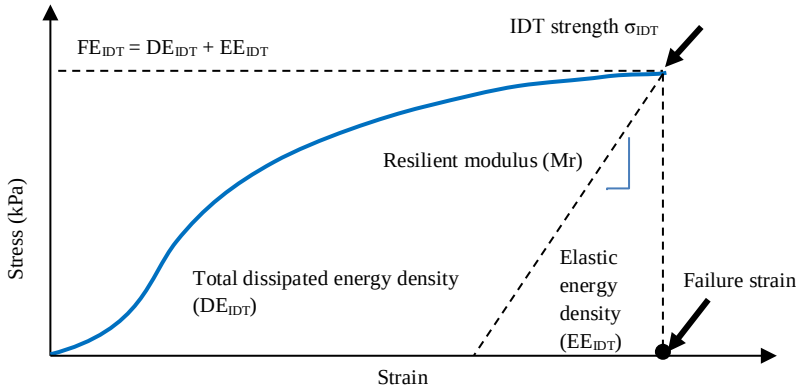

Figure 2-9. Fracture and dissipated energy density from IDT strength test [72]

Baburamani[75] states that as viscoelastic materials, asphalt mixtures can be analyzed in terms of the energy dissipated in the specimen during testing. He argues that the rheology of asphalt mixtures as a function of temperature, loading frequency and strain/stress level influences the energy dissipated. As Van Dijk *et al.* cited in Baburamani[75] state, the total energy dissipated during a fatigue test may be controlled with the fatigue life and change in the mechanical properties of asphalt mixtures. Further, the energy dissipated can be used to explain the decrease in mechanical properties such as flexural stiffness loss during the test. Pronk[94] argues that dissipated energy per cycle is the most relevant parameter and the fatigue life based on dissipated energy is more reliable than prediction based on the tensile strain criterion. Hopman *et al.*[95] note that the energy dissipated per cycle controls the fatigue damage of asphalt mixtures. According to Hassan and Khalid[96] the dissipated energy is the difference between the induced energy and released energy due to load application and relief. Thus, the energy dissipated in each pulse of a loading cycle causes incremental damage to the asphalt mixtures, then leads to crack extension, plastic deformation and thermal energy[83].

In viscoelastic materials, deformation and strain increase over time as long as a constant load is applied, and when the load is removed, some deformation is recoverable and some is unrecoverable. For a viscoelastic material, the DE in each loading cycle for asphalt mixtures is observed as the area under the stress-strain curve of the hysteresis loop and calculated using the following Equation 2-18[70, 72, 75, 83, 96]. The unloaded material has a different path to that when a load is applied. Thus, the phase lag is recorded between the applied stress and the measurement strain. Further, the energy is dissipated in the form of mechanical work, heat generation or damage. In the strain-controlled fatigue test, the energy decreases when the number of load cycles increases as the stress decreases, while for the stress-controlled fatigue test the dissipated energy per cycles increases when the number of cycles increases[97, 98].

$$DE_i = \pi . \sigma_i . \varepsilon_i . \sin(\delta_i) \quad (2\text{-}18)$$

where DE_i : dissipated energy in cycle i

σ_i : stress level in cycle i

ε_0 : strain level in cycle i

δi : phase angle in cycle i

Van Dijk cited in Maggiore *et al.*[82, 99] used an equation to relate the cumulative dissipated energy and the number of cycles to failure as shown in Equation 2-19.

$$W_f = A(N_f)^z \quad (2\text{-}19)$$

where W_f : cumulative dissipated energy to failure

N_f : number of load cycle to failure

A, z : mixture dependent constants

Further, some researchers have proposed several failure criteria based on the dissipated energy concept. Pronk and Hopman[86] proposed an energy-ratio (ER) concept to define the fatigue life of asphalt mixtures in the strain-controlled tests by using Equation 2-20. The energy ratio is defined as the ratio of the initial dissipated energy to the dissipated energy at the i_{th} cycle multiplied by the load cycle n. The energy ratio is then plotted against the number of cycles, and the failure point is recognised as the point at which there is a significant change in the slope of the curve. The fatigue life is defined as the number of loading cycles where the curve (energy ratio) deviates from a straight (tangent) line.

$$Energy\ ratio = \frac{n.w_0}{w_i} \quad (2\text{-}20)$$

where: n : the number of load cycles

w_0 : initial dissipated energy/cycles at the start of the test

w_i : dissipated energy at the cycles i_{th}

Pronk[100] proposed the concept of energy ratio to define failure as the ratio of the cumulative dissipated energy at cycle *n* to the dissipated energy for cycle *n* based upon Equation 2-21**.** Pronk used a similar procedure to that used by Pronk and Hopman to define the failure point (fatigue life). However, Khiavi and Ameri[70] and Abojaradeh[98] argue that the number of load cycles to failure in both the Pronk-Hopman and Pronk methods is not an exact value since it is not easy to locate where the energy ratio deviates from a straight line based on the fact that the early part of the curve is not a truly straight line.

$$Energy\ ratio = \frac{\sum_{i=1}^{n} w_i}{w_n} \quad (2\text{-}21)$$

where n : the number of load cycles

w_i : dissipated energy at cycle i_{th}

w_n : dissipated energy for cycles n

In addition, Rowe and Bouldin[101] developed the definition of failure by introducing a new definition as the load cycle multiplied by the stiffness at that cycle using Equation 2-22. The energy ratio for different cycles is then plotted *versus* the number of load cycles. This function produces a peak value, which can be identified easily by fitting a high order polynomial function and differentiating[98]. The point at the peak value of the curve is defined as the failure point.

$$Energy\ ratio = n\,S_i \quad (2\text{-}22)$$

where n : number of load cycle

S_i : stiffness at cycles i_{th}

Abojaradeh[98] introduced a fatigue failure criterion based on the Rowe and Bouldin failure definition. The energy stiffness ratio was developed using Equation 2-23. A peak value can be obtained by plotting the energy stiffness ratio versus the number of load cycles, and it is recognized as the failure point of fatigue life.

$$Energi\ stiffness\ ratio = \frac{N_i\ S_i}{S_0} \quad (2\text{-}23)$$

where N_i : the cycle number

S_i : stiffness at cycles i_{th}

S_0 : initial stiffness taken at cycle number 50

Furthermore, Ghuzlan and Carpenter[99, 102] and Carpenter *et al.*[92] developed and proposed the dissipated energy ratio (DER) method to define the failure point of fatigue life in asphalt mixtures. The DER was defined as the change in dissipated energy between two cycles, cycle *n* and *n+1* (ΔDE), divided by the dissipated energy of the first cycle (cycle *n*). Some researchers[70, 72, 82, 93, 98] have used the DER as a parameter to relate the damage accumulation to fatigue life of asphalt mixtures. The DER is represented by Equation 2-24.

$$DER = \frac{[DE_{n+1} - DE_n]}{DE_n} \quad (2\text{-}24)$$

where DER : dissipated energy ratio

DE_{n+1} : dissipated energy produced in load cycle $n+1$

DE_n : dissipated energy produced in load cycle n

The RDEC values plotted versus the number of load cycles creates a curve that decreases rapidly at the beginning application of the load cycle then reaches a steady state at a large number of cycles and increases rapidly at the end. The failure point (N_f) is defined as the number of load cycles at which the dissipated energy ratio begins to increase rapidly.

2.5 Asphalt Binder

2.5.1 The nature of asphalt binder

Asphalt binder used for road construction is obtained generally from fractional distillation of crude oils, although other different forms can also be obtained, such as lake asphalt, rock asphalts and gilsonite. Asphalt binder is material formed from hydrocarbon, sulphur, nitrogen and oxygen. Table 2-2 presents the composition of asphalt binder derived from crude oil[5].

Table 2-2. Composition of asphalt binder

Component	Percentage
Carbon	82 – 88
Hydrogen	8 – 11
Sulphur	0 – 6
Oxygen	0 – 1.5
Nitrogen	0 – 1

According to the Shell Bitumen Handbook, the chemical composition of asphalt bitumen can be grouped into two types, which are called as asphaltenes and maltenes. The maltenes, further, can be divided into saturated, aromatic and resin[18].

In addition, Fordyce and O'Donnell state that asphalt binder is composed of three forms of structure: oils, asphaltenes and maltenes. Oils have the physical form of a chain. The complexity of the chains influences the viscosity (resistance to flow) of asphalt binder. Asphaltenes are a chemical structure composed flat plates forming an irregularly shaped solid. Resin consists of plate-like structures with chains extending from them. Therefore, asphalt binders are a solution constructed of particles of asphaltene surrounded by resins within oils. The viscosity of asphalt binder is affected by the proportion of the three chemical groups and the temperature. The energy and movement of the individual particles increase with increased temperature, however, the associated bonds between the particles decreases and results in a lower resistance to shear[2].

Rheology is defined as an effort to study of the deformation and flow of materials. According to Bahia[103], rheology is used to study materials whose deformation characteristics vary with the application of load and the time rate of the load. Asphalt binders are included among rheological materials because temperature and rate (or time) loading affect their behaviour[103]. Asphalt binders have two rheological properties which are thermoplastic and viscoelastic. Thermoplastic means that the viscosity of the asphalt binder decreases on heating and increases on cooling, while viscoelastic means that when a force is applied, the asphalt binder will become distorted as well as flow. The distortion is recoverable and it describes elastic behaviour while the viscous flow is irrecoverable. The chemical composition and temperatures influence the elastic and viscous response of asphalt binder. At lower temperatures, asphalt binder is more viscous and its response is more elastic when a short time force is applied. By contrast, at high temperatures, asphalt binder is less viscous and sometimes, flow will occur when a force is applied. Furthermore, the shape of the asphalt binder will show a little recovery when the force is removed.

A function of the mechanical properties of asphalt binder is to respond to an applied force in the form of stress over a contact area. The response of asphalt binder may occur in the form of recoverable (recorded as strain) and irrecoverable (recorded as rate of strain) movement. For liquid materials, the response is referred to as viscosity, which is the ratio of shearing stress to the corresponding rate of shearing strain, whereas for elastic solid materials such as asphalt binder, the term of elastic modulus (stiffness modulus) is used as the ratio of applied stress to corresponding strain, as discussed in Section 2.5.2.

2.5.2 Concept of asphalt binder stiffness

Asphalt binder becomes elastic or viscous depending on the temperature and rate of loading. At low temperatures and under short periods of loading (high frequencies), the binder behaves as an elastic (brittle) solid, whereas at high temperature and under long periods of loading (low frequencies), the binder behaves as a viscous material. Under intermediate temperatures and periods of loading, asphalt binder becomes a viscoelastic material.

The concept of stiffness modulus was introduced as a basic parameter to explain the mechanical properties of asphalt binder in order to specify the viscoelastic behaviour by analogy with the elastic modulus of a solid. Basically, the elastic modulus of material (E) followed Hooke's law, with the stiffness modulus being used to express the dependence of asphalt binder on temperature and loading period[5, 18]. Stiffness modulus is, generally defined as the ratio between the applied stress and the resulting strain at loading time (t) and temperature (T) as shown in Equation 2-25:

$$S_{t,\,T} = \frac{\sigma}{\varepsilon_{t,T}} \qquad (2\text{-}25)$$

where: $S_{t,T}$: Stiffness at loading time t and temperature T

σ : Stress

$\varepsilon_{t,T}$: Strain at loading time t and at temperature T

2.5.3 Determination of asphalt binder stiffness

The stiffness modulus of asphalt binder is related to shear deformation. To determine the resistance to shear, it is necessary to find out the shear stress and shear strain. The definition of resistance to shear is the ratio of shear stress to shear strain. The shear modulus at frequency *f*, is given as Equation 2-26[18].

$$G_f = \left(\frac{\tau}{\gamma}\right)_f \quad (2.26)$$

where: G_f : Shear modulus

τ : Shear stress

γ : Shear strain

According to The Shell Bitumen Handbook, the phase difference (ϕ) is the lag between shear stress and shear strain as shown in Figure 2-10. This lag is a measure of the degree of elasticity of the bitumen under the test condition and can range from 0 to 90°. The elastic materials could not show a difference phase between shear stress and shear stain, whereas the viscous materials might have a phase lag of 90°. For viscoelastic materials such as asphalt binder, the phase lag is between 0 and 90° depending on the type and grade of bitumen, temperature and frequency. At low temperature and high frequency, there is a small phase lag for asphalt binder, and vice versa, indicating that asphalt binder behaviour is approximately elastic and viscous[18].

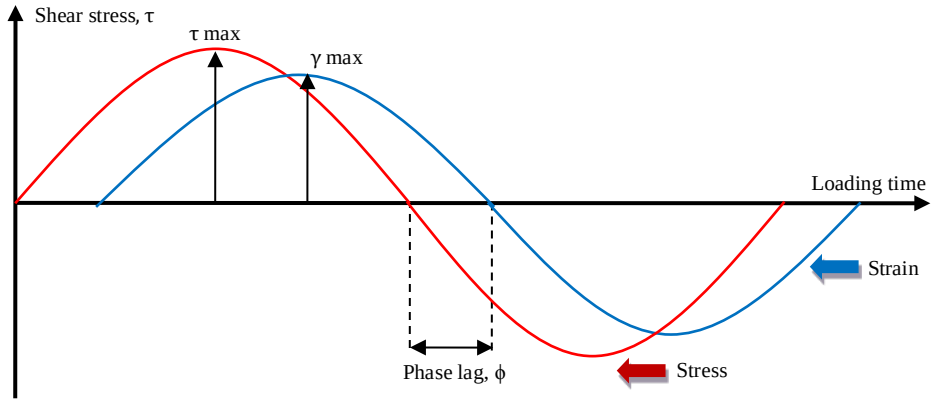

Figure 2-10. Concept of lag between stress and s train [18]

Shear stress can be applied during a test by combining creep tests with dynamic tests. The creep test is used to simulate the effect of environment (the load is applied as a constant load for a long period of time), whereas the dynamic loading is used to simulate the effect of traffic (with varying stress, constant amplitude and frequency, and for shorter loading periods). The combined test data can be used for covering stiffness versus loading time, as the asymptote represents the approximation of elastic and viscous response at short and long loading time (Figure 2-11). In addition, the stiffness modulus as a function of loading time at various temperatures is presented in Figure 2-12.

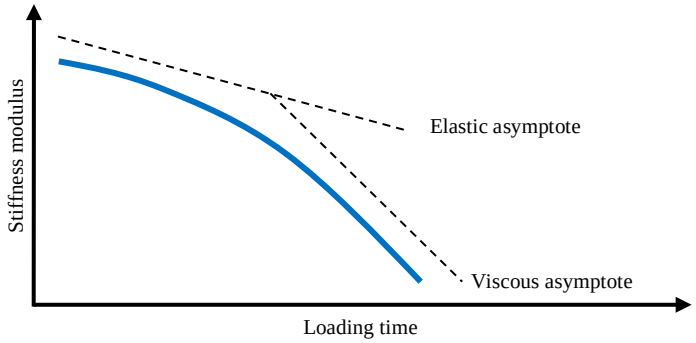

Figure 2-11. Stiffness modulus as a function of loading time or frequency [18]

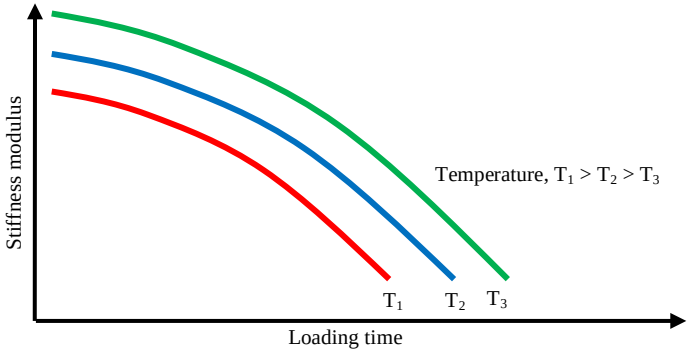

Figure 2-12. Stiffness modulus as a function of loading time, different temperature [18]

2.5.4 Asphalt binder characterization

Asphalt binder has a complex response to stress because it is a complex material. The response of asphalt binder to stress is dependent on the temperature and loading time, as discussed in Section 2.5.2. Consequently, the nature of the test must be appropriate to the nature of the material. Joshi *et al.*[104] argued that conventional methods such as penetration, viscosity, ductility, and ring and ball softening point have limitations in accurately utilize the performance of modified binder.

The Dynamic Shear Rheometer (DSR) test is used to characterize the viscoelastic behaviour of asphalt binder at different temperature and frequencies, and may be used to evaluate the potential of asphalt binder for rutting and cracking, according to Mallick and El-Korchi[105]. The experimental data results in a viscoelastic function showing a complex shear modulus (G*) and phase angle (δ) under loading times where shear was repeatedly applied.

Lu *et al.*[106] explained that the ratio of the peak applied shear stress (τ) to the resulting peak shear strain (γ) is defined as the complex shear modulus (G*), which is a measure of the total resistance of a material to deformation when repeatedly

sheared. The complex shear modulus consists of two components which are defined as the storage modulus *(G')* and the loss modulus *(G'')*. The storage modulus and the loss modulus can be defined as the elastic shear modulus and viscous shear modulus, respectively. *G'* is proportional to the stress in-phase with the strain and related to the elastic response of the materials, while *G''* is proportional to the stress out-of-phase and related to the viscous effect.

Furthermore, the phase angle *(δ)* is defined as the difference between the stress and strain in an oscillatory deformation. This parameter is a measure of the viscoelastic character of the material, as an indicator of the relative amount of recoverable and non-recoverable deformation. An elastic material demonstrates *δ* of 0° while the purely viscous liquid material demonstrates *δ* of 90°[106].

Bahia *et al.*[107], explained the relationship between the complex shear modulus *(G*)*, elastic shear modulus *(G')*, viscous shear modulus *(G'')* and phase angle *(δ)* as shown in Figure 2-13**.** The phase angle *(δ)* is used to describe the viscoelastic behaviour of asphalt binder as follows. If a material is purely viscous then the phase angle *(δ)* is 90°, which means that elastic shear modulus *(G')* is 0 and viscous shear modulus *(G'')* is equal to the complex shear modulus *(G*)*, *G'' = G**. If a material is elastic then the phase angle *(δ)* is 0°, which means that elastic shear modulus *(G')* is equal to complex shear modulus *(G*)*, *G' = G**, and the viscous shear modulus (*G''*) is 0.

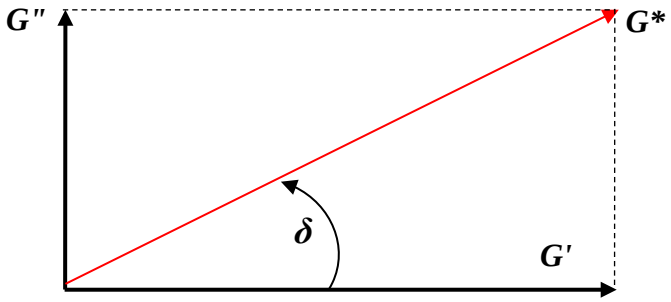

Figure 2-13. Relationship between complex shear modulus *(G*)*, elastic shear modulus *(G')*, viscous shear modulus *(G'')* and phase angle *(δ)*

From the definition above, these parameters can be controlled and this means that the asphalt pavement performance can also be controlled. The rheological technique was used to predict the asphalt mixtures performance based on the main two rheological parameters, complex shear modulus (G*) and phase angle (δ). According to Joshi *et al.*[104] and Chen *et al.*[108], the parameter of G*/sin δ is defined as the rutting resistance parameter, which could be correlated with permanent

deformation susceptibility of a bitumen, while G*sin δ is the fatigue resistance parameter. Gonzales *et al.*[109] explained that the maximum temperature for good viscoelastic response of the binder facing the rutting is given by the temperature at which G*/sin δ = 1 kPa at a frequency of 10 rad/s. Accordingly, at the average maximum temperature reached by an asphalt pavement, the value should remain above 1 kPa for bitumen to resist asphalt pavement rutting. Further, the fatigue resistance parameter may be used to determine the fatigue cracking potential. Under a strain-controlled process, the fatigue is proportional to G*sin δ, and hence a lower value of G*sin δ means a lower potential for fatigue cracking[5].

As discussed in Section 2.5.1, the viscoelastic parameters of asphalt binder are a function of temperature and frequency, which may be modified by the inclusion of additives. There are many studies on using the rheological technique on the viscoelastic parameters of bitumen.

2.5.5 Asphalt binder modification

The need for asphalt modification is caused by limitation in the capability of the base asphalt binder to resist distresses. When the rheological and mechanical properties of base asphalt binder are not ideal for accommodating changes in traffic load, traffic volume, environment and pavement structure requirements, modification has been used as an alternative to improve asphalt binder properties. The rheological and durability properties of base asphalt binders are not sufficient for resisting the on distresses caused by increases in traffic and changes in environmental conditions.

Modified bitumen is formulated with additives to improve its service performance. Bahia[103] has explained that the modification of asphalt binder is performed to improve one or more basic properties of asphalt binder related to one or more types of pavement distress, including rigidity, elasticity, brittleness, storage stability and durability, and resistance to accumulated damage.

Rigidity is total resistance to deformation. Higher rigidity at high temperature or low loading rates is desirable to prevent rutting. However at intermediate and low temperature, lower rigidity is needed to resist fatigue and thermal cracking, respectively. Elasticity is the ability of asphalt mixture to recover from deformation using stored energy. Greater elasticity is favourable for resisting rutting and fatigue damage. Brittleness is a type of failure that happens at low strain. Brittleness should be reduced to improve resistance to fatigue and thermal cracking.

Binder modifier can be classified in several ways: based on the mechanism, on the composition and physical nature of the modifier; or on the target asphalt property that needs improvement or enhancement. The objective of using the binder modifier corresponds to the main distress that the additive is expected to reduce with regard to road deterioration, such as permanent deformation, fatigue cracking, low-temperature cracking, moisture damage and oxidative aging[107].

Modification of pure binder is performed through the use of chemicals, particles or polymers to enhance a target property. Chemical modification improves the physical properties of asphalt binder and produces a binder that shows adequate stiffness at high temperatures or suffers less cracking at low temperatures. Particles such as fillers[110] and cellulose fibres[30, 46] and polymers[30, 42, 46, 52, 55] increase the resistance to permanent deformation at certain traffic loads and temperatures. Polymers also form a continuous network in asphalt binder and transmit their elastic properties to the homogenous blend.

Binder modifiers display diverse reactions in modified binder, for example, they can disperse completely or dissolve in the binders. As organic or inorganic materials, they can react with binders or are only added as in fillers. The most frequently used types of binder modifier as reported by NHCRP[107] are listed in Table 2-3.

Table 2-3. Types of asphalt modifiers

Type	Class
Polymer-elastomer	Styrene butadiene styrene (SBS), styrene butadiene (SB), styrene butadiene rubber latex (SBR), tyre rubber.
Polymer-Plastomer	Ethyl vinyl acetate (EVA)
Anti-Stripping Agents	Fatty amidoamines, polyamines, hydrated lime, others
Hydrocarbons	Natural asphalts
Fibres	Cellulose, polypropylene, polyester, mineral
Processed-Based	Air blowing
Mineral fillers	Lime
Anti-oxidants	Hydrated lime
Extenders	Sulphur

2.6 Buton Rock Asphalt

The granular Buton Rock Asphalt (BRA) binder modifier used in this study is processed from natural rock asphalt. The raw materials for natural rock asphalt are found on Buton Island in Indonesia as seen in Figure 2-14, and this is traditionally known as asphalt Buton (Asbuton). The total deposit of Asbuton is about 677 million tons and should be sufficient for use in Indonesian road construction for 100 - 200

years[111, 112]. The deposit is spread out across the island in particular from Sampolawa Bay to Lawele Bay in area about 75 km long and 25 km wide. The process of mining Asbuton is illustrated in Figure 2-15.

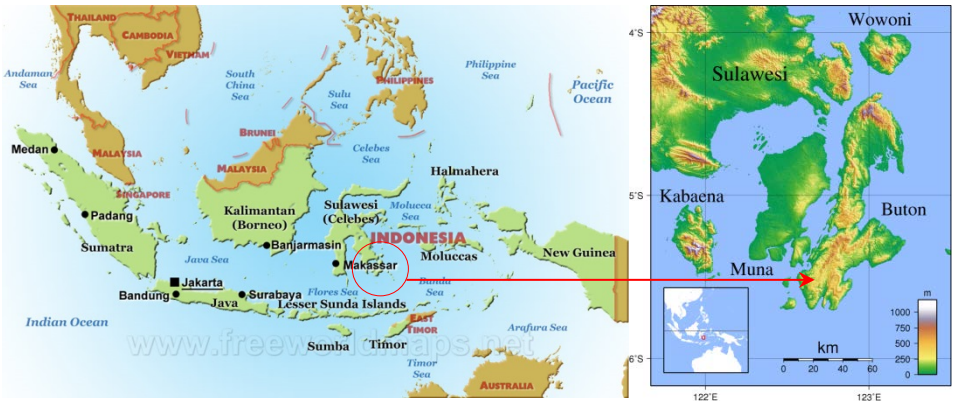

Figure 2-14. The location of Buton Island
(source of figure: [113])

Figure 2-15. Process of mining asphalt Buton
(source of figure: [114])

2.6.1 Properties of asphalt Buton

Generally, Asbuton can be divided into two categories: hard and soft, based on the area where the deposit of Asbuton is sourced. The Asbuton from the Kabungka area is hard, and it is easy to process further, while the softer Asbuton is found in the Lawele area.

Asbuton consists of mineral and asphalt binder. According to Affandy[115], Asbuton contains 70% minerals and 30% asphalt binder, Kurniadji[112] says that

Asbuton contains 10% to 50% asphalt binder, and according to Suarnaya[116], asphalt binder content in Asbuton is about 10% to 40%. Furthermore, a recent study by Affandy[115] has shown that the fine mineral content in Asbuton affects the physical properties of asphalt binder, such as penetration, softening point, ductility and others. His study compared the physical properties of three asphalt binders: semi extraction Asbuton (contains 30% mineral), pure extraction Asbuton (contains less than 1% mineral), and asphalt binder 60/80 penetration grade (pen 60/80). As shown in Table 2-4, generally, the hardness of semi extraction Asbuton is the highest compared to the pure extraction and pen 60/80 asphalt binder due to the effect of the mineral content in the asphalt binder. Accordingly, the semi extraction and pure extraction Asbuton can be concluded to be asphalt mastics. Asphalt mastics are generally considered to contain asphalt binders and filler particles no larger than 75 microns[117, 118].

Table 2-4. Physical properties of Asphalt buton [115]

Properties	Method	Asphalt binder		
		Semi extraction	Pure extraction	Pen 60/80 grade
Penetration (25°C, 100 g, 5s), 0.1 mm	SNI 06-2456-1991	48.1	68.4	62
Softening point, °C	SNI 06-2434-1991	58.8	51	50.3
Flash point, °C	SNI 06-2433-1991	-	200	317
Ductility (25°C, 5 cm/minute), cm	SNI 06-2432-1991	83	>140	>140
Specific gravity of bitumen	SNI 06-2441-1991	1.25	1.053	1.036
Specific gravity of Asbuton mineral	SNI 1964-2008	2.68	-	-
Solubility in C_2HCL_3, %	SNI 06-2438-1991	68.2	99.8	99.52
Loss of heating (TFOT), %	SNI 06-2440-1991	0.0176	2.18	0.0041
Penetration after TFOT, %	SNI 06-2456-1991	61.8	54.1	76
Softening point after TFOT, °C	SNI 06-2434-1991	-	-	51.3
Ductility after TFOT, cm	SNI 06-2432-1991	24	126	140
Temperature of mixing, °C	AASHTO-27-1990	-	170-176	153
Temperature of compaction, °C	AASHTO-27-1990	-	155-162	142

As reported by Delaporta *et al.*, mineral filler can affect the properties of bituminous mixture and measuring its mechanical properties can contribute to understanding how they correlate with the behaviour of the bituminous mixture. Mineral filler-bitumen composite has potential for reinforcement and this may depend on different parameters such as type, size, grading or concentration[119]. The amount of natural binder in Buton Rock Asphalt (BRA) modifier outruns that of BRA modified asphalt mixtures. This behaviour can be attributed to the aggregate grading of these mixtures, where the amount of BRA mineral (fine aggregates) is also changed. The mechanical properties of these mixtures mostly rely on the properties of mastic, and the mixtures dependency on properties of fine aggregates increases. Further, based on the DSR test, Affandy[115] classified pure extraction

Asbuton as Performance Grade 70 (PG-70) and showed that the phase angles of pure extraction Asbuton were smaller compared with the pen 60/80 asphalt binder, indicating that pure extraction asphalt binder is more elastic than pen 60/80 asphalt binder.

In addition, based on the chemical composition, Asbuton contains relatively higher nitrogen and lower parafin than the base asphalt binder, resulting in the bonding strength of Asbuton being is better than that of the base asphalt binder. The chemical properties of Asbuton asphalt binder and Asbuton mineral are presented in Table 2-5 and Table 2-6.

Table 2-5. Chemical properties of Asbuton binder [115]

Component	Content	
	Asbuton Kabungka	Asbuton Lawele
Nitrogen bases (N)	29.04	27.01
Acidaffins (A1)	6.6	9.33
Acidaffins (A2)	8.43	12.98
Paraffin (P)	8.86	11.23
Maltene parameter	2.06	1.50
Nitrogen/Paraffin (N/P)	3.28	2.41
Asphaltene content, %	46.92	39.45

Table 2-6. Chemical properties of Asbuton mineral [115]

Component	Content	
	Asbuton Kabungka	Asbuton Lawele
$CaCO_3$	86.66	72.90
$MgCO_3$	1.43	1.28
$CaSO_4$	1.11	1.94
CaS	0.36	0.52
H_2O	0.99	2.94
SiO_2	5.64	17.06
$Al_2O_3 + Fe_2O_3$	1.52	2.31
Residu	0.96	1.05

2.6.2 Review of studies into the mechanical properties of A*sbuton* asphalt mixtures

The possibility of using Asbuton fillers as material derived from Asbuton in asphalt mixtures was investigated by Subagio *et al.*[8-10]. Several tests, including resilient modulus and wheel tracking, were conducted by by Subagio *et al.*[8] on HRA mixtures using Asbuton mineral as a filler substitute in the HRA mixture. The resilient modulus tests were conducted at temperatures of 25°C, 45°C and 60°C, while for wheel tracking, the tests were conducted at test temperatures of 25°C and 45°C. For all of the test temperatures, the results indicated that the mechanical performance of HRA-Asbuton modified mixtures in term of resilient modulus and rut

depth were better than for the HRA-fly ash modified mixtures. Subagio *et al.*[9] conducted a study on the fatigue performance of HRA by using Asbuton mineral as filler. The specimens were tested at a frequency of 10 Hz, three stress levels of 0.26 MPa, 0.39 MPa, and 0.51 MPa, and under sinusoidal wave loading. However, the exact temperature at which the tests were carried out is not clear, because this was simply described as room temperature. The results showed that the numbers of cycles to failure and the initial stiffness for HRA-Asbuton modified mixtures were higher than for the HRA-fly ash modified mixtures. Further, Subagio *et al.*[10] conducted several tests, including the resilient modulus and wheel tracking test, on HRS asphalt mixtures using Asbuton mineral as a partial fine aggregate and filler. The results showed that resilient modulus values were inconsistent for HRS mixtures with 5% and 10% Asbuton filler tested at 25°C, 35°C and 45°C. The resilient modulus values of HRS modified at a test temperature of 25°C were lower when compared with unmodified HRS mixtures. By contrast, at a test temperature of 45°C the resilient modulus of modified HRS mixtures were greater than those of the unmodified HRS mixtures. For the wheel tracking test, unmodified HRS mixtures had their lowest dynamic stability tested at 45°C and their highest dynamic stability at a test temperature of 60°C.

A more recent study was conducted by Hadiwardoyo and Fikri[14] on asphalt concrete wearing course (AC-WC) dense graded. AC-WC with 20%, 25%, 30% and 40% buton natural asphalt (BNA) was mixed to produced hot-mix buton asphalt modified (HMBAM) with the same optimum bitumen content and air voids as unmodified mixtures. However the research methods was not clear in dealing with the final aggregate gradation used for HMBAM as well as the final bitumen content in HMBAM, considering that the BNA was composed of mineral and natural binder. Several tests were done including the Marshall test, indirect tensile strength test and wheel tracking test. The wheel tracking test were conducted at test temperatures of 30°C and 60°C while for indirect tensile test this was not specified. The results showed that the tensile stress and resilient modulus of 25% HMBAM were higher than for the unmodified mixture. Moreover, the rut depth of HMBAM was lower compared with the unmodified asphalt mixtures at both test temperatures.

In another study, Zamhari *at al.*[15] presented the use of granular buton rock asphalt (granular BRA) and pure buton rock asphalt (pure BRA) in hot mix asphalt as a partial or total replacement to evaluate the performance of hot-mix asphalt

(HMA) specimens containing Asbuton materials. The test was conducted on HMA containing 10% and 15% granular BRA and pure BRA modified as well as unmodified HMA. Several tests on asphalt mixtures were conducted, including the ITSM test and dynamic creep test. The ITSM tests were carried out at test temperatures of 30°C, 40°C and 50°C, while the dynamic creep test was carried out at a test temperature of 45°C and 1800 loading cycles (3600 seconds) with one second of load followed by one second off. The ITSM test results revealed that the resilient moduli of granular and pure BRA modified mixtures were higher than those of the unmodified mixtures. Furthermore, the creep test results showed that the rate of permanent deformation of unmodified mixtures was higher than for granular and pure BRA asphalt mixtures. In addition, the creep stiffness values of pure and granular BRA asphalt mixtures were higher compared with the unmodified asphalt mixtures.

A study on the feasibility of using Asbuton materials for asphalt mixture was carried out by Affandy[115]. Several tests were conducted on asphalt mixtures containing semi extraction Asbuton as well as on unmodified asphalt mixtures, including the ITSM test and wheel tracking test. The same gradation was used for both asphalt mixtures taking into consideration the mineral content of the semi extraction Asbuton used as filler in the gradation of the asphalt mixtures. However, once again the study was not clear with regard to the final bitumen content and percentage of semi extraction Asbuton used in asphalt mixtures. The stiffness modulus tests were performed at temperatures of 25°C, 35°C and 55°C, while for the wheel tracking test, the tests were carried out at a temperature of 45°C for 60 minutes. The results show that the stiffness modulus values of semi extraction Asbuton mixtures were higher compared with the unmodified asphalt mixtures at all testing temperatures. The rut depth values for unmodified asphalt mixtures were higher compared with the semi extraction Asbuton mixtures.

2.7 Summary, Research Gaps, and Research Objective

2.7.1 Summary

After reviewing the literature, the following main conclusions can be drawn:

(1) In recent times, it has been found that the viscoelastic properties of asphalt mixtures based on the mechanical approach are needed in order to carry out analytical design methods of pavement design.

(2) The two most common forms of road deterioration are permanent deformation and fatigue cracking. Accordingly, the characterization of asphalt mixtures is important to provide data relating to the elastic response of materials (stress-strain relationship) and failure conditions.

(3) One important challenge is that the mechanical properties of asphalt mixtures are mostly affected by the performance of asphalt binder relating to its rheological behaviour. Various factors affect the performance of asphalt binder and asphalt mixtures such as rate of loading, loading time, rest period, temperature, stress-strain state, mode of loading, aging and moisture, all of which need to be observed.

(4) The mechanical properties of asphalt mixtures can be predicted based on the rheological parameters of the asphalt binder: complex shear modulus (G*) and phase angle (δ);

(5) Asphalt binder modification is mostly needed to improve the mechanical performance of asphalt mixtures including rigidity, elasticity, brittleness, stability, durability and resistance to accumulated damage, through the chemical and physical properties of the materials;

(6) In general, the use of Asbuton or materials derived from Asbuton in asphalt mixtures is beneficial to the mechanical properties of asphalt mixtures. However it is still insufficient to show the effect of Asbuton on the mechanical properties of asphalt mixtures under various conditions as mention in point (3) above. Moreover, more sophisticated testing devices and complex parameters are required to gain a better understanding of the mechanical properties of BRA modified asphalt binder and BRA modified asphalt mixtures.

2.7.2 Research gaps

Further research is needed to improve the fundamental understanding of the mechanical properties of BRA modified binder and the mechanical properties of BRA modified asphalt mixtures, including:

(1) Characterizing the viscoelastic behaviour of Asbuton modified binder at different temperatures and frequencies in order to evaluate the potential of Asbuton modified binder for its rutting and cracking potential.

(2) Developing a comprehensive study on the resilient modulus of Asbuton modified asphalt mixtures.

(3) Understanding the behaviour of Asbuton modified asphalt mixtures on the deformation and fatigue cracking system.

2.7.3 Research objective

As identified by the above literature review, there are various research gaps in the mechanical properties of Asbuton (or Asbuton product) modified binders and Asbuton (or Asbuton product) modified asphalt mixtures. However, this research study, this study will focus on the mechanical properties of BRA modified asphalt mixtures by using granular BRA modifier binder as one of the commercial products derived from Asbuton, in terms of the two main research objectives of this study, as follows:

(1) To study the potential effect of using granular BRA modifier binder in asphalt mixtures on the permanent deformation resistance of asphalt mixtures;

(2) To study the potential effect of using granular BRA modifier binder in asphalt mixtures on the resistance to fatigue cracking.

Accordingly, to address these two objectives, five studies were carried out including:

(1) The effect of granular BRA modifier binder on the resilient modulus of asphalt mixtures, dealing with the effect of temperature, rest period, traffic volume, and loading time on resilient modulus values.

(2) The effect of granular BRA modifier binder on the deformation resistance of asphalt mixtures, dealing with the progression of total permanent strain and creep modulus, strain rate, and using the stepwise concept to find out the flow number, flow point and minimum strain rate.

(3) The effect of granular BRA modifier binder on the rut depth and tracking rate of asphalt mixtures based on the Australian method, velocity, and dynamic stability.

(4) The effect of granular BRA modifier binder on the fatigue life of asphalt mixtures, dealing with the initial flexural stiffness, initial phase angle, fatigue life of asphalt mixtures using the classical and energy ratio approach, fatigue life prediction based on the strain method and strain-stiffness method, dissipated energy.

(5) The effect of granular BRA modifier binder on the dynamic modulus of asphalt mixtures, dealing with the dynamic modulus, phase angle, master curve of dynamic modulus and black space diagram.

CHAPTER 3
RESEARCH METHODOLOGY

3.1 Introduction to Methodology

This chapter presents the research methodologies employed to achieve the thesis objectives outlined in Chapter 2. The background of the materials used in the experiments, the mix design for unmodified and BRA modified asphalt mixtures, and the testing standards/procedures are presented. The chapter then describes a series of experiments conducted in the laboratory to study the potential effect of granular BRA modifier binder on the permanent deformation resistance and resistance to fatigue cracking. In general, the experimental program consisted of: indirect tensile stiffness modulus tests to determine the resilient modulus of the asphalt mixtures, dynamic creep tests to determine the permanent compressive strain characteristics of the asphalt mixtures, wheel tracking tests to determine the deformation resistance of the asphalt mixtures, repeated flexural bending tests to determine the fatigue life of the asphalt mixtures, and the asphalt mixture performance test (AMPT) to determine the dynamic modulus of asphalt mixtures. The overall research methodology for achieving the thesis objective is shown in Figure 3-1.

3.2 Selection of Materials

3.2.1 Base asphalt binders

Class-170 (pen 60/80) base asphalt binder was used for the unmodified asphalt mixtures. The binder was classified in accordance with the Australian Standard AS-2008[120]. C-170 is a soft grade bitumen and has the highest flexibility and durability appropriate for use in asphalt mixtures in cool climate regions and for light traffic. The properties of the base asphalt binder are summarized in Table 3-1.

Table 3-1. Properties of base binder

Properties	Test Method	Value
Density, Kg/L	AS 2341.7	1.03
Flash point, ºC	AS 2341.14	>250
Viscosity at 60ºC, Pa.S	AS 2341.2	170
Viscosity at 135ºC, Pa.S	AS 2341.2	0.35

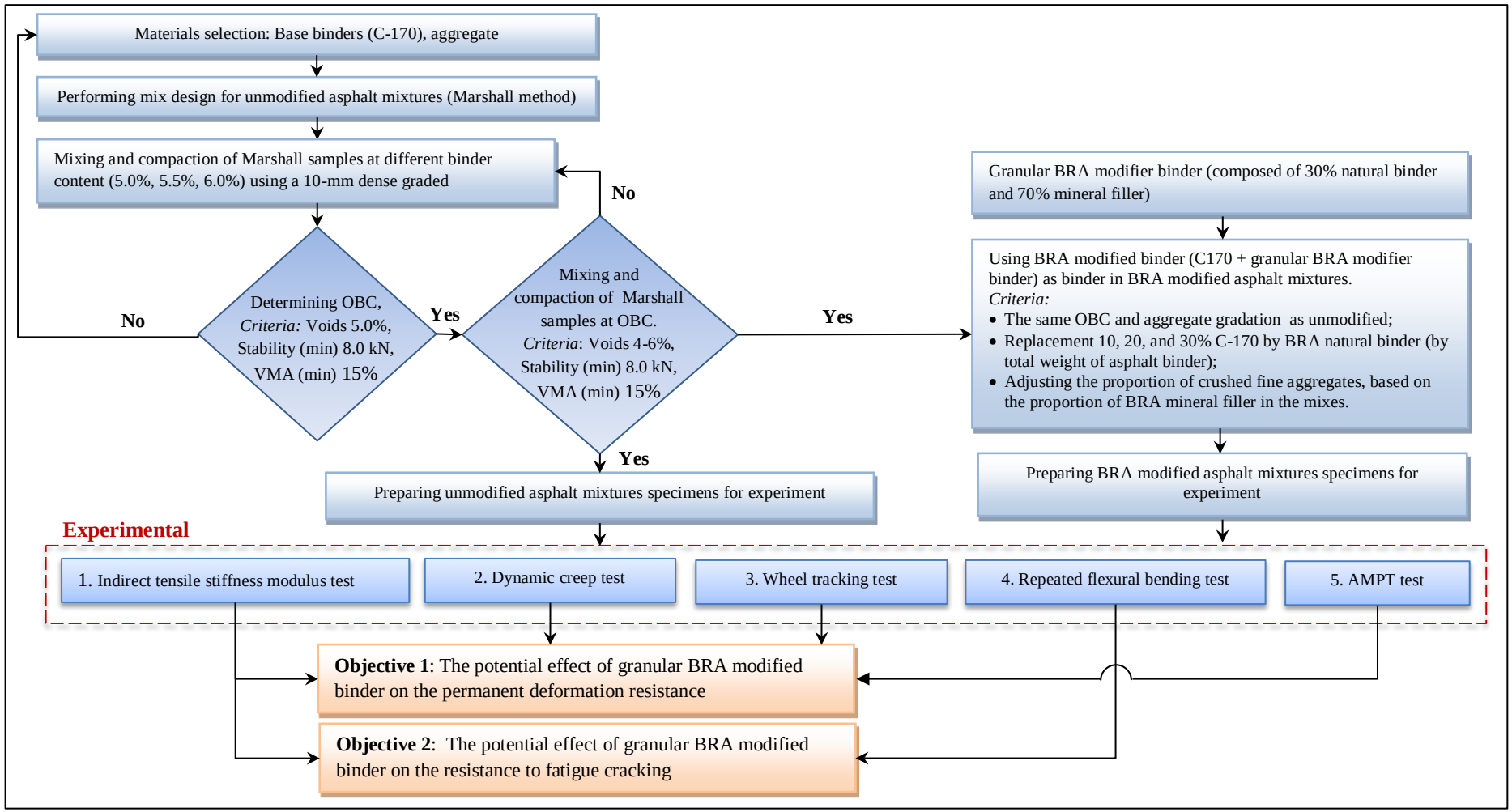

Figure 3-1. Research methodology

3.2.2 Aggregates

A crushed granite aggregate from a local quarry in Western Australia was used in all of the mixtures. The coarse and fine aggregates required to prepare the mixes were obtained by sieving on each sieve diameter. The unmodified and BRA modified asphalt mixtures used a typical dense graded aggregate with a maximum aggregate size of 9.5 mm (DG-10) based on Specification 504[121]. The results of determination of aggregates properties are presented in Appendix A1 to Appendix A4 and summarized in Table 3-2.

Table 3-2. Properties of aggregates

Properties	Test Method	Value		
		Average	SD	CV
Los angeles value (%)	AS 1141.23-1995	21.8	0.24	1.1
Flakiness index (%)	AS 1141.15-1999	14.14	0.74	5.2
Apparent coarse aggregate density (t/m^3)	AS 1141.5-2000	2.63	0.04	1.35
Apparent fine aggregate density (t/m^3)	AS 1141.5-2000	2.60	0.05	1.82

3.2.3 Granular BRA modifier binder

Figure 3-2 shows the form of the BRA modifier binder (pellets) with a diameter of 7 mm to 10 mm used in this study. The brand was *Retona Pellets,* a commercial product manufactured by PT. Olahbumi Mandiri in Jakarta, Indonesia. In this research, these materials are known as granular BRA modifier binder. The raw materials of this product are obtained from Buton Island in Indonesia.

Figure 3-2. Typical of granular BRA modifier binder

3.2.3.1 Bitumen content test

A bitumen content test for granular BRA modifier binder was carried out following the WA standard 730.1-2011[122]. The objective of this test was to determine the content of natural bitumen in granular BRA modifier binder. The content of

natural bitumen will be further used to quantify the weight of granular BRA modifier binder mixed with base asphalt binder.

a. Apparatus

The apparatus used to determine bitumen content was a centrifugal extractor, consisting of a bowl in which the samples were placed, and then revolved at a controlled speed of up to 3600 rpm as seen in Figure 3-3. The apparatus was also provided with a container for catching the solvent thrown from the bowl and a drain for removing the solvent.

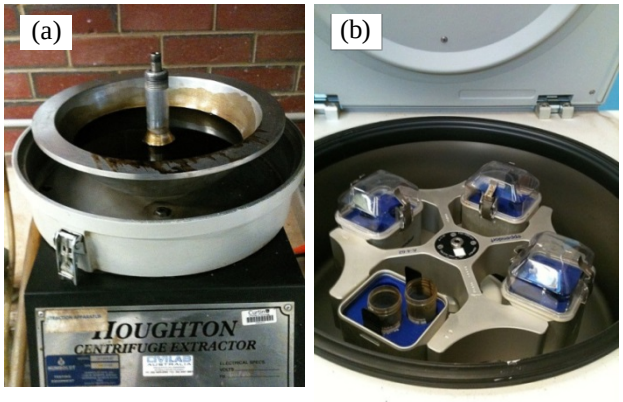

Figure 3-3. Apparatus used for bitumen content test, (a) Centrifuge extractor, and (b) centrifuge

b. Sample preparation

Triplicate portions of granular BRA modifier binder were prepared for extraction, with a minimum mass of 750 g for each test portion. In this study, the mass of the three samples was 758, 762 and 768 g. Each sample portion was put in a bowl before the test was run.

c. Bitumen content test results

The test portions were placed in the extraction bowl, and sufficient solvent was added to cover the samples. The filter was placed on the bowl in the extraction apparatus, and the cover of the apparatus was clamped tightly to the assembly. The machine then started revolving slowly, gradually increasing to a maximum speed of 3600 rpm. The machine was stopped when the solvent discharge had ceased. This procedure was repeated until the discharge was clear. Further, two centrifuge tubes were prepared and then approximately half of the aliquot was poured into each centrifuge tube. The centrifuge tubes were put in the centrifuge machine which was running until it stopped automatically.

The bitumen content test results found that, on average, the granular BRA modifier binder consisted of about 70% mineral and 30% binder by total weight of materials. The determination of the bitumen content in the granular BRA modifier binder is presented in Appendix A5.

3.2.3.2 Particle size distribution test

The objective of the particle size distribution test in this study was to determine the particle size distribution of the BRA mineral in accordance with WA standard 210.1-2011[123].

a. Apparatus

A mechanical sieve shaker and one set of sieves as seen in Figure 3-4 were used to sieve the BRA minerals following the Australian standard of sizes. The set of sieve sizes used in this test were 2.36, 1.18, 0.600, 0.425, 0.300, 0.150 and 0.075 mm.

b. Sample preparation

BRA minerals obtained from the bitumen content test (Section 3.2.3.1) were dried in an oven at a temperature of 105°C for 24 hours. Three test portions, each with a minimum mass of 500 g, were prepared. Every test portion was placed in the top sieve which was agitated automatically by the sieve shaker for about 30 minutes.

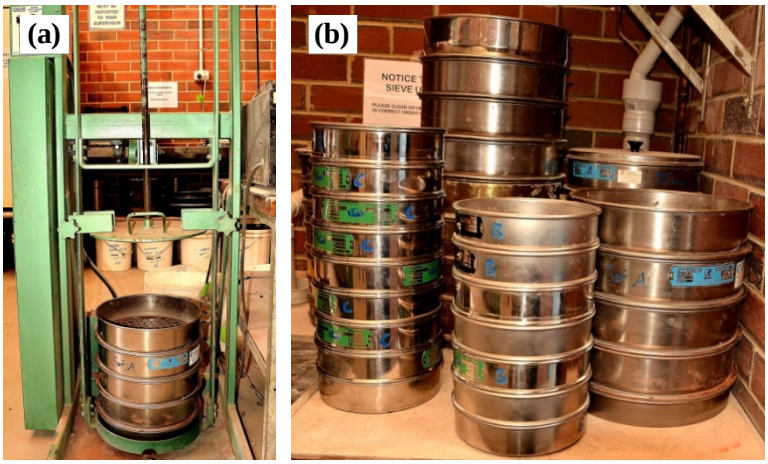

Figure 3-4. Apparatus used for particle size distribution test,
(a) sieve shaker, and (b) a set of sieves

c. Particle size distribution of BRA mineral test results

The mass of BRA mineral retained in each sieve was weighed and the results for each test portion are presented in Appendix A6. The mean particle size distributions of BRA mineral for each sieve are shown in Table 3-3. As an alternative means of showing the distribution for the BRA mineral particle sizes, Figure 3-5 shows the relationship between the particle size diameter and percentage passing.

Table 3-3. The mean particle size distribution of BRA mineral and soil classification

Sieve size (mm)	: 2.36	1.18	0.600	0.300	0.150	0.075
Passing (%)	: 100	97	92	81	61	36
Classification of soil based on the USCS						
Grain diameter at 10% passing (D_{10})	: 0.075 mm					
Grain diameter at 30% passing (D_{30})	: 0.075 mm					
Grain diameter at 60% passing (D_{60})	: 0.15 mm					
Coefficient of Uniformity (C_u)	: 2.00					
Coefficient of Curvature (C_c)	: 0.50					

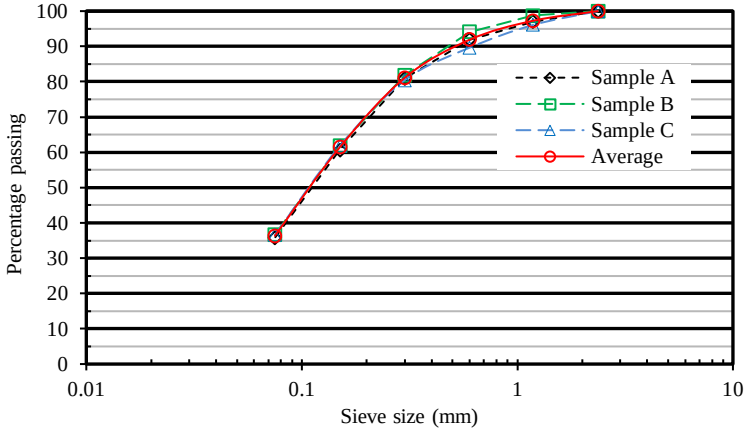

Figure 3-5. Particle size distribution of BRA mineral

3.3 Mix Design for Unmodified Asphalt Mixtures

The objective of the mix design is to balance the composition of material used in asphalt mixtures, such as aggregate and bitumen, in order to produce the asphalt mixtures with optimal properties such as high resistance to deformation, cracking and fatigue. The process, therefore, started with the selection of the appropriate standard specification. In this research, the standards used the most were the Main Roads Western Australia Standard and the Australian Standard.

The mix design results from the choice of aggregate type, gradation of aggregates, binder grades and the setting of binder content which will optimize the mechanical properties in relation to the desired behaviour in service. In this study, the focus was the involvement of bitumen content in mix design. According to the Shell Bitumen Handbook[18], the objective of mix design is to combine the use of economical materials with local resources while meeting the engineering requirements.

3.3.1 Criteria used to obtain optimum binder content

All of the mixtures were designed for high volume traffic (75 blows Marshall compaction). This study used the Marshall mix design as a method for determining the optimum asphalt content of unmodified asphalt mixtures based on Specification

504 [121]. It included several processes and decision points. Based on this specification, dense graded asphalt mixes were assessed in accordance with the standard procedure for the Marshall method of design as shown in Table 3-4 in order to find out the optimum binder content and to achieve the limiting values for various Marshall properties as shown in Table 3-5. In this research, the optimum binder content was determined as the binder content required for achieving an air void content of 5.0% at 75 blows Marshall compaction, where the air void range is between 4.0% and 6.0% in accordance with Specification 504[121] as shown in Table 3-5. A particle size distribution of dense graded asphalt mixture corresponding to Specification 504[121] as shown in Table 3-6 was chosen for all mixtures to maintain consistency for comparison purposes, as it was reported that the coarse aggregate ratio had an effect on the rutting performance of asphalt mixtures[124]. Range regions for binder content of 5.0%. 5.5%, and 6.0% were chosen to find out the optimum binder content.

Table 3-4. Design parameter for dense graded asphalt mixtures

Parameter	Standard
Maximum density of asphalt: Rice method	Test method WA 732.2
Bulk density and void content of asphalt	Test method WA 733.1
Stability and flow of asphalt : Marshall method	Test method WA 731.1

Table 3-5. Marshall properties for dense graded asphalt mixtures

Parameter	Value	
	Minimum	Maximum
Marshall stability	8.0 kN	-
Marshall flow	2.0 mm	4.0 mm
Air voids, Nominal 10 mm – Perth and	4.0%	6.0%
Voids in mineral aggregates, Nominal 10-mm	15.0%	-

Table 3-6. Particle size distribution for dense graded asphalt mixtures

Sieve size	Nominal 10mm Granite, percentage passing	
(mm)	Design mid-point	Upper-lower limit
13.20	100	100
9.50	97.5	95-100
6.70	83.0	78-88
4.75	68.0	63-73
2.36	44.0	40-48
1.18	28.5	25-32
0.600	21.0	18-24
0.300	14.5	12-17
0.150	10.0	8-12
0.075	4.0	3-5
Bitumen content (by percentage mass of whole mixture)		5.4% ± 0.3% (Class 170 Bitumen)
Hydrated lime (by percentage mass of total aggregate)		1.5% ± 0.5%

3.3.2 Maximum density of asphalt test

The objective of the maximum density of asphalt mixtures test based on the Rice method is to determine the maximum density of asphalt mixtures in a loose state free from occluded air by using the water displacement method in accordance with the WA standard 732.2-2011[125]. Maximum density is a critical asphalt mixture characteristic because it will be used to calculate the percentage of air voids in compacted asphalt mixtures.

a. Apparatus

The apparatus used to obtain the maximum density of asphalt mixtures consists of a pycnometer with 2L capacity, water bath, and vacuum pump as shown in Figure 3-6. The pycnometer will be connected to a vacuum pump.

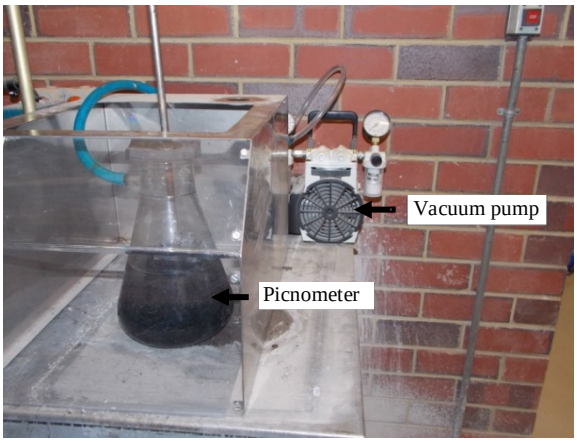

Figure 3-6. Apparatus used for maximum density test

b. Sample preparation

Three test portions of loose asphalt mixtures with a minimum mass of 1000 g for each portion, were prepared for each asphalt mixture with the binder content of of 5.0%, 5.5%, and 6.0%. Sample preparation for the maximum density test follows the WA standard 705.1[126]. A sample of a test portion for the maximum density test is shown in Figure 3-7.

c. Maximum density test results

The mean, standard deviation and coefficient of variation for the maximum density of asphalt mixtures over the range of binder content are presented in Table 3-7. The details of the maximum density of asphalt tests are presented in Appendix B1. It can be seen that a higher binder content resulted in a lower maximum density for the asphalt mixtures due to the decrease in aggregate content in the mixtures.

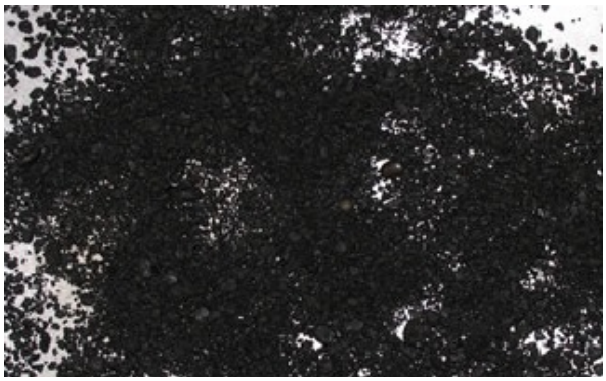

Figure 3-7. A test portion of loose asphalt mixtures for maximum density

Table 3-7. Results of the maximum density of asphalt mixtures test

Parameters	Binder content (%)								
	5.0			5.5			6.0		
	Mean	SD	CV (%)	Mean	SD	CV (%)	Mean	SD	CV (%)
Maksimum density (t/m^3)	2.475	0.001	0.02	2.449	0.002	0.06	2.442	0.001	0.05

3.3.3 Bulk density and void content of asphalt test

The objective of this test is to determine the bulk density, air voids, voids in mineral aggregates, and voids filled with bitumen in asphalt mixtures with a range of bonder contents, using the water displacement method in accordance with WA standard 733.1-2011[127].

a. Apparatus

The apparatus used to determine the bulk density of compacted asphalt mixtures based on the water displacement method consisted of a water bath and digital scale as shown in Figure 3-8.

Figure 3-8. Apparatus used for bulk density and binder content test

b. Sample preparation

The procedure employs Marshall compaction to fabricate the asphalt specimens using an automatic Marshall compactor as seen in Figure 3-9. Specimens in triplicate with dimension of 101.6±0.5 mm diameter and 57 - 70 mm height were compacted by applying 75 blows of the steel hammer with a weight of 4.535 kg falling freely from a height of 457 mm to each side of the specimen. The mould containing the compacted sample was removed from the compaction pedestal and the specimen was allowed to air cool before being removed from the mould. Triplicate specimens were prepared for each level of bitumen content.

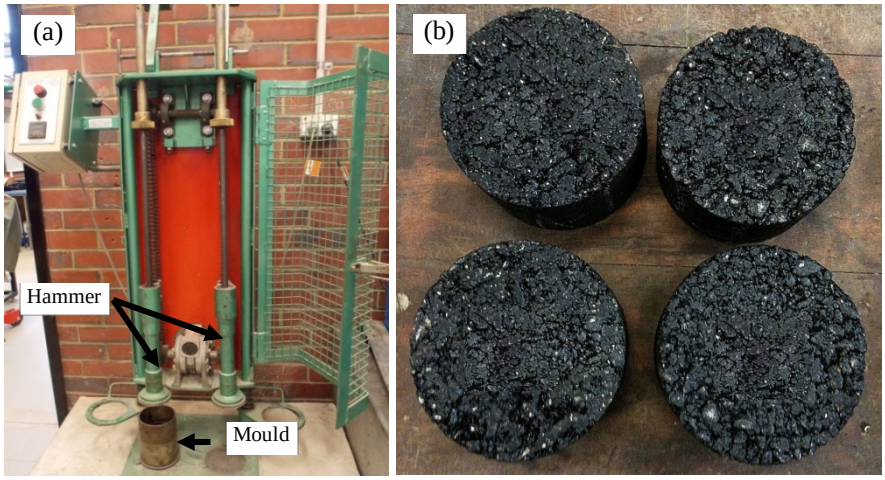

Figure 3-9. (a) Marshall compactor apparatus, and (b) compacted asphalt mixtures specimens

c. Bulk density and void content test results

The results of the bulk density and void content of asphalt test are presented in Table 3-8. It can be seen that a higher percentage of binder content resulted in less air voids (VIM), while by contrast, a higher percentage of binder content resulted in more voids in mineral aggregate (VMA) and voids filled with bitumen (VFB). The details of the bulk density and void content of asphalt tests are presented in Appendix B2.

Table 3-8. Results of bulk density and void content of asphalt mixtures test

Parameters	Binder content (%)								
	5.0			5.5			6.0		
	Mean	SD	CV (%)	Mean	SD	CV (%)	Mean	SD	CV (%)
VIM (%)	5.7	0.3	5.3	4.9	0.10	2.2	4.7	0.06	1.4
VMA (%)	17.0	0.26	1.6	17.3	0.09	0.5	18.2	0.06	0.3
VFB (%)	66.6	1.25	1.9	71.9	0.47	0.7	74.3	0.28	0.4

3.3.4 Stability and flow of asphalt test

The objective of the stability and flow of asphalt test based on the Marshall method is to determine the stability and flow value of asphalt mixtures in the laboratory in accordance with the WA standard 731.1-2010[128].

a. Apparatus

An automatic Marshall testing machine was used in this test to find out the stability and flow values of asphalt mixtures as shown in Figure 3-10.

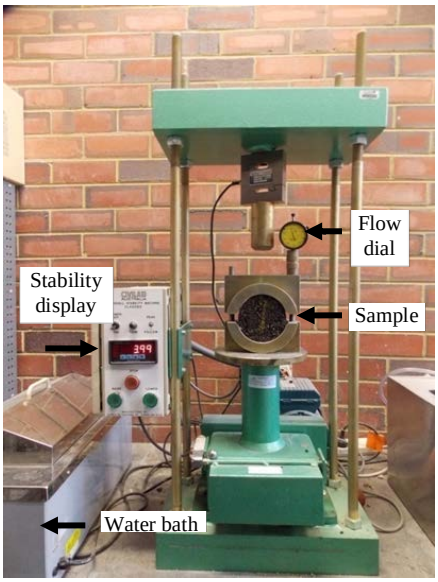

Figure 3-10. Automatic Marshall testing machine

b. Sample preparation

The stability and flow of asphalt test used the same specimens as for the bulk density and void content of asphalt test. The samples were put in a water bath at a temperature of 60±1 °C for 30 minutes. The samples were then removed from the water bath and placed centrally in the lower segment of the testing head. The upper segment of the testing head was placed on the test specimen and the complete assembly then placed in position in the testing machine. The base travelling at a rate of 48 - 54 mm/minute was then applied.

c. Stability and flow

The mean, standard deviation (SD), and coefficient of variation (CV) of the stability and flow test results over the range of binder content are presented in Table 3.9. The same values for stability and flow are illustrated in Figure 3-11. The detailed results of the stability and flow test are presented in Appendix B3. As shown in

Table 3-9, a higher percentage of binder content resulted in lower stability and a higher flow value.

Table 3-9. Results of stability and flow of asphalt test

Parameters	Binder content (%)								
	5.0			5.5			6.0		
	Mean	SD	CV (%)	Mean	SD	CV (%)	Mean	SD	CV (%)
Stability (kN)	12.04	0.07	0.5	10.04	0.12	1.2	8.75	0.21	2.3
Flow (mm)	3.33	0.16	4.8	3.69	0.04	1.1	5.03	0.47	9.4

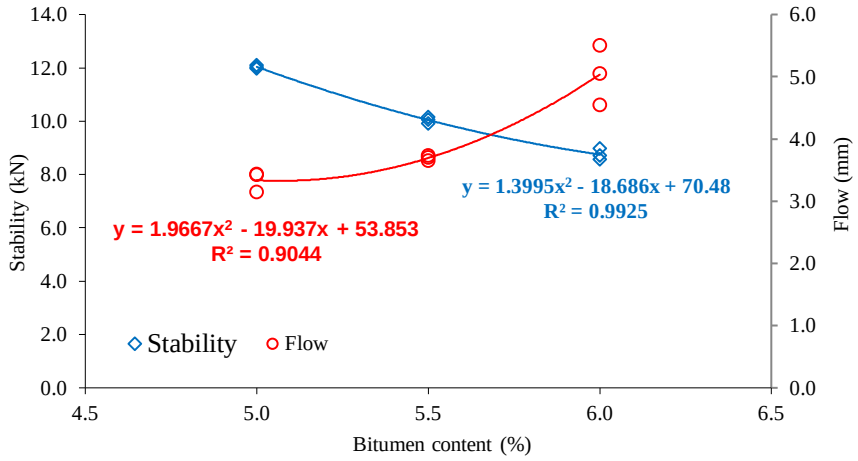

Figure 3-11. Stability and flow test results

3.3.5 Determination of optimum binder content

According to Specification 504[121], the optimum binder content (OBC) was defined as the amount of binder in asphalt mixtures required to achieve 5.0% air voids. The VIM values obtained from Section 3.3.3 were then plotted corresponding to the binder content as shown in Figure 3-12. Then, a VIM of 5.0% was chosen to give a binder content of 5.4% as the optimum binder content (by mass of asphalt mixture).

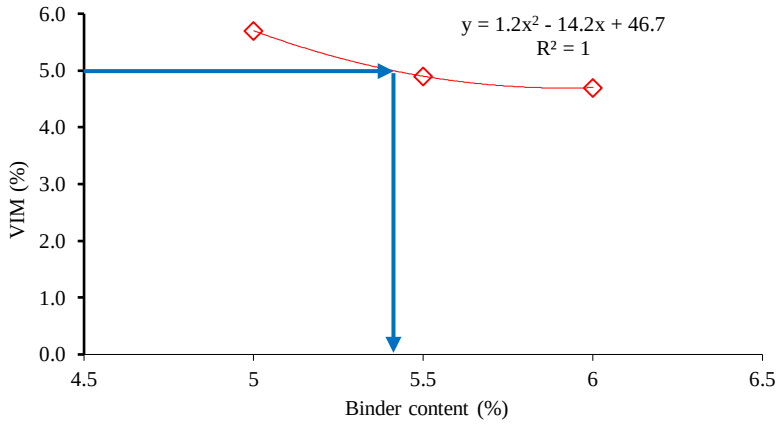

Figure 3-12. Determining the optimum binder content

Furthermore, three Marshall asphalt mixture specimens with 5.4% binder content and the same particle size distribution were prepared to address the Marshall properties satisfying the limits specified in Table 3.5. The results for the design parameter of 5.4% binder content are presented in Table 3.10 and the detailed results of the test are presented in Appendix B4.

Table 3-10. Design parameters for unmodified asphalt mixtures at OBC of 5.4%

Parameters	Value	SD	CV
Maximum density (t/m^3)	2.458	0.002	0.07
Stability (kN)	10.25	0.17	1.7
Flow (mm)	3.45	0.08	2.3
Air voids (%)	5.2	0.05	1.0
Voids in mineral aggregates (%)	17.3	0.05	0.3
Voids filled with bitumen (%)	69.8	0.23	0.4

3.4 Mix Design for BRA Modified Asphalt Mixtures

After the optimum bitumen content of the unmodified asphalt mixtures was determined, the BRA modified asphalt mixtures were designed to exhibit the benefits arising from mixing granular BRA modifier binder into the asphalt mixtures. Therefore, the same binder content as for unmodified asphalt mixtures was used for the BRA modified asphalt mixtures in order to maintain consistency for comparison purposes. Hence, the optimum binder content of 5.4% by weight of the total mixtures was also used for the BRA modified asphalt mixtures.

Table 3-11 shows the proportion of the base asphalt binder and the BRA modifier binder in unmodified and BRA modified asphalt mixtures, as well as the proportion of granular BRA (pellets) mixed into the mixtures. It can be seen in this table that three percentages of BRA natural binder, including 10%, 20% and 30% by total weight of asphalt binder, were chosen as a substitute for the base asphalt binder in the BRA modified asphalt mixtures. The BRA modified asphalt mixtures were designed according to the fact that 70% minerals and 30% natural binder (by total weight of materials) formed the granular BRA modifier binder as presented in Section 3.2.3.1.

Table 3-11. Proportion of materials used in asphalt mixtures

	Percentage by total weight of mixtures (%)			
	Unmodified asphalt mixtures	BRA Modified asphalt mixtures		
		10%	20%	30%
1. Total binder content	5.4	5.4	5.4	5.4
a. Base asphalt binder	5.4	4.9	4.3	3.8
b. BRA modifier binder	0.0	0.5	1.1	1.6
2. Total aggregate content	94.6	94.6	94.6	94.6
a. Crushed aggregate	94.6	93.3	92.1	91.0
b. BRA mineral	0.0	1.3	2.5	3.6
3. Granular BRA (Pellets) (%)	0.0	1.8	3.6	5.2

To focus on the contribution of granular BRA modifier binder, a range of different percentages of granular BRA modifier binder was used in a single mix composition to produce nominally identical mixes. Table 3-13 shows that in the BRA modified asphalt mixtures, the substitution of the base asphalt binder allowed the proportion of fines passing 2.36 mm to be adjusted. The total mass of crushed fine aggregate was decreased and replaced with the mineral contained in the granular BRA modifier with the aim of minimizing the variance in the gradation of aggregates. The percentage of crushed aggregate in the BRA modified asphalt mixture for dense graded 10 mm was decreased by increasing the percentage of granular BRA modifier binder.

3.4.1 Maximum density of BRA modified asphalt mixtures test

The objective of this test is to determine the maximum density of the BRA modified asphalt mixtures in a loose state free from occluded air by using the water displacement method in accordance with the WA standard 732.2-2011[125] for each BRA modifier binder content. Moreover, the maximum density of BRA modified asphalt mixtures is used to calculate the percentage of air voids in compacted BRA modified asphalt mixtures.

The apparatus used and the sample preparation for determining the maximum density of BRA modified asphalt mixtures were the same as presented in Section 3.3.2 and the results of this test are presented in Table 3-12. The details of the maximum density test of the BRA modified asphalt mixtures are presented in Appendix B5.

Table 3-12. Results of maximum density of BRA modified asphalt test

Parameters	10% BRA modified			20% BRA modified			30% BRA modified		
	Mean	SD	CV (%)	Mean	SD	CV (%)	Mean	SD	CV (%)
Max density (t/m^3)	2.454	0.002	0.09	2.456	0.001	0.05	2.464	0.02	0.10

Table 3-13. Final aggregate gradation used for unmodified and BRA modified asphalt mixtures

Sieve size (mm)	Unmodified mixtures[a]	BRA modified mixtures[b] composition									Lower-upper limit[c], Passing (%)
		10%			(20%)			30%			
	Crushed aggregate	Crushed aggregate	BRA mineral	Final	Crushed aggregate	BRA mineral	Final	Crushed aggregate	BRA mineral	Final	
13.20	100	100.0		100	100		100	100.0		100	100
9.50	97.5	97.5		97.5	97.5		97.5	97.5		97.5	95-100
6.70	83.0	83.0		83.0	83.0		83.0	83.0		83.0	78-88
4.75	68.0	68.0		68.0	68.0		68.0	68.0		68.0	63-73
2.36	44.0	44.0	100	44.0	44.0	100	44.0	44.0	100.0	44.0	40-48
1.18	28.5	28.5	100.0	28.5	28.6	99.9	28.5	28.6	99.9	28.5	25-32
0.600	21.0	21.1	99.9	21.0	21.2	99.8	21.0	21.3	99.7	21.0	18-24
0.300	14.5	14.8	99.7	14.5	15.0	99.5	14.5	15.2	99.3	14.5	12-17
0.150	10.0	10.5	99.5	10.0	11.0	99.0	10.0	11.5	98.5	10.0	8-12
0.075	4.0	4.9	99.1	4.0	5.7	98.3	4.0	6.4	97.6	4.0	3-5
Proportion[d] (%)	100	98.6	1.4		97.4	2.6		96.2	3.8		

[a] : The gradation used for unmodified asphalt mixtures as a target gradation in the middle point of limit values.

[b] : The gradation used for BRA modified asphalt mixtures in three different percentages of BRA modifier binder (by weight of total asphalt binder).

[c] : Limit values in accordance with Specification 504[121]

[d] : Proportion of crushed aggregate and BRA mineral remaining in the asphalt mixtures (by weight of total aggregate

3.5 Experimental

3.5.1 Determining the resilient modulus of asphalt mixtures

Indirect tensile stiffness modulus (ITSM) tests were performed to determine the resilient modulus of unmodified and BRA modified asphalt mixtures based on standard AS 2891.13.1-1995[129].

The determination of the resilient modulus was divided into two stages. The purpose of the first stage was to record the effect on the stiffness modulus of asphalt mixtures of using three percentages (10%, 20% and 30%) of granular BRA modifier binder as described in Section 3.4, compared to unmodified asphalt mixtures. In this stage, the specimens were tested under the standard conditions. The purpose of the second stage was to find out the effect of temperature, rise time and pulse period on the unmodified and BRA modified asphalt mixtures. Hence, in the second stage, the unmodified and BRA modified asphalt mixtures specimens were tested under different conditions of temperature, rise time and pulse period. However, for the second stage, mixtures contained only 20% BRA modifier binder.

a. Apparatus

ITSM tests were performed using a universal testing machine (UTM 25) as shown in Figure 3-13. The apparatus is a servo hydraulic testing machine designed and built to IPC Global's specifications, and is capable of applying an approximately triangular shaped or haversine load pulse with a rise time in the range of 0.025 s to 0.1 s. The apparatus is also provided with a temperature controlled chamber that is capable of holding the loading frame and a dummy specimen for indicating the temperature in the core and skin of the specimens and allowing for analysis on materials to be performed at non ambient temperatures.

b. Sample preparation

The specimens were cylindrical with dimension of 100±2 mm in diameter and 35 - 70 mm in height, prepared according to the standard AS 2891.13.1-1995[129]. Based on the target height of the specimen (65 mm), the weight of the loose asphalt mix was calculated using Equation 3-1. Related to the proportion of materials as shown in Table 3-11, the weight of materials was calculated and the results are presented in Table 3-14.

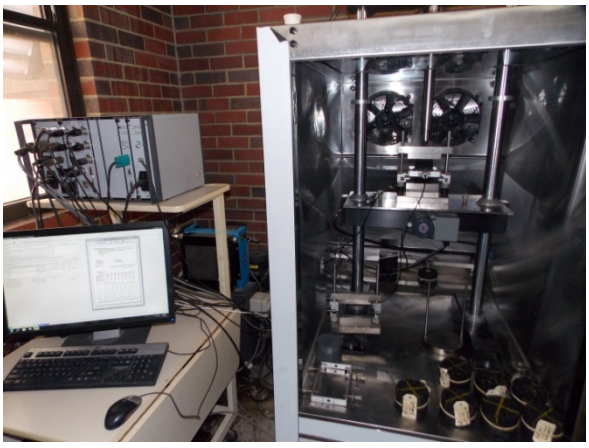

Figure 3-13. UTM-25 equipment used for ITSM testing

Further, related to the gradation of crushed aggregate and BRA mineral as shown in Table 3-12, the weight of crushed aggregates and BRA minerals on each sieve size were calculated and the results are presented in Table 3-15.

$$\text{Weight of asphalt mixtures} = \tfrac{1}{4}\pi.(d^2).\,h.\,\rho_{max}.(100\text{-VIM}) \quad (3\text{-}1)$$

where d : Diameter of the sample (cm)

h : Height of the sample (cm)

ρ_{max} : Maximum density of asphalt mixtures (t/m^3)

VIM : Target of voids in mixtures (%)

Table 3-14. Weight of materials used for ITSM test

	Unmodified asphalt mixtures	BRA modified		
		10%	20%	30%
1. Weight of loose asphalt mixtures[1] (g)	1192.6	1190.6	1191.5	1195.48
a. Weight of base asphalt binder[2] (g)	64.4	58.3	51.2	45.4
b. Weight of BRA modifier binder[2] (g)	0.0	6.0	13.1	19.1
c. Weight of crushed aggregate[2] (g)	1128.2	1110.8	1097.4	1087.9
d. Weight of BRA mineral[2] (g)	0.0	15.5	29.8	43.0
2. Weight of granular BRA (pellets) (g)	0.0	21.5	42.9	62.1

[1] Obtained from Equation 3.1, with d=10 cm; h=6.5 cm; target VIM=5.0; and ρ_{max} obtained from Table 3-10 and Table 3-13

[2] Proportion of materials obtained from Table 3.11

After each size of crushed aggregates had been weighed, they were then blended manually in a pan and then heated in an oven at a temperature of 105ºC for 24 hours. After that, the blend aggregates were heated in the same oven at 150ºC prior to mixing with asphalt binder for approximately two hours.

Table 3-15. Weight of crushed aggregates and BRA minerals used for ITSM tests

Sieve size (mm)	Weight of materials (g)							
	Unmodified		BRA modified (10%)		BRA modified (20%)		BRA modified (30%)	
	Crushed Agg.	BRA mineral	Crushed Agg.	BRA mineral	Crushed Agg.	BRA mineral	Crushed Agg	BRA mineral
13.20	0.0		0.0		0.0		0.0	
9.50	28.2		28.2		28.2		28.3	
6.70	163.6		163.3		163.5		164.0	
4.75	169.2		168.9		169.1		169.6	
2.36	270.77	0.00	270.31	0.00	270.54	0.00	271.43	0.00
1.18	174.87	0.00	174.11	0.46	173.83	0.89	174.01	1.29
0.600	84.61	0.00	83.70	0.77	83.05	1.49	82.67	2.15
0.300	73.33	0.00	71.51	1.70	69.99	3.28	68.78	4.73
0.150	50.77	0.00	47.59	3.10	44.77	5.96	42.28	8.61
0.075	67.69	0.00	63.71	3.87	60.19	7.45	57.10	10.76
Pan	45.13	0.00	39.48	5.57	34.37	10.72	29.74	15.49
Total	1,128.2	0.00	1,110.8	15.5	1,097.4	29.8	1,087.9	43.0

In the other side, the base asphalt binder and granular BRA modifier binder (pellets) were placed in the same bowl. The mixture was then put in an oven at a temperature of 150±5 ºC for 30 to 60 minutes with frequent manual stirring intended to blend and incorporate the two binders as BRA modified binder.

Then the previously blended aggregates were put in the same bowl as the BRA modified binder and mixed using mixing equipment for 1.5 minutes. Laboratory mixtures were prepared based on the procedure for sampling loose asphalt described in AS 2891.1.1-2008[130], and then were immediately compacted. Figure 3-14 shows the blended aggregate used for asphalt mixtures and loose asphalt mixtures prior to mixes.

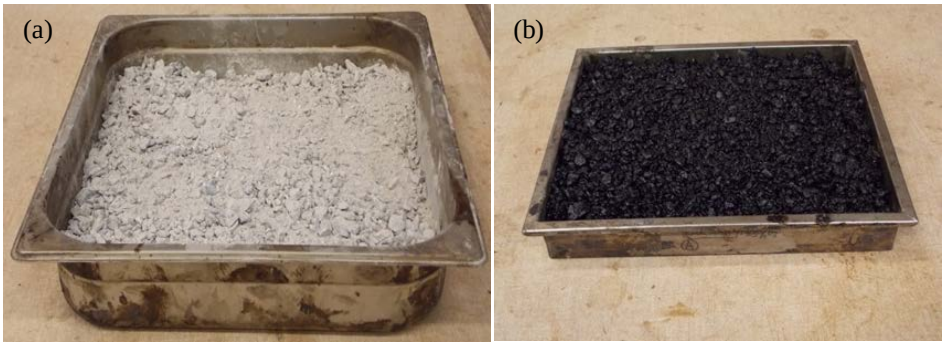

Figure 3-14. Preparation of specimen, (a) aggregate blended, (b) loose asphalt mixtures

The compactions were done using a gyratory compactor, as set out in AS 2891.2.2-1995[131], carries out at an angle of 2º angle and 240 kPa vertical loading stress. By controlling the mass added to the mould, samples were produced with approximately the same dimensions and air void content. The number of gyrations

was set at the required value to obtain a target void content of 5±0.5%. Any samples outside this range were rejected. According to the standard, a test result comprises the mean of calculated from values obtained from three cylinders. In total twelve specimens were tested for the first stage (three identical specimens for each percentage of BRA modifier binder) and thirty specimens were tested for the second stage (three identical specimens for each test temperature).

c. Indirect tensile stiffness modulus test

The equipment cabinet was used to bring the specimens to the required test temperature before each test was performed, to allow the temperature in the specimen to reach equilibrium. A dummy specimen in the cabinet was used to record the equilibrium temperature. Normally, the specimens were placed in the cabinet for at least two hours to reach temperature equilibrium.

The ITSM test was non-destructive where the compressive load pulse with haversine or other waveforms was applied vertically in the vertical diameter of a cylindrical specimen through a curved loading strip. The resulting horizontal recoverable deformation was measured by attaching two linear variable differential transformers (LVDT) at the mid thickness at each end of the horizontal diameter. The test frame according to UTM 25 is shown in Figure 3-15. Initially, the application of five pulses of load at a required rise time to the peak load and at a required pulse period was performed for a conditioning test. The average of a further five load pulses was then used to calculate the measured resilient modulus of the asphalt mixtures. The resilient modulus (E) for each load pulse was determined by using Equation 3-2[129]. The resume of test conditions for the first and second stage is presented in Table 3.16.

$$E = P \times \frac{(\nu + 0.27)}{(H \times h_c)} \qquad (3\text{-}2)$$

where E : resilient modulus (MPa)

P : peak load (N)

ν : Poisson ratio

H : recovered horizontal deformation of specimen after application of load (mm)

h_c : height of the specimen (mm)

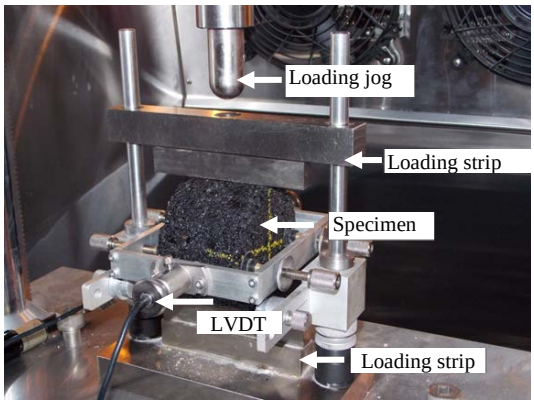

Figure 3-15. Set-up for the ITSM test

Table 3-16. Test conditions for the first and second stages of the ITSM test

Parameters	First stage	Second stage
Test temperature, °C	25 ± 0.5	5, 15, 25, 40, 60 ± 0.5
Rise time t_u (10% to 90%), ms	40 ± 5	40, 60, 80 ± 5
Pulse repetition period (10% to 10%), ms	3000 ± 5	1000, 2000, 3000 ± 5
Recovered horizontal strain, με	50 ± 20	50 ± 20
Air voids, %	5 ± 0.5	5 ± 0.5
Content of BRA modifier binder, %	0, 10, 20, 30	20

The loading conditions are illustrated in Figure 3-16. During the testing, the time taken for the applied load to increase from 10% to 90% was defined as the rise time. The load pulse (pulse repetition period) was defined as the period between the 10% of the load application and the 10% of the next load application.

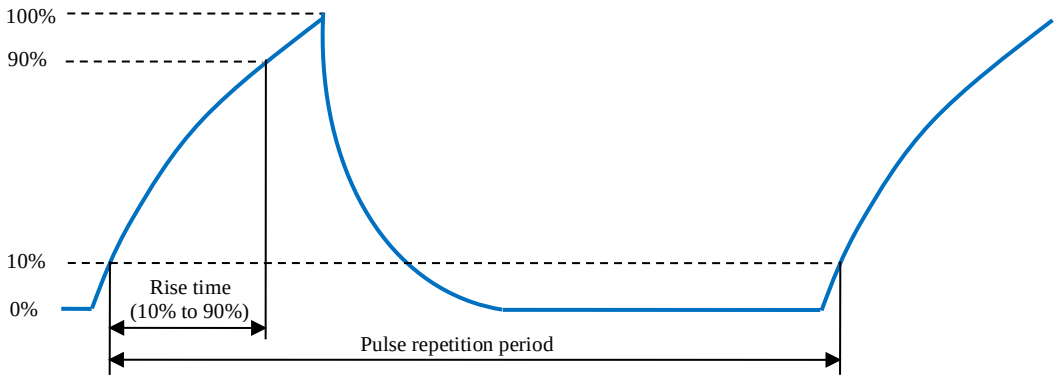

Figure 3-16. Force and horizontal deformation pulse shapes

3.5.2 Determining the permanent compressive strain of asphalt mixtures

Dynamic creep tests were performed to determine the permanent compressive strain characteristics of unmodified and BRA modified asphalt mixtures according to standard AS 2891.12.1-1995[132]. In this test, BRA modified asphalt mixtures were formed by substituting the base asphalt binder with 10%, 20%, and 30% BRA

modifier binder (by weight of total asphalt binder) containing granular BRA modifier binder as presented in Section 3.4.

a. Apparatus

Dynamic creep tests were performed using UTM 25 equipment which is the same equipment used for the ITSM tests.

b. Sample preparation

Cylindrical specimens of 100±2 mm in diameter and 50±2 mm in height were prepared in accordance with the standard[132]. However, the height of the specimens was set at 65 mm in order to calculate the weight of loose asphalt mix using Equation 3.1. Further, the height of the specimens after compacting was trimmed to a final height of 50±2 mm using a diamond saw on the top and bottom faces to make them smooth.

The results of the weight of the materials and the weight of the crushed aggregates and BRA minerals on each size used for the unmodified and BRA modified asphalt mixtures are the same as those presented in Table 3-14 and Table 3-15, respectively. The procedures for preparing and heating blended aggregates, mixing, and compacting asphalt mixtures are the same as those presented in Section 3.5.1.

The compactions also used a gyratory compactor, as set out in AS 2891.2.2-1995[131], carried out at an angle of 2º and 240 kPa vertical loading stress. The mass of loose mix added to the mould was controlled to produce approximately the same dimension and air void content. The number of gyrations was set at the required value to obtain a target air void content of 5±0.5%. Any samples with a void content outside this range were rejected. Triplicate specimens were prepared for each asphalt mixture.

c. Dynamic creep test

A specimen was placed between two platens before testing was carried out and was then put inside the equipment cabinet at the required test temperature of 50±0.5°C for about two hours to allow the specimen temperature to reach equilibrium. Following that, the specimens were exposed to uniaxial and periodically repeated loading using an upper platen under the test conditions listed in Table 3-17, until the test was terminated at 30,000 maximum cyclic counts or 3% accumulative axial strain. The test frame according to UTM-25 is shown in Figure 3-17. This an

hydraulic testing machine applying a rectangular shaped load pulse through a hemispherical ended loading ram for 0.5±0.05 s hold time with a peak load equivalent to an applied compressive stress of 200±5 kPa and then removing the load and resting for a period of 1.5±0.5 s before the application of the next pulse.

Table 3-17. The test conditions of the dynamic creep test

Parameters	Values
Air voids	5±0.5%
Test temperature	50±0.5°C
Compressive stress	200±5 kPa
Loading period (t_1)	0.5±0.05 s
Pulse repetition period (t_p)	2.0±0.05 s

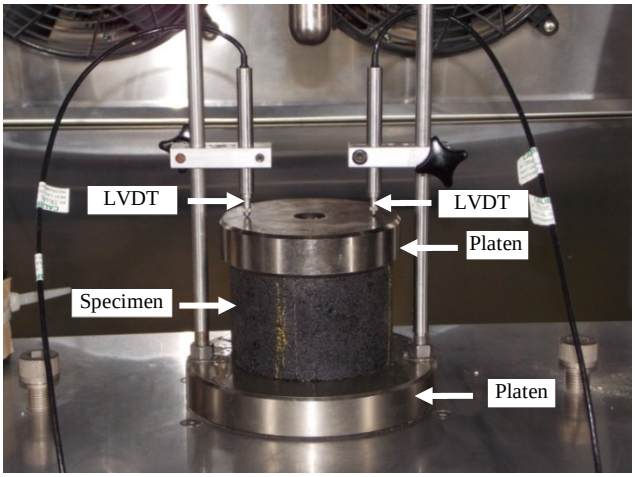

Figure 3-17. The set-up of dynamic creep test

3.5.3 Determining the rutting performance of asphalt mixtures

Wheel tracking machine (WTM) tests were performed to determine the rutting performance of unmodified and BRA modified asphalt mixtures based on the Austroads standard AG:PT/T231[54]. BRA modified mixtures were made by substituting the base asphalt binder with 10%, 20%, and 30% BRA modifier binder (by weight of total asphalt binder) containing granular BRA modifier binder as described in Section 3.4.

a. Apparatus

The WTM tests were performed using a relatively simple testing apparatus as illustrated in Figure 3-18. The apparatus consists of a loaded wheel that bears the specimen held on a moving table. A vertical load is applied to the top of a specimen with a 200 mm diameter wheel. This is a steel wheel with a thick, smooth rubber tread and a width of 50 mm. The table oscillates beneath the loaded wheel and a

displacement measuring device is provided that measures the vertical depth of the rut as it develops continuously. When the termination conditions are reached the test is completed.

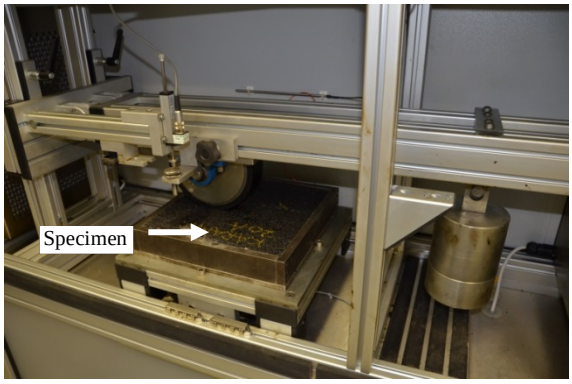

Figure 3-18. Set-up of wheel tracking test

b. Sample preparation

The specimens consisted of slabs with dimension of 300 mm in length, 300 mm in width, and 50 mm in height prepared in accordance with the Austroads Standard[54]. The total weight of the loose asphalt mixtures was calculated using Equation 3-3. The weight of the materials and the weight of the crushed aggregate and BRA mineral of each size used for the unmodified and BRA modified asphalt mixtures are presented in Table 3-18 and Table 3-19, respectively.

$$\text{Weight of asphalt mixtures} = l \times w \times h \times \rho_{max} \times (100 - \text{VIM}) \quad (3\text{-}3)$$

where: l : length of the sample (cm)

w : width of the sample (cm)

h : height of the sample (cm)

ρ_{max} : maximum density of asphalt mixtures (ton/m^3)

VIM : target of voids in mixtures (%)

Table 3-18. Weight of materials used for the WTM tests

	Asphalt mixtures			
	Unmodified	BRA 10%	BRA 20%	BRA 30%
1. Weight of loose asphalt mixtures[1]	10508.0	10490.9	10499.4	10533.6
a. Weight of base asphalt binder[2]	567.4	514.1	451.5	400.3
b. Weight of BRA modifier binder[2]	0.0	52.5	115.5	168.5
c. Weight of crushed aggregate[2]	9940.5	9788.0	9669.9	9585.6
d. Weight of BRA minerals[2]	0.0	136.4	262.5	379.2
2. Weight of granular BRA (pellets)	0.0	188.8	378.0	547.7

[1] Obtained from Equation 3.3 with l=30 cm; w=30.5 cm; h=5.0 cm, target VIM=5.0%, and ρ_{max} obtained from Table 3-10 and 3-13.

[2] Proportion of materials obtained from Table 3-11

The procedures for preparing and heating blended aggregate and mixing asphalt mixtures were the same as the procedure presented in Section 3.5.1. The loose asphalt mixtures were then immediately compacted in the slab mould by using a roller compactor in accordance with Austroads AG:PT/T220[133] as seen in Figure 3-20. After 24 hours prior to the compaction process, the slab was put in the apparatus cabinet to be tested. Triplicate samples were prepared for unmodified and BRA modified asphalt mixtures.

Table 3-19. Weight of crushed aggregate and BRA minerals used for the WTM test

Sieve size (mm)	Weight of materials (g)							
	Unmodified		BRA modified (10%)		BRA modified (20%)		BRA modified (30%)	
	Crushed Agg.	BRA mineral	Crushed Agg.	BRA mineral	Crushed Agg.	BRA mineral	Crushed Agg	BRA mineral
13.20	0.0		0.0	0.0	0.0	0.0	0.0	0.0
9.50	248.5		248.1	0.0	248.3	0.0	249.1	0.0
6.70	1441.4		1439.0	0.0	1440.2	0.0	1444.9	0.0
4.75	1491.1		1488.7	0.0	1489.9	0.0	1494.7	0.0
2.36	2385.7	0.00	2381.8	0.0	2383.8	0.0	2391.5	0.0
1.18	1540.8	0.00	1534.2	4.1	1531.7	7.9	1533.2	11.4
0.600	745.5	0.00	737.5	6.8	731.8	13.1	728.4	19.0
0.300	646.1	0.00	630.1	15.0	616.7	28.9	606.0	41.7
0.150	447.3	0.00	419.3	27.3	394.5	52.5	372.6	75.8
0.075	596.4	0.00	561.4	34.1	530.3	65.6	503.1	94.8
Pan	397.6	0	347.9	49.1	302.8	94.5	262.1	136.5
Total	9940.5	0.00	9788.0	136.4	9669.9	262.5	9585.6	379.2

c. Wheel tracking test

Before testing was started, the specimen was put in the device cabinet at the required test temperature of 60°C for about two hours to allow the specimen temperature to reach equilibrium. The tests were then performed until the wheel travelling stopped automatically after reaching 10,000 loading passes. The test conditions are presented in Table 3-20. The behaviour of asphalt mixtures is generally expressed in term of the number of load repetitions the materials is able to carry before acceptable level of permanent deformations. The results of the test shows that test temperature had significant influence on permanent deformations. Increase in temperature leads to more increase in permanent deformations[36, 134]. Air voids are needed to ensure compliance with the desired criteria.

Table 3-20. Test conditions for WTM tests

Parameter	Test condition
Test temperature, ºC	60 ± 1.0
Sample thickness, mm	50 ± 5.0
Air void content, %	5 ± 0.5
Vertical load, N	700 ± 20

3.5.4 Determining the fatigue life of compacted of asphalt mixtures

Repeated flexural bending tests were performed to determine the fatigue life of compacted asphalt mixtures in accordance with Austroads standard AG:PT/T233[90]. In this test, the BRA modified binder used for BRA modified asphalt mixtures was made by replacing 20% base asphalt binder (by total weight of asphalt binder in the mixtures) with 20% BRA natural binder.

a. Apparatus

Repeated flexural bending tests were performed using a servo-pneumatic four point bending apparatus as illustrated in Figure 3-19. The apparatus consists of a pneumatically powered loading system, a beam cradle and an environmental chamber IMACs integrated multi-axis system and Windows application software. The beam cradle is designed to subject an asphalt beam specimen with backlash-free rotation and horizontal translation of all load and reaction points.

Figure 3-19. Four point bending apparatus

b. Sample preparation

The specimens consisted of slabs of 400 mm in length, 305 mm in width and 75 mm in height prepared in accordance with Austroads standard AG:PT/T233[90]. The total weight of the loose asphalt mixtures was calculated using Equation 3-3. The weight of the materials and the weight of the crushed aggregates and BRA minerals of each size for unmodified and BRA modified asphalt mixtures are presented in Table 3-21 and Table 3-22, respectively.

Table 3-21. Total weight of materials used for the flexural bending test

	Asphalt mixtures	
	Unmodified	BRA modified (20%)
1. Weight of loose asphalt mixtures[1] (g)	21366.2	21348.8
a. Weight of base asphalt binder[2] (g)	1153.8	918.0
b. Weight of BRA modifier binder[2] (g)	0.0	234.8
c. Weight of crushed aggregate[2] (g)	20212.4	19662.3
d. Weight of BRA mineral[2] (g)	0.0	533.7
2. Weight of granular BRA (pellets) (g)	0.0	768.6

[1] Obtained from Equation 3.3 with l=40 cm; w=30.5 cm; h=7.5 cm, and ρ_{max} obtained from Table 3-10 and 3-13.

[2] Proportion of materials obtained from Table 3-11.

Table 3-22. Weight of crushed aggregates and BRA minerals for the flexural bending test

Sieve size (mm)	Weight of materials (gr)			
	Unmodified		BRA modified (20%)	
	Crushed Aggregate	BRA mineral	Crushed Aggregate	BRA mineral
13.20	0.0		0.0	
9.50	505.3		504.9	
6.70	2930.8		2928.4	
4.75	3031.9		3029.4	
2.36	4850.98	0.00	4847.03	0.00
1.18	3132.93	0.00	3114.36	16.01
0.600	1515.93	0.00	1488.01	26.69
0.300	1313.81	0.00	1254.03	58.71
0.150	909.56	0.00	802.07	106.74
0.075	1212.75	0.00	1078.33	133.43
Pan	808.50	0.00	615.70	192.14
Total	20212.4	0.00	19662.345	533.7

The procedures for preparing and heating the blended aggregates, and mixing and compacting the asphalt mixtures were as the same as the procedure presented in Section 3.5.1. Laboratory mixtures were prepared based on the procedure for sampling loose asphalt described in AS 2891.1.1-2008[130], and then were immediately compacted in a slab mould by using a roller compactor as seen in Figure 3-20 in accordance with Austroads standard AG:PT/T220[133].

After 24 hours prior to the compaction process, the slabs were then cut to produce the final beam specimens with dimensions of 390±5 mm in height, 50±5 mm in depth and 63.5±5 mm in width as illustrated in Figure 3-21. Triplicate specimens were prepared for each test condition.

c. Repeated flexural bending test

Before each test was started, the specimen was placed inside the device cabinet for two hours to ensure that the temperature recorded during the test was the temperature of the test specimen and to maintain the temperature during the test.

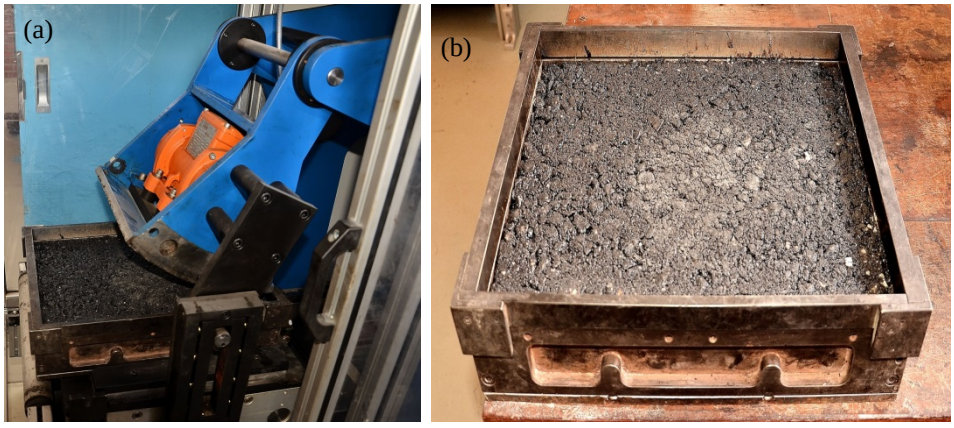

Figure 3-20. Compaction process for the slabs for the flexural bending test

Figure 3-21. Final beam specimens

Then the specimen was placed in the loading frame cradle and clamped at the four points to hold the specimen in place as seen in Figure 3-22. After being clamped and before the test was run, the specimen was left for a minimum of 30 minutes to enable the specimen clamping stress to be relieved. The tests were performed under the strain-controlled mode of loading under the test conditions presented in Table 3-23. The deflection at the centre of the beam was measured with a linear variable differential transformer. Initially, an application of 50 load cycles was used to determine and calculate the initial flexural stiffness.

Table 3-23. Test conditions for the repeated flexural bending test

Parameter	Test condition
Test temperature, ºC	20 ± 0.5
Loading frequency, Hz	10 ± 0.1
Mode of loading	Continuous haversine
Peak tensile strain, με	400, 600, 800
Air void content, %	5± 0.5

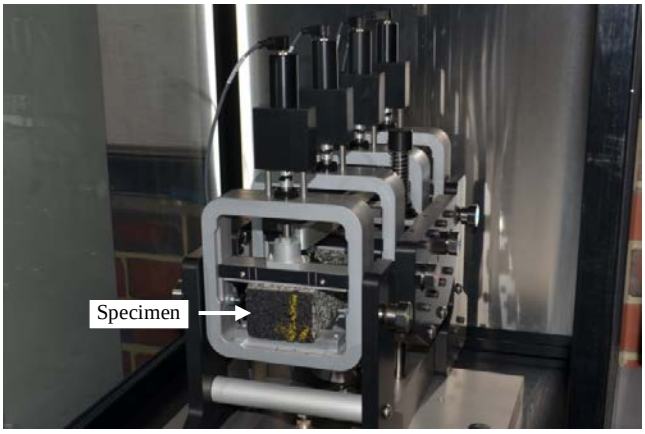

Figure 3-22. The set-up of the repeated flexural bending test

3.5.5 Determining the dynamic modulus of asphalt mixtures

The asphalt mixture performance tester (AMPT) tests were performed to measure the dynamic modulus and phase angle of unmodified and BRA modified asphalt mixtures under a range of temperatures and loading frequencies according to the specifications of the American Association of State Highway Transportation Officials (AASHTO) Designation: T342-11 Determining Dynamic Modulus of Hot Mix Asphalt (HMA)[135]. In this test, BRA modified asphalt mixtures were made by substituting the base asphalt binder with 10%, 20%, and 30% BRA modifier (by weight of total asphalt binder) as detailed in Section 3.4.

a. Apparatus

The AMPT servo hydraulic apparatus manufactured by IPC Global, illustrated in Figure 3-23, was used in this test. It consists of an environmental chamber for conditioning specimens to the desired testing temperature, a high performance hydraulic actuator and digital control and data acquisition system.

Figure 3-23. AMPT test equipment

b. Sample preparation

Dynamic modulus testing was performed on test specimens cored from gyratory 150 mm compacted mixtures. The specimens were prepared according to the procedure for sampling loose asphalt described in standard AS 2891.1.1-2008[130]. The total weight of the loose asphalt mixtures was also calculated by using Equation 3-1. The weights of the materials used for unmodified and BRA modified asphalt mixtures are presented in Table 3-24 and Table 3-25. The procedures used for preparing and heating blended aggregate and mixing asphalt mixtures were the same as those described in Section 3.5.1. All specimens were compacted with a Servopac Gyratory Compactor, over a gyratory angle of 3° and vertical loading stress of 240 kPa to a height of 170 mm.

24 hours after the compaction process, the specimens were cored to produce the final cylindrical specimen as illustrated in Figure 3-24. The final diameter and height of the specimen were 100 mm and 150 mm, respectively. Dynamic modulus specimens in triplicate were fabricated for unmodified and BRA modified asphalt mixtures.

Table 3-24. Total weight of materials used for the AMPT test

	Unmodified	BRA modified		
		10%	20%	30%
1. Weight of loose asphalt mixtures[1] (g)	7017.8	7006.4	7012.1	7034.9
a. Weight of base asphalt binder[2] (g)	379.0	343.3	301.6	267.3
b. Weight of BRA modifier binder[2] (g)	0.0	35.0	77.1	112.5
c. Weight of crushed aggregate[2] (g)	6638.8	6537.0	6458.1	6401.8
d. Weight of BRA mineral[2] (g)	0.0	91.1	175.3	253.3
2. Weight of granular BRA (pellets) (g)	0.0	126.1	252.4	365.8

[1] Obtained using Equation 3.1, with d=150 mm, h=170 mm, target VIM = 5.0%, and ρ_{max} obtained from Table 3-10 and 3-13.

[2] Proportion of materials obtained from Table 3-11.

Table 3-25. Weight of crushed aggregates and BRA minerals used for the AMPT test

Sieve size (mm)	Weight of materials (g)							
	Unmodified		BRA modified (10%)		BRA modified (20%)		BRA modified (30%)	
	Crushed Agg.	BRA mineral	Crushed Agg.	BRA mineral	Crushed Agg.	BRA mineral	Crushed Agg	BRA mineral
13.20	0.0		0.0	0.0	0.0	0.0	0.0	0.0
9.50	166.0		165.7	0.0	165.8	0.0	166.4	0.0
6.70	962.6		961.1	0.0	961.8	0.0	965.0	0.0
4.75	995.8		994.2	0.0	995.0	0.0	998.3	0.0
2.36	1593.3	0.00	1590.7	0.0	1592.0	0.0	1597.2	0.0
1.18	1029.0	0.00	1024.6	2.7	1022.9	5.3	1023.9	7.6
0.600	497.9	0.00	492.5	4.6	488.7	8.8	486.5	12.7
0.300	431.5	0.00	420.8	10.0	411.9	19.3	404.7	27.9
0.150	298.7	0.00	280.0	18.2	263.4	35.1	248.8	50.7
0.075	398.3	0.00	374.9	22.8	354.2	43.8	336.0	63.3
Pan	265.6	0.00	232.3	32.8	202.2	63.1	175.0	91.2
Total	6638.8	0.00	6537.0	91.1	6458.1	175.3	6401.8	253.3

c. AMPT test

The loading configuration for the sample is shown in Figure 3-25. The specimen was prepared by attaching three mounting studs for the axial LVDTs to the sides of the specimen with epoxy cement. Before testing was started, the test specimen was conditioned in the equipment chamber and allowed to equilibrate to the specified testing temperature. Minimum equilibrium temperature times are provided in Table 3-26. The tests were performed at four different temperatures and ten loading frequencies (listed in Table 3-27) in order to develop a master curve for use in the pavement response and performance analysis.

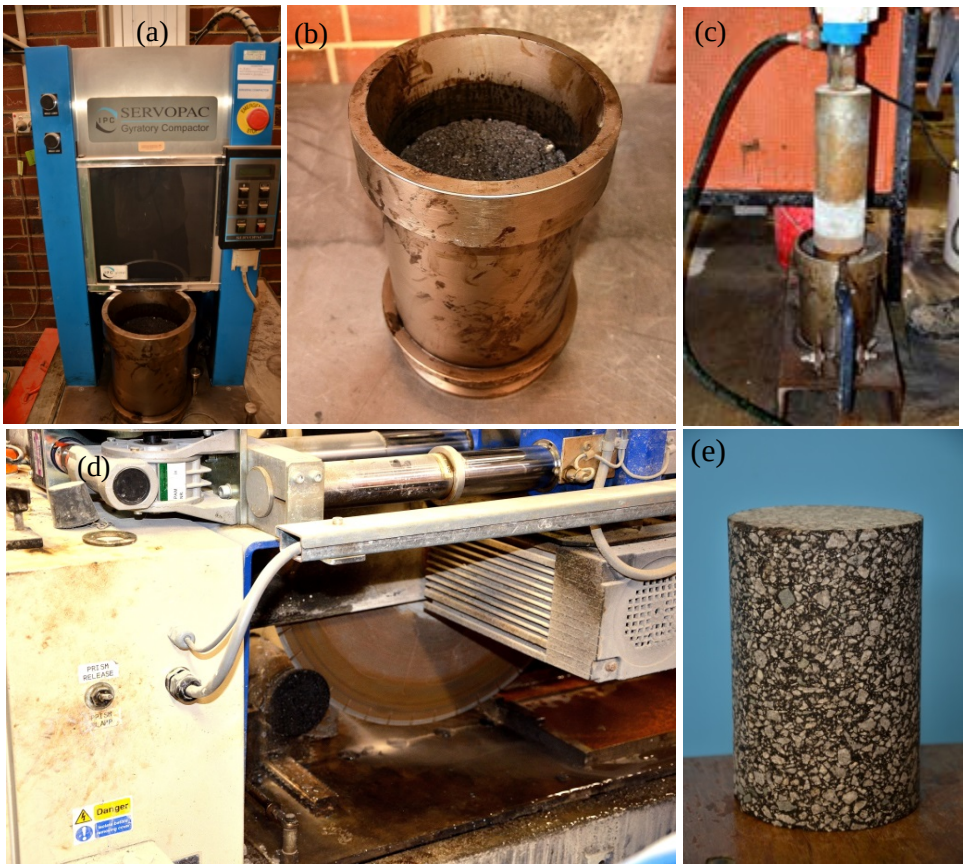

Figure 3-24. Dynamic modulus specimen preparation: (a) compaction, (b) after compaction, (c) coring processes, (d) cutting process, and (e) final form of specimen

Table 3-26. Equilibrium times for dynamic modulus test [135]

Specimen temperatures (°C)	Time from room temperature 25°C, h	Time from previous test temperature, h
4.4	Overnight	4 h or overnight
21.1	1	3
37.8	2	2
54.0	3	1

Table 3-27. Test conditions for dynamic modulus test

Test temperatures (°C)	4.4, 21.1, 37.8, and 54.0
Loading frequencies (Hz)	0.01, 0.1, 0.2, 0.5, 1.0, 2.0, 5.0, 10, 20, and 25
Mode of loading	Haversine
Air void content	5±0.5%

The test combinations of temperature and loading frequency began with the lowest temperature and proceeded to the highest. Testing at a given temperature began with the highest loading frequency and proceeded to the lowest. Dynamic modulus testing was performed under conditions of unconfined uniaxial compression and the specimens were subjected to sinusoidal (haversine) axial compressive stress over the range of temperatures and frequencies. Dynamic modulus and phase angle values for each loading frequency at a test temperature were computed automatically after the application of 10 conditioning cycles, and this was immediately followed by the application of 10 test cycles at the same frequency.

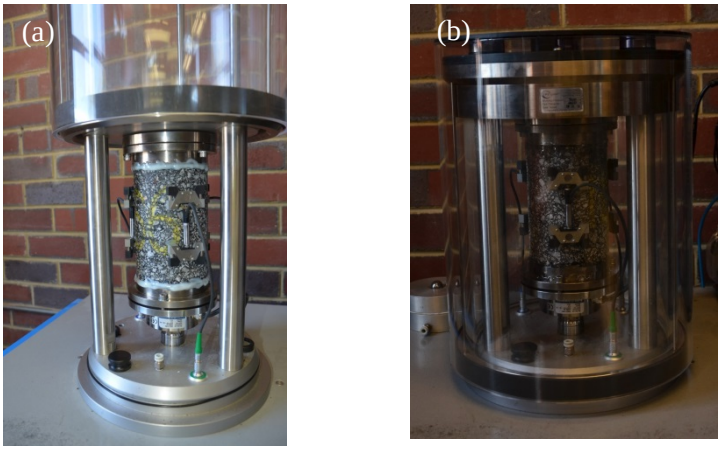

Figure 3-25. The set-up of the dynamic modulus test, (a) preparation of the axial LVDTs, (b) specimens were conditioned in the chamber

CHAPTER 4

EVALUATION OF THE EFFECT OF GRANULAR BRA MODIFIER BINDER ON THE RESILIENT MODULUS OF ASPHALT MIXTURES

4.1 Introduction

A good understanding of the resilient modulus characteristics of BRA modified asphalt mixtures is important when considering the benefits of using BRA modifier binder in asphalt mixtures. As discussed in Section 2.4.1, the resilient modulus is an important parameter for studying the potential elastic properties of asphalt mixtures and is used as an input for modelling and predicting the life of a pavement.

The objective of Chapter 4 is therefore to analyze the potential for using granular BRA modifier binder in asphalt mixtures with the purpose of increasing the resilient modulus values over a range of temperatures, loading times, and traffic volumes.

The ITSM test was divided into two stages as outlined in Section 3.5.1 and the analysis of the results included: (1) the resilient modulus of unmodified and BRA modified asphalt mixtures tested under standard conditions; (2) the impact of temperature on the resilient modulus of unmodified and BRA modified mixtures; (3) the impact of rest period on the resilient modulus of unmodified and BRA modified asphalt mixtures; (4) the impact of traffic volume on the resilient modulus of unmodified and BRA modified asphalt mixtures; (5) the impact of loading time on the resilient modulus of unmodified and BRA modified asphalt mixtures; and (6) the resilient modulus master curve for unmodified and BRA modified asphalt mixtures.

4.2 Analysis of ITSM Test Results and Discussion

4.2.1 Resilient modulus of asphalt mixtures

Table 4-1 shows the mean, standard deviation (SD), and coefficient of variation (CV) for the air voids and resilient modulus for unmodified and BRA modified asphalt mixtures. The CV values for the resilient modulus for both mixtures are a maximum of 5%. In addition, Table 4-2 summarizes the statistical analysis of air void content and the resilient modulus for unmodified and BRA modified asphalt mixtures. A *paired sample t-test* with a 95% level of confidence was used to

statistically analyze the mean air void values and the resilient modulus using the IBM SPSS statistics 21 program. The results of the determination of bulk density-air voids, and ITSM tests for each specimen are presented in Appendix C1 and Appendix C2, respectively. No significant difference in voids was found between the unmodified and BRA modified asphalt mixtures, while the air void content was within the range of 5.0 ± 0.5%.

It is accepted that the resilient modulus is related to air void content for a given mix. Generally a higher air void content results in a lower resilient modulus. This meant that test allowed for preparation of samples with similar mean air void contents for each triplicate group.

Table 4-1. Results of the air void content and indirect tensile stiffness modulus tests

Asphalt mixtures	Voids			Resilient Modulus		
	Mean (%)	SD (%)	CV (%)	Mean (MPa)	SD (MPa)	CV (%)
Unmodified	5.0	0.10	2	4366	45	1
BRA modified (10%)	5.1	0.16	3	5213	216	5
BRA modified (20%)	5.0	0.16	3	7216	101	2
BRA modified (30%)	5.1	0.12	3	7593	259	4

Table 4-2. *Paired sample t-test* results for air void content and resilient modulus

Asphalt mixtures	Air void				Resilient modulus			
	t	*df*	*Sig. (2-t)*	*d*	*t*	*df*	*Sig. (2-t)*	*d*
Unmodified – BRA modified (10%)	-1.0	2	0.423	-0.57	-7.7	2	0.017	-4.42
Unmodified – BRA modified (20%)	1.0	2	0.423	0.57	-59.3	2	0.000	-34.22
Unmodified – BRA modified (30%)	-0.4	2	0.742	-0.22	-20.0	2	0.002	-11.54
BRA modified (10%)–BRA modified (20%)	2.0	2	0.184	1.15	-30.3	2	0.001	-17.47
BRA modified (10%)–BRA modified (30%)	0.0	2	1.000	0.00	-16.7	2	0.004	-9.62
BRA modified (20%)–BRA modified (30%)	-1.0	2	0.423	0.58	-2.9	2	0.102	1.67

As presented in Table 4-2, the resilient modulus of the BRA modified asphalt mixtures was statistically significantly higher than that of the unmodified asphalt mixtures. Comparison of the resilient modulus of unmodified and BRA modified asphalt mixtures, showed that the resilient modulus for BRA modified asphalt mixtures prepared with 10%, 20% and 30% BRA modifier binder was about 19%, 65% and 74%, respectively, higher than the unmodified asphalt mixtures as illustrated in Figure 4-1. However, the resilient modulus value for the unmodified asphalt mixtures did not exceed the criterion (below 5000 MPa) set out by Main Roads Western Australia[136]. A higher percentage of BRA modifier binder content resulted in a higher resilient modulus. However, there was no significant difference between the resilient modulus for the 20% and 30% BRA modified asphalt mixtures (significance > 0.05).

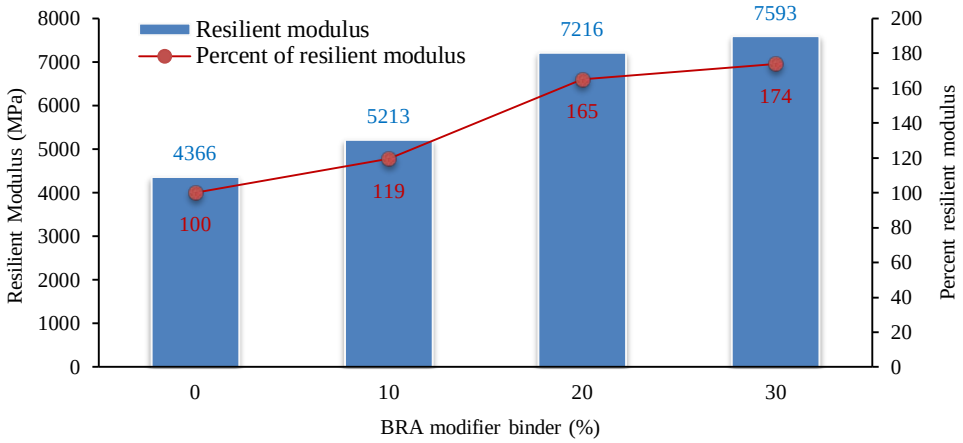

Figure 4-1. Resilient modulus for unmodified and BRA modified – first stage ITSM test

Many factors influence the resilient modulus of asphalt mixtures. Accordingly, in order to enhance the opportunity of achieving the objectives of this research, the first stage of the ITSM test was considered using the same gradation, aggregate source, total binder content and air void content (bulk density). Based on the results, substituting base asphalt binder with granular BRA modifier binder improved the mechanical properties of the asphalt mixtures. BRA modifier binder helps the mixture to resist horizontal deformation. The higher the content of granular BRA modifier binder, the greater the tensile strength will be, leading to an increase in the resilient modulus of the mixtures.

By comparing the unmodified with BRA modified asphalt ones that both used the same type and grading of aggregates, the BRA modified asphalt specimens have higher resilient modulus. The BRA modified binder is stiffer and has better tensile strength. Thus, the improvement in resilient modulus of BRA modified asphalt mixtures is attributed to the stiffer BRA modified binder.

Similar observations have been reported by other researchers. Subagio *et al.*[8] conducted resilient modulus test at temperature of 25°C, 45°C and 60°C. For all of the test temperature, the results indicated that the mechanical performance of HRA Asbuton modified mixtures in term of resilient modulus were better than unmodified asphalt mixtures. In another study, Zamhari *et al.*[15] presented the use of granular buton rock asphalt and pure buton rock asphalt in hot-mix asphalt. The ITSM test results revealed that the resilient moduli of granular and pure BRA modified mixtures were higher than those of the unmodified mixtures.

As described in Section 2.3, the resilient modulus is related to the load spreading capacity[24]. Asphalt mixtures with a high resilient modulus will distribute

loads over a wider area. It is expected that the BRA modified asphalt mixtures with a higher resilient modulus would have greater tensile strain and resistance to cracking. The resilient modulus of asphalt mixtures is a very important factor in pavement design with regard to calculating the required pavement thickness[137]. A higher resilient modulus means a reduction in the necessary thickness of the asphalt mixtures layer.

In addition, the resilient modulus values for the three replicates at each testing temperature for unmodified and BRA modified asphalt in the second stage of the ITSM tests were plotted in the form of X-Y plots. Using a power regression, regression equations were developed between the resilient modulus and rise time as presented in Table 4-3. The coefficient of determination (R^2) was used to determine how well the model fits the data and the results showed that the R^2 values were between 0.55 (at 60°C) and 0.96 (at 40°C). Further, the average resilient modulus values obtained from these equations were used for analysis.

The air void values of the specimens used in the second stage of the ITSM tests were provided within a range of 5.0±0.5% with the aim of limiting the effect of density on the resilient modulus of asphalt mixtures. The results of determining the air void content for unmodified and BRA modified asphalt mixtures are presented in Appendix C3 and Appendix C4, respectively.

The resilient modulus values for the second stage of the ITSM test obtained from individual specimens are presented in Appendix C5 and Appendix C6 for unmodified and BRA modified asphalt mixtures respectively. Using a power regression analysis yielded excellent coefficients of correlation of between 0.94 and 1.0 for unmodified asphalt mixtures, and between 0.91 and 1.0 for BRA modified asphalt mixtures. With the variation in loading conditions (rise time and repetition period) presented in Table 4-4, and using the regression equation developed in Table 4-3, the resilient modulus values for unmodified and BRA modified asphalt mixtures were determined and these are summarized in Table 4-5 and Table 4-6, respectively, and illustrated in Figure 4-2.

Table 4-3. Developed regression equation for resilient modulus at the second stage

Testing temperature (°C)	Asphalt mixtures	Pulse repetition period (ms)	Equation[1]	R^2
5	Unmodified	1000	$y = 27692.309x^{-0.155}$	0.898
	Unmodified	2000	$y = 25220.375x^{-0.128}$	0.840
	Unmodified	3000	$y = 22982.688x^{-0.092}$	0.697
	BRA Modified	1000	$y = 34567.427x^{-0.128}$	0.832
	BRA Modified	2000	$y = 31427.543x^{-0.099}$	0.865
	BRA Modified	3000	$y = 30358.117x^{-0.080}$	0.912
15	Unmodified	1000	$y = 21281.490x^{-0.219}$	0.713
	Unmodified	2000	$y = 21235.835x^{-0.230}$	0.729
	Unmodified	3000	$y = 21746.324x^{-0.239}$	0.763
	BRA Modified	1000	$y = 25320.082x^{-0.178}$	0.828
	BRA Modified	2000	$y = 24982.692x^{-0.180}$	0.809
	BRA Modified	3000	$y = 25721.289x^{-0.186}$	0.812
25	Unmodified	1000	$y = 17773.527x^{-0.405}$	0.817
	Unmodified	2000	$y = 13897.884x^{-0.375}$	0.780
	Unmodified	3000	$y = 14391.167x^{-0.393}$	0.788
	BRA Modified	1000	$y = 19080.082x^{-0.288}$	0.929
	BRA Modified	2000	$y = 19812.853x^{-0.316}$	0.914
	BRA Modified	3000	$y = 20146.454x^{-0.328}$	0.853
40	Unmodified	1000	$y = 4152.254x^{-0.508}$	0.939
	Unmodified	2000	$y = 2577.166x^{-0.412}$	0.787
	Unmodified	3000	$y = 2286.208x^{-0.389}$	0.749
	BRA Modified	1000	$y = 6898.153x^{-0.438}$	0.924
	BRA Modified	2000	$y = 5559.128x^{-0.411}$	0.963
	BRA Modified	3000	$y = 5271.487x^{-0.405}$	0.954
60	Unmodified	1000	$y = 348.243x^{-0.221}$	0.585
	Unmodified	2000	$y = 370.539x^{-0.249}$	0.550
	Unmodified	3000	$y = 415.445x^{-0.290}$	0.648
	BRA Modified	1000	$y = 824.259x^{-0.258}$	0.817
	BRA Modified	2000	$y = 726.250x^{-0.237}$	0.762
	BRA Modified	3000	$y = 677.955x^{-0.233}$	0.878

[1]: *y = resilient modulus (MPa); x = rise time (ms)*

Table 4-4. Variation of experiment parameters for the second stage of the ITSM tests

Pulse repetition period (ms)	Frequency (Hz)	Rise time (ms)	Loading time (ms)	Rest period (ms)	R/L[1]
1000	1.0	40	100	900	9
1000	1.0	60	150	850	5.7
1000	1.0	80	200	800	4
2000	0.5	40	100	1900	19
2000	0.5	60	150	1850	12.3
2000	0.5	80	200	1800	9
3000	0.33	40	100	2900	29
3000	0.33	60	150	2850	19
3000	0.33	80	200	2800	14

[1] *R/L = rest period/loading time*

Table 4-5. Resilient modulus values (MPa) for unmodified asphalt mixtures

Rise time (ms)	Pulse repetition period (ms)	Temperature (°C)				
		5	15	25	40	60
40	1000	15633	9487	3990	637	154
40	2000	15729	9091	3485	564	148
40	3000	16369	9005	3377	544	143
60	1000	14681	8681	3386	519	141
60	2000	14933	8281	2993	477	134
60	3000	15769	8173	2879	465	127
80	1000	14040	8151	3013	448	132
80	2000	14393	7751	2687	424	124
80	3000	15357	7630	2571	416	117

Table 4-6. Resilient modulus values (MPa) for BRA modified asphalt mixtures

Rise time (ms)	Pulse repetition period (ms)	Temperature (°C)				
		5	15	25	40	60
40	1000	21558	13131	6595	1371	318
40	2000	21813	12861	6176	1221	303
40	3000	22600	12951	6008	1183	287
60	1000	20467	12217	5868	1148	287
60	2000	20954	11956	5433	1033	275
60	3000	21879	12010	5260	1004	261
80	1000	19727	11607	5401	1012	266
80	2000	20366	11352	4961	918	257
80	3000	21381	11385	4786	894	244

4.2.2 Effect of temperature on resilient modulus of asphalt mixtures

Table 4-7 shows the resilient modulus ratio based on the resilient modulus values displayed in Table 4-5 and Table 4-6. The resilient modulus ratio was calculated by dividing the resilient modulus values for BRA modified asphalt mixtures in a given loading period and pulse period with the resilient modulus values for unmodified asphalt mixtures in the same loading period, pulse repetition period and temperature. Table 4-5 and Table 4-6 show that the modulus of the asphalt mixes decreased as temperature increased. This is caused by a decrease in the ductility of the binder under increased temperature, resulting in a decrease in the strength of asphalt mixtures[31].

Table 4-7 shows that the resilient modulus ratio increases as the temperature increases. At a test temperature of 5°C, the average resilient modulus ratio is 1.39, while it increases to 2.18 at a test temperature of 40ºC. This confirms previous findings by Tabatabaie *et al.*[138] demonstrating that the asphalt binder grade has a significant impact on the resilient modulus of asphalt mixtures. This explains that the resilient modulus for BRA modified asphalt mixtures prepared with 20% BRA modifier binder increased under the same conditions of test temperature, rise time and pulse period. As an alternative means of showing the influence of BRA modifier

binder on resilient modulus values, Figure 4-3 illustrates the relationship between the resilient modulus of unmodified and BRA modified (20%) asphalt mixtures. The points are above the equality line, representing an increase by about 1.4 times in the resilient modulus due to the substitution of BRA modifier binder.

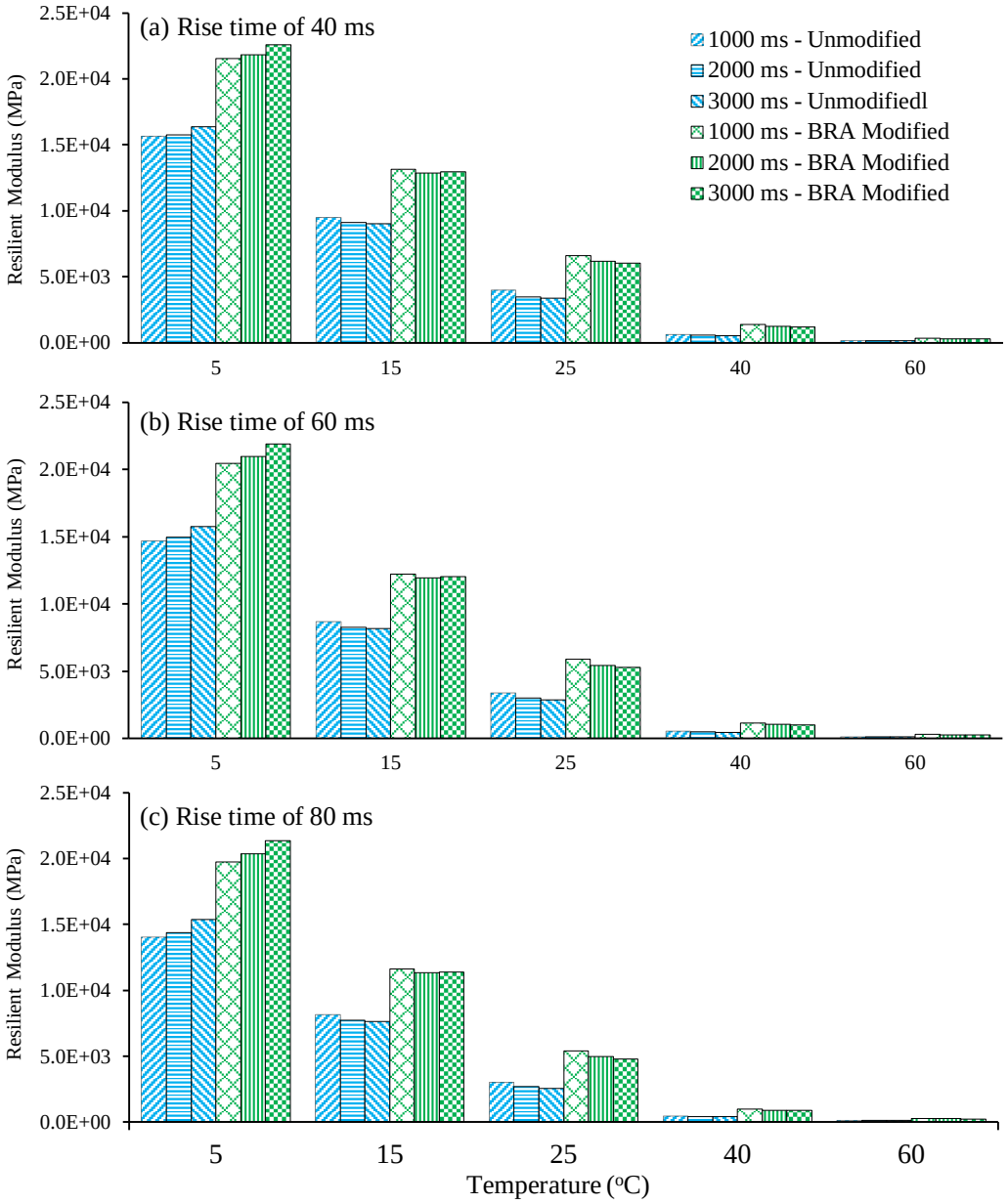

Figure 4-2. Resilient modulus for asphalt mixtures

Moreover, in comparing the ITSM test values a similar increase in resilient modulus for the first and second stage was observed. For the first stage, the BRA modified asphalt mixture prepared with 20% BRA modifier binder showed an increase in the resilient modulus of 65%, and an increase of 78% for the second stage.

Table 4-7. Resilient modulus ratio

Rise time (ms)	Pulse repetition period (ms)	Temperature (°C)				
		5	15	25	40	60
40	1000	1.38	1.38	1.65	2.15	2.06
40	2000	1.39	1.41	1.77	2.16	2.05
40	3000	1.38	1.44	1.78	2.17	2.01
60	1000	1.39	1.41	1.73	2.21	2.04
60	2000	1.40	1.44	1.82	2.17	2.05
60	3000	1.39	1.47	1.83	2.16	2.06
80	1000	1.41	1.42	1.79	2.26	2.02
80	2000	1.41	1.46	1.85	2.17	2.07
80	3000	1.39	1.49	1.86	2.15	2.09
	Average	1.39	1.44	1.79	2.18	2.05

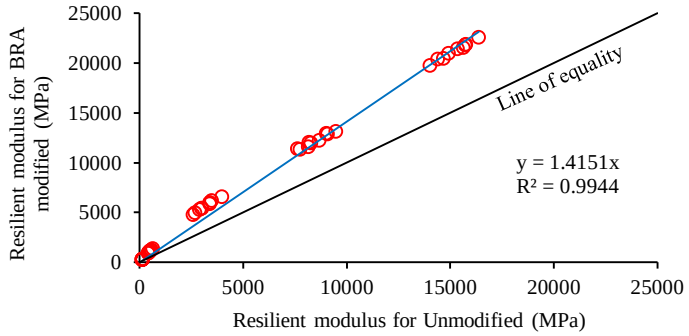

Figure 4- 3. Relationship between resilient modulus of unmodified and BRA modified asphalt

From the previous study[30], stiffness modulus values are likely to converge at test temperatures of 25°C and 40°C. Similarly, this study found that the stiffness modulus tends to converge at test temperatures of 15°C, 25°C, 40°C and 60°C. Table 4-8 shows a decrease in resilient modulus for both asphalt mixtures due to the increase in test temperature. It can be seen that the resilient modulus values decreased by about 39-85% and 39-82% for unmodified and BRA modified asphalt mixtures respectively, between two adjacent temperatures. The resilient modulus decreased by up to approximately 85% with an increase in temperature from 25°C to 40°C. This shows that resilient modulus is highly dependent on temperature as a result of the softening point of asphalt binder. As expected, the results of this study showed that the resilient modulus of asphalt mixtures decreases as temperature increases. The resilient modulus of the unmodified mixtures decreased by 2-3% more than the BRA modified asphalt mixtures tested under the same rise time and pulse period conditions. These results confirmed that BRA modified asphalt mixtures are less sensitive to temperature change than unmodified asphalt mixtures. Increasing the temperature led to an increase in the deformation of the asphalt mixtures due to a

lower base asphalt binder viscosity at higher temperatures. BRA modifier binder is needed for conditions of higher temperature.

Table 4-8. Decrease in resilient modulus (%)

Rise time (ms)	Pulse repetition period (ms)	Asphalt mixtures	Temperature range (°C)			
			5 to 15	15 to 25	25 to 40	40 to 60
40	1000	Unmodified	-39.3	-57.9	-84.0	-75.8
40	2000	Unmodified	-42.2	-61.7	-83.8	-73.8
40	3000	Unmodified	-45.0	-62.5	-83.9	-73.7
60	1000	Unmodified	-40.9	-61.0	-84.7	-72.8
60	2000	Unmodified	-44.5	-63.9	-84.1	-71.9
60	3000	Unmodified	-48.2	-64.8	-83.8	-72.7
80	1000	Unmodified	-41.9	-63.0	-85.1	-70.5
80	2000	Unmodified	-46.1	-65.3	-84.2	-70.8
80	3000	Unmodified	-50.3	-66.3	-83.8	-71.9
40	1000	BRA Modified	-39.1	-49.8	-79.2	-76.8
40	2000	BRA Modified	-41.0	-52.0	-80.2	-75.2
40	3000	BRA Modified	-42.7	-53.6	-80.3	-75.7
60	1000	BRA Modified	-40.3	-52.0	-80.4	-75.0
60	2000	BRA Modified	-42.9	-54.6	-81.0	-73.4
60	3000	BRA Modified	-45.1	-56.2	-80.9	-74.0
80	1000	BRA Modified	-41.2	-53.5	-81.3	-73.7
80	2000	BRA Modified	-44.3	-56.3	-81.5	-72.0
80	3000	BRA Modified	-46.8	-58.0	-81.3	-72.7

4.2.3 Effect of rest period ratio on resilient modulus of asphalt mixtures

The effect of the rest period ratio on the resilient modulus of unmodified and BRA modified asphalt mixtures is shown in Figure 4-4. The rest period ratio is obtained by dividing the rest period by the loading time (R/L), while the resilient modulus ratio is defined by dividing the resilient modulus in a given rest period ratio with the resilient modulus under a standard loading time of 100 ms and repetition period of 3000 ms at the same temperature[31, 139].

The R/L ratio affected the resilient modulus for both the unmodified and BRA modified asphalt mixtures. Figure 4-4 shows that the resilient modulus ratio for unmodified and BRA modified asphalt mixtures increased with an increase in the R/L ratio at 5°C. However, by contrast, the resilient modulus ratio for both asphalt mixtures decreased with an increase in the R/L ratio at other test temperatures. Law[140], and Shafabakhsh and Tanakizadeh[31] have concluded that a lower R/L ratio will yield greater resilient modulus values under the same loading period.

The differences in resilient modulus are more obvious with an increase in temperature for both asphalt mixtures. A lower R/L ratio resulted in a higher resilient modulus ratio of up to 1.182 and 1.159 for unmodified asphalt mixtures at a test temperature of 25°C and BRA modified asphalt mixtures at a test temperature of 40°C, respectively.

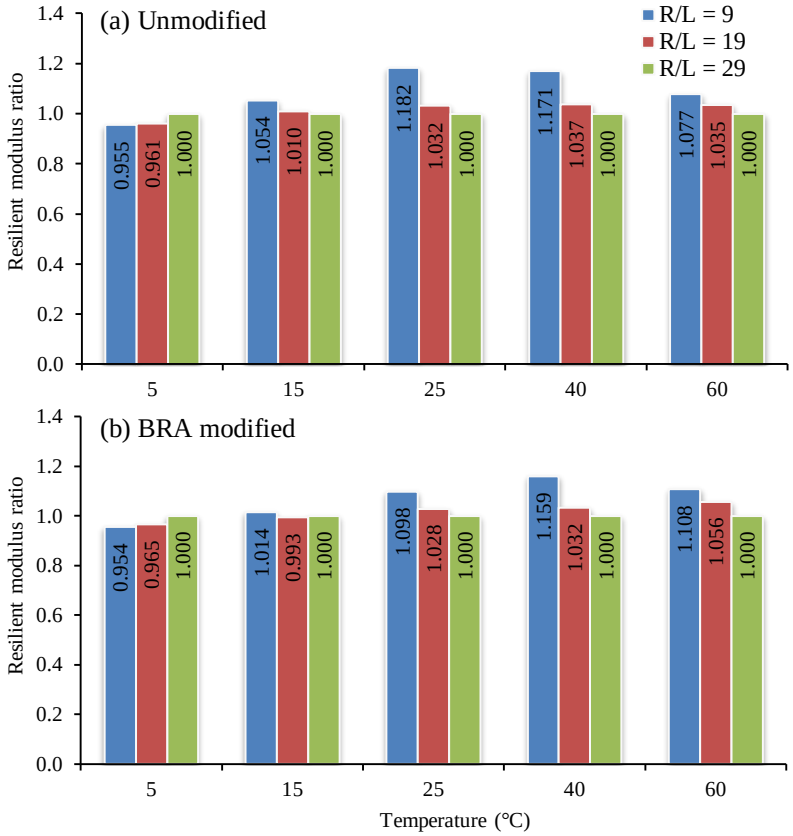

Figure 4-4. Effect of rest period ratio on resilient modulus of asphalt mixtures: (a) Unmodified, (b) BRA modified

This shows that the resilient modulus increases when the frequency of the load cycle increases from 0.33 Hz or 0.5 Hz to 1.0 Hz. A shorter rest period resulted in less time for strain recovery to occur under a higher load cycle frequency, resulting in a higher resilient modulus[141]. Kim *et al.*[139] have showed that the rest period ratio has a direct effect on the recovery strain of asphalt mixtures. A greater resilient modulus value is obtained from a smaller recoverable strain. However they found that a R/L ratio approaching 8 and higher had only a minor effect on the resilient modulus. The resilient modulus of asphalt mixtures decreases as the R/L ratio increases. Moreover, the dependency of the R/L ratio decreases with a decrease in temperature. Monismith[142] reported that an R/L ratio of 8 and higher does not show the beneficial effect of a longer R/L ratio. Similarly, Barkdale *et al.*[143] showed that an R/L ratio of 4 to 27 brings about less variation in the resilient modulus.

The change in resilient modulus ratio due to the decrease in the rest period ratio for unmodified asphalt mixtures was the highest at the same test temperature. It is apparent that the replacement of 20% base binder with BRA modifier binder reduced the effect of the rest period ratio on the resilient modulus of BRA modified mixtures.

4.2.4 Effect of traffic volume on resilient modulus of asphalt mixtures

In order to investigate the effect of traffic volume on the resilient modulus of asphalt mixtures, 1000 ms and 3000 ms pulse periods were used to simulate a high and low volume of traffic, respectively[30], and the results are presented in Figure 4-5. It can be seen in Figure 4-5(a), that at a test temperature of 5°C, the unmodified and BRA modified asphalt mixtures under low traffic volume conditions had a resilient modulus higher than that of asphalt mixtures under high traffic volume conditions. By contrast, at other test temperatures (illustrated in Figures 4-5(b) through 4-5(e)), the resilient modulus values for both mixtures under a low volume of traffic (3000 ms) were lower compared with those mixtures under a higher volume of traffic (1000 ms). Furthermore, the increase in rise time from 40 ms to 80 ms resulted in a decrease in the resilient modulus.

The change in resilient modulus for unmodified and BRA modified asphalt as a result of an increase in traffic volume and rise time[30] are presented in Table 4-9. The resilient modulus for both asphalt mixtures decreased by up to 8.6% as the repetition period decreased from 3000 ms to 1000 ms at a test temperature of 5°C. However, at other test temperatures, the resilient modulus of both asphalt mixtures increased by up to about 17-18% when the repetition period decreased from 3000 ms to 1000 ms, especially at a moderate temperature (25°C) and high temperature (40°C). Similar findings were reported by Tayfur *et al*.[30]. The resilient modulus of polymer modified asphalt mixtures increased by about 8% when the repetition period was decreased to 1000 ms.

In addition, the effect of loading frequency on the resilient modulus of unmodified and BRA modified asphalt mixtures is illustrated in Figure 4-6. The frequency as shown in Table 4-4 was calculated using Equation 4.1. Further, a linear relationship was found between the loading frequency and resilient moduli for both asphalt mixtures as calculated using Equation 4.2.

The constant coefficients obtained from fitting Figure 4-6 to the data for unmodified and BRA modified asphalt mixtures are listed in Table 4-10. As can be seen, at a temperature of 5°C, the constant coefficient "*a*" is a negative value, indicating that an increase in loading frequency results in a decrease in the resilient modulus of unmodified and BRA modified asphalt mixtures.

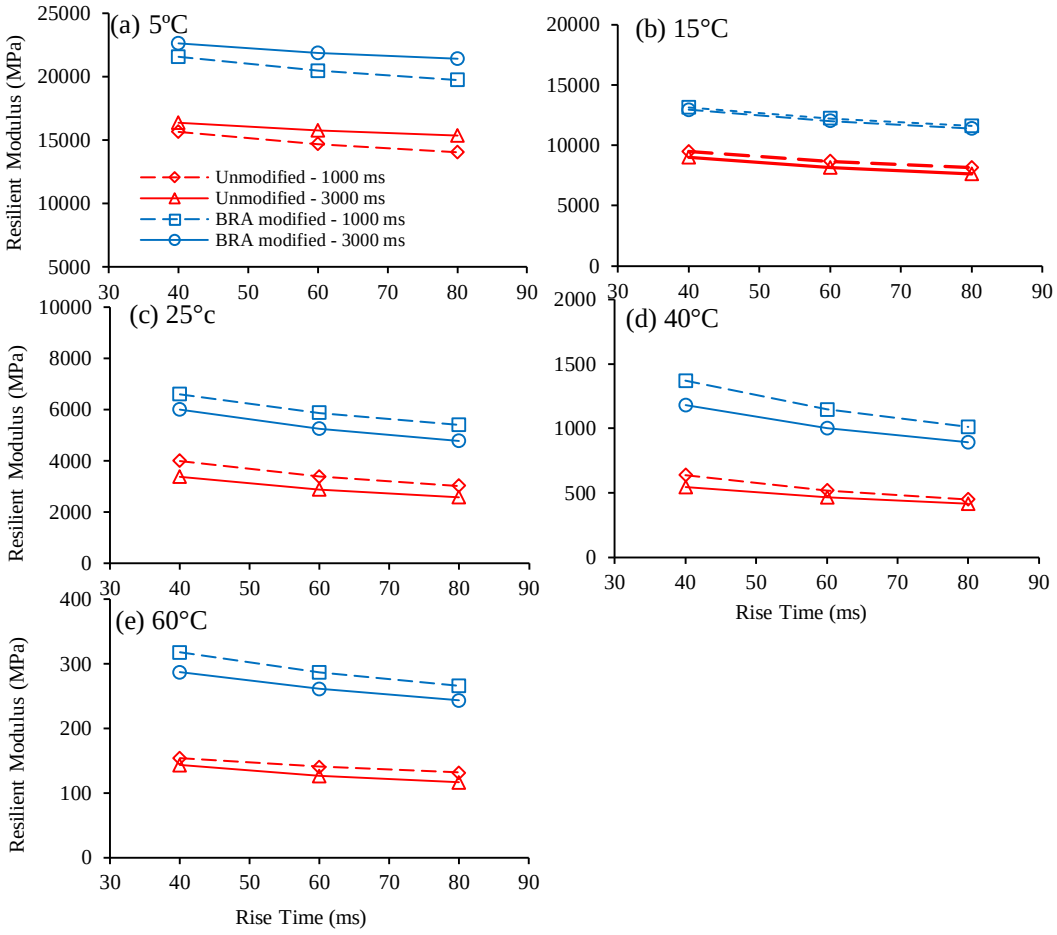

Figure 4-5. Resilient modulus for asphalt mixtures at various test temperatures

Table 4-9. Effect of traffic volume change on resilient modulus of asphalt mixes (%)

Asphalt mixtures	Rise time (ms)	Pulse repetition period (ms)	Temperature (ºC)				
			5	15	25	40	60
Unmodified	40	3000 to 1000	-4.5	5.4	18.2	17.1	7.7
Unmodified	60	3000 to 1000	-6.9	6.2	17.6	11.6	11.0
Unmodified	80	3000 to 1000	-8.6	6.8	17.2	7.7	12.8
BRA Modified	40	3000 to 1000	-4.6	1.4	9.8	15.9	10.8
BRA Modified	60	3000 to 1000	-6.5	1.7	11.6	14.3	10.0
BRA Modified	80	3000 to 1000	-7.7	1.9	12.8	13.2	9.0

$$f = \frac{1}{d} \tag{4.1}$$

$$\log (M_r) = a \log (f) + b \tag{4.2}$$

where f : loading frequency (Hz)

d : loading duration (s)

M_r : resilient modulus (MPa)

a,b : constant coefficients of the model

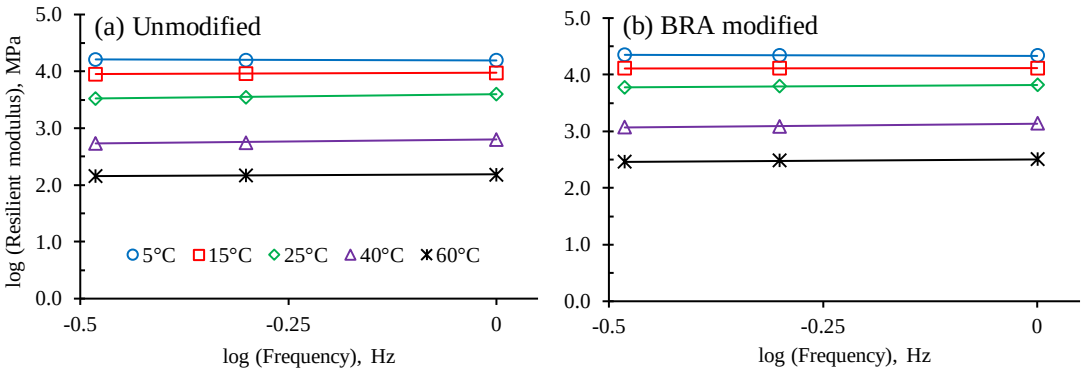

Figure 4-6. Effect of loading frequency on resilient modulus of asphalt mixtures

Table 4-10. Coefficient of linear relationship frequency – resilient modulus

Temperature	Unmodified			BRA modified		
(°C)	*a*	*b*	R^2	*a*	*b*	R^2
5	-0.0382	4.1916	0.7318	-0.0400	4.3317	0.8296
15	0.0485	3.9761	0.9573	0.0142	4.1170	0.5691
25	0.1550	3.5977	0.9600	0.0852	3.8184	0.9923
40	0.1458	2.8017	0.9746	0.1365	3.1345	0.9697
60	0.0659	2.1882	0.9897	0.0902	2.5041	0.969

However at other test temperatures, the constant coefficient "*a*" is a positive value, demonstrating that the resilient modulus for both unmodified and BRA modified asphalt mixtures increases with an increase in the loading frequency. According to Fakhri and Ghanizadeh[34], the constant coefficient "*a*" indicates the change in modulus rate corresponding to the change in loading frequency. The results show that the minimum value of coefficient "*a*" is at a temperature of 5°C and increases as the temperature increases. The maximum value of this coefficient was recorded at the temperatures of 25°C and 40°C for unmodified and BRA modified asphalt mixtures, respectively. Similar observations were reported by Fakhri and Ghanizadeh[34]. At the same test temperature, the constant coefficient "*a*" for unmodified asphalt mixtures was higher than for the BRA modified asphalt mixtures. This confirms that BRA modified asphalt mixtures are less sensitive to changes in the frequency than unmodified asphalt mixtures. Moreover, the constant coefficient "*b*" for both unmodified and BRA modified asphalt mixtures decreased with an increase in test temperature, indicating that presenting that the resilient modulus values for both asphalt mixtures decreases as temperature increases.

4.2.5 Effect of loading time on resilient modulus of asphalt mixtures

Figure 4-7 illustrates the effect of loading time on the resilient modulus of unmodified and BRA modified asphalt mixtures. The resilient modulus ratio was

defined as the resilient modulus for a given loading time divided by the resilient modulus for a standard loading time of 100 ms and a repetition period of 3000 ms[31]. The resilient modulus ratio for unmodified asphalt mixtures decreased by up to 0.76 at a test temperature of 25°C and 40°C as the loading time increased to 200 ms, while for BRA modified asphalt mixtures, the resilient modulus ratio decreased by up to 0.76 at a test temperature of 40°C. Furthermore, at a low temperature (5°C), the effect of loading time on resilient modulus was less significant. At this temperature, the behaviour of the asphalt mixtures is close to elastic and therefore the materials are largely independent of the change in loading time. Similar observations have been reported by other researchers[30, 140, 143]. However, at moderate (15°C and 25°C) and high temperatures (40°C and 60°C), the resilient modulus decreased significantly as loading time increased to 200 ms. According to other researcher[143, 144], at these temperatures there is a great deformation with less recovery from deformation when a high loading time is applied. It was observed the resilient modulus decreased in about 24%-26% for BRA modified asphalt mixtures and 24%-29% for unmodified asphalt mixtures.

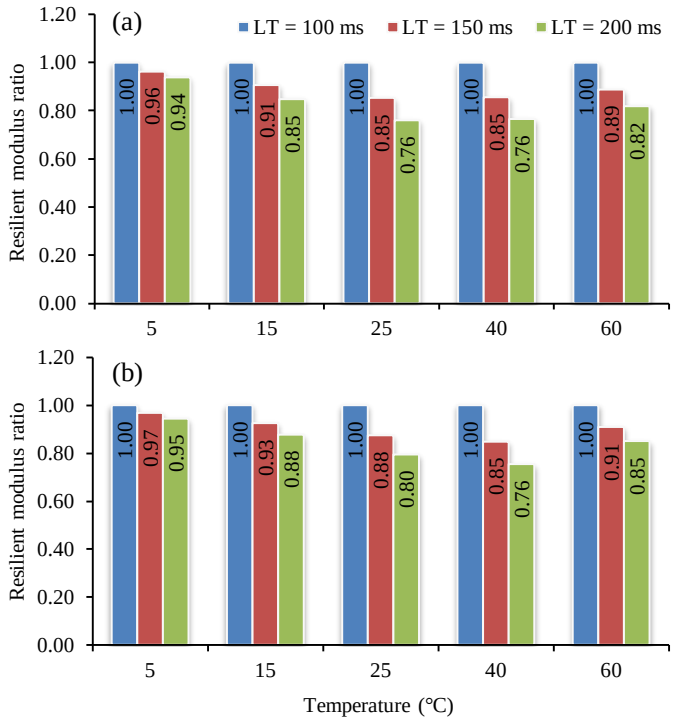

Figure 4-7. Effect of loading time on resilient modulus of (a) unmodified asphalt mixtures, and (b) BRA modified asphalt mixtures

Generally, the decrease in resilient modulus ratio due to the increase in loading time for unmodified asphalt mixtures was greater than for the BRA modified asphalt

mixtures. Similar observation have been reported by Kamal *et al.*[144]. According to their research, the resilient modulus values for polymer modified asphalt mixtures decreases with an increase in loading time from 150 ms to 450 ms at the same temperature. Tayfur *et al.*[30] reported that the resilient modulus values for polymer modified asphalt mixtures increased by about 25% when the loading time decreased from 80 ms to 40 ms. Shafabakhsh and Tanakizadeh[31] observed that the effect of loading time on the resilient modulus of asphalt mixes was significant. They stated that with an increase in loading time from 100 ms (for R/L of 9) to 1000 ms at 40°C, the resilient modulus ratio decreased by about 0.16 for haversine loading and 0.21 for square loading, and vice versa; with a decrease in loading time to 50 ms, the resilient modulus ratio decreased by about 1.45 for haversine loading and 1.41 for square loading.

In addition, Table 4-11 shows the decrease in resilient modulus with increase in loading time. Loading times of 100 ms and 200 ms were chosen for simulating high and low vehicle speeds respectively. The results show that the resilient modulus of unmodified and BRA modified asphalt mixtures decreased as loading time increased to 200 ms under various temperature and pulse period conditions. The resilient modulus decreased by up to 29.7% and 26.2% for unmodified and BRA modified asphalt mixtures, respectively, with an increase in loading time from 100 ms to 200 ms. The decrease in resilient modulus for BRA modified asphalt was lower than for with the unmodified asphalt mixtures tested at various temperatures and pulse repetition periods. It was obvious that the addition of 20% BRA modifier binder to asphalt mixtures reduced the effect of loading time on the resilient modulus of the asphalt mixtures.

Table 4-11. Effect of the decrease in loading time from 100 to 200 ms on asphalt mixes

Asphalt mixtures	Pulse repetition period (ms)	Decrease in loading time (%),				
		5	15	25	40	60
Unmodified	1000	-10.2	-14.1	-24.5	-29.7	-14.2
Unmodified	2000	-8.5	-14.7	-22.9	-24.8	-15.9
Unmodified	3000	-6.2	-15.3	-23.8	-23.6	-18.2
BRA Modified	1000	-8.5	-11.6	-18.1	-26.2	-16.4
BRA Modified	2000	-6.6	-11.7	-19.7	-24.8	-15.1
BRA Modified	3000	-5.4	-12.1	-20.3	-24.5	-14.9

4.2.6 Resilient modulus master curve for asphalt mixtures

The effects of temperature and loading frequency were combined to find out the different susceptibilities of the various asphalt mixtures to temperatures. The resilient modulus master curve for asphalt mixtures is developed based on the time-

temperature superposition principal, similarly to the dynamic modulus master curve described in Section 2.4.3. The master curve for the resilient modulus is modelled by the sigmoidal function described by Equation 4-3[34].

$$\text{Log } |S| = \delta + \frac{\alpha}{1 + e^{\beta + [\gamma (\log f_r)]}} \quad (4\text{-}3)$$

where: f_r : reduced frequency of loading at reference temperature

δ : minimum value of S

$\delta + \alpha$: maximum value of S

β, γ : parameter describing the shape of sigmoidal function

$$a(T) = \frac{f}{f_r} \quad (4.4)$$

where: $a(T)$: shift factor as a function of temperature

f : loading frequency at desired temperature

f_r : loading frequency at reference temperature

T : temperature of interest

According to Witczak and Bari[62], the second order polynomial can be used to show the relationship between the logarithm of the shift factor as shown in Equation 4-5.

$$Log\ a(T_i) = aT_i^2 + bT_i + c \quad (4\text{-}5)$$

where $a(T_i)$: shift factor as a function of temperature T_i

T_i : time of loading at desired temperature

a, b, and c : reduced time of loading at reference temperature

The laboratory resilient modulus data for the five testing temperatures and three frequencies for each asphalt mixture were combined to construct the resilient modulus master curve. Equation 4-3 was used to construct this master curve for a reference temperature of 21°C for all asphalt mixtures. The resilient modulus data were then shifted into a master curve for the analysis of the performance of asphalt mixtures by simultaneously solving shift parameters. Figure 4-8 shows the relationship between the logarithm of the shift factors (log a(Ti)) and test temperature for each mixture. The shift factor for unmodified and BRA modified asphalt mixtures was found to be similar. All of the shift factors followed a second order polynomial with respect to temperature. The seven parameters in accordance with Equations 4-3 and 4-5 presented in Table 4-12 were used to calculate the

resilient modulus for unmodified and BRA modified asphalt mixtures (20%) over the range of temperatures and loading frequencies used in the testing.

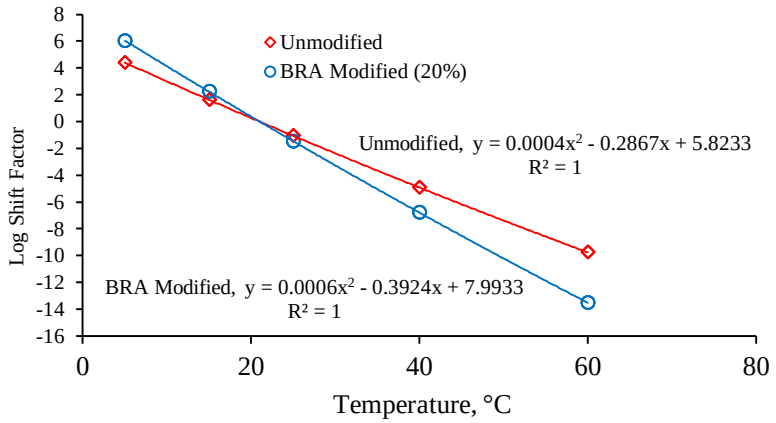

Figure 4-8. Shift factor for unmodified and BRA modified asphalt mixtures

Table 4-12. Resilient modulus and shift parameter

Asphalt mixtures	Dynamic modulus parameter				Shift parameter			
	δ	α	β	γ	a	b	c	R^2
Unmodified	1.129	2.376	-1.076	-0.362	0.0004	-0.287	5.823	1.0
BRA modified (20%)	1.357	2.301	-1.112	-0.234	0.0006	-0.392	7.993	1.0

Fitted master curves for asphalt mixtures were shown in Figure 4-9 plotted in a log-log scale. The measured and master curve resilient moduli were then compared in order to check the accuracy and effectiveness of the master curve. A plot master curve resilient modulus ($S_{master\ curve}$) and laboratory resilient modulus (S_{lab}) for unmodified and BRA modified asphalt mixtures are shown in Figure 4-10. It can be seen that the resilient modulus data obtained from the master curve for both asphalt mixtures is almost identical to laboratory resilient modulus data.

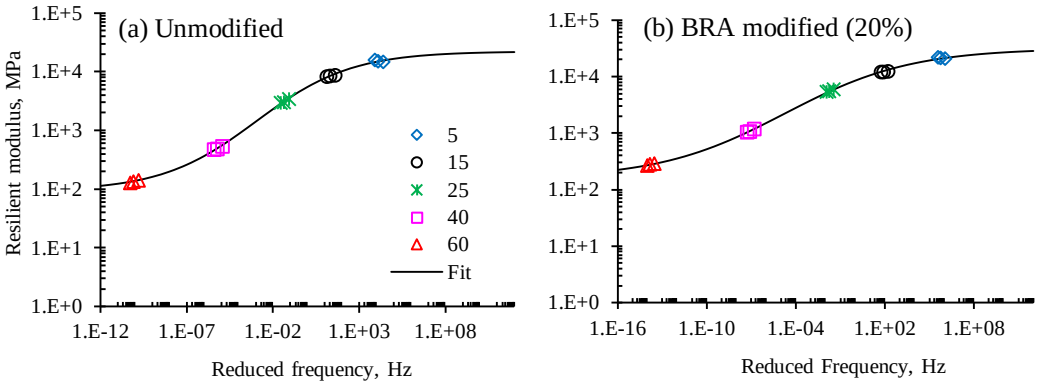

Figure 4-9. Fitted of resilient modulus master curve of asphalt mixtures

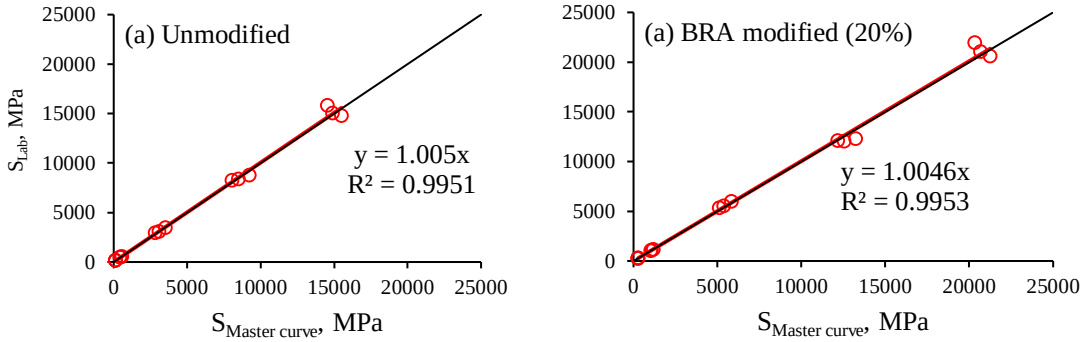

Figure 4-10. Comparison between the measured and master curve resilient modulus

The resilient modulus master curves for unmodified and BRA modified asphalt mixtures at a reference temperature of 21°C as shown in Figure 4-9 are plotted in Figure 4-11. This figure illustrates the comparison of the effect of granular BRA modifier binder on the resilient modulus of asphalt mixtures at a reference temperature and various loading frequencies. The resilient modulus for BRA modified asphalt mixtures was observed to be higher than for unmodified mixtures especially in the high-intermediate temperature range and at low frequency. Therefore, the viscoelastic behaviour of BRA modified asphalt mixtures containing 20% BRA modifier binder was higher than for unmodified asphalt mixtures.

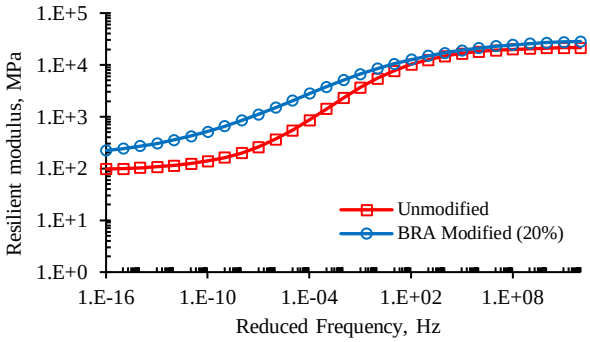

Figure 4-11. Resilient modulus master curve for unmodified and BRA modified asphalt mixtures

4.2.7 Statistical analysis

The resilient modulus results for the second stage were also analyzed statistically using the analysis of covariance (Ancova). The purpose of the statistical analysis at this stage was to determine whether granular BRA modifier binder seemed to have an effect on the resilient modulus of asphalt mixtures when the test temperature, rise time and pulse repetition period were controlled.

The response examined was the resilient modulus of the asphalt mixtures. Independent variables included two asphalt mixtures as fixed variables (unmodified

and BRA modified asphalt mixtures) and three testing variables as covariates (temperature, rise time and pulse repetition period). The results of the Ancova are summarized in Table 4-13, indicating which effects are statistically significant at the 95 percent ($p < 0.05$) probability level and described as thereafter.

Table 4-13. Statistically significant effect of variables in ITSM test

Variables	Resilient modulus
Asphalt mixtures	Yes
Temperatures	Yes
Rise time	No
Pulse repetition period	No

The results of Levene's test (Appendix C8-a) when temperature, rise time, and pulse repetition period are included in the model as covariates are non-significant. This indicates that the variances are equal (hence the assumption of the homogeneity of variances has been met). It is clear that the covariates (temperature, rise time, and pulse repetition period) significantly predict the dependent variable (resilient modulus).

Looking at the significance values (Appendix C8-b), only the temperature as a covariate significantly predicts the resilient modulus of asphalt mixtures because the significant value is less than 0.05, where $F(1, 175) = 614.724$, and $p = 0.000$. Therefore the resilient modulus of asphalt mixtures is significantly influenced by the temperature, while rise time and pulse repetition period seem to have no significant effect on the resilient modulus. The significant values for rise time and pulse repetition period were 0.161 and 0.939 respectively.

Other than that, even though the effects of temperature, rise time and pulse repetition period were not included, the effect of BRA modifier binder on the resilient modulus values of asphalt mixtures was significant, where $F(1, 175) = 27.485$, and $p = 0.000$. The model as a whole was still significant, therefore it is possible to predict the resilient modulus of asphalt mixtures from these variables (asphalt mixtures, temperature, rise time and pulse repetition periods) where the significance for the corrected model was less than 0.05 ($p = 0.000$).

The results of the normal post hoc test (Appendix C8-d) showed that using granular BRA modifier binder in the asphalt mixtures had a significant effect on the resilient modulus; specifically the resilient modulus of the BRA modified asphalt mixtures was significantly higher than the unmodified asphalt mixtures.

4.3 Summary

Several tests for determining the resilient modulus of unmodified and BRA modified mixtures were evaluated under the ITSM test in accordance with Australian standard AS-2891.13.1-1995. Included in this evaluation were: (a) first stage: the effect of using BRA modifier binder at 10%, 20%, and 30% (by weight of total binder) in base asphalt binder on the resilient modulus of asphalt mixtures tested under standard conditions (such as a test temperature of 25°C, rise time of 40 ms, repetition period of 3000 ms); (b) second stage: the effect of variation in the test condition variables such as test temperature, rise time, and pulse repetition period, on unmodified and BRA modified asphalt mixtures. All specimens were tested with statistically the same air void values which were within 5.0±0.5%. The following observations have been made based on the analysis in this study:

(1) The resilient modulus of BRA modified asphalt mixtures was significantly higher than that of unmodified asphalt mixtures. This indicates that the substitution of BRA modifier binder led to an increase in the shear resistance and thus an increase in the stiffness of BRA modified asphalt mixtures.

(2) The resilient modulus of unmodified and BRA modified asphalt mixtures was influenced by temperature. The resilient modulus of asphalt mixtures decreased with an increase in temperature. However, the BRA modified asphalt mixtures were less sensitive to the temperature changes than the unmodified asphalt mixtures.

(3) The ratio of rest period to loading time (R/L ratio) affected the resilient modulus of the asphalt mixtures. The substitution of 20% BRA modifier binder reduced the effect of the R/L ratio on the resilient modulus of the asphalt mixtures. Moreover, the BRA modified asphalt mixtures were less sensitive to changes in the frequency than the unmodified asphalt mixtures.

(4) The resilient modulus of unmodified and BRA modified asphalt mixtures decreased with increased loading time. However, the decrease in resilient modulus for BRA modified asphalt mixtures was lower than that for unmodified asphalt mixtures.

(5) Based on statistical analysis using the analysis of covariance (Ancova), two factors, temperature and granular BRA modifier binder, had the greatest and most statistically significant influence on resilient modulus compared to other

variables, while the loading time and pulse repetition period seemed to have no statistically significant effect on resilient modulus.

CHAPTER 5

EVALUATION OF THE EFFECT OF GRANULAR BRA MODIFIER BINDER ON THE DEFORMATION RESISTANCE OF ASPHALT MIXTURES

5.1 Introduction

Permanent deformation of asphalt mixtures in the pavement structure reduces the serviceability of asphalt pavement during its service life. As discussed in Section 2.4.2, rutting increases gradually when the traffic load increases, especially heavy loads, in combination with high temperature.

The objective of Chapter 5 is to analyze the influence of granular BRA modifier binder on the resistance to permanent deformation of BRA modified asphalt mixtures. Therefore, two laboratory tests were conducted as described in Sections 3.5.2 and 3.5.3: (1) the dynamic creep test, to determine the permanent compressive strain characteristics of the asphalt mixtures; and (2) the wheel tracking test, to determine the rutting resistance of the asphalt mixtures.

The analysis of the dynamic creep test results included: (1) the effect of granular BRA modifier binder on the loading cycles-permanent strain of asphalt mixtures; (2) the effect of granular modifier binder on the creep modulus of asphalt mixtures; (3) the flow number, flow point and strain rate of asphalt mixtures. In addition, the analysis of the wheel tracking test results included: (1) the effect of granular BRA modifier on the rut depth and tracking rate of asphalt mixtures; (2) the effect of granular BRA modifier on the velocity of asphalt mixtures; (3) the effect of granular BRA modifier binder on the dynamic stability of asphalt mixtures.

5.2 Analysis of Dynamic Creep Test Results and Discussion

5.2.1 Loading cycle – permanent strain of asphalt mixtures

The total permanent strain calculated by averaging three replicates (except two replicates for 30% BRA modified asphalt mixtures) using a linear regression was plotted in the format of X-Y plots as shown in Figure 5-1. The regression equation developed from fitting Figure 5-1 for every mixture is presented in Table 5-1. The loading cycles were set to reach 3% of total permanent strain; however the testing processes were stopped automatically for BRA modified asphalt mixture containing 30% BRA modifier binder after they reached about 30,000 cycles, according to AS

2891.12.1-1995[132]. This indicates that the asphalt mixtures might have greater stiffness as described in Section 4.2.1, resulting in a lower permanent strain after passing the cycle limit. Table 5-1 also shows the loading cycles obtained to reach 3% total permanent strain by using the regression equation in Table 5-1.

The mean, standard deviation (SD), and coefficient of variation (CV) of the air void content for unmodified and BRA modified asphalt mixtures specimens were also shown in Table 5-1. A *paired t-test method* with 95% confidence level was carried out using the IBM SPSS statistic 21 program to statistically analyze the means of the void values and it was found that there were no significant differences between the void values for the unmodified and BRA modified asphalt mixtures as shown in Table 5-2, while the air void contents were within the range of 5±0.5%[132]. The results of the determination of bulk density – void contents for each specimen are presented in Appendix D1 and the dynamic creep test results for each specimen are presented in Appendix D2.

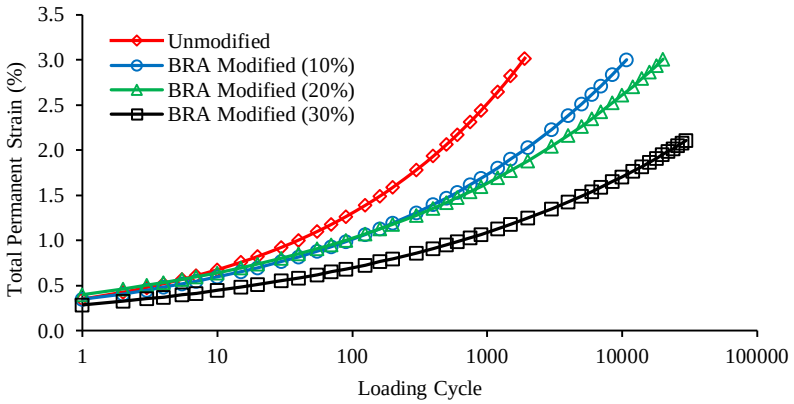

Figure 5-1. Permanent strain progression curve

Table 5-1. Regression equation developed and the results of air void contents

Asphalt mixtures	Regression equation		Voids (%)			Loading cycle
	Equation	R^2	Mean	SD	CV	
Unmodified	$y = 0.3510x^{0.2849}$	0.967	5.1	0.15	3	1900
BRA modified (10%)	$y = 0.3489x^{0.2316}$	0.981	5.1	0.10	2	10,850
BRA modified (20%)	$y = 0.4022x^{0.2029}$	0.984	5.1	0.06	1	20,200
BRA modified (30%)	$y = 0.2859x^{0.1938}$	0.978	5.1	0.14	3	30,000[1]

[1]: *The cycles obtained about 2.11% of total permanent strain instead of 3%*

The mean values have been quoted for each asphalt mixtures as shown in Table 5-1. To compare the number of cycles to achieve 3% accumulation of axial strain, the BRA modified asphalt mixtures required a higher number of cycles than the unmodified asphalt mixtures.

Table 5-2. *Paired sample t-test* results for air void contents

Asphalt mixtures	Air void			
	t	*df*	*Sig.*	*d*
Unmodified – BRA modified (10%)	-0.5	2	0.667	-0.29
Unmodified – BRA modified (20%)	0.0	2	1.000	0.00
Unmodified – BRA modified (30%)	-0.5	2	0.667	-0.29
BRA modified (10%)–BRA modified (20%)	1.0	2	0.423	0.61
BRA modified (10%)–BRA modified (30%)	0.6	2	0.592	0.36
BRA modified (20%)–BRA modified (30%)	-0.7	2	0.547	-0.41

The increase in the content of BRA modifier binder to 10%, 20%, and 30% resulted in an increase of the number of cycles by 471%, 963%, and 1478% respectively. This indicates that modifying asphalt binder with granular BRA modifier binder decreases the temperature sensitivity of asphalt mixtures. The results show that the permanent deformation of BRA modified asphalt is less dependent on temperature than that of unmodified asphalt mixtures.

In addition, Figure 5-2 allows additional analysis concerning the number of cycles to achieve an accumulative permanent strain after one million load cycles. The total permanent strain versus load cycles were plotted on a log-log scale. The same regression analysis as for Figure 5-1 was used to calculate the fatigue laws ($\varepsilon = a \times N^b$) and the coefficient of correlation showed the accuracy of the equation (R^2) summarized in Table 5-1. Increasing the content of BRA modifier binder to 10%, 20%, and 30% resulted in a decrease in the total permanent strain (ε) after one million load cycles to 52%, 63%, and 76% respectively. This indicated that the total permanent strain values reveal that the BRA modified asphalt has much better resistance to rutting than unmodified at any percentage level of BRA modifier binder.

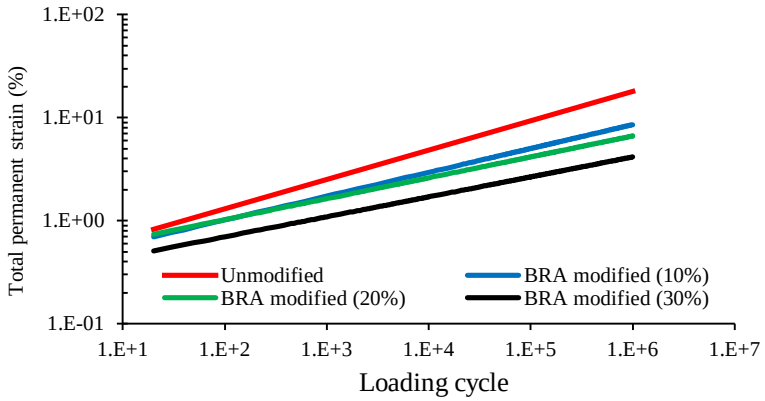

Figure 5-2. The fatigue laws from the dynamic creep test by regression analysis

The BRA modifier binder tends to reduce the damage caused by each number of cycles to the specimens, allowing more cycles until permanent strain is attained. The slopes determined between the number of cycles from 20 and one million show that the average of strain rate for unmodified asphalt was higher than for BRA modified asphalt mixtures at any percentage of BRA modifier binder, while the average minimum strain rate for unmodified asphalt mixture was higher than that for BRA modified asphalt mixtures as shown in Figure 5-3. This suggested that BRA modified asphalt mixtures were more stable than unmodified asphalt mixtures because the rate of deformation was lower than for the unmodified one.

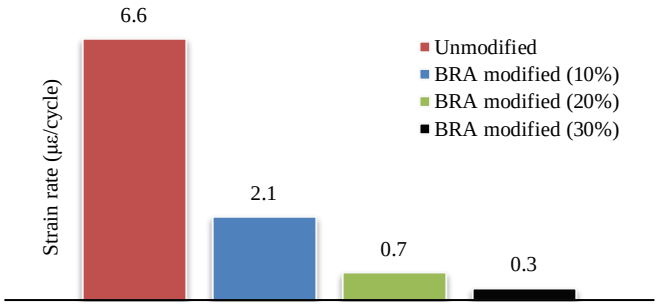

Figure 5-3. Average strain rate of the asphalt mixtures obtained from the test

5.2.2 Creep modulus of asphalt mixtures

The creep modulus can be used to indicate the permanent axial deformation of asphalt mixtures. The creep modulus is obtained from Equation 2-5 as the ratio of deviator stress to total deformation (strain).

There was a significant increase in the creep modulus of the BRA modified asphalt mixtures compared to unmodified asphalt mixtures as shown in Figure 5-4, even when the creep modulus for all mixtures showed a downward tendency. As there were three replicates tested for each asphalt mixture, the diagram was obtained from the average number of parameters in each loading using a regression analysis. The developed regression equation from fitting Figure 5-4 for every mixture is presented in Table 5-3. The creep modulus of BRA modified asphalt for any level of BRA modifier was higher than that for unmodified mixtures.

Figure 5-5 shows the results of the creep modulus at a loading cycle of 1800 cycles, which was 3600 seconds. The creep modulus increased by about 44%, 61% and 144% for the BRA modifier binder contents of with 10%, 20% and 30%.

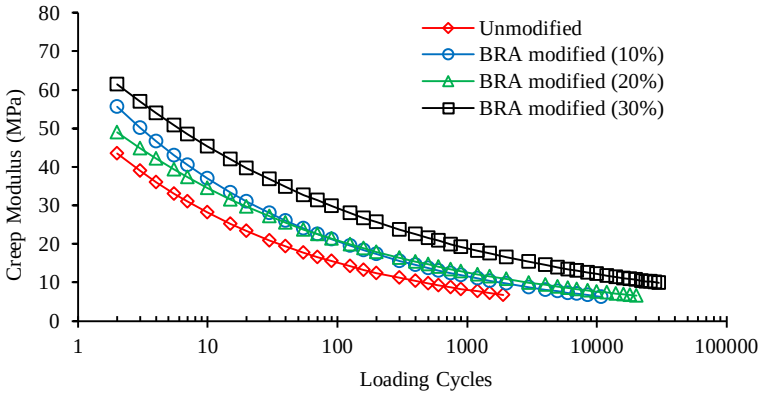

Figure 5-4. The average of the creep modulus of the asphalt mixtures after being fitted

Table 5-3. Regression equation developed for creep modulus

Asphalt mixtures	Regression equation	
	Equation	R^2
Unmodified	$y = 52.461x^{-0.271}$	0.980
BRA modified (10%)	$y = 66.191x^{-0.253}$	0.969
BRA modified (20%)	$y = 56.943x^{-0.218}$	0.970
BRA modified (30%)	$y = 70.124x^{-0.19}$	0.989

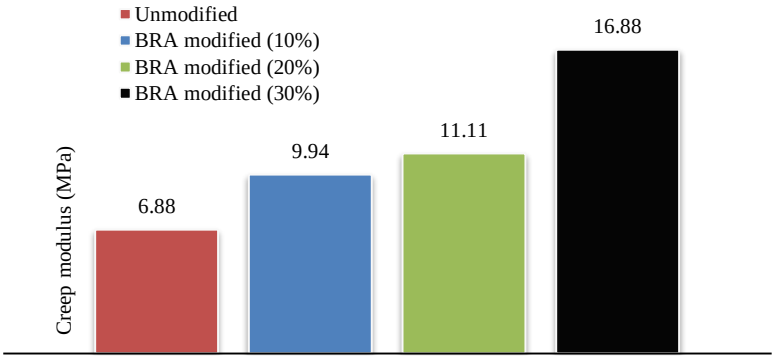

Figure 5-5. Average creep modulus of asphalt mixtures at 1800 cycles

As could be expected, unmodified asphalt mixture has the least resistance to rutting. BRA modifier binder had a positive effect in improving the rutting performance of BRA modified asphalt mixtures. As a result of the reduced temperature susceptibility of BRA modified asphalt mixtures, it is possible to increase the stiffness of BRA modified asphalt mixtures at high temperature (50°C) in order to reduce the rutting. Adding BRA modifier binder to asphalt mixtures remarkably decrease their susceptibility to permanent deformation. The results indicated the most significant enhancement in the behaviour of asphalt mixture especially for asphalt mixtures with content of 30% BRA modifier, which can be due to their higher dependency on mastic properties particularly at high temperatures.

Similar observation has been reported by other researcher. Zamhari *et al.*[15]

presented the dynamic creep test on unmodified and BRA asphalt mixtures. The test results showed that the rate of permanent deformation of unmodified mixtures was higher than for BRA asphalt mixtures while the creep stiffness values of BRA asphalt mixtures were higher compared with the unmodified asphalt mixtures.

5.2.3 Determine the flow number, flow point and minimum strain using the stepwise concept

The stepwise concept described in Section 2.4.2.2 was used in this study to determine FN, flow point, and minimum strain rate for unmodified and BRA modified asphalt mixtures. The mean, SD, and CV values for FN, flow point and minimum strain rate are shown in Table 5-4. The results for the determination of FN, flow point, minimum strain rate and slope at steady state for each specimen are presented in Appendix D4. It was concluded that a higher percentage of granular BRA modifier binder in asphalt mixtures resulted in a higher flow number and lower flow point as well as minimum strain rate.

It is indicated that the addition of granular BRA modifier binder increased the viscosity of asphalt binder which slightly reduced the development of permanent shear strain. Additionally, the gradation of the mixture affected the shear strain significantly. A higher shear strain rate was found under fewer flow number and higher flow point.

When granular BRA modifier is used and the percentage of granular BRA modifier binder is changed from 10% to 30%, the BRA modified asphalt mixtures contained a higher percentage of mineral, which it behaviour can be attributed to the aggregate grading of these mixtures. The mechanical properties of BRA modified asphalt mixtures mostly rely on the properties of mastic. Therefore, it is expected that BRA modified asphalt mixtures will be more resistant to permanent deformation than unmodified asphalt mixtures.

Furthermore, the relationship between flow number and rate of deformation is shown in Figure 5-6. The equation was built only at a testing temperature of 50°C with 5±0.5% air voids. From the data presented, it can be seen that there was a strong correlation between the flow number (FN) and rate of deformation slope at a steady state (R^2=0.96). This showed that the criteria for subjective class goodness of fit is good[51]. Similarly, Goh and You[48] reported that the rate of deformation correlated well with permanent deformation. They indicated that the flow number (FN) of an

asphalt mixture can be computed using the rate of deformation at various temperatures and air void levels using the flow number equation described in Equation 2-3, so that FN and slope at steady state maintain a good relationship in between on the stepwise concept.

Table 5-4. Flow number, flow point and minimum strain rate based on the stepwise concept

Asphalt mixtures	FN (cycles)			Flow point (%)			Minimum strain rate (με/cycle)		
	Mean	SD	CV (%)	Mean	SD	CV (%)	Mean	SD	CV (%)
Unmodified	1506	161	10.7	2.8	0.1	3.5	7.1	1.1	14.4
BRA modified (10%)	4664	601	12.9	2.6	0.2	7.5	2.2	0.4	19.6
BRA modified (20%)	8876	1482	16.7	2.5	0.2	7.3	0.8	0.1	5.1
BRA modified (30%)	25521	2738	10.7	2.4	0.4	16.4	0.3	0.1	38.4

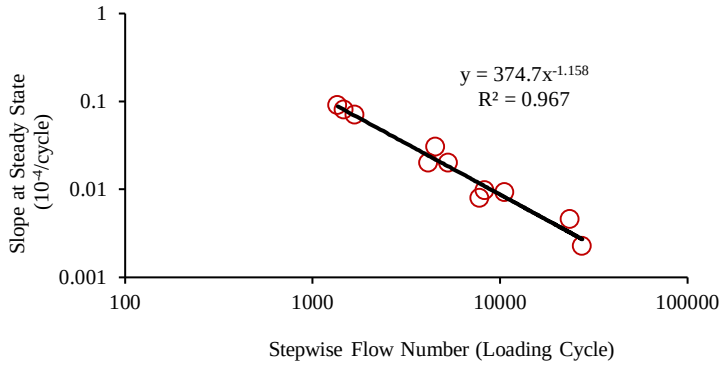

Figure 5-6. Relationship between flow number and slope

5.3 Analysis of Wheel Tracking Test Results and Discussion

The rutting performance of unmodified and BRA modified asphalt mixtures was compared based on laboratory performance. In this study, the wheel tracking test was expressed by rut depth and tracking rate in accordance with AG:PT/T231[54] to obtain the rut resistance. Furthermore, velocity and dynamic stability were used as other parameters.

5.3.1 Performance of asphalt mix using the rut depth and tracking rate

A *paired t-test* method with a 95% level of confidence was also used to statistically analyze the mean air voids of the wheel tracking test specimens using the IBM SPSS Statistics 21 program. The results show no significant difference in the void content between unmodified and BRA modified asphalt mixtures as shown in Table 5-5. The mean, SD, and CV of air void content were presented in Table 5-6. The mean air void content of asphalt mixtures was within the range of 5±1% in accordance with the Austroads Standard AG:PT/T231[54]. The results of the determination of bulk density – void content for each specimen are presented in Appendix E1.

Table 5-5. *Paired sample t-test* results for air void contents

Asphalt mixtures	Air void			
	t	*df*	*Sig*	*d*
Unmodified – BRA modified (10%)	3.4	2	0.076	1.98
Unmodified – BRA modified (20%)	2.7	2	0.111	1.59
Unmodified – BRA modified (30%)	0.4	2	0.742	2.18
BRA modified (10%)–BRA modified (20%)	1.6	2	0.236	0.97
BRA modified (10%)–BRA modified (30%)	-0.4	2	0.719	-0.24
BRA modified (20%)–BRA modified (30%)	-1.9	2	0.196	-1.10

Table 5-6. Results of air void contents and regression equation developed

Asphalt mixtures	Voids (%)			Regression equation	
	Mean	SD	CV	Equation	R^2
Unmodified	5.1	0.10	1.9	$y = 0.0771x^{0.4998}$	0.996
BRA modified (10%)	5.0	0.11	2.1	$y = 0.0122x^{0.6802}$	0.986
BRA modified (20%)	4.9	0.14	2.8	$y = 0.0977x^{0.381}$	0.984
BRA modified (30%)	5.1	0.11	2.2	$y = 0.1120x^{0.3302}$	0.970

In the laboratory, the rut was measured automatically by apparatus after chosen cycle intervals in the wheel path by measuring the settlement of the surface of the specimen. The measurements are reported in mm. Figure 5-7 presents the relationship between the number of wheel cycles and the rut (mm) for unmodified and BRA modified asphalt mixtures obtained from the wheel tracking test tested at the 60°C test condition. The curve plots the average progression of rut depth from averaging three replicates using a linear regression. The wheel travelling was stopped automatically after reaching 10,000 loading passes. Regression equations were developed between the numbers of passes and rut depth from fitting Figure 5-7 as presented in Table 5-6. The results of the determination of rut depth obtained from individual specimens are presented in Appendix E2.

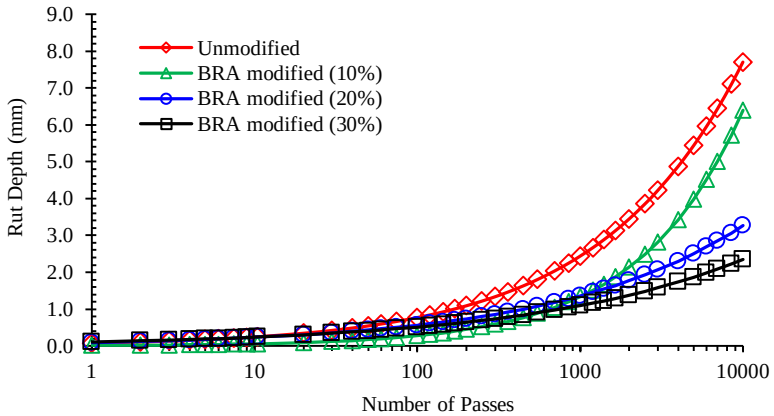

Figure 5-7. Rut progression curve of wheel tracking test

Figure 5-7 clearly shows that the rut progression curves for BRA modified asphalt mixtures are very different from unmodified asphalt mixtures. The results obtained for rut depth revealed that BRA modified performs better than unmodified

asphalt mixtures after 10,000 cycles. These values for the rut depth after 10,000 cycles as shown in Figure 5-7 are illustrated in Figure 5-8.

Based on the tracking depth according to the Austroads method[137], the unmodified asphalt mixtures had a medium performance with an average 7.7 mm rut depth, whereas the 10% BRA modified mixtures had a good performance with an average rut depth of 6.4 mm. For 20% and 30% BRA modified asphalt mixtures, their performance is included as a superior performance with 3.3 mm and 2.3 mm rut depths respectively after reaching the passes limit. It seems that the substitution of BRA modifier binder increases the shear resistance of BRA modified binder resulting in enhanced rut resistance to the mix. The percentage expressed the rut depth in percentage according to the total thickness of the specimens (50 mm). Based on those rut depths, BRA modified asphalt mixtures with 10%, 20%, and 30% BRA modifier binder had a rut depth that was shallower by about 16%, 57%, and 70%, respectively, than for unmodified mixtures. This indicated that the use of BRA modifier binder in asphalt mixtures resulted in an increase in resistance to permanent deformation (rutting) in comparison with the unmodified asphalt mixtures. The increase in the BRA modifier binder content resulted in a decrease in the rut depth for the BRA modified asphalt mixtures.

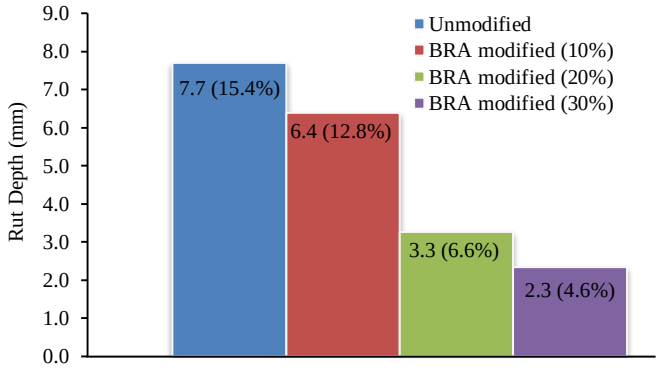

Figure 5-8. Rut depth values for asphalt mixtures after 10,000 cycles

In addition, according to Choi[3], a binder with high viscosity will have a higher shear resistance. Accordingly, this binder provides a better rut resistance in asphalt mixtures. It is believed that the role of BRA modifier binder used in BRA modified asphalt mixtures provides enhanced rut resistance compared to base asphalt binder used in unmodified asphalt mixtures.

Figure 5-9 shows the stress-strain paths for the materials in asphalt mixtures subjected to wheel tracking tests. According to Perraton *et al.*, stress-strain occurs

according to the position of the wheel on the top surface and the depth of the materials. The stress-strain paths are very complex and they are affected by the rotation and cycle of axes[23]. At point A1 (top), the materials may be subjected to a principal horizontal and vertical compression stress and at point A2 (middle), the materials may be subjected to a principal vertical compression stress and horizontal tension stress. However, at point A3 (bottom), the materials are subjected to a principal tension stress.

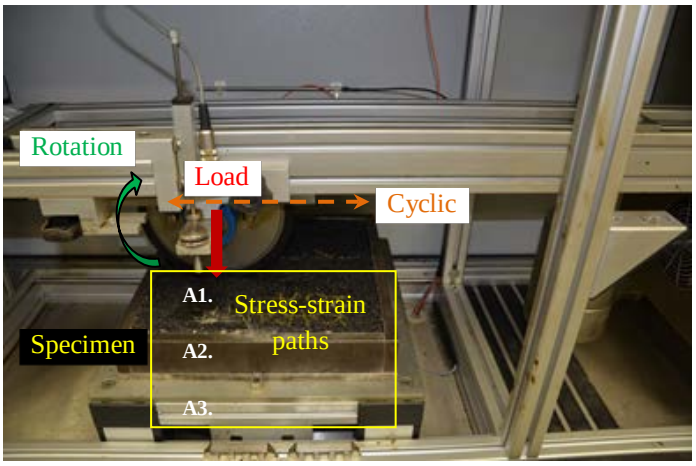

Figure 5-9. Stress-strain distributions in the specimen under cyclic load

As described in Section 2.4, the visco-plastic deformation is influenced by the rheological behaviour of the bitumen. In visco-plastic deformation, the sliding and rotation of the aggregates are mostly influenced by the ability of asphalt binder to bind the aggregates. Hence, the rheological characteristic of asphalt binder has great importance for the ability of aggregates to move in the asphalt mix.

Asphalt binders are notable for their thermo-sensitive materials. Accordingly, at a high temperature (60°C), unmodified asphalt binder has a lower stiffness compared to BRA modified binder, resulting in an increase in the lubricant effect of unmodified asphalt binder and promoting the visco-plastic deformation of unmodified asphalt mixtures, even though the effect of visco-elastic deformation at low temperature has little influence. Therefore, the unmodified mixtures had a lower resistance to permanent deformation

From the wheel tracking test results, rut resistance can also be represented by tracking rate. The tracking rate is obtained by steady tracking rate over 4,000 to 10,000 loading passes[54] as shown in Figure 5-10. Furthermore, Figure 5-11 shows the tracking rate values for unmodified and BRA modified asphalt mixtures. It can be seen in this figure that the BRA modified asphalt mixtures showed a lower tracking

rate than the unmodified asphalt mixtures. The tracking rate decreased by about 24%, 77%, and 86% for 10%, 20% and 30% BRA modifier binder, respectively.

In addition, Figure 5-12 shows that the correlation between the rut depth and tracking rate for individual specimens was strong ($R^2 = 0.983$). Mixtures with low rut depth exhibit a low tracking rate. The results obtained from individual specimens are presented in Appendix E3 and E4.

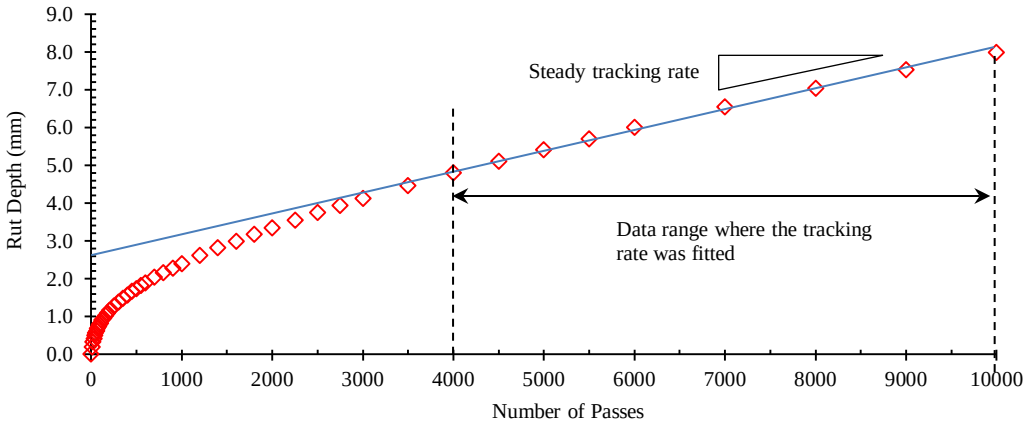

Figure 5-10. Rut depth progression curve

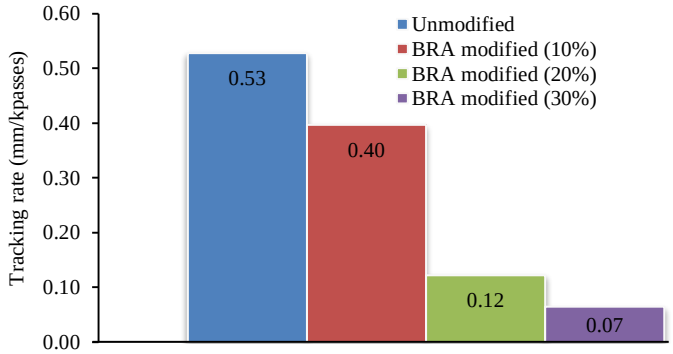

Figure 5-11. Average tracking rate values for asphalt mixtures

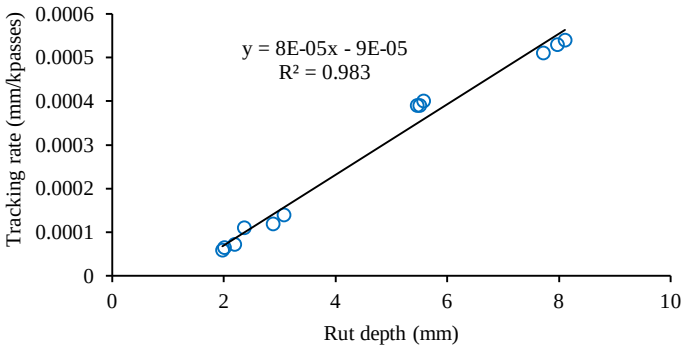

Figure 5-12. Correlation between rut depth and tracking rate

5.3.2 Performance of asphalt mix using the velocity

Development of the rut profile was also analyzed in terms of the velocity of deformation. In accordance with Fontes *et al.*[42], and Dias *et al.*[52], the velocities of deformation were obtained by corresponding the deformation verified between 120 minutes and 105 minutes using Equation 2-15.

According to Dias *et al* [52], based on the LT-173, the average rate is acceptable when the $R_{rd\text{-}105/120}$ is less than or equal to $15x10^{-3}$ mm/min. Figure 5-13 shows the results of the wheel tracking test, expressed in terms of velocity of deformation of the slab. There were noticeable differences due to the granular BRA modifier asphalt binder used. The velocity of unmodified and 10% BRA modified asphalt mixtures does not pass the criteria in accordance with NLT-173 where the velocity of those mixtures was higher than 0.015 mm/minute. However, the velocity values for 20% and 30% BRA modified asphalt mixtures is much lower than the limit. The results obtained from individual specimens are presented in Appendix E5.

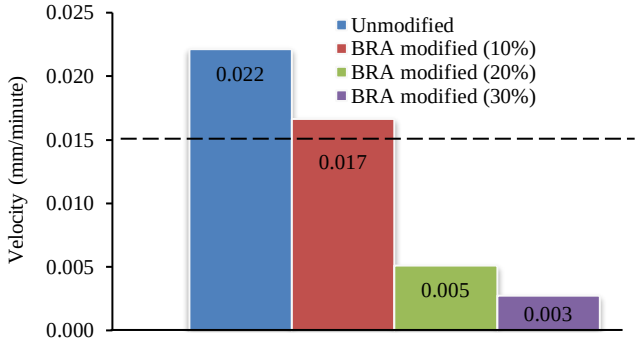

Figure 5-13. Average velocity for asphalt mixtures

5.3.3 Performance of asphalt mix using the dynamic stability

The results for dynamic stability were also used to evaluate the rutting characteristics of unmodified and BRA modified asphalt mixtures. In accordance with Chen *et al* [53], the dynamic stability of asphalt mixtures was determined during a test of 45 minutes to 60 minutes to generate a 1-mm rut depth. Equation 2-6 was used to calculate the dynamic stability of asphalt mixtures.

Figure 5-14 shows the average dynamic stability of asphalt mixtures. The results obtained from individual specimens are presented in Appendix E6. It can be summarized that unmodified asphalt mixtures lead to relatively lower dynamic stability values than BRA modified asphalt mixtures. The increase in the BRA modifier binder content resulted in an increase in dynamic stability for the BRA modified asphalt mixtures. The increase in the content of BRA modifier binder to

10%, 20%, and 30% resulted in an increase in the dynamic stability by 48%, 197% and 386% respectively. According to Chen *et al*, the dynamic stability should be more than 1500 cycles/mm[53].

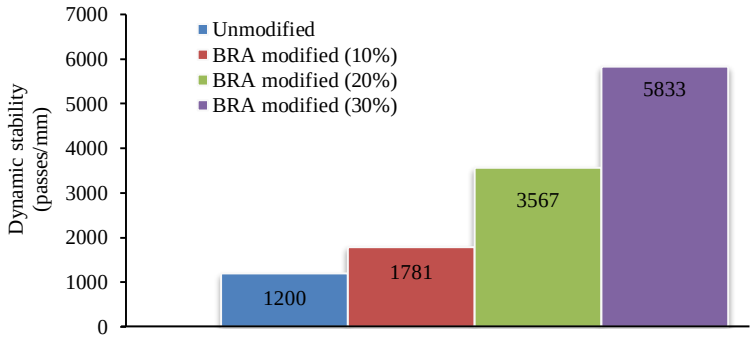

Figure 5-14. Dynamic stability values for asphalt mixtures

5.4 Summary

Dynamic creep tests were performed on unmodified and BRA modified asphalt mixtures in accordance with AS 2891.12.1-1995 under the following test conditions: test temperature of 50°C, air void content of 5.0±1.0%, and compressive stress of 200±5 kPa. The proportion of BRA modifier binder substituted base binder was 10%, 20%, and 30% by total weight of asphalt binder. The following observations have been made based on the analysis in this study:

(1) The addition of granular BRA modifier binder in asphalt mixtures at 10%, 20%, and 30% by total weight of asphalt binder increased the number of cycles to achieve 3.0% accumulation axial strain by 471%, 961%, and 1478%, respectively. Accordingly, the increase in the content of BRA modifier binder resulted in a lower permanent strain/a higher number of cycles due to greater stiffness.

(2) The average minimum strain rate of BRA modified asphalt mixtures was lower compared with the unmodified asphalt mixtures. The minimum strain rate for BRA modified asphalt mixtures decreased as the percentage of BRA modifier binder increased. This reveals that the BRA modified asphalt mixtures were more stable than unmodified asphalt mixtures.

(3) A significant increase in creep modulus for BRA modified asphalt mixtures was achieved compared to unmodified asphalt mixtures. The BRA modified asphalt mixtures had a higher creep modulus than unmodified asphalt mixtures for each value of loading cycles. Comparing the creep modulus at loading cycles of 1800

(3600 seconds), the creep modulus of BRA modified asphalt mixtures with 10%, 20%, and 30% BRA modifier binder increased by 44%, 61% and 144%, respectively.

(4) Based on the stepwise method, the addition of BRA modifier binder to asphalt mixtures had an effect on the flow number, flow point, and minimum strain rate of asphalt mixtures. A higher percentage of BRA modifier binder resulted in a higher flow number, however, the flow point and minimum strain rate decreased with an increase in the percentage of BRA modifier binder.

(5) The flow number was higher for BRA modified asphalt mixtures than for unmodified asphalt mixtures. A higher percentage of granular BRA modifier in asphalt mixtures resulted in a higher flow number, a lower flow point, and a lower minimum strain rate.

Furthermore, wheel tracking tests were performed on unmodified and BRA modified asphalt mixtures based on the Austroads standard AG:PT/T231 under a range of condition as follows: test temperature of 60°C, air void content of 5±1.0% and vertical load of 700±20 N. The proportion of BRA modifier binder substituted for base binder was 10%, 20% and 30% by total weight of asphalt binder. The following observations have been made based on the analysis in this study:

(1) The addition of BRA modifier binder in asphalt mixtures increased the resistance of BRA modified asphalt mixtures to rutting depth. The rut depth of BRA modified asphalt mixtures decreased by 16%, 57% and 70% as the percentage of BRA modifier binder increased by 10%, 20% and 30%, respectively.

(2) The tracking rate of BRA modified asphalt mixtures measured over 4,000 to 10,000 loading passes decreased by 24%, 77% and 86% with an increase in the percentage of BRA modified binder by 10%, 20% and 30%, respectively.

(3) The velocity for BRA modified asphalt mixtures was lower than for unmodified asphalt mixtures. A higher percentage of BRA modifier binder in asphalt mixtures resulted in lower velocity values for the BRA modified asphalt mixtures.

(4) The dynamic modulus of BRA modified asphalt mixtures was higher than for unmodified asphalt mixtures. The dynamic modulus of BRA modified asphalt mixtures increased with an increase in the percentage of BRA modifier binder.

CHAPTER 6

EVALUATION OF THE EFFECT OF GRANULAR BRA MODIFIER BINDER ON THE FATIGUE LIFE OF ASPHALT MIXTURES

6.1 Introduction

Fatigue cracking is considered to be one of the most common forms of distress relating to repeated loading during asphalt pavement life, as described in Section 2.4.4. The reliable evaluation of fatigue strength for asphalt mixtures is necessary to determine the flexible pavement strength. In this study, a thorough understanding of BRA modified asphalt mixtures in terms of fatigue strength characteristics is required for minimizing the fatigue failure of asphalt mixtures.

The objective of Chapter 6 is, however, to assess the effect of granular BRA modifier binder on the fatigue life of asphalt mixtures. Laboratory evaluation methods for fatigue strength on four point bending equipment under repeated flexural bending test was done as described in Section 3.5.4. The repeated flexural bending test results were analyzed by examining the parameters including: (a) flexural initial stiffness and phase angle of asphalt mixtures, (b) fatigue life of asphalt mixtures based on the classical approach and energy stiffness ratio, (c) fatigue life prediction based on the strain approach and strain-mix stiffness approach, and (d) damage rate based on the flexural stiffness progression curve and cumulative dissipated energy.

6.2 Analysis of Repeated Flexural Bending Test Results and Discussion

6.2.1 Flexural stiffness and phase angle of asphalt mixtures

Flexural stiffness and phase angle are used for evaluating the fatigue resistance of asphalt mixtures. These concepts are widely used to study the fatigue failure criteria for asphalt mixtures and grouped into linear viscoelastic properties.

The asphalt mixture is subjected to the flexural stress from the localized negative bending due to repetitive stress and strains caused by load. Thus, flexural stiffness (the stiffness measured in bend) is a potential indicator for characterizing the property of asphalt mixtures. According to Daniel *et al.*[145] and Abojaradeh *et al*,[88] the flexural stiffness has been widely used to study fatigue performance of asphalt mixtures and it is well accepted as the fundamental properties of asphalt mixtures. Hence, the flexural stiffness is importance in evaluating both the load induced and

thermal stress-strain distribution in asphalt mixtures. Furthermore, phase angle is used to manifest fatigue damage as an increase in the phase angle, and a decrease in the flexural stiffness. In this term, phase angle accounts for the effect of damage.

Typical results for the repeated flexural bending test for flexural stiffness and phase angle are presented in Figure 6-1. This figure plotted the relationship between flexural stiffness and number of cycles. Three phases were observed for flexural stiffness, which is similar to those presented by Hassan and Khalid[96], Di Benedetto *et al.*[74], and Maggiore *et al.*[146, 147]. Phase 1 is characterized by a rapid reduction in flexural stiffness due to repetitive excitation, which is then followed by Phase 2, where the reduction in the stiffness modulus is approximately linear.

Di Benedetto *et al*. discussed that in Phase 1, the decrease in flexural stiffness is not only considered to be caused by fatigue damage, but heating and a third phenomenon also play important role. In this phase, the stiffness loss is totally recoverable. In Phase-2, the role of fatigue in the decrease in flexural stiffness is predominant. The effect of thermal heating is small during this phase, however it has still to be considered. Phase 1 and Phase 2 correspond to the crack initiation process in the asphalt mixtures. Finally, the flexural stiffness exhibits a marked drop in Phase 3, after passing through an inflection point with load cycles culminating in failure. In Phase 3, local crack propagation occurs. Further, the macrocrack or cracks starts to develop and global failure is obtained at the end of this phase. The damage could be isolated and characterized only by Phase 2[74]. However, the phase angle tends to show constant behaviour during the test after a rapid increase in Phase 1.

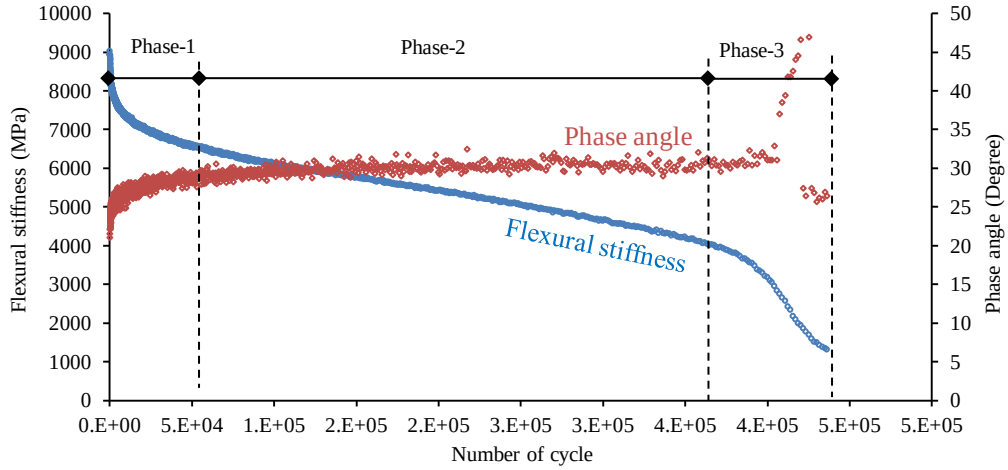

Figure 6-1. Progression curve of flexural stiffness and phase angle

The mean, standard deviation (SD), and coefficient of variation (CV) for air void, initial flexural stiffness and phase angle for both unmodified and BRA

modified asphalt mixtures are presented in Table 6-1. The initial flexural stiffness values were recorded at 50 cycles, where the CV values of initial flexural stiffness for both mixtures are maximum 10%. Furthermore, Table 6-2 summarizes the statistics analysis for air void, initial flexural stiffness and phase angle of unmodified and BRA modified asphalt mixtures. A *paired sample t-test* method with 95% level of confidence was used to statistically analyze using IBM SPSS Statistics 21 program.

Table 6-1. Average air void content, flexural stiffness and phase angle

Asphalt mixtures	Initial tensile strain (με)	Air void (%)			Initial flexural stiffness (MPa)			Phase angle (degree)		
		Mean	*SD*	*CV*	*Mean*	*SD*	*CV*	*Mean*	*SD*	*CV*
Unmodified	400	5.1	0.06	1.1	5044	509	10	33.8	2.4	7
Unmodified	600	5.0	0.06	1.1	5155	174	3.4	34.1	0.3	1
Unmodified	800	5.1	0.10	2.0	5365	309	5.7	33.7	1.1	3
BRA modified	400	4.9	0.06	1.2	8639	197	2.3	21.9	0.9	4
BRA modified	600	5.0	0.00	0.0	8562	396	4.6	25.9	2.6	10
BRA modified	800	5.0	0.10	2.0	9002	135	1.5	22.8	1.1	5

Table 6-2. The summary of *paired sample t-test* of air voids, initial flexural stiffness and phase angle

Asphalt mixtures	Initial tensile strain (με)	Air void				Initial flexural stiffness				Phase angle			
		t	*df*	*Sig.*	*d*	*t*	*df*	*Sig.*	*d*	*t*	*df*	*Sig.*	*d*
Unmodified	400 – 600	1.7	2	0.225	1.75	-0.3	2	0.779	-0.18	-0.196	2	0.862	-0.19
	400 – 800	0.5	2	0.667	0.49	-2.6	2	0.118	-1.53	-0.206	2	0.856	-0.21
	600 – 800	-0.8	2	0.529	-0.75	-0.8	2	0.484	0.49	0.813	2	0.502	0.47
BRAmodified	400 – 600	-2.0	2	0.184	-2.03	0.2	2	0.831	0.14	-4.223	2	0.052	-4.22
	400 – 800	-2.0	2	0.184	-2.03	-2.8	2	0.106	-1.63	-1.623	2	0.246	-1.62
	600 – 800	0.0	2	1.000	0.00	2.3	2	0.151	1.31	1.623	2	0.246	1.62
Unmodified - BRAmodified	400	3.4	2	0.074	3.46	-8.8	2	0.013	-5.09	14.321	2	0.005	14.33
	600	1.0	2	0.423	1.00	-16.3	2	0.004	-9.42	5.657	2	0.030	5.66
	800	1.7	2	0.225	1.73	-16.6	2	0.004	-9.58	8.738	2	0.013	8.73

According to studies, the density (air voids) affects the fatigue life of asphalt mixtures. Vazquez *et al.*[38] included the air void content as one of the factors most affecting the resistance to fatigue cracking of asphalt mixtures. Nejad *et al.*[148] stated that adequate binder content and density should be used in asphalt mixtures to increase the resistance to fatigue cracking. Low asphalt content and high air voids in asphalt mixtures also tend to show fatigue cracking. Mogawer *et al.*[149] also had gave attention to the density of asphalt mixtures as a factor related to fatigue cracking potential. Baburamani[75] and Hartman *et al.*[27] described that the degree of compaction (air void content) achieved in the mix affected the flexural stiffness and fatigue life of asphalt mixtures.

The beam fatigue samples in this study were provided with statistically the same density with the aim of limiting the effect of density on flexural stiffness, while the mean air voids were within the range of 5.0 ± 0.5%. The results of the determination of bulk density – air voids, initial flexural stiffness, and phase angle

for each specimen are presented in Appendix F1, F2 and F3, respectively. In addition, related to this research methodology, Tarefder *et al.*[150], Nejad *et al.*[148], and Bhattacharje and Mallick[151] included mix aggregate gradation as a factor affecting the cracking in asphalt mixtures.

As presented in Table 6-2, the difference in the initial tensile strain did not significantly affect the initial flexural stiffness values in the same mixtures for both unmodified and BRA modified asphalt mixtures (significance > 0.05). The tensile strain occurring in the bottom of the asphalt layer is considered to be a parameter controlling fatigue cracking.

However, comparing the flexural stiffness at the same strain level indicates that the initial flexural stiffness of BRA modified mixtures was statistically significantly higher than for unmodified mixtures (significance < 0.05). The initial flexural stiffness for BRA modified asphalt mixtures at 400, 600, and 800 με was 71%, 61%, and 67%, respectively, higher than for unmodified asphalt mixtures as presented in Figure 6-2. It can be concluded the behaviour of the BRA modified mixtures at a given initial tensile strain and measured at a loading frequency of 10 Hz was more elastic.

The flexural strain of BRA modified asphalt mixtures is generated by the cohesive strength of the BRA modified binder and the bond strength of the BRA modified binder–aggregate interface. Asphalt mixture with higher tensile strength provides better resistance to fatigue. This would further imply that modified mixtures appear to be capable of withstanding larger tensile strain prior to cracking. Therefore, BRA modifier binder added in the asphalt mixtures can generate a higher tensile strength in the BRA modified asphalt mixtures which improve the long-term performance of asphalt pavement.

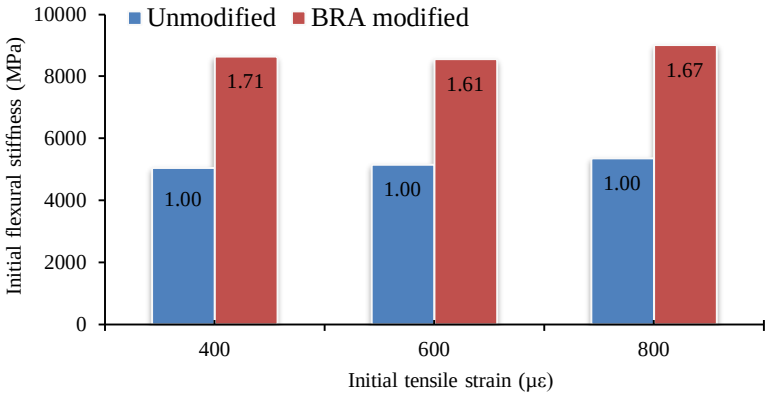

Figure 6-2. The initial flexural stiffness values for asphalt mixtures

In addition, Figure 6-3 shows the phase angle for unmodified and BRA modified asphalt at a given initial tensile strain. The phase angle for the two asphalt mixtures did not indicate sensitivity to initial tensile strain (significance > 0.05), while the phase angle values for the unmodified asphalt mixtures at 54%, 37%, and 47% were significantly higher than the values obtained for the BRA modified asphalt mixtures for a given initial tensile strain (significance < 0.05) as shown in Table 6-2. This means that the BRA modified mixtures show less viscous behaviour than the unmodified mixtures.

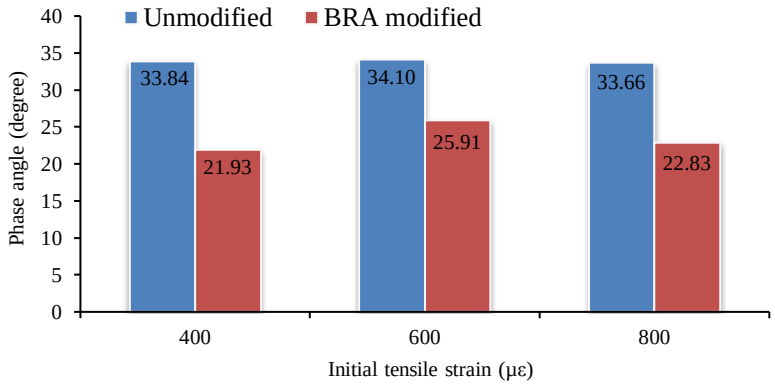

Figure 6-3. Average phase angle for unmodified and BRA modified asphalt mixtures

6.2.2 Fatigue life of asphalt mixtures

Fatigue is a phenomenon defined as progressive damage which is capable of leading to its rupture caused by load and environmental factors as described in Section 2.4.4. In the fatigue test, a finding is normally based on the type of test and the geometry of the specimen. In this context, the most critical situation is based on the control of the displacement amplitude where a large number of repetitions is carried out in order to obtain a set of results which represents the fatigue phenomenon for bituminous mixtures. Hence, this correlates the number of cycles applied to bituminous mixtures until its ruptures. Fatigue life is the number of cycles that a specimen sustains before failure.

The results of the flexure fatigue tests in term of fatigue life obtained in this study were analyzed using the classical approach and energy stiffness ratio (ER) method developed by Abojaradeh[152]. In the classical method, the failure point (N_{f50}) is assumed to be the number of loading corresponding to the 50% reduction of initial flexural stiffness. This failure criterion of asphalt mixtures has been widely defined in the strain controlled test to present fatigue crack initiation as described in Section

2.4.4. Furthermore, Kim *et al.*[153] and Li *et al.*[72] have used the 50% reduction of initial flexural stiffness as a failure criterion in fatigue testing.

The ER method defines the energy stiffness ratio as the ratio of the flexure stiffness at cycle-*i* (S_i) to the initial flexure stiffness (S_o) multiplied by the load cycle value at cycle-*i* (N_i) as shown by Equation 2-23. Figure 6-4 shows the relationship between the number of cycles and the energy stiffness ratio, where the fatigue failure (N_f) is determined by plotting the peak value of energy stiffness ratio to the number of cycles. During the test, it can be seen that the values of the energy stiffness ratio improves as the number of cycles (N_i) increases until it reaches a peak value. During this time, the value of the load cycle (N_i) is continuously increases, whereas the value of initial flexural stiffness (S_0) is constant and the value of flexural stiffness at cycle – *i* (S_i) might slightly decrease. Further, the value of the energy stiffness ratio decreases suddenly after reaching its peak value. During this time, the stiffness of materials (S_i) is suddenly decreases even though the number of cycles (N_i) increases. Accordingly, Abojaradeh[98] has defined the fatigue failure as the number of load repetition at the peak value of the curve.

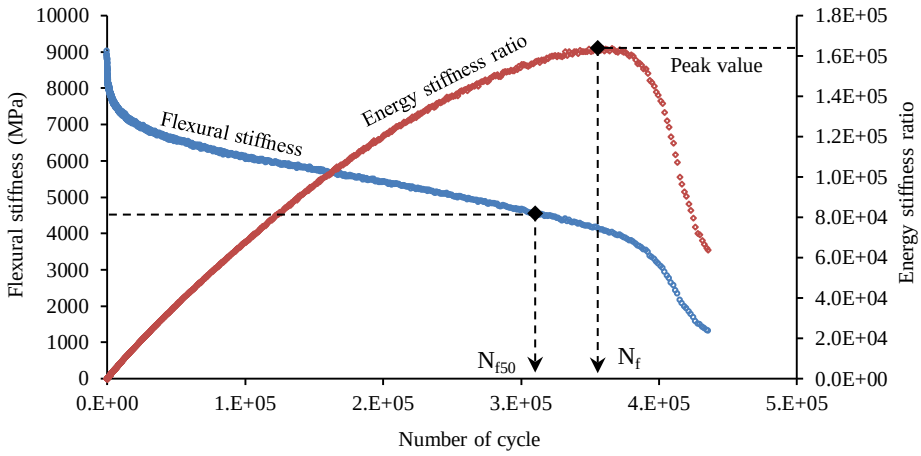

Figure 6-4. Energy stiffness ratio *versus* loading cycles (for a specimen tested at 20°C and 400 εμ)

The results for the mean fatigue life of the asphalt mixtures using both classical and energy stiffness ratio approaches are summarized in Table 6-3, while the results from the determination of fatigue life obtained from individual specimens are presented in Appendix F4 and F5. The fatigue life ratio presented in Table 6-3 was defined by dividing the fatigue life of BRA modified by the fatigue life of unmodified asphalt mixtures. Comparison of the fatigue life for unmodified and BRA modified asphalt mixtures at the same initial tensile strain, indicates that the fatigue life of BRA modified was about 2.0 – 2.4 and 1.6 – 2.1 by using the classical

and ER approaches, respectively, higher fatigue lives when compared to unmodified asphalt mixtures.

To compare the unmodified and BRA modified asphalt mixtures, the fatigue life at 400, 600, and 800 με was assessed by developing a fatigue curve for each mixture and this is presented in Figure 6-5. The analysis of fatigue life presents evidence that the fatigue life of the mixtures is identical for both classical and ER approaches.

Table 6-3. The summary of fatigue life and fatigue life ratio for unmodified and BRA modified

Initial tensile strain (με)	Fatigue life, N_f (cycle)				Fatigue life ratio	
	Classical		ER		Classical	ER
	Unmodified	BRA modified	Unmodified	BRA modified		
400	134,487	306,933	163,113	341,953	2.3	2.1
600	42,663	85,283	56,247	88,283	2.0	1.6
800	9,617	22,933	11,990	24,050	2.4	2.0

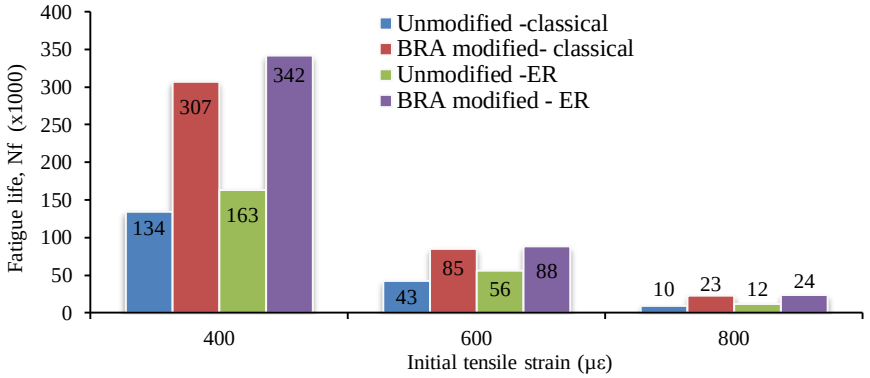

Figure 6-5. Mean fatigue life of asphalt mixtures

Asphalt mixtures are complex materials in term of viscoelastic behaviour when applied to loading and environment conditions. A continued flexing occurs in the asphalt mixture when traffic loading is applied. Therefore, the stiffness and nature of asphalt mixtures affect the magnitude of the strain[18]. The better performance of BRA modified asphalt mixtures in fatigue life may be attributed to the unique combination of base asphalt binder and BRA modifier binder compared to unmodified asphalt mixtures. Binder can be an important factor for higher fatigue life in BRA modified asphalt mixtures. As shown in the ITSM test presented in Chapter 4, BRA modified asphalt mixtures are stiffer which may contribute to greater strength within the mix, thereby increasing the fatigue life. The mixtures which have greater interlocking between the aggregates have a better tensile stress resistance and consequently have better fatigue life[148]. Vazquez *et al.*[38] and Tarefder *et al.*[150] included asphalt binder grade and asphalt binder content as the factors most affecting resistance to fatigue cracking in asphalt mixtures. As Guler[154] and Khiavi and Ameri[70] argued, binder

type is considered to be an important factor among the other factors in mixture variables such as aggregate gradation, aggregate type, binder content, compaction temperature and traffic loading, which can have a significant effect on the fatigue life of the bituminous mixes.

In addition, the ratio of flexural stiffness was introduced in accordance with the ER method. The ratio of flexural stiffness was defined by dividing the flexural stiffness for a given fatigue failure (S_f) by the initial flexural stiffness (S_0). The results of these values are presented in Table 6-4. It can be seen that the mean ratios of flexural stiffness obtained were 0.42 – 0.44 for unmodified asphalt mixtures and 0.48 for BRA modified asphalt mixtures, respectively. The results confirmed that the fatigue life of unmodified and BRA modified asphalt mixtures developed by using the ER method are longer compared with the fatigue life of asphalt mixtures analyzed by using the classical method (50% initial stiffness reduction). Similar observations have been reported by other researchers. Khiavi and Ameri[70] stated that the fatigue life based on the RDEC and DER criteria corresponds to 65% and 55% initial stiffness reduction. Maggiore *et al.*[146] found that the fatigue life was longer than the 50% initial stiffness reduction. Other researchers, Rowe[155] and Walubita[156] stated that this phenomenon usually occurs in a range of 40-50%.

Table 6-4. Flexural stiffness ratio of asphalt mixtures using energy-stiffness ratio method

Initial tensile strain (με)	Unmodified			BRA modified		
	Initial stiffness (S_0) (MPa)	Stiffness at failure (S_f) (MPa)	Ratio (S_f/S_0)	Initial stiffness (S_0) (MPa)	Stiffness at failure (S_f) (MPa)	Ratio (S_f/S_0)
400	5044	2238	0.44	8639	4120	0.48
600	5155	2160	0.42	8562	4153	0.48
800	5365	2242	0.42	9002	4337	0.48

Figure 6-6 shows the sensitivity of the energy stiffness ratio change due to the change in strain. The value of the energy stiffness ratio (N_i x S_i/S_0) at failure corresponded to the number of cycles at failure for all specimens on the log-log scale. The results show a straight line with a much higher coefficient of determination R^2 (0.996). The regression equation developed in Figure 6-6 is:

$$y = 0.332x^{1.028} \quad (6\text{-}1)$$

The (N_i x S_i/S_0) at failure is then expressed by (N_f x S_f/S_0), so Equation 6-1 is then changed to become as follows:

$$\frac{N_f \times S_f}{S_o} = 0.332(N_f)^{1.028}$$

As the power of 1.023 is close to 1.0, the Equation 6-1 can be approximated by:

$$\frac{S_f}{S_o} = 0.332 \qquad (6-2)$$

The result is similar to data gathered by another researcher. According to Abojaradeh[98], the (S_f/S_0) value is 0.3512 for controlled strain, and there is no difference between the curves for controlled strain and controlled stress.

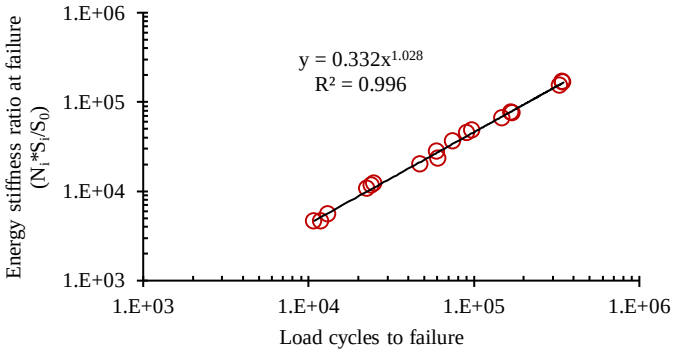

Figure 6-6. Energy stiffness ratio at failure vs load cycles at failure for controlled strain

6.2.3 Fatigue life prediction of asphalt mixtures

The strain approach and strain-mix stiffness approach are used to predict the fatigue life of unmodified and BRA modified asphalt mixtures. A simple form of strain approach model was established for the control strain test using the linear regression analysis between fatigue life logarithm (log N_f) and the initial strain logarithm (log ε_0). The strain approach model can be represented as Equation 2-15**.** This model was also presented by Awanti *et al.*[76], Shukla and Das[157], Li *et al.*[72], Pereira *et al.*[158], and Bhattacharjee and Mallick[151]. As a study by Pell; Di Benedetto and De la Roche cited in Baburamani[75] shows, the asphalt binder and asphalt mixture stiffness strongly influences the critical horizontal strain or stress due to traffic load on the asphalt layer and contributes to the slope of the initial strain line. Further, the incorporation of the applied strain and the stiffness in the mix were expressed as Equation 2-16[75, 91, 159].

Following Equation 2-15, an empirical relationship between fatigue life (N_f) and initial tensile strain (ε_0) for unmodified and BRA modified mixtures was developed and used to determine the phenomenological (classical) and ER approach during the regression analysis as shown in Figure 6-7. The fatigue life from three replicates of each initial tensile strain for unmodified and BRA modified asphalt were plotted in the form of X-Y plots. Using a power regression, the equations for fatigue life-initial tensile strain were developed for unmodified and BRA modified

asphalt mixtures. The fatigue equations shown are developed from best fit to these data. The classical (phenomenological) and ER relationship between the number of cycles (N_f, in cycle) and the initial strain (ε_0, in με) for asphalt mixtures tested was obtained as:

(a) For unmodified asphalt mixtures using classical approach

$$N_f = 8.662E + 14\left(\frac{1}{\varepsilon_0}\right)^{3.752} \qquad R^2 = 0.958 \qquad (6-3)$$

(b) For unmodified asphalt mixtures using energy-stiffness ratio approach

$$N_f = 7.534E + 14\left(\frac{1}{\varepsilon_0}\right)^{3.694} \qquad R^2 = 0.953 \qquad (6-4)$$

(c) For BRA modified asphalt mixtures using classical approach

$$N_f = 1.430E + 15\left(\frac{1}{\varepsilon_0}\right)^{3.705} \qquad R^2 = 0.984 \qquad (6-5)$$

(d) For BRA modified asphalt mixtures using energy-stiffness ratio

$$N_f = 2.777E + 15\left(\frac{1}{\varepsilon_0}\right)^{3.800} \qquad R^2 = 0.988 \qquad (6-6)$$

From Figure 6-7, it can be concluded that for a given initial tensile strain, the BRA modified mixtures results in a longer fatigue life compared to unmodified asphalt mixtures tested at 20 ºC. Further, these curves can be used to perform the structural design of asphalt mixtures with regard the number of loads required and the tensile strain level developing in the pavement.

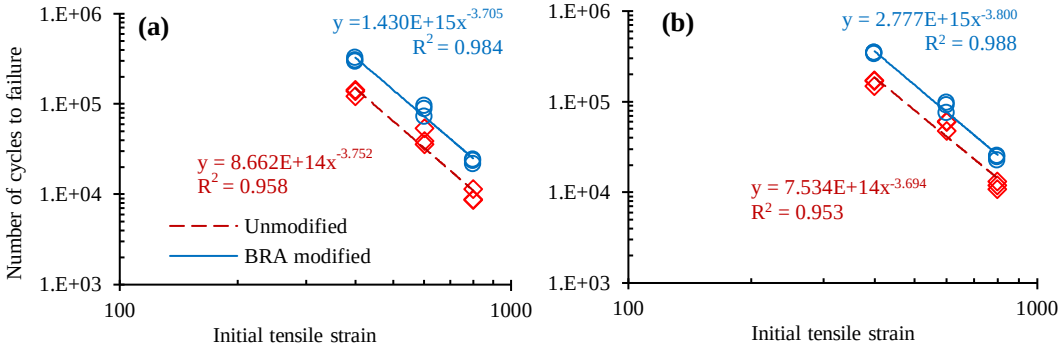

Figure 6-7. Fatigue characteristics of unmodified and BRA modified asphalt mixtures, (a) Classical approach, (b) ER approach

Carpenter *et al.*[92] stated that strains at the bottom of the pavement layer subjected to traffic and used in the structural design are extremely low, typically below 100 με, and are usually developed through a linear extrapolation of the traditional fatigue data, even though the fatigue behaviour at low strain levels does not follow the same relationship as the materials subjected to strains at the normal levels developed above 300 με.

Fatigue tests carried out at normal strain level can clearly indicate the fatigue curve of different mixes. However, traditional fatigue test carried out at a low strain level of 300 με or lower will be a time-consuming fatigue test even though the results appear to show distinctly different performance for mixtures tested at low strain levels compared to the normal strain level[92].

Furthermore, Awanti *et al.* described that the tensile strains at the bottom of the bituminous layer in a typical pavement are about 30 to 200 με under a standard axle load[76]. Hence, for this reason, using fatigue life-initial tensile strain the fatigue lives of unmodified and BRA modified asphalt were compared at 200με levels. It was found that at a testing temperature of 20ºC, the BRA modified asphalt mixtures showed 1.91 times greater fatigue lives than unmodified asphalt mixtures.

The intercept and the slope, k_1 and k_2 respectively, are the important variables obtained from the test. Under the strain-controlled mode of loading, these variables represent the properties of materials used in asphalt mixtures and typical values for asphalt mixtures. According to Ghuzlan and Carpenter[160], k_1 and k_2 can be used in the fatigue based mechanism design procedures and the typical range of k_2 values are between 3 and 6. In this study, it was noted that all of the slopes of the fatigue curve (k_2) were within this range even though in some fatigue models k_2 was fixed to specific number, as in the Asphalt Institute and Illinois fatigue equation, where the k_2 value is fixed to 3.29 and 3.0 respectively[160]. Ghuzlan and Carpenter[99] argue that k_1 and k_2 is fundamental values of the asphalt mixtures.

Figure 6-8 shows the correlation between the k_1 and k_2 values obtained from the flexural beam fatigue test for unmodified and BRA modified asphalt mixtures included in this study which gives a good correlation (R^2 = 0.895 and 0.927). As shown in this figure, the k_1 and k_2 values are located in one line in spite of the different mixture properties. The k_1 and k_2 variables for each sample are presented in Appendix F6. The relationship shown here is consistent with the finding of other researchers[160]. The relation between k_1 and k_2 from all sets of data is given in Equation 6-7 and 6-8:

(a) For asphalt mixtures using the classical approach:

$$k_2 = 0.341.Log\,(k_1) - 1.400 \qquad (6-7)$$

(b) For asphalt mixtures using the ER approach:

$$k_2 = 0.309.Log\,(k_1) - 0.940 \qquad (6-8)$$

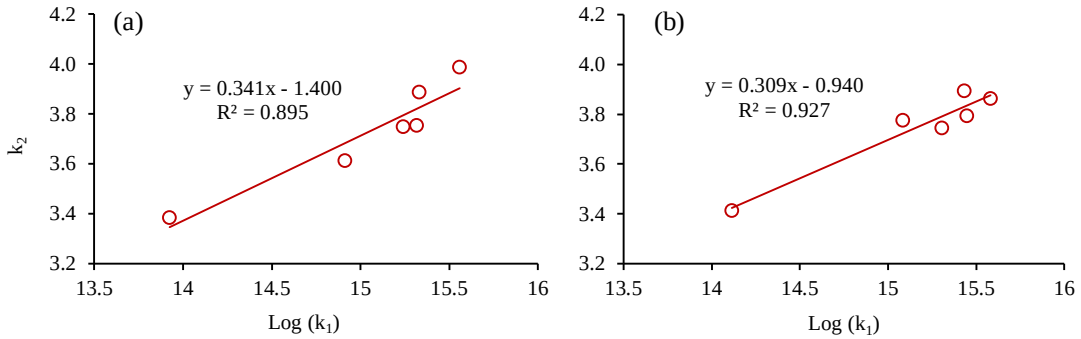

Figure 6-8. The relation of k_1-k_2 for all of asphalt mixtures using: (a) classical approach, (b) ER approach

In addition, Figure 6-9 shows the effect of using BRA modifier binder on k_1-k_2 relation. It can be seen that both lines are not close and it can be proven that there is a significance difference between two lines (at 95% level of significance). Therefore, it is concluded that the use of BRA modified binder in asphalt mixtures has a significant effect on the k_1-k_2 relation. According to Ghuzlan and Carpenter, asphalt type, air void level and aggregate do not significantly influence the k_1-k_2 relationship. In contrast, the mode of loading, the testing temperature, and asphalt content have a significant effect on the k_1-k_2 relationship[160].

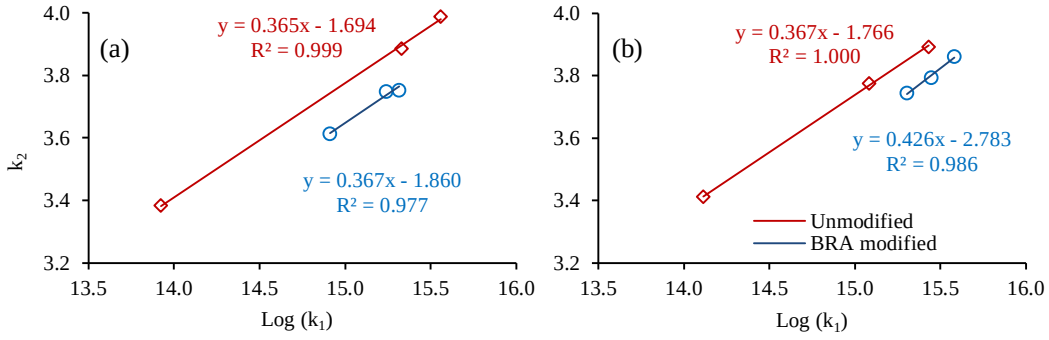

Figure 6-9. The relation of k_1-k_2 for unmodified and BRA modified asphalt mixtures, (a) using classical approach, (b) using energy-stiffness ratio approach

Furthermore, in accordance with Equation 2-16, statistical analysis was carried out to develop the strain-stiffness relationship between the number of cycles (N_f, in cycles) as a dependent variable and initial strain (ε_0, in με) and the initial flexural stiffness (S_0, in MPa) as independent variables for the unmodified and BRA modified asphalt mixtures. The following prediction models for N_f are presented:

(a) For unmodified asphalt mixtures using the classical approach

$$N_f = 5.105E + 17\left(\frac{1}{\varepsilon_0}\right)^{3.711}\left(\frac{1}{S_0}\right)^{0.770} \qquad R^2 = 0.937 \qquad (6.9)$$

(b) For unmodified asphalt mixtures using the ER approach

$$N_f = 1.505E + 16\left(\frac{1}{\varepsilon_0}\right)^{3.660}\left(\frac{1}{S_0}\right)^{0.375} \qquad R^2 = 0.938 \qquad (6.10)$$

(c) For BRA modified asphalt mixtures using the classical approach

$$N_f = 1.832E + 28\left(\frac{1}{\varepsilon_0}\right)^{3.518}\left(\frac{1}{S_0}\right)^{3.457} \qquad R^2 = 0.992 \qquad (6.11)$$

(d) For BRA modified asphalt mixtures using the ER approach

$$N_f = 9.332E + 27\left(\frac{1}{\varepsilon_0}\right)^{3.620}\left(\frac{1}{S_0}\right)^{3.304} \qquad R^2 = 0.996 \qquad (6.12)$$

Figure 6-10 shows the effect of initial flexural stiffness on the fatigue life of unmodified and BRA modified asphalt mixtures, in accordance with Equations 6-9 to 6-12. The equations are plotted at various values of initial tensile strain (200 με to 1200 με) and initial flexural stiffness (1000 MPa to 20,000 MPa). It can be seen that the cycle to failure (N_f) decreases as initial flexural stiffness (S_0) increases for both unmodified and BRA modified asphalt mixtures. The cycle to failure of BRA modified is higher than for the unmodified asphalt mixtures until initial flexural stiffness (S_0) reaches about 13,030 MPa and 11,500 MPa for the classical and ER approaches, respectively. However, the cycle to failure (N_f) values were observed to be lower for the BRA with a higher initial flexural stiffness (S_0) than those mentioned above.

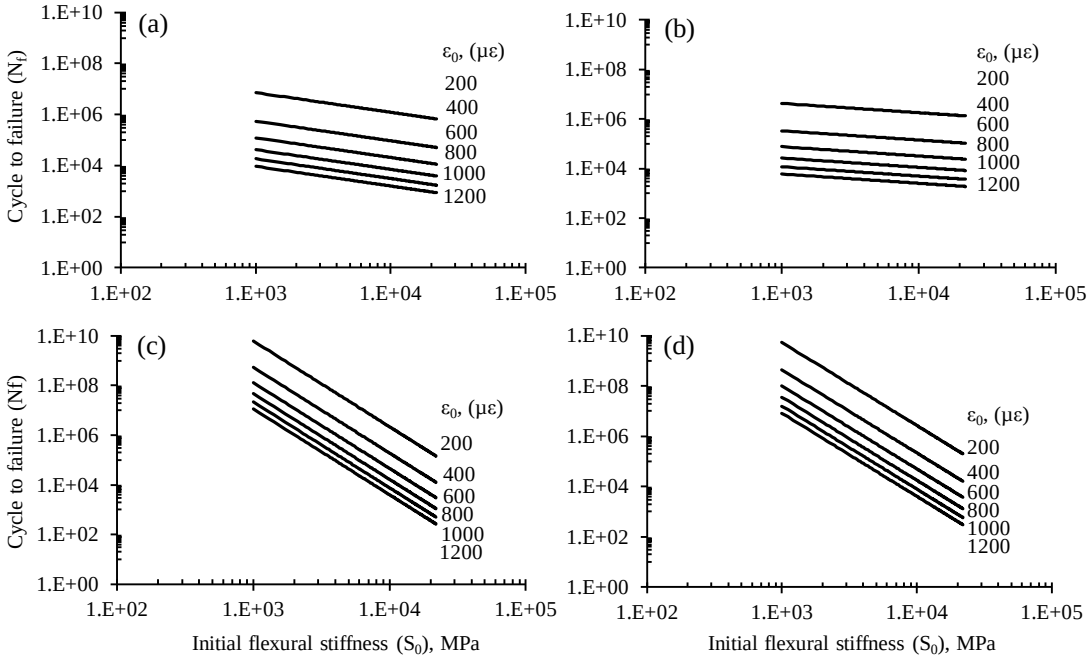

Figure 6-10. Strain-stiffness relationship between N_f, ε_0, and S_0: (a) Unmodified (classical), (b) Unmodified (ER), (c) BRA modified (classical), and (d) BRA modified (ER)

Similar observations have been reported by other researchers, such as Monismith *et al.*[159] who stated that fatigue life is influenced by the flexural stiffness of asphalt mixtures. Accordingly, the substitution of base asphalt binder with BRA modifier binder which resulted in an initial flexural stiffness of BRA modified asphalt mixtures greater than 13,030 MPa (using the classical approach) or 11,500 MPa (using the ER approach), respectively, will have a cycle to failure lower than for unmodified asphalt mixtures.

6.2.4 Dissipated energy

The energy dissipated can be used as a great indicator of fatigue response during each loading cycle, because it captures both elastic and viscous effects. An example of dissipated energy evolution with the number of cycles obtained in this study is given in Figure 6-11. The figure shows that during a fatigue test, the stiffness of asphalt mixtures reduces, resulting in microcracks in the materials when repeated stresses are applied to the specimen below the failure stress; therefore the dissipated energy varies per each loading cycle and decreases for controlled strain tests. As Carpenter and Shen[161] have said, the energy dissipated in a loading cycle is affected by the energy applied in the previous cycles. Baburamani[75] suggested that the rate of dissipated energy change per cycle is a better indicator of the initiation and growth of damage or cracking. In this study, the dissipated energy was obtained for each cycle for both unmodified and BRA modified asphalt mixtures. Further, typical results for cumulative dissipated energy in this study are presented in Figure 6-12.

As seen in Figure 6-12, with the test carried out in constant strain mode, the increase in number of loading cycles resulted in a decrease in flexural stiffness, and increase in cumulative dissipated energy. With a rapid reduction in flexural stiffness at phase 1, however, the cumulative dissipated energy increases rapidly.

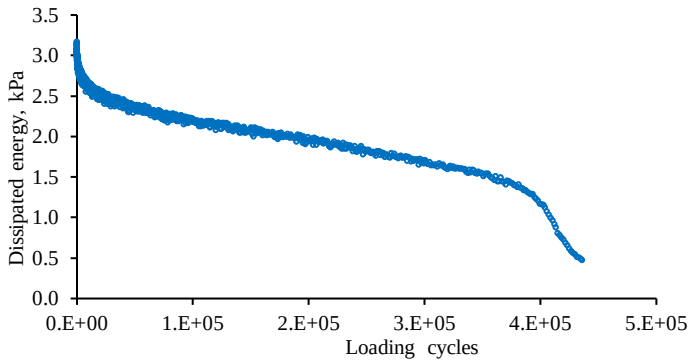

Figure 6-11. Evolution of dissipated energy per cycle

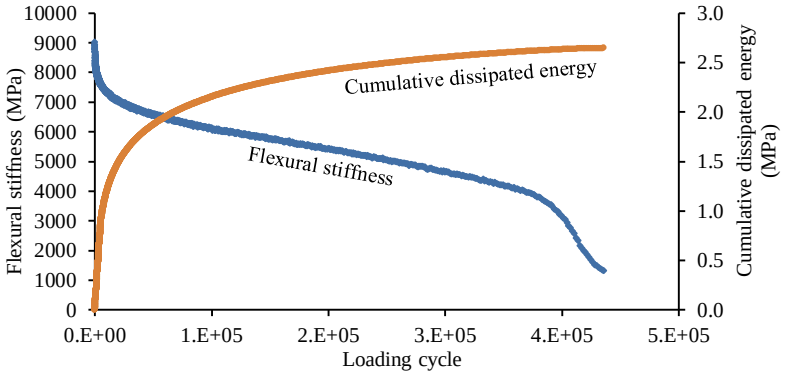

Figure 6-12. Progression curve of flexural stiffness and cumulative dissipated energy (20°C, 400με)

Further, the cumulative dissipated energy increases linearly at phase 2. According to Di Benedetto *et al.*[74], the fatigue damage could be characterized only by phase 2, and Equation 6-13[96] was used to obtain the damage rate *dD/dN* as a function of the slope of the line in phase 2.

$$\frac{dD}{dN} = \left(\frac{1}{E_{00}}\right) * \left(\frac{dE^*}{dN}\right) \tag{6-13}$$

where, E_{00} : y-axis intercept of the fitted straight line

dE^*/dN : Slope of the fitted straight line of phase 2

The results of the damage parameters obtained in accordance with the progression curve of flexural stiffness and cumulative dissipated energy are presented in Tables 6-5 and 6-6 respectively, from which it can be noticed that BRA modifier binder had an influence on the damage parameters for asphalt mixtures. The data for the damage parameters for each triplicate specimen of unmodified and BRA modified asphalt mixtures based on the flexural stiffness and cumulative dissipated energy are summarized in Appendix F7 and F8, respectively. Lytton *et al.*[162] suggested that the rate of change of dissipated energy per cycle is a better indicator of the initiation and growth of damage or cracking. Comparing the damage parameter at the same initial tensile strain, the slopes and damage rate values for unmodified asphalt mixtures in both flexural stiffness and the cumulative dissipated energy progression curve were higher compared with the BRA modified asphalt mixtures. These results revealed that BRA modified asphalt mixtures have much better resistance to fatigue failure than unmodified asphalt mixtures.

Table 6-5. The summary of damage parameters of unmodified and BRA modified asphalt mixtures based on the flexural stiffness progression curve

Initial tensile strain (με)	Unmodified			BRA modified		
	dE/dN*	E_{00}	*dD/dN*	*dE*/dN*	E_{00}	*dD/dN*
400	0.00775	3641	2.153E-06	0.00768	6885	1.116E-06
600	0.0267	3696	7.210E-06	0.0159	5839	2.701E-06
800	0.1581	4175	3.776E-05	0.0606	5962	9.894E-06

Table 6-6. The summary of damage parameters of unmodified and BRA modified asphalt mixtures based on the cumulative dissipated energy

Initial tensile strain (με)	Unmodified			BRA modified		
	dE/dN*	E_{00}	*dD/dN*	*dE*/dN*	E_{00}	*dD/dN*
400	1.861E-06	1.357	1.368E-06	1.303E-06	2.148	5.616E-07
600	0.0012	59	2.136E-05	0.0006	123	6.109E-06
800	0.0032	21	1.755E-04	0.0016	70	2.281E-05

In addition, as Hopman *et al.*[163] has stated, cumulative dissipated energy has a good correlation with crack initiation. A study by Van Dijk cited in Baburamani established a relationship between the number of cycles to fatigue failure and total dissipated energy per unit volume to the failure point[75]. Figure 6-13 shows a relationship between the number of cycles to failure and cumulative dissipated energy to the failure point for unmodified and BRA modified asphalt mixtures using the classical and ER approach. The figure was developed for all specimens tested at 400 με, 600 με, and 800 με as some factors such as temperature, loading frequency, and mode of loading did not seem to have an effect on this relationship. It can be seen that the slopes (k_2) of the curves for BRA modified asphalt mixtures was higher than for unmodified asphalt mixtures. The results reveal that the sensitivity of cumulative dissipated energy to the number of cycles to failure was higher than for the unmodified asphalt mixtures.

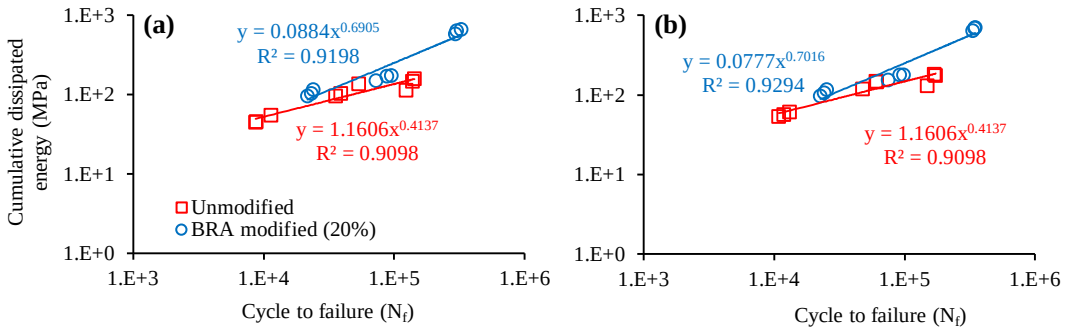

Figure 6-13. Relationship between cycle to failure and cumulative dissipated energy: (a) classical approach; (b) ER approach

Furthermore, Figure 6-14 shows the cumulative initial dissipated energy values for unmodified and BRA modified asphalt mixtures recorded at 50 cycles. The initial tensile strain seems to have a significant effect on cumulative initial dissipated

energy for both asphalt mixtures. A higher initial strain resulted in a higher cumulative initial dissipated energy. It can be seen that the cumulative initial dissipated energy values for BRA modified asphalt mixtures are higher than for unmodified asphalt mixtures. The cumulative initial dissipated energy values for BRA modified asphalt mixtures increased by 1.5 to 1.8 times.

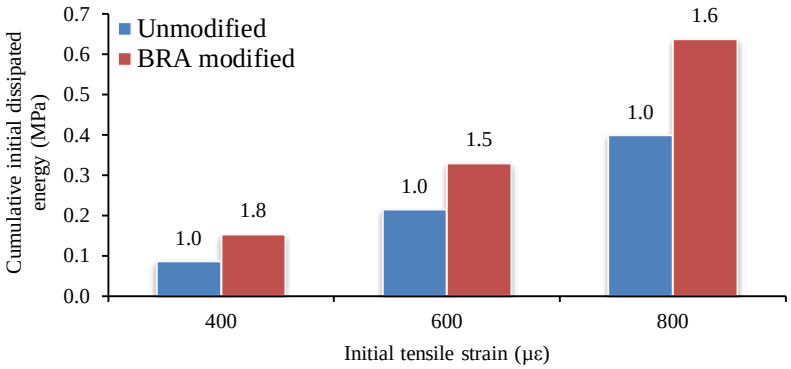

Figure 6-14. Cumulative initial dissipated energy for asphalt mixtures

6.3 Summary

Repeated flexural bending tests were performed on unmodified and BRA modified asphalt mixtures at initial tensile strains of 400, 600 and 800 με, a test temperature of 20°C, loading frequency of 10 Hz, and loading mode of continuous haversine on controlled strain test in accordance with the Austroads AG:PT/T233 test method to find out the effect of BRA modifier binder on the fatigue strength of BRA modified asphalt mixtures. The proportion of BRA modifier binder in BRA modified asphalt mixtures was 20% by total weight of asphalt binder. All specimens were tested with statistically the same air voids and were within the range of 5.0±0.5%. The following observations have been made based on the analysis in this study:

(1) Initial flexural stiffness for BRA modified asphalt mixtures tested at initial tensile strains of 400, 600, and 800 με were 71%, 61%, and 67%, respectively, higher than for unmodified asphalt mixtures. In addition, the phase angle values for unmodified asphalt mixtures for given initial tensile strain were 54%, 37%, and 47% higher than that for BRA modified asphalt mixtures. The results indicate that the behaviour of BRA modified asphalt mixtures was more elastic (less viscous) than the unmodified asphalt mixtures. The change in the initial tensile strain in the testing process did not significantly affect the initial flexural stiffness and phase angle values for both unmodified and BRA modified asphalt mixtures.

(2) Two methods were used to compare the fatigue lives of asphalt mixtures: the classical (phenomenological) and energy stiffness ratio approach. It is shown that the number of cycles to failure obtained by the energy stiffness ratio analysis is generally greater than the classical method. The ratio of flexural stiffness were 0.42–0.44 and 0.48 for unmodified and BRA modified asphalt mixtures, respectively (less than 50% reduction).

(3) The number of cycles for BRA modified asphalt mixtures were longer than for the unmodified asphalt mixtures. When the asphalt mixtures were prepared with 20% BRA modifier binder, the number of cycles for BRA modified asphalt mixtures increased by 2.0-2.4, and 1.6-2.1 observed by the using classical and energy stiffness ratio approaches, respectively.

(4) The regression equation models in accordance with the strain approach and strain-stiffness approach were used to predict the fatigue life of unmodified and BRA modified asphalt mixtures. According to the strain approach, the number of cycles to failure for BRA modified asphalt mixtures was higher when compared with unmodified asphalt mixtures. Furthermore, based on the strain-stiffness approach, the initial flexural stiffness (S_0) affected the fatigue life of unmodified and BRA modified asphalt mixtures. The cycles to failure of BRA modified asphalt mixtures were higher than for unmodified asphalt mixtures as initial flexural stiffness increased by up to 13,030 MPa and 11,500 MPa for classical and energy stiffness ratio approach, respectively. However, the cycles to failure of BRA modified asphalt mixtures were lower compared with unmodified when the initial flexural stiffness increased.

(5) The regression equations model used to predict the fatigue life of unmodified and BRA modified asphalt mixtures based on the strain approach and strain-mix stiffness approach were developed. The use of BRA modifier binder in asphalt mixtures had a significant effect on the relationship between intercept (k_1) and slope (k_2) variables.

(6) The damage to asphalt mixtures due to their fatigue response was observed by using an energy dissipated and flexural stiffness progression curve. The damage rate for BRA modified asphalt mixtures was lower than for the unmodified asphalt mixtures. The results showed that BRA modified asphalt mixtures have better resistance to fatigue failure than unmodified asphalt mixtures.

CHAPTER 7

EVALUATION OF THE EFFECT OF GRANULAR BRA MODIFIER BINDER ON THE DYNAMIC MODULUS OF ASPHALT MIXTURES

7.1 Introduction

The dynamic modulus of asphalt mixtures (|E*|) is categorized as one of the primary properties for determining a material's response during the application of dynamic loading over a range of testing temperatures and loading frequencies.

The objective of Chapter 7 is therefore to assess the effect on the dynamic modulus of asphalt mixtures of using granular BRA modifier binder. The laboratory evaluation method using the AMPT test was employed as described in Section 3.5.5. The analysis of the AMPT test results included: (1) the dynamic modulus values for the asphalt mixtures and the prediction of the rutting potential of the asphalt mixtures based on the dynamic modulus values; (2) developing the dynamic modulus master curve and comparing the measured and master curve dynamic moduli; (3) comparing the effect of granular BRA modifier binder based on the dynamic modulus master curve; (4) the phase angle values of asphalt mixtures and the rutting performance indicator used to evaluate the resistance of asphalt mixtures to rutting; (5) the black space diagram; and (6) the relationship between the dynamic modulus and resilient modulus of asphalt mixtures, and between the dynamic modulus and rutting depth.

7.2 Analysis of Dynamic Modulus Test Results and Discussion

7.2.1 Laboratory dynamic modulus of asphalt mixtures

Table 7-1 summarizes the mean, standard deviation and coefficient of variation of the air voids for unmodified and BRA modified asphalt mixtures. In order to avoid the air voids having an effect on the dynamic modulus test results, the unmodified and BRA modified asphalt specimens were tested at the same air void level. According to Mogawer *et al.*[149], the density of asphalt mixtures affects the dynamic modulus results for mixtures tested at different temperatures and frequencies. Cho *et al.*[164] investigated the effect of air voids on the dynamic modulus and found that the dynamic modulus decreases as the air voids increase, while the phase angle shows the opposite trend. Shu and Huang[165] also argued that air voids have an effect on the dynamic modulus of asphalt mixtures.

A *paired sample t-test* with a 95% level of confidence was used to statistically analyze the mean air voids using the IBM SPSS Statistics 21 program and revealed no significant different in air voids between the asphalt mixtures as shown in Table 7-2, with the air void contents being within the range of 5.0 ± 0.5%. The results of the determination of bulk density – void contents for each specimen are presented in Appendix G1.

Table 7-1. Summary of air void contents for the AMPT test

Asphalt mixtures	Voids		
	Mean (%)	SD (%)	CV (%)
Unmodified	5.0	0.03	0.67
BRA modified (10%)	5.1	0.1	1.0
BRA modified (20%)	5.0	0.1	2.0
BRA modified (30%)	5.1	0.06	1.25

Table 7-2. Summary of *paired sample t-test* results for air voids of the AMPT test specimen

Asphalt mixtures	Air void			
	t	*df*	*Sig. (2-t)*	*d*
Unmodified – BRA modified (10%)	1.7	2	0.225	1.75
Unmodified – BRA modified (20%)	0.5	2	0.667	0.49
Unmodified – BRA modified (30%)	-0.8	2	0.529	-0.75
BRA modified (10%)–BRA modified (20%)	-2.0	2	0.184	-2.03
BRA modified (10%)–BRA modified (30%)	3.4	2	0.074	3.46
BRA modified (20%)–BRA modified (30%)	1.0	2	0.423	1.00

The mean dynamic modulus values for unmodified and BRA modified asphalt mixtures obtained from laboratory tests at ten different loading frequencies and four different testing temperatures are presented in Figure 7-1, and the data for each set of triplicate samples and their overall averages are summarized in Appendix G2. As expected, the dynamic modulus decreases as loading frequency decreases under a constant testing temperature. Under a constant frequency, the dynamic modulus also decreases with an increase in the test temperature for the same mixtures. The change in dynamic modulus is consistent with the temperature among the asphalt mixtures. The dynamic modulus of the unmodified asphalt mixtures was the lowest at all loading frequencies and testing temperatures. For BRA modified asphalt mixtures, the addition of BRA modifier binder seems to have a significant effect on dynamic modulus values. A higher percentage of BRA modifier binder resulted in a higher dynamic modulus for the asphalt mixtures.

Figure 7-1 shows that the dynamic modulus is dependent not only on the loading frequency but also on the testing temperature. Change in the dynamic modulus was found to occur as either the loading frequency and/or temperature was varied. The behaviour of asphalt mixtures in term of the dynamic modulus is strongly influenced by a combination of temperature and frequency.

The dependency on the loading frequency is more evident at high temperatures (37 ºC and 54 ºC) than intermediate (21.1 ºC) and low temperature (4.4 ºC). A higher temperature resulted in a lower dynamic modulus which indicates more viscous behaviour. For example, at 54 ºC, the dynamic modulus of the BRA modified asphalt mixture with 30% BRA modifier binder increased by 24 times when the loading frequency increased from 0.01 Hz to 25 Hz, while it only increased by 2.3 times at 4.4 ºC. This reveals that asphalt mixtures display more viscous behaviour in term of high temperature resulted in a lower aggregates interlocking. This indicates that aggregate interlocking seems to have a significant effect on dynamic modulus values.

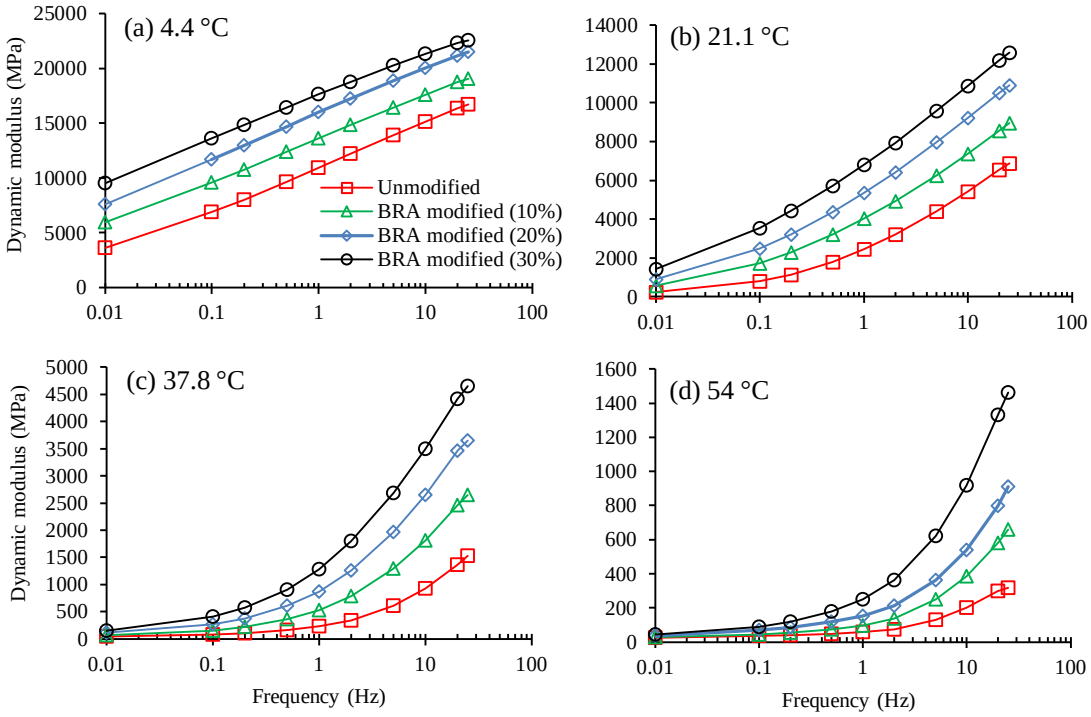

Figure 7-1. Average dynamic modulus test results for asphalt mixtures

As an alternative means of showing the consequence of adding BRA modifier binder to asphalt mixtures, Figure 7-2 shows the relationship between the dynamic modulus values for unmodified and BRA modified asphalt mixtures. The points are above the line of equality, representing an increased dynamic modulus value due to the BRA modifier binder substitution. Figures 7-2(a) through 7-2(c) show the effect for each percentage of BRA modifier binder. A higher percentage of BRA modifier binder in the asphalt mixtures resulted in a higher dynamic modulus. The dynamic modulus increase by 1.17, 1.38, and 1.50 for the mixtures prepared with 10%, 20%, and 30% BRA modifier binder, respectively. Figure 7-2(d) illustrates the average increase in dynamic modulus by 1.35 due to the substitution of BRA modifier binder.

Currently the dynamic modulus is under consideration as a parameter for determining resistance to permanent deformation of asphalt mixtures based on the Superpave volumetric mixtures design procedure[166]. In order to predict the permanent deformation potential, Wang *et al.*[39] recommended conducting the dynamic modulus test at loading frequencies of 10 Hz and 0.1 Hz to represent highway speed and intersection traffic respectively. The dynamic modulus at 0.1 Hz represents the worst conditions for rutting potential. According to Zhou *et al.*[167], the rutting performance of asphalt mixtures can be evaluated by using the dynamic modulus values tested at a loading frequency of 10 Hz and high temperature. Accordingly, the dynamic modulus values for unmodified and BRA modified mixtures tested at loading frequencies of 10 Hz and 0.1 Hz and high testing temperatures of 37.8 and 54.0 °C were used in this study to evaluate the rutting performance of asphalt mixtures as shown in Figure 7-3. The dynamic modulus values for unmodified asphalt mixtures were lower than for the BRA modified asphalt mixtures, indicating that the unmodified asphalt mixtures had a greater rutting potential than the BRA modified asphalt mixtures. Hence, the substitution of base asphalt binder with granular BRA modifier binder can improve the rutting resistance performance of asphalt mixtures.

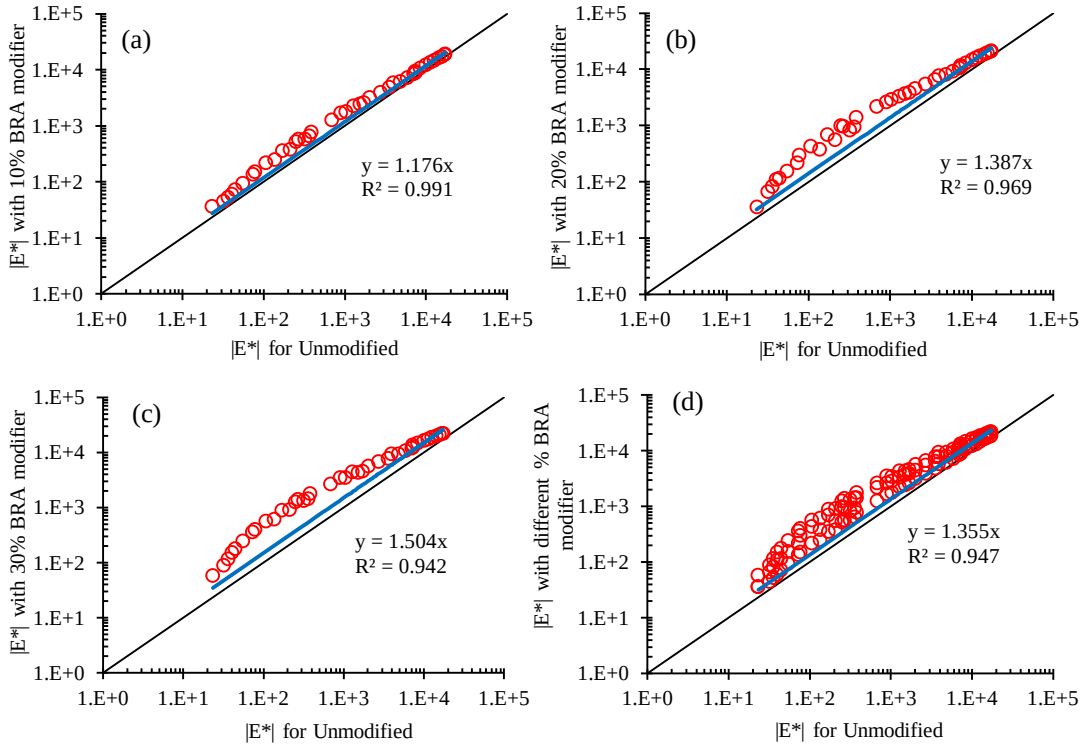

Figure 7-2. Dynamic modulus relationship between unmodified and BRA modified mixtures

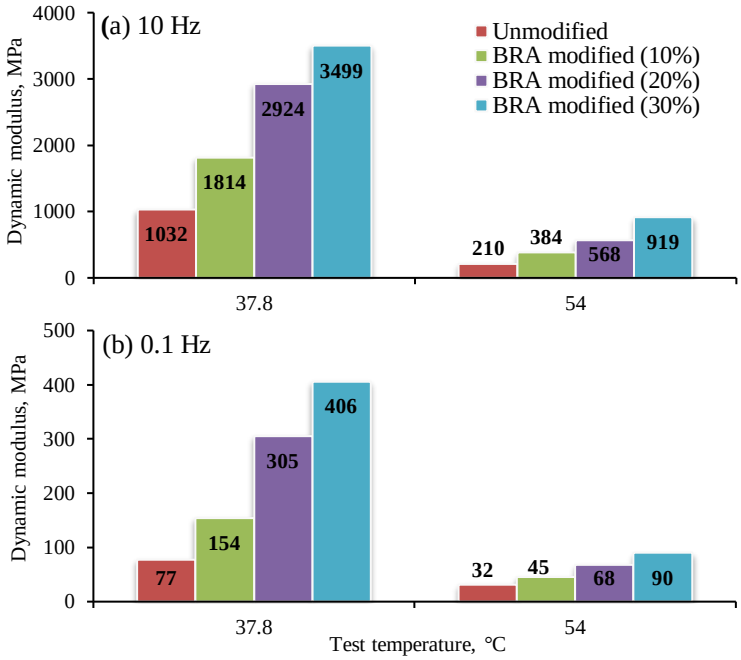

Figure 7-3. Dynamic modulus of asphalt mixtures tested at 10 and 0.1 Hz

7.2.2 Developing the dynamic modulus master curve for the asphalt mixtures

The objective of the master curve is to determine the dynamic moduli of asphalt mixtures at various conditions as described in Section 2.4.3. For further analysis, the effect of temperatures and loading frequencies were combined to show the susceptibility to different temperatures of the asphalt mixtures with different BRA modifier binder contents. The concept of the time-temperature superposition principle was used to utilize the effect of the combination of temperature and frequency on dynamic modulus by establishing master curves.

The laboratory dynamic modulus test data at the ten testing frequencies and four testing temperatures for each asphalt mixture, as detailed in Appendix G2, were combined to develop master curves for the dynamic modulus. A master curve was constructed using a sigmoidal model shown as Equation 2-10 for a reference temperature of 21°C for all of the asphalt mixtures. The dynamic modulus data were then shifted into a master curve for the analysis of the asphalt mixtures performance by simultaneously solving shift parameters. The relationship between the logarithm of the shift factors and test temperature is illustrated in Figure 7-4. The shift factors were similar for all asphalt mixtures. At 37.8°C and 54°C, the curves seemed slightly out of alignment. For all mixtures, the shift factors followed a second-order polynomial with respect to temperature. The seven parameters in accordance with Equations 2-20 and 2-22 as seen in Table 7-3 were then used to calculate the dynamic modulus |E*| for unmodified and BRA modified asphalt mixtures with

particular percentages of BRA modifier binder over the range of test temperatures and loading frequencies used in this testing.

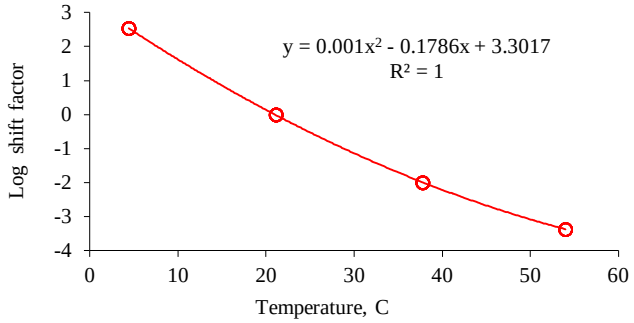

Figure 7-4. Shift factor of asphalt mixtures (30% BRA modified asphalt mixtures)

Table 7-3. Dynamic modulus and shift parameter

Asphalt mixtures	Dynamic modulus parameter				Shift parameter			
	δ	α	β	γ	a	b	c	R^2
Unmodified	0.269	3.142	-1.051	-0.733	0.001	-0.169	3.117	1.0
BRA modified (10%)	0.310	3.137	-1.330	-0.682	0.001	-0.172	3.188	1.0
BRA modified (20%)	0.130	3.419	-1.523	-0.581	0.001	-0.158	3.020	1.0
BRA modified (30%)	0.335	3.192	-1.663	-0.617	0.001	-0.178	3.301	1.0

Figure 7-5 illustrates the measured dynamic modulus data and fitted master curve for each asphalt mixture plotted on a log scale. The accuracy and effectiveness of the master curve were checked by comparing the measured and master curve dynamic moduli. Figure 7-6 is a plot of the master curve dynamic modulus ($|E^*|_{Master\ curve}$) calculated from Equation 2-10 and the laboratory dynamic modulus test data ($|E^*|_{Lab}$) for unmodified and BRA modified asphalt mixtures.

The dynamic modulus data calculated from Equation 2-10 are presented in Appendix G3. Figure 7-6 shows that the master curve dynamic modulus data gives identical results when compared to the laboratory dynamic modulus data. Accordingly, the dynamic modulus obtained from the master curve can be used to substitute for the laboratory dynamic modulus data.

The errors in the dynamic modulus master curve were normalized using Equation 7-1 obtained by using the same set of shift factors and different sets of shift factors following Zhao *et al.*[168]. The results of the normalized error are presented in Appendix G4.

$$NE = \frac{\left|E^*_{Lab} - E^*_{Master\ curve}\right|}{E^*_{Lab}} \times 100\% \qquad (7\text{-}1)$$

where: *NE* : Normalized error

E^*_{Lab} : Laboratory dynamic modulus (MPa)

$E^*_{Master\ curve}$: Master curve dynamic modulus (MPa)

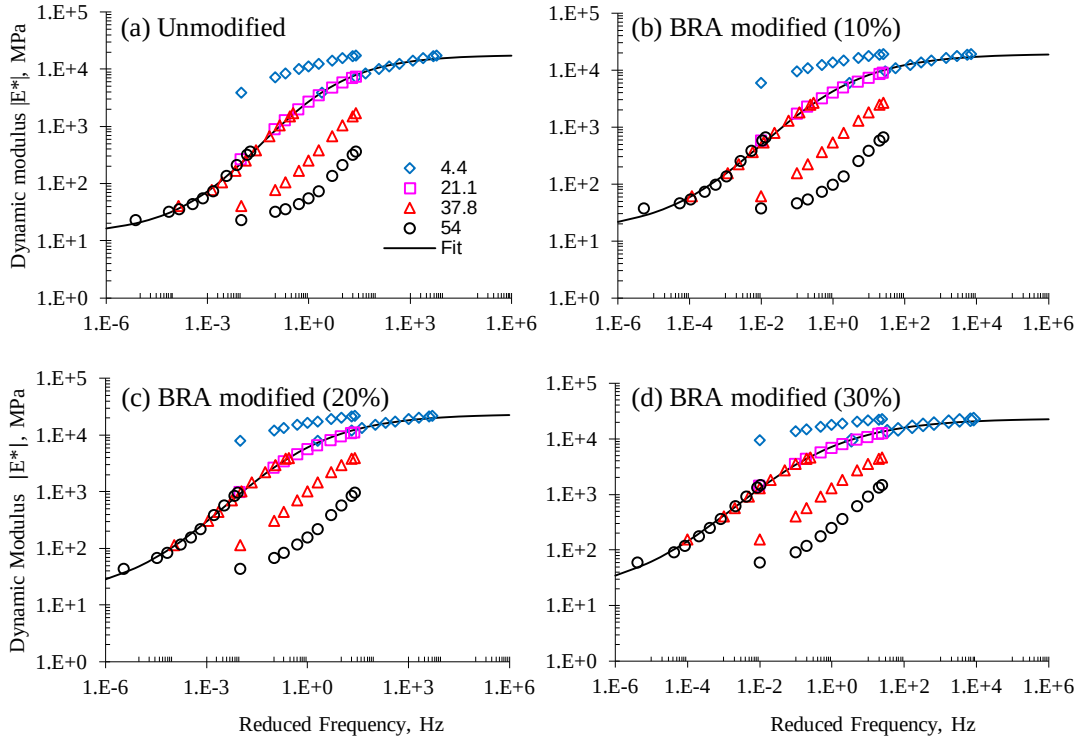

Figure 7-5. Fitted master curve for asphalt mixtures

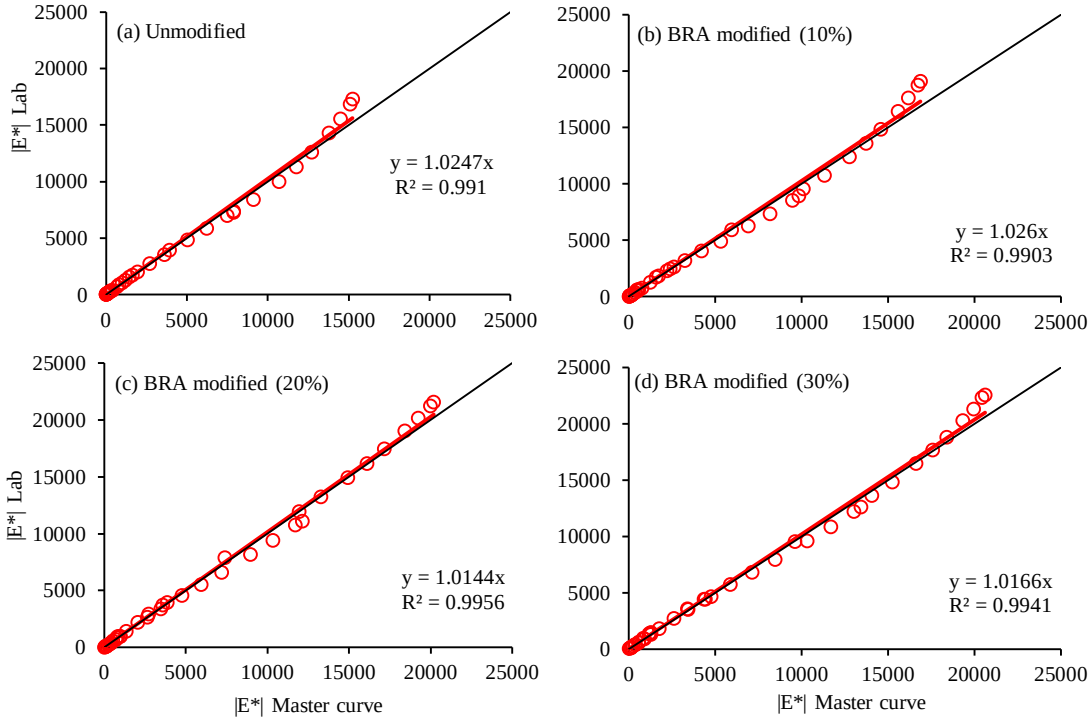

Figure 7-6. Comparison between the laboratory and master curve dynamic moduli

7.2.3 Effect of granular BRA modifier binder on dynamic modulus

The master curves for the dynamic modulus for unmodified and BRA modified asphalt mixtures at a reference temperature of 21°C obtained from Figure 7-5 are shown in Figure 7.7. The curves represent a sigmoidal function fit through the data averaged from three replicate specimens as described in Section 3.5.5. This figure illustrates the comparison of the effect of granular BRA modifier binder on the dynamic modulus of asphalt mixture.

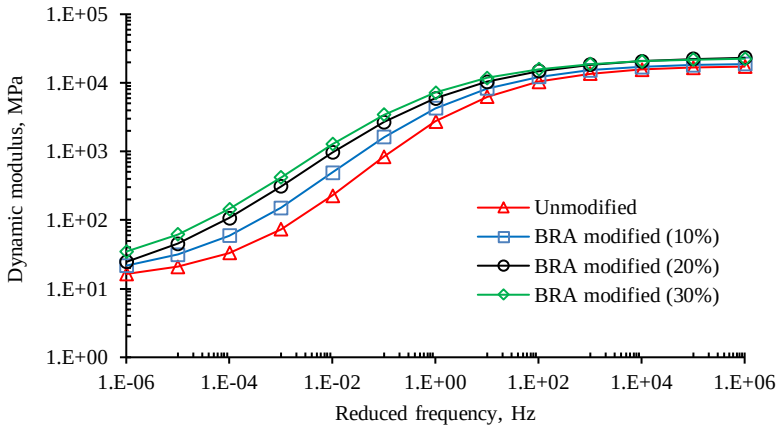

Figure 7-7. Master curve of the dynamic modulus for unmodified and BRA modified asphalt mixtures

For the mixtures tested, the dynamic modulus of BRA modified asphalt mixtures was observed to be slightly higher than for the unmodified mixtures at all frequencies. In addition, the dynamic modulus was observed to be higher for BRA modified asphalt mixtures with a higher percentage of BRA modifier binder at the same temperature and frequency. Accordingly, the BRA modified asphalt mixtures with 30% BRA modifier binder yielded the largest dynamic modulus. The dynamic modulus of BRA modified asphalt mixtures with each percentage of BRA modifier binder were higher than for the unmodified asphalt mixtures, especially in the high-intermediate temperature range and at low frequency. It was observed that the viscoelastic behaviour of BRA modified asphalt mixtures was greater than that of unmodified mixtures, and greater viscoelastic behaviour was seen in the mixture with a higher percentage of BRA modifier binder. However, the dynamic modulus of the BRA modified asphalt mixtures was closer to that of the unmodified asphalt at high frequencies than at low frequencies because the elastic behaviour of asphalt mixtures increases, while the viscous behaviour decreases when the loading speed increases[165]. Further, Shu and Huang[165] have said that the dynamic modulus of asphalt mixtures is always controlled by the asphalt mastic or asphalt binder.

7.2.4 Phase angle of asphalt mixtures and rutting indicator

The mean phase angle values for the unmodified and BRA modified asphalt mixtures obtained from dynamic modulus tests at various loading frequencies and test temperatures are presented in Figure 7-8, with the phase angle results for each specimen being detailed in Appendix G5. A comparison of the phase angle for all of the asphalt mixtures indicates that the phase angle values for the unmodified asphalt mixtures were higher than for the BRA modified asphalt mixtures at all test temperatures and loading frequencies. A higher percentage of BRA modifier binder content resulted in a lower phase angle, which indicates less viscous behaviour.

As shown in Figure 7-8, the behaviour of asphalt mixtures in terms of the phase angle is strongly influenced by a combination of temperature and frequency. The patterns for the phase angle are more complex than for the dynamic modulus tested over the range of frequencies and temperatures. However, unmodified and BRA modified mixtures show the same pattern. At test temperatures of 4.4°C and 21.1°C, the phase angle of the asphalt mixtures decreased as the loading frequency increased. However, at a test temperature of 37.8°C, the phase angle increased when the frequency increased up to 1.0 Hz (for BRA modified 10% and 20%), 0.5 Hz (for BRA modified 30%) and 2 Hz (for unmodified), respectively, followed by a decrease in phase angle with an increase in loading frequency. This reveals that unmodified asphalt mixtures display more viscous behaviour in term of loading frequency/loading time, with unmodified asphalt mixtures having the greatest phase angle at 2 Hz. At a test temperature of 54.0 °C, the phase angle increased with the increase in loading frequency. Figure 7-9 shows an increase in the phase angle of asphalt mixtures with an increase in the test temperature from 4.4ºC to 21.1ºC, but a decrease in the phase angle with an increase in test temperature from 37.8ºC to 54 ºC. This indicates that aggregates interlocking affect the behaviour of asphalt mixtures.

Furthermore, Witczak[51] recommended using the rutting performance indicator, in term of E*/sin(δ) measured at 5 Hz, to evaluate the resistance of asphalt mixtures to rutting. Zhou *et al.*[167] proposed using |E*|/sin (δ) as rutting performance indicator for asphalt mixtures tested at a temperature of 40°C and loading frequency of 10 Hz. Zhou and Scullion[169] noted that a loading time of 0.1 second in the laboratory can be used to represent actual traffic loadings times in the field.

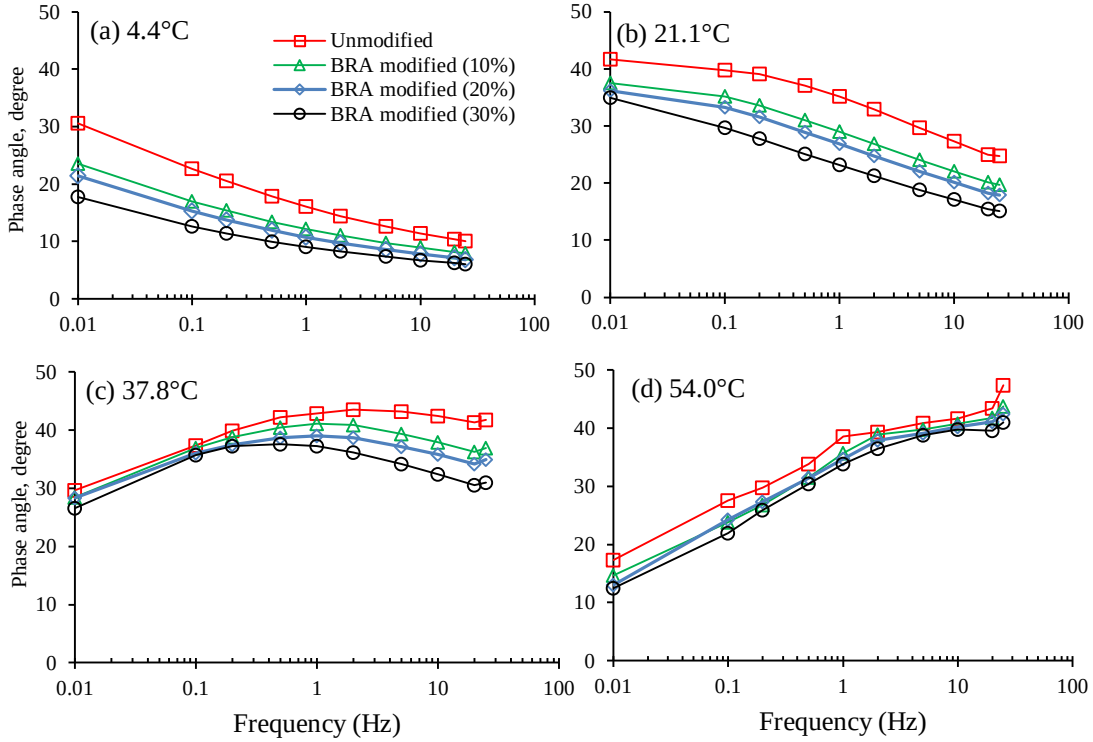

Figure 7-8. Phase angle of asphalt mixtures at various loading frequencies and temperatures

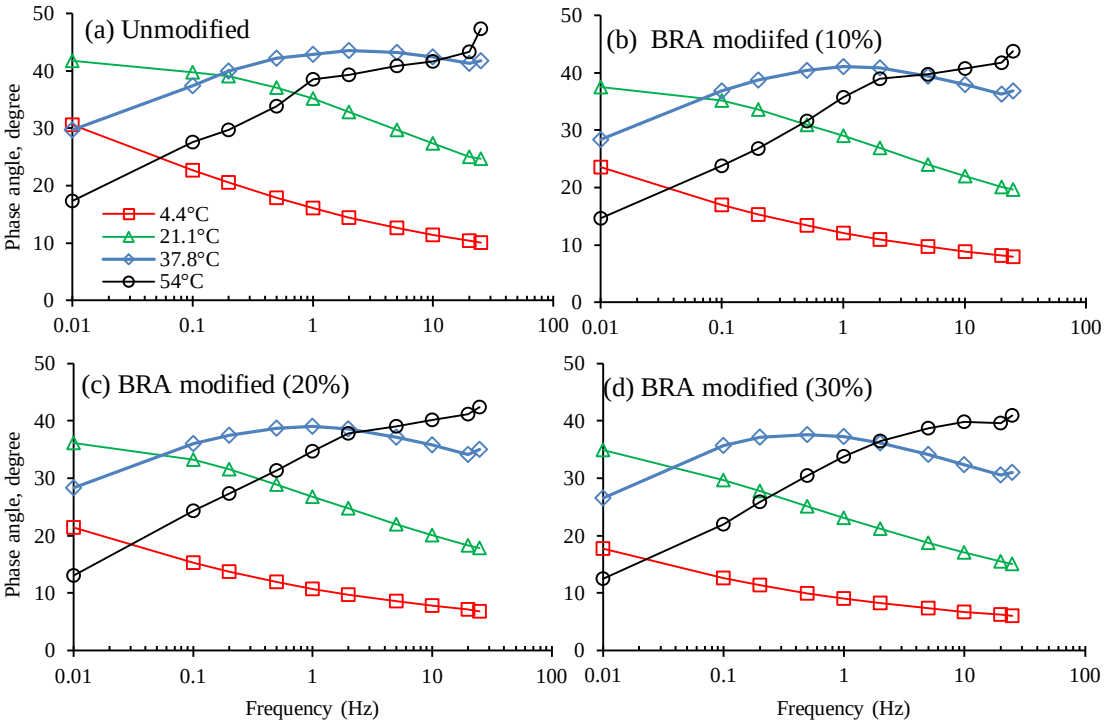

Figure 7- 9. Phase angle vs loading frequency for asphalt mixtures

Meanwhile, the dynamic moduli test results at loading frequencies of 5 Hz and 10 Hz and test temperatures of 37.8°C and 54.0°C to represent high temperatures were selected in this analysis to evaluate the resistance deformation of unmodified

and BRA modified asphalt mixtures. The results presented in Figure 7-10 show that the values of |E*|/sin (δ) for unmodified asphalt mixtures were the lowest at all test temperatures and loading frequencies. The low value of |E*|/sin (δ) relates to the poor resistance of unmodified asphalt mixtures to rutting.

The master curves for phase angle versus frequency for each mixture were created as shown in Figure 7-11 by using the same shift factor as used in the construction of the dynamic modulus master curve. The phase angle follows the behaviour of viscoelastic materials, decreasing as the frequency increases, except at higher test temperatures of 37.8°C and 54°C.

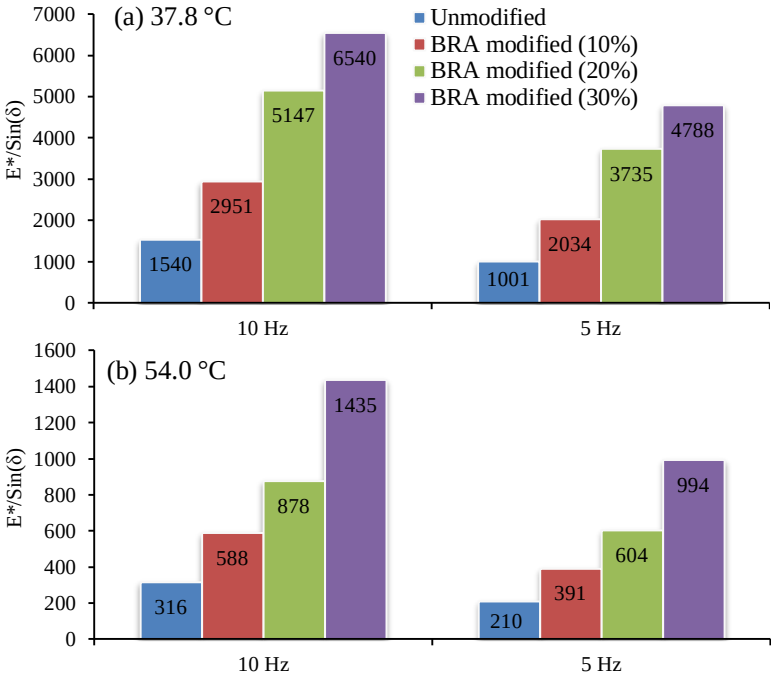

Figure 7-10. The E*/sin(δ) values of asphalt mixtures

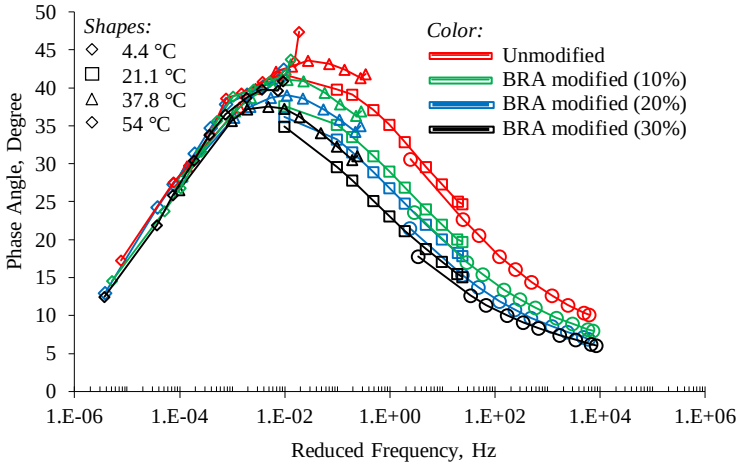

Figure 7-11. Phase angle curve for asphalt mixtures

7.2.5 Black space diagrams

Figure 7-12 shows the black space diagram for various levels of BRA modifier binder content. Figures 7-12(a) through 7-12(d) show the black space diagram for each triplicate specimen of all asphalt mixtures. These show the black space diagrams converging at higher stiffness values. However, this result is different at lower stiffness values. Figure 7-12(e) illustrates the black space diagrams for various levels of BRA modifier binder content constructed from the data averaged from three replicate specimens. Similar trends were observed in this figure, with the black space diagrams for the various BRA modifier binder levels converging at higher stiffness values. However, the higher levels of BRA modifier binder had lower phase angles at lower stiffness values. The BRA modified asphalt mixture with 30% of BRA modifier binder content had the lowest phase angle at lower stiffness values. As Daniel *et al.*[170] have said, asphalt mixtures with lower phase angles display a reduced capacity for relaxation and the materials will be more susceptible to cracking in the stiffness range, even though the materials will have a greater resistance to rutting.

7.2.6 Relationship between dynamic modulus and resilient modulus

A number of studies have been conducted to establish the correlation between dynamic modulus and resilient modulus. Birgisson *et al.*[171] have shown the correlation between dynamic modulus and resilient modulus and testing frequency, for a range of testing temperatures and frequencies of 0.33 Hz, 0.5 Hz, 1.0 Hz, 4 Hz and 8 Hz. A study by Lee *et al.*[33] compared of dynamic modulus values measured in uniaxial and IDT tests at three temperatures and five different frequencies and found good agreement between the dynamic modulus and resilient modulus. Ping and Xiao[172] compared the dynamic modulus and resilient modulus at loading frequencies of 10 Hz, 5 Hz, and 1 Hz. Based on the empirical correlation, they found the dynamic modulus and resilient modulus to be relatively equal at a loading frequency of 4.0 Hz. Therefore, the regression lines for loading frequencies lower than 4.0 Hz were below the equality line, and by contrast, above the equality line for loading frequencies higher than 4.0 Hz.

For the comparison of the dynamic modulus and resilient modulus in this research at loading frequencies of 0.33 Hz, 0.5 Hz, and 1.0 Hz and test temperatures of 5°C, 15°C, 25°C, 40°C and 60°C, the dynamic modulus values were needed. For that purpose, the shift factors at these temperatures were first determined, then the

reduced frequencies were calculated using Equation 2-10. Finally, the regressed sigmoidal equation for the master curve was used to calculate the corresponding dynamic modulus value. The resilient modulus data were obtained from the second stage of the ITSM test as presented in Table 4.5 and Table 4.6 in Chapter 4. ITSM test data were compared to the dynamic modulus test data for two asphalt mixtures - unmodified and BRA modified asphalt mixtures (20%) and the results are shown in Figure 7-13. Linear regression equations are presented in this figure for illustration. It can be seen that the linear regression line for unmodified and BRA modified asphalt mixtures with loading frequencies of 0.33 Hz, 0.5 Hz and 1.0 Hz are below the line of equality. Similar findings have been reported in another study[172]. Furthermore, the resilient modulus was greater than the dynamic modulus at low temperature (high modulus values), while at a high temperature (low modulus values), the values were close to each other.

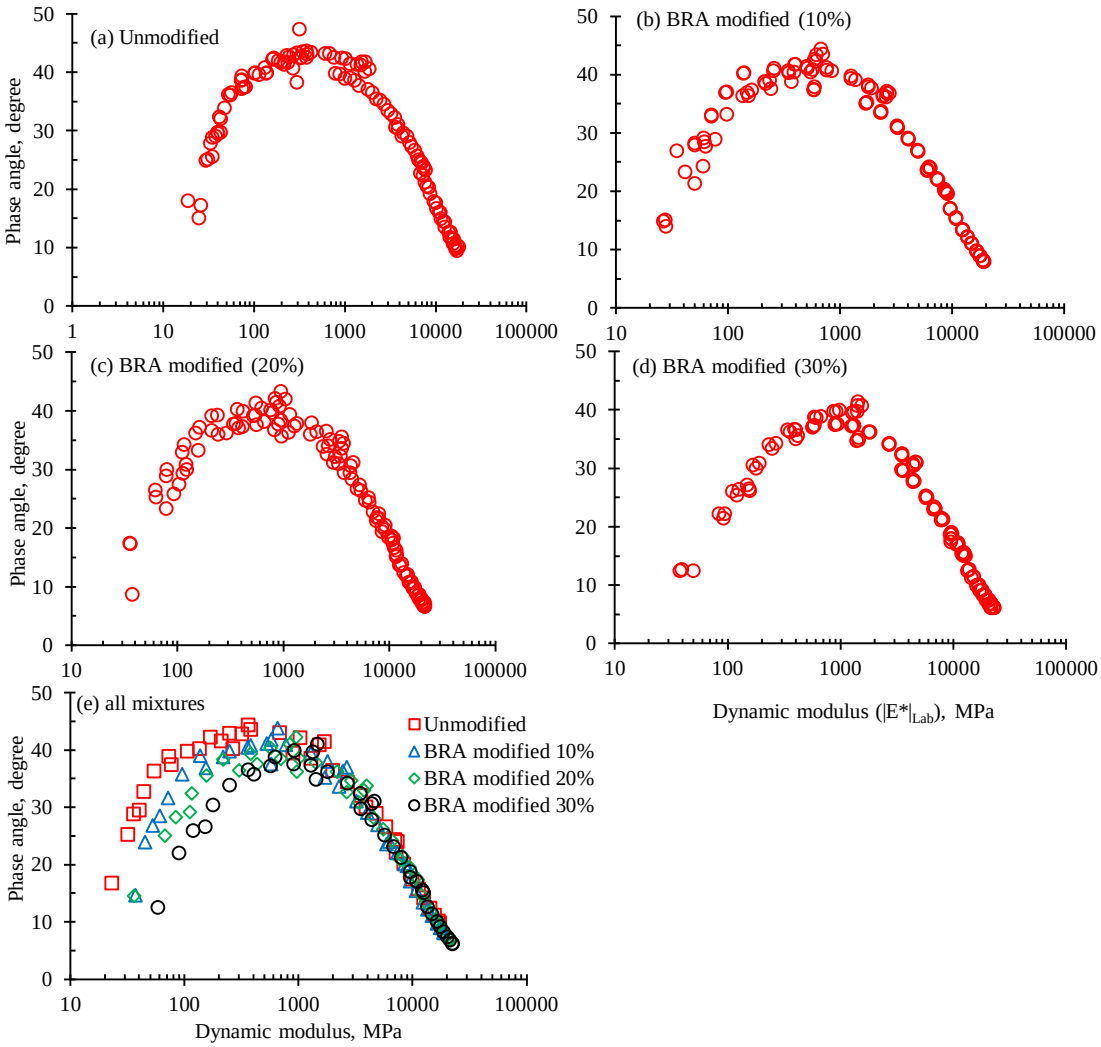

Figure 7-12. Black space diagram for unmodified and BRA modified asphalt mixtures

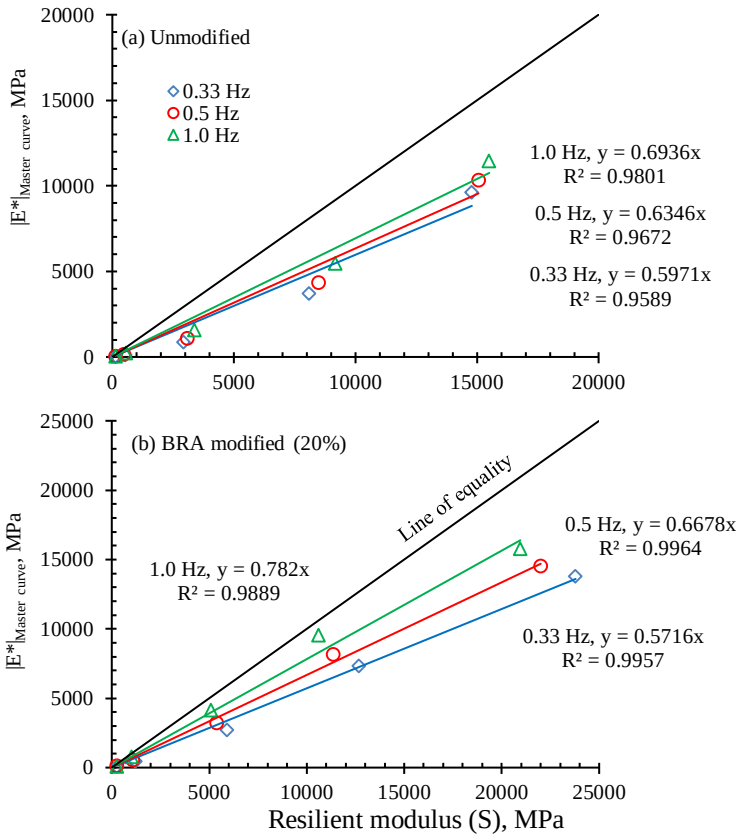

Figure 7-13. Dynamic modulus versus resilient modulus at various frequencies

7.2.7 Relationship between dynamic modulus and rutting depth

The plots of the relationship between dynamic modulus and rutting depth at the same loading frequency are presented in Figure 7.14. The rutting depth data were obtained from the wheel tracking test presented in Figure 5-7 in Chapter 5. The rut depth results were obtained after 10,000 loading passes were reached at a test temperature of 60°C with the moving table of the wheel tracking test at a frequency of 42 ± 0.5 load passes per minute. Hence, a frequency of 0.7 Hz was chosen for use in this analysis to develop the relationship between the dynamic modulus and rutting depth test results. The dynamic modulus values were found after a master curve had been constructed using a sigmoidal model for a reference temperature of 60°C and loading frequency of 0.7 Hz for unmodified and BRA modified asphalt mixtures.

Figure 7-14 shows that the dynamic modulus of asphalt mixtures increases as the rut depth decreases. This figure also shows that the rut depth for the unmodified asphalt mixtures was higher than for the BRA modified asphalt mixtures.

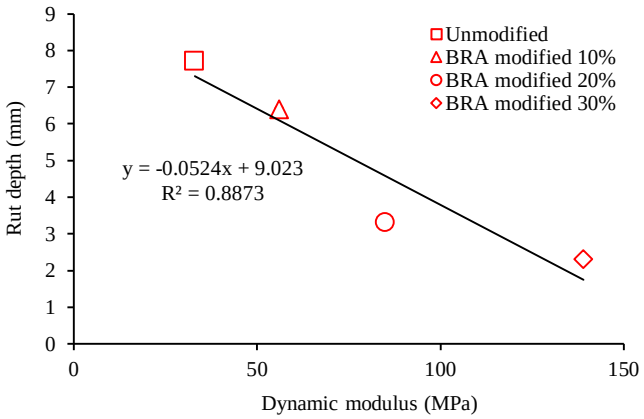

Figure 7-14. Dynamic modulus versus rutting depth at frequency of 0.7 Hz and temperature of 60°C

7.3 Summary

Dynamic modulus tests were performed on unmodified and BRA modified asphalt mixtures at four test temperatures (4.4°C, 21.1°C, 37.8°C and 54°C) and ten loading frequencies (0.01 Hz, 0.1 Hz, 0.2 Hz, 0.5 Hz, 1.0 Hz, 2.0 Hz, 5.0 Hz, 10 Hz, 20 Hz and 25 Hz) in accordance with the specifications of American Association of State Highway Transportation Officials (AASHTO) Designation: T 342-11 Determining Dynamic Modulus of Hot Mix Asphalt (HMA), in order to find out the effect of granular BRA modifier binder on the dynamic modulus of BRA modified asphalt mixtures. Four asphalt mixtures containing 0% (unmodified), 10%, 20%, and 30% BRA modifier binder were used to produce the dynamic modulus test specimens using 10 mm dense graded aggregate. The analysis included the evaluation of dynamic modulus test results and dynamic modulus master curve, effect of granular BRA modifier binder on dynamic modulus values, phase angles, rutting indicator, and the relationship between the dynamic modulus and resilient modulus. The following observations have been made based on the analysis in this study:

(1) The dynamic modulus values of asphalt mixtures decreases with an increase in temperature under a constant loading frequency, and increases with an increase in the frequency under a constant testing temperature.

(2) The substitution of base asphalt binder with 10%, 20% and 30% BRA modified binder significantly increases the dynamic modulus (|E*|) values of asphalt mixtures. A higher percentage of BRA modifier binder resulted in higher dynamic modulus values.

(3) The effect of BRA modifier binder on the dynamic modulus was shown to be most significant at higher temperatures (such as 37.8°C and 54°C) and slow loading rates. This characteristic of BRA modified asphalt mixtures can lead to a reduced tendency to deform elastically.

(4) The phase angle decreases as the loading frequency increases at testing temperatures of 4.4°C and 21.1°C. At 37.8°C, the phase angle seems to increase up to frequencies of 0.5 Hz – 2.0 Hz and then starts to decrease with an increase in frequency. At 54.0°C, the phase angle increases with an increase in frequency.

(5) Black space diagrams show convergence at higher stiffness values while BRA modified asphalt mixtures have lower phase angles at lower stiffness values than unmodified asphalt mixtures. This reveals that BRA modified asphalt mixtures are more susceptible to cracking and more resistant to rutting in the low stiffness ranges.

(6) Based on the linear regression analysis, the relationship between the dynamic modulus and resilient modulus test results showed that the dynamic modulus increased with an increase in resilient modulus at loading frequencies of 0.33 Hz, 0.5 Hz and 1.0 Hz. The linear regressions for unmodified and modified mixtures at those frequencies were below the line of equality.

(7) The relationship between dynamic modulus and rut depth test results showed that the dynamic modulus of asphalt mixtures increases as the rut depth of asphalt mixtures decreases.

CHAPTER 8
CONCLUSIONS AND RECOMMENDATIONS

8.1 Introduction

This chapter summarizes the key research outcomes of this study. Generally, this research has delivered a fundamental understanding of the impact of granular BRA modifier binder on the mechanical properties of BRA modified asphalt mixtures, including resilient modulus, permanent compressive strain, rutting performance, fatigue life, and dynamic modulus. The main findings are presented below. Additionally, based on the data and findings of this research, some recommendations are made for further work required in this study area.

8.2 Conclusions

8.2.1 Resilient modulus of asphalt mixtures

(1) The addition of granular BRA modifier binder seems to have a significant effect on increasing the resilient modulus values of BRA modified asphalt mixtures. A higher percentage of BRA modifier binder resulted in a greater resilient modulus in asphalt mixtures, indicating an increase in the shear resistance of BRA modified asphalt mixtures. Accordingly, BRA modified asphalt mixtures are predicted to have better loads-spreading ability, resistance to cracking and resistance to permanent deformation.

(2) The BRA modified asphalt mixtures showed less sensitivity to changes in temperature, ratio of rest period to loading time, frequency, and loading time, compared to unmodified asphalt mixtures.

(3) The resilient modulus values for unmodified and BRA modified asphalt mixtures with the same gradation and air void contents are mostly affected by the temperature and asphalt binder types.

8.2.2 Permanent compressive strain of asphalt mixtures

(1) The addition of granular BRA modifier binder resulted in good performance compared to unmodified asphalt mixtures, with the permanent strain of BRA modified asphalt mixtures decreasing with an increasing percentage of BRA modifier binder. In addition, the rate of deformation of

BRA modified asphalt mixtures decreased with the increase in granular BRA modifier content, revealing that BRA modified asphalt mixtures are more stable compared to unmodified asphalt mixtures.

(2) The creep modulus values for BRA modified asphalt mixtures were higher compared to unmodified asphalt mixtures. A higher percentage of BRA modifier binder resulted in a higher creep modulus for BRA modified asphalt mixtures.

(3) Flow number and flow point are influenced by granular BRA modifier binder. The flow number of BRA modified asphalt mixtures increased with an increase in the percentage of BRA modifier binder, while the flow point decreased with an increase in the percentage of BRA modifier binder.

8.2.3 Rutting performance of asphalt mixtures

(1) The addition of granular BRA modifier binder to asphalt mixtures resulted in shallower rut depth in BRA modified asphalt mixtures compared to unmodified asphalt mixtures. This indicates that the shear resistance of BRA modified asphalt mixtures is better than that of unmodified asphalt mixtures.

(2) Based on velocity and dynamic stability, the performance of BRA modified asphalt mixtures is better than unmodified asphalt mixtures. The values of velocity decrease and the values of dynamic stability increase as the percentage of BRA modifier binder in asphalt mixtures increases.

8.2.4 Fatigue life of asphalt mixtures

(1) The addition of granular BRA modifier binder to asphalt mixtures resulted in the BRA modified asphalt mixtures being more elastic (less viscous) than unmodified asphalt mixtures.

(2) The fatigue life performance of BRA modified asphalt mixtures is much better than for unmodified asphalt mixtures. However, the initial flexural stiffness affects the fatigue life of asphalt mixtures. Hence, the BRA modified asphalt mixtures with an initial flexural stiffness greater than 11,500 MPA are predicted to have a shorter fatigue life than unmodified asphalt mixtures. In other words, the addition of BRA modifier binder in asphalt mixtures at an amount greater than 20% might potentially result in a greater stiffness modulus

but will have a negative impact on the fatigue life performance of BRA modified asphalt mixtures.

(3) The addition of granular BRA modifier binder to asphalt mixtures increases the cumulative dissipated energy of the BRA modified asphalt mixtures, resulting in a better fatigue failure resistance than for unmodified asphalt mixtures.

8.2.5 Dynamic modulus of asphalt mixtures

(1) The addition of granular BRA modifier binder significantly increases the dynamic modulus of asphalt mixtures. A higher percentage of BRA modifier binder resulted in a higher dynamic modulus for the asphalt mixtures.

(2) Loading frequencies of 10 Hz and 0.1 Hz and testing temperatures of 37.8°C and 54°C were used to evaluate the rutting performance of asphalt mixtures. The dynamic modulus values for BRA modified asphalt mixtures were higher than for unmodified asphalt mixtures, revealing that the rutting performance of BRA modified asphalt mixtures is much better than for unmodified asphalt mixtures.

(3) At all test temperatures and frequencies, phase angle values for unmodified asphalt mixtures were higher than for BRA modified asphalt mixtures. This reveals that the behaviour of unmodified asphalt mixtures was more viscous than BRA modified asphalt mixtures.

(4) The $E^*/\sin(\delta)$ parameter measured at frequencies of 5 Hz and 10 Hz and test temperatures of 37.8°C and 54°C was used to predict the rutting potential of asphalt mixtures. Based on this parameter, the rutting performance of BRA modified asphalt mixtures was better than the unmodified asphalt mixtures as the value of $E^*/\sin(\delta)$ for BRA modified asphalt mixtures was higher than for unmodified asphalt mixtures.

8.3 Recommendations

The concept of BRA modified asphalt mixtures design and the laboratory test results outlined in this study provide the foundation for understanding the mechanical properties of BRA modified asphalt mixtures. However, there are some areas related to the use of BRA modifier binder in asphalt mixtures that could not be studied in this research. The following require further investigation:

(1) An evaluation of the mechanical properties of BRA modified asphalt mixtures with more than one mix gradation should be performed to illustrate the effect of BRA modifier binder on other asphalt mixtures.

(2) Different optimum asphalt content may be obtained between unmodified and BRA modified asphalt mixtures. Accordingly, the mechanical performance of unmodified and BRA modified asphalt mixtures should be compared at different optimum levels of bitumen content.

(3) A comprehensive evaluation of the mechanical properties of BRA modified asphalt mixtures with different testing parameters is necessary to illustrate the effect of loading and environment. For example, the effect of variations in testing temperature and loading frequency on the repeated flexural bending test.

(4) Asphalt binder is a viscoelastic material whose behaviour is affected by temperature and loading frequency. Accordingly, it is necessary to characterize the viscoelastic behaviour of BRA modified binder at different temperatures and frequencies in order to evaluate the rutting and cracking potential of BRA modified asphalt mixtures and develop the relationship between the characteristics of BRA modified binder and the mechanical properties of BRA modified asphalt mixtures.

References

1. Newcomb DE, Buncher M, Huddleston IJ. Concepts of Perpetual Pavements. Transportation Research Board; 2001.
2. Fordyce D, O'Donnell E. Bituminous pavement materials: their composition and specification. Thomas Telford House - London: Thomas Telford Service Ltd; 1994; p. 1-42.
3. Choi YK. Visco-elastic analysis of the elastomeric binder shear resistance in relation to asphalt rutting. Road Materials and Pavement Design. 2011; 12(4):767-794. Available
4. Corte JF. Development and Use of Hard-Grade Asphalt and of High-Modulus Asphalt Mixes in France. Transportation Research Board; 2001.
5. Mallick RB, El-Korchi T. Pavement Engineering - Principle and Practice Taylor and Francis group.
6. Edwards Y, Tasdemir Y, Isacsson U. Influence of commercial waxes and polyphosporic acid on bitumen and asphalt concrete performance at low and medium temperature. Material and Structure. 2006; 39:725-737. Available
7. Zaman AA, Fricke AL, Beatty CL. Rheological properties of rubber-modified asphalt. Transportation Engineering. 1995:461-467. Available
8. Subagio BS, Siswosoebrotho B, Karsaman R Development of laboratory performance of indonesia rock asphalt (ASBUTON) in hot rolled asphalt mix. Proceeding of the Eastern Asia Society for Transportation Studies; 2003 p. 436-449.
9. Subagio BS, J. Adwang, R.H. Karsaman, and I. Fahmi. Fatigue performance of HRA (hot rolled asphalt) and superpave mixes using Indonesian rock asphalt (asbuton) as fine aggregates and filler. Journal of the Eastern Asia Society for Transportation Studies 2005; 6:1207-1216. Available
10. Subagio BS, Rahman H, Fitriadi H, Lusiana L Plastic Deformation Characteristics and Stiffness Modulus of Hot Rolled Sheet (HRS) containing Buton Asphalt (ASBUTON). Proceedings of the Eastern Asia Society for Transportation Studies; 2007 Eastern Asia Society for Transportation Studies p. 262-262.
11. Ali N, Tjaronge MW, Samang L, Ramli MI Experimental Study on Effects of Flood Puddle to Durability of Asphaltic Concrete Containing Refined Butonic Asphalt. Proceedings of the Eastern Asia Society for Transportation Studies; 2011 Eastern Asia Society for Transportation Studies p. 273-273.
12. Hadiwardoyo SP, Sinaga ES, Fikri H. The influence of Buton asphalt additive on skid resistance based on penetration index and temperature. Construction and Building Materials. 2013; 42:5-10. DOI:10.1016/j.conbuildmat.2012.12.018.
13. Ali N. The Experimental Study on the Resistance of Asphalt Concrete with Butonic Bitumen againts Water Saturation. 2013; Available
14. Hadiwardoyo SP, Fikri H. Use of Buton Asphalt Additive on Moisture Damage Sensitivity and Rutting Performance of Asphalt Mixtures. Civil and Environmental Research. 2013; 3(3):100-108. Available
15. Zamhari KA, M. Merhadi, and M.H. Ali. Comparing the Performance of Granular and Extracted Binder from Buton Rock Asphalt. International Journal Pavement Research Technology 2014; 7(1):25-30. Available
16. Singh D, Zaman M, Commuri S. Evaluation of predictive models for estimating dynamic modulus of hot-mix asphalt in Oklahoma. Transportation

Research Record: Journal of the Transportation Research Board. 2011; (2210):57-72. Available
17. Brown S. Properties of Road Layers. Thomas Telford House - London; 1994; p. 43-63.
18. The Shell Bitumen Handbook. Riversdale House, Guildford street, Cherstsey, Surrey - UK: Shell Bitumen UK; 1990; p. 1-336.
19. Brown S. Material characteristics for analytical pavement design. Developments in highway pavement engineering. 1978; 1:41-92. Available
20. Peattie K. Flexible pavement design. Developments in highway pavement engineering. 1978; 1 Available
21. Apeagyei AK, Diefenderfer BK, Diefenderfer SD. Development of dynamic modulus master curves for hot-mix asphalt with abbreviated testing temperatures. International Journal of Pavement Engineering. 2012; 13(2):98-109. Available
22. Venudharan V, Biligiri KP. Estimation of phase angles of asphalt mixtures using resilient modulus test. Construction and Building Materials. 2015; 82:274-286. Available
23. Perraton D, Di Benedetto H, Sauzéat C, De La Roche C, Bankowski W, Partl M, et al. Rutting of bituminous mixtures: wheel tracking tests campaign analysis. Materials and structures. 2011; 44(5):969-986. Available
24. Zoorob S, Suparma L. Laboratory design and investigation of the properties of continuously graded Asphaltic concrete containing recycled plastics aggregate replacement (Plastiphalt). Cement and Concrete Composites. 2000; 22(4):233-242. Available
25. Pourtahmasb MS, Karim MR, Shamshirband S. Resilient modulus prediction of asphalt mixtures containing Recycled Concrete Aggregate using an adaptive neuro-fuzzy methodology. Construction and Building Materials. 2015; 82:257-263. Available
26. Ji SJ. Investigation of factors affecting resilient modulus for hot mix asphalt. Christchurch, New Zealand: University of Canterbury; 2006.
27. Hartman AM, M. D. Gilchrist, Walsh G. Effect of Mixture Compaction on Indirect Tensile Stiffness and Fatigue. Journal of Transportation Engineering. 2001; 127(5):0370–0378. Available
28. Kok BV, Kuloglu N. Effects of Two-Phase Mixing Method on Mechanical Properties of Hot Mix Asphalt. Road Materials and Pavement Design. 2011 [cited 2015/02/16]; 12(4):721-738. DOI:10.1080/14680629.2011.9713892.
29. Mokhtari A, Moghadas Nejad F. Mechanistic approach for fiber and polymer modified SMA mixtures. Construction and Building Materials. 2012; 36:381-390. DOI:10.1016/j.conbuildmat.2012.05.032.
30. Tayfur S, Ozen H, Aksoy A. Investigation of rutting performance of asphalt mixtures containing polymer modifiers. Construction and Building Materials. 2007; 21(2):328-337. DOI:10.1016/j.conbuildmat.2005.08.014.
31. Shafabakhsh G, Tanakizadeh A. Investigation of loading features effects on resilient modulus of asphalt mixtures using Adaptive Neuro-Fuzzy Inference System. Construction and Building Materials. 2015; 76:256-263. DOI:10.1016/j.conbuildmat.2014.11.069.
32. Lavasani M, Latifi Namin M, Fartash H. Experimental investigation on mineral and organic fibers effect on resilient modulus and dynamic creep of stone matrix asphalt and continuous graded mixtures in three temperature levels.

Construction and Building Materials. 2015; 95:232-242. DOI:http://dx.doi.org/10.1016/j.conbuildmat.2015.07.146.
33. Lee H, Kim S, Choubane B, Upshaw P. Construction of dynamic modulus master curves with resilient modulus and creep test data. Transportation Research Record: Journal of the Transportation Research Board. 2012; (2296):1-14. Available
34. Fakhri M, Ghanizadeh AR. An experimental study on the effect of loading history parameters on the resilient modulus of conventional and SBS-modified asphalt mixes. Construction and Building Materials. 2014; 53:284-293. DOI:10.1016/j.conbuildmat.2013.11.091.
35. Alavi AH, M. Ameri, A.H. Gandomi, and M.R. Mirzahosseini. Formulation of flow number of asphalt mixes using a hybrid computational method. Construction and Building Materials. 2011; 25(3):1338-1355. DOI:10.1016/j.conbuildmat.2010.09.010.
36. Khodaii A, Mehrara A. Evaluation of permanent deformation of unmodified and SBS modified asphalt mixtures using dynamic creep test. Construction and Building Materials. 2009; 23(7):2586-2592. DOI:10.1016/j.conbuildmat.2009.02.015.
37. BMT-Institute. Dun-troi-be-tong-nhua. 4 February 2015 [Available from: http://bmt-rnd.vn/wp-content/uploads/2013/09/dun-troi-be-tong-nhua.jpg.
38. Vazquez CG, J.P. Aguiar-Moya, A. de F. Smit, and J.A. Prozzi. Laboratory Evaluation of Influence of Operational Tolerance (Acceptance Criterion) on Performance of Hot-Mix Asphalt Concrete. Austin, USA: Center for Transportation Research The University of Texas, USA; 2010.
39. Wang H, Al-Qadi, I., Faheem, A., Bahia, H., Yang, S.H., Reinke, G. Effect of mineral filler characteristics on asphalt mastic and mixture rutting potential. Transportation Research Record: Journal of the Transportation Research Board. 2011; (2208):33-39. Available
40. Apeagyei AK. Rutting as a Function of Dynamic Modulus and Gradation. Journal of Materials in Civil Engineering. 2011; 23(9):1302-1310. DOI:10.1061/(asce)mt.1943-5533.0000309.
41. Xiao F, V.S. Punith, B. Putman, and S.N. Amirkhanian. Utilization of Foaming Technology in Warm-Mix-Asphalt Mixtures Containing Moist Aggregates. Journal of Materials in Civil Engineering. 2011; 23(9):1328-1337. DOI:10.1061/(asce)mt.1943-5533.0000297.
42. Fontes LPTL, G. Trichês, J.C. Pais, and P.A.A Pereira. Evaluating permanent deformation in asphalt rubber mixtures. Construction and Building Materials. 2010; 24(7):1193-1200. DOI:10.1016/j.conbuildmat.2009.12.021.
43. Kalyoncuoglu SF, Tigdemir M. A model for dynamic creep evaluation of SBS modified HMA mixtures. Construction and Building Materials. 2011; 25(2):859-866. DOI:10.1016/j.conbuildmat.2010.06.101.
44. Dehnad MH, Khodaii A, Moghadas Nejad F. Moisture sensitivity of asphalt mixtures under different load frequencies and temperatures. Construction and Building Materials. 2013; 48:700-707. DOI:10.1016/j.conbuildmat.2013.07.059.
45. Ahmedzade P, Sengoz B. Evaluation of steel slag coarse aggregate in hot mix asphalt concrete. J Hazard Mater. 2009; 165(1-3):300-5. DOI:10.1016/j.jhazmat.2008.09.105.

46. Sengul CE, S. Oruc, E. Iskender, and A. Aksoy. Evaluation of SBS modified stone mastic asphalt pavement performance. Construction and Building Materials. 2013; 41:777-783. DOI:10.1016/j.conbuildmat.2012.12.065.
47. Archilla AR, Diaz LG, Carpenter SH. Proposed Method to Determine the Flow Number in Bituminous Mixtures from Repeated Axial Load Tests. Journal of Transportation Engineering 2007; 133(11):610-617. DOI:10.1061//ASCE/0733-947X/2007/133:11/610.
48. Goh SW, You Z. A simple stepwise method to determine and evaluate the initiation of tertiary flow for asphalt mixtures under dynamic creep test. Construction and Building Materials. 2009; 23(11):3398-3405. DOI:10.1016/j.conbuildmat.2009.06.020.
49. Zhou F, Scullion T. Discussion: Three Stages of Permanent Deformation Curve and Rutting Model. International Journal of Pavement Engineering. 2002 [cited 2015/03/08]; 3(4):251-260. DOI:10.1080/1029843021000083676.
50. Yilmaz M, Çeloğlu ME. Effects of SBS and different natural asphalts on the properties of bituminous binders and mixtures. Construction and Building Materials. 2013; 44:533-540. DOI:10.1016/j.conbuildmat.2013.03.036.
51. Witczak M, Kaloush K, Pellinen T, El-Basyouny M, Von Quintus H. Simple performance test for superpave mix design, NCHRP Report 465. Transportation Research Board, Washington, DC, USA. 2002; Available
52. Dias JLF, Picado-Santos LG, Capitão SD. Mechanical performance of dry process fine crumb rubber asphalt mixtures placed on the Portuguese road network. Construction and Building Materials. 2014; 73:247-254. DOI:10.1016/j.conbuildmat.2014.09.110.
53. Chen JS, Sun YC, Liao MC, Huang CC, Tsou KW. Evaluation of Permeable Friction Course Mixes with Various Binders and Additives. Journal of Materials in Civil Engineering. 2013; 25(5):573-579. DOI:10.1061/(ASCE)MT.
54. Austroads. AG:PT/T231. Deformation Resistance of Asphalt Mixtures by Wheel Tracking Test, 2006. Sydney, New South Wales:
55. Xu T, Wang H, Li Z, Zhao Y. Evaluation of permanent deformation of asphalt mixtures using different laboratory performance tests. Construction and Building Materials. 2014; 53:561-567. DOI:10.1016/j.conbuildmat.2013.12.015.
56. Clyne TR, Li X, Marasteanu MO, Skok EL. Dynamic and resilient modulus of Mn/DOT asphalt mixtures. 2003.
57. Hu X, Zhou F, Hu S, Walubita LF. Proposed loading waveforms and loading time equations for mechanistic-empirical pavement design and analysis. Journal of Transportation Engineering. 2009; 136(6):518-527. Available
58. Witczak MW. Specification criteria for simple performance tests for rutting. Transportation Research Board; 2007.
59. Flintsch GW, Loulizi A, Diefenderfer SD, Galal KA, Diefenderfer BK. Asphalt materials characterization in support of implementation of the proposed mechanistic-empirical pavement design guide. 2007; Available
60. Schwartz CW Evaluation of the Witczak dynamic modulus prediction model. Proceedings of the 84th Annual Meeting of the Transportation Research Board, Washington, DC; 2005.
61. Yao B, Cheng G, Wang X, Cheng C. Characterization of the stiffness of asphalt surfacing materials on orthotropic steel bridge decks using dynamic

modulus test and flexural beam test. Construction and Building Materials. 2013; 44:200-206. Available
62. Witczak M, Bari J. Development of a master curve (E*) database for lime modified asphaltic mixtures. Arizona State University Research Report, Tempe (Arizona, USA): Arizona State University. 2004; Available
63. Garcia G, Thompson M. HMA dynamic modulus predictive models (a review). 2007; Available
64. Kim Y, Lee HD, Heitzman M. Dynamic modulus and repeated load tests of cold in-place recycling mixtures using foamed asphalt. Journal of Materials in Civil Engineering. 2009; 21(6):279-285. Available
65. Dougan CE, Stephens J, Mahoney J, Hansen G. E*-Dynamic Modulus: Test Protocol-Problems and Solutions. 2003.
66. Coffey S, DuBois E, Mehta Y, Nolan A, Purdy C. Determining the impact of degree of blending and quality of reclaimed asphalt pavement on predicted pavement performance using pavement ME design. Construction and Building Materials. 2013; 48:473-478. Available
67. Christensen DW, Anderson DA. Interpretation of dynamic mechanical test data for paving grade asphalt cements (with discussion). Journal of the Association of Asphalt Paving Technologists. 1992; 61 Available
68. Pellinen T, Witczak M. Stress dependent master curve construction for dynamic (complex) modulus (with discussion). Journal of the Association of Asphalt Paving Technologists. 2002; 71 Available
69. Zhu H, Sun L, Yang J, Chen Z, Gu W. Developing master curves and predicting dynamic modulus of polymer-modified asphalt mixtures. Journal of Materials in Civil Engineering. 2011; Available
70. Khiavi AK, Ameri M. Laboratory evaluation of strain controlled fatigue criteria in hot mix asphalt. Construction and Building Materials. 2013; 47:1497-1502. DOI:10.1016/j.conbuildmat.2013.06.062.
71. Hakimelahi H, Saadeh S, Harvey J. Investigation of fracture properties of California asphalt mixtures using semicircular bending and beam fatigue tests. Road Materials and Pavement Design. 2013; 14(sup2):252-265. DOI:10.1080/14680629.2013.812835.
72. Li Q, Lee HJ, Kim TW. A simple fatigue performance model of asphalt mixtures based on fracture energy. Construction and Building Materials. 2012; 27(1):605-611. DOI:10.1016/j.conbuildmat.2011.07.001.
73. Zhou F, X. Hu, S. Hu, L.F. Walubita, and T.Scullion. Incorporation of Crack Propagation in the M-E Fatigue Cracking Prediction. Road Materials and Pavement Design. 2008; 9(sup1):433-465. DOI:10.1080/14680629.2008.9690178.
74. Di Benedetto H, C. De La Roche, H. Baaj, A. Pronk, and R. Lundström. Fatigue of bituminous mixtures. Materials and Structures. 2004; 37(3):202-216. Available
75. Baburamani P. Asphalt fatigue life prediction model - a literature review. Victoria - Australia; 1999.
76. Awanti SS, Amarnath MS, Veeraragavan A. Influence of rest periods on fatigue characteristics of SBS polymer modified bituminous concrete mixtures. International Journal of Pavement Engineering. 2007; 8(3):177-186. DOI:10.1080/10298430601017501.

77. Brovelli C, M. Crispino, J. Pais, and P. Pereira. Using polymers to improve the rutting resistance of asphalt concrete. Construction and Building Materials. 2015; 77:117-123. DOI:10.1016/j.conbuildmat.2014.12.060.
78. Kim TW, J. Baek, H.J. Lee, and J.Y. Choi. Fatigue performance evaluation of SBS modified mastic asphalt mixtures. Construction and Building Materials. 2013; 48:908-916. DOI:10.1016/j.conbuildmat.2013.07.100.
79. Sibal A, Das A, Pandey BB. Flexural Fatigue Characteristics of Asphalt Concrete with Crumb Rubber. International Journal of Pavement Engineering. 2000; 1(2):119-132. DOI:10.1080/10298430008901701.
80. Teltayev B. A New Failure Criterion for Asphalt Mixtures Under Fatigue Loading. International Journal of Pavement Research & Technology. 2015; 8(4) Available
81. Yuan MM, Z.X. Ning, C.W. Qiang, and Z.S. Xian. Ratio of Dissipated Energy Change-based Failure Criteria of Asphalt Mixtures. Research Journal of Applied Sciences, Engineering and Technology. 2013; 6(14):514-2519. Available
82. Maggiore C, J. Grenfell, G. Airey, and A.C. Collop Evaluation of fatigue life using dissipated energy methods. 7th RILEM International Conference on Cracking in Pavements; 2012 Springer p. 643-652.
83. Dondi G, M. Pettinari, C. Sangiorgi, and S.E. Zoorob. Traditional and Dissipated Energy approaches to compare the 2PB and 4PB flexural methodologies on a Warm Mix Asphalt. Construction and Building Materials. 2013; 47:833-839. DOI:10.1016/j.conbuildmat.2013.05.091.
84. Pérez-Jiménez F, R. Miró, A. Martínez, R. Botella, O. Reyes, G. Valdés. False Failure in Flexural Fatigue Tests. 2nd Workshop on Four Point Bending, Pais (ed.), University of Minho. 2009; Available
85. Pell PS Fatigue of asphalt pavement mixes. The Second International Conference on the Structural Design of Asphalt Pavements; 1967; Michigan: p. 577-594.
86. Pronk A, Hopman P. Energy dissipation: the leading factor of fatigue. 1991. Report No.: 0727716352.
87. Tayebali AA, Rowe GM, Sousa JB. Fatigue response of asphalt-aggregate mixtures (with discussion). Journal of the Association of Asphalt Paving Technologists. 1992; 61 Available
88. Abojaradeh M, Witczak MW, Mamlouk MS, Kaloush KE. Validation of initial and failure stiffness definitions in flexure fatigue test for hot mix asphalt. Journal of Testing and Evaluation. 2007; 35(1):95. Available
89. Shen S, Lu X. Energy based laboratory fatigue failure criteria for asphalt materials. J. of Test. Eval. 2011; 39(3):846-852. Available
90. Austroads. AG:PT/T233. Fatigue life of compacted bituminous mixes subject to repeated flexural bending Issue 1-17, 2006. Sydney, New South Wales:
91. Shen S, and S.H. Carpenter. Dissipated energy concepts for HMA performance: fatigue and healing. Urbana, Illinois - USA: Departmen of Civil and Environmental Engineering - University of Illinois; 2007.
92. Carpenter S, Ghuzlan K, Shen S. Fatigue endurance limit for highway and airport pavements. Transportation Research Record: Journal of the Transportation Research Board. 2003; (1832):131-138. Available
93. Shen S, Carpenter S. Application of the dissipated energy concept in fatigue endurance limit testing. Transportation Research Record: Journal of the Transportation Research Board. 2005; (1929):165-173. Available

94. Pronk A. Evaluation of the dissipated energy concept for the interpretation of fatigue measurements in the crack initiation phase. 1900; Available
95. Hopman PC, A.C. Pronk, P.A. Kunst, A.A. Molenaar, and J.M. Molenaar Application of the visco-elastic properties of asphalt concrete. International Conference on Asphalt Pavements, 7th, 1992, Nottingham, United Kingdom; 1992.
96. Hassan M, Khalid H. Fracture characteristics of asphalt mixtures containing incinerator bottom ash aggregate. Transportation Research Record: Journal of the Transportation Research Board. 2010; 2180(1):1-8. Available
97. Al-Khateeb G, and A. Shenoy. A distinctive fatigue failure criterion. Association of Asphalt Paving Technology. 2004; 73:585-622. Available
98. Abojaradeh M. Development of Fatigue Failure Criterion for Hot-Mix Asphalt Based on Dissipated Energy and Stiffness Ratio. Jordan Journal of Civil Engineering 2013; 7(1):54-69. Available
99. Ghuzlan KA, Carpenter SH. Fatigue damage analysis in asphalt concrete mixtures using the dissipated energy approach. Canadian Journal of Civil Engineering. 2006; 33(7):890-901. Available
100. Pronk A Comparison of 2 and 4 point fatigue tests and healing in 4 point dynamic bending test based on the dissipated energy concept. Eighth International Conference on Asphalt Pavements; 1997.
101. Rowe GM, Bouldin MG Improved techniques to evaluate the fatigue resistance of asphaltic mixtures. 2nd Eurasphalt & Eurobitume Congress Barcelona; 2000.
102. Ghuzlan K, Carpenter S. Energy-derived, damage-based failure criterion for fatigue testing. Transportation Research Record: Journal of the Transportation Research Board. 2000; (1723):141-149. Available
103. Bahia HU. Modelling of Asphalt Binder Rheology and Its Application to Modified Binders. McGraw Hill; 2009; p. 11-64.
104. Joshi C, A. Patted, M.R. Archana, and M.S. Amarnath Determining the rheological properties of asphalt binder using dynamic shear rheometer (DSR) for selected pavement stretches. International Journal of Research in Engineering and Technology; 2013 p. 192-196.
105. Mallick RB, El-Korchi T. Pavement engineering: principles and practice. CRC Press; 2013.
106. Lu X, Isacsson U, Ekblad J. Rheological properties of SEBS, EVA and EBA polymer modified bitumens. Materials and Structures. 1999; 32(2):131-139. Available
107. Bahia HU, D. I. Hanson, M. Zeng, H. Zhai, M.A. Khatri and R. M. Anderson. Characterization of Modified Asphalt Binders in Superpave Mix Design. NCHRP Report 459. 2001:1-45. Available
108. Chen JS, C.C. Huang, P.Y. Chu, and K.Y. Lin. Engineering characterization of recycled asphalt concrete and aged bitumen mixed recycling agent. Materials and Science. 2007; 42:9867-9876. DOI:10.1007/s10853-007-1713-8.
109. González O, Munoz M, Santamaría A. Bitumen/polyethylene blends: using m-LLDPEs to improve stability and viscoelastic properties. Rheologica acta. 2006; 45(5):603-610. Available
110. Baig MG, Wahhab HIA. Mechanistic Evaluation of Hedmanite and Lime Modified Asphalt Concrete. Journal of Materials in Civil Engineering. 1998; 10(3):153-160. Available

111. Ali A, Poernomo. Jati diri aspal buton di era naiknya harga aspal minyak. Majalah Teknik Jalan dan Transportasi 2007:16-20.
112. Kurniadji Tinjauan Campuran Beraspal Panas untuk Simpangan dan Tanjakan (Hot Mix Asphalt used for Crossroad and Grade - an Overview). Mewujudkan Teknologi Infrastruktur Jalan yang Inovatif; 2007; Bandung - Indonesia: Pusat Penelitian and Pengembangan Jalan dan Jembatan-Departemen Pekerjaan Umum (The Center for Road Research and Development-Department of Public Work).
113. Free World Maps. Indonesia-map-political-big. 26 March 2015 [Available from: http://www.freeworldmaps.net/asia/indonesia/indonesia-map-political-big.jpg; http://en.wikipedia.org/wiki/Buton.
114. Satyotito. Mengenal Aspal Alam di Pulau Buton. 2016 [cited 3 January]. Available from: https://tulisantulisansatyo.wordpress.com/2014/10/20/mengenal-aspal-alam-di-pulau-buton/.
115. Affandy F. 25th ARRB Conference. The performance of bituminous mixes using Indonesia natural asphalt, 2012. Perth, Western Australia:
116. Suaryana N Analsis Faktor-Faktor yang Dapat Mendorong kegagalan dalam Pelaksanaan Asbuton (Analysis of the Factors Caused the Unsuccesful of the Implementation of Asbuton). 2007; Bandung - Indonesia: Pusat Penelitian and Pengembangan Jalan dan Jembatan-Departemen Pekerjaan Umum (The Center for Road Research and Development-Department of Public Work).
117. Abbas AR, Papagiannakis AT, Masad EA. Linear and Nonlinear Viscoelastic Analysis of the Microstructure of Asphalt Concretes. Materials in Civil Engineering 2004; 16(2):133–139. DOI:10.1061//ASCE/0899-1561/2004/16:2/133.
118. Airey GD, Rahimzadeh B, Collop AC. Linear Rheological Behavior of Bituminous Paving Materials. Materials in Civil Engineering. 2004; 16(4):212-220. DOI:10.1061//ASCE/0899-1561/2004/16:3/212.
119. Delaporte B, Di Benedetto, H., Chaverot, P., Gauthier, G. Linear Viscoelastic Properties of Bituminous Materials Including New Products Made with Ultrafine Particles. Road Materials and Pavement Design. 2009; 10(1):7-38. DOI:10.1080/14680629.2009.9690180.
120. Australian Standard. AS 2008-1997. Residual bitumen for pavements Issue 1-11, 1997. New South Wales, Australia:
121. Main Road Western Australia. Specification 504. Asphalt Wearing Course, 2010. Perth:
122. Main Roads Western Australia. Test method WA 730.1-2011. Bitumen content and particle size distribution of asphalt and stabilised soil: centrifuge method Issue 1-4, 2011. Perth:
123. Main Roads Western Australia. WA 210.1-2011. Particle size distribution of aggregate Issue 1-3, 2011. Perth:
124. Mohammad L.N, Al-Shamsi K. Transportation Research Circular (Number E-C124) - Practical Approaches to Hot-Mix Asphalt Mix Design and Production Quality Control Testing. A Look at the Bailey Method and Locking Point Concept in Superpave Mixture Design Issue Number E-C124, 2007. Washington DC: Transportation Research Board;
125. Main Roads Western Australia. WA 732.2-2011. Maximum density of asphalt - Rice method Issue 1-2, 2011. Perth:

126. Main Road Western Australia. WA 705.1-2011. Preparation of Asphalt for Testing Issue 1-7, 2011. Perth:
127. Main Road Western Australia. WA 733.1 – 2011. Bulk density and void content of asphalt Issue 1-4, 2011. Perth:
128. Main Roads Western Australia. WA 731.1-2010. Stability and flow of asphalt: Marshal method Issue 1-3, 2010. Perth:
129. Australian Standard. AS 2891.13.1-1995. Methods of sampling and testing asphalt - Methods 13.1: Determination of resilient modulus of asphalt - Indirect tensile method Issue 1-8, 1995. New South Wales, Australia
130. Australian Standard. AS 2891.1.1-2008. Methods of sampling and testing asphalt - Method 1.1: Sampling loose asphalt Issue 1-12, 2008. New South Wales, Australia:
131. Australian Standard. AS 2891.2.2-1995. Methods of sampling and testing asphalt - Method 2.2: Sample preparation - Compaction of asphalt test specimens using a gyartory compactor, 1995. New South Wales, Australia:
132. Australian Standard. AS 2891.12.1-1995. Methods of sampling and testing asphalt - Method 12.1: Determination of the permanent compressive strain characteristics of asphalt - Dynamic creep test Issue 1-8, 1995. New South Wales, Australia:
133. Austroads. AG:PT/T220. Sample preparation - compaction of asphalt slabs suitable for characterisation Issue 1-11, 2005. Sydney, New South Wales
134. Yusoff NIM, Breem AAS, Alattug HNM, Hamim A, Ahmad J. The effects of moisture susceptibility and ageing conditions on nano-silica/polymer-modified asphalt mixtures. Construction and Building Materials. 2014; 72:139-147. DOI:http://dx.doi.org/10.1016/j.conbuildmat.2014.09.014.
135. American Association of State Highway and Transportation Officilas. AASHTO Designation: T 342-11. Determining Dynamic Modulus of Hot Mix Asphalt (HMA) Issue 1-18, 2011. Washington:
136. Main Road Western Australia. Engineering Road Note 9. Procedure for the Design of Road Pavements Issue 1-52, 2012. Perth:
137. Austroads. Testing Asphalt in Accordance with the Austroads Mix Design Procedures. New South Wales, Australia; 2008.
138. Tabatabaie S, Ziari H, Khalili M. Modeling temperature and resilient modulus of asphalt pavements for tropic zones of Iran. Asian Journal of Scientific Research. 2008; 1(6):579-588. Available
139. Kim Y, Shah K, Khosla N. Influence of test parameters in SHRP P07 procedure on resilient moduli of asphalt concrete field cores. Transportation Research Record. 1992; (1353) Available
140. Law TL. Resilient modulus of asphalt concrete mixtures. 2004; Available
141. Fairhurst C, Kosla N, Kim Y Resilient modulus testing of asphalt specimens in accordance with ASTM D4123-82. Mechanical Tests for Bituminous Mixes. Characterization, Design and Quality Control. Proceedings of the Fourth International Symposium held by RILEM; 1990.
142. Monismith C Resilient modulus testing: interpretation of laboratory results for design purposes. Proceedings of the Workshop on Resilient Modulus Testing; 1989 Oregon State University Corvallis, OR.
143. Barksdale RD, Alba J, Khosla NP, Kim R, Lambe PC, Rahman M. Laboratory determination of resilient modulus for flexible pavement design. 1997.

144. Kamal M, Shazib F, Yasin B. Resilient behaviour of asphalt concrete under repeated loading & effects of temperature. Journal of the Eastern Asia Society for Transportation Studies. 2005; 6:1329-1343. Available
145. Daniel JS, Kim YR. Laboratory evaluation of fatigue damage and healing of asphalt mixtures. Journal of Materials in Civil Engineering. 2001; 13(6):434-440. Available
146. Maggiore C, Grenfell J, Airey G, Collop AC Evaluation of fatigue life using dissipated energy methods. 7th RILEM International Conference on Cracking in Pavements; 2012 Springer p. 643-652.
147. Maggiore C, Airey G, Marsac P. A dissipated energy comparison to evaluate fatigue resistance using 2-point bending. Journal of Traffic and Transportation Engineering (English Edition). 2014; 1(1):49-54. Available
148. Nejad FM, Aflaki E, Mohammadi MA. Fatigue behavior of SMA and HMA mixtures. Construction and Building Materials. 2010; 24(7):1158-1165. DOI:10.1016/j.conbuildmat.2009.12.025.
149. Mogawer WS, A.J. Austerman, J.S. Daniel, F. Zhou, and T. Bennert. Evaluation of the effects of hot mix asphalt density on mixture fatigue performance, rutting performance and MEPDG distress predictions. International Journal of Pavement Engineering. 2011; 12(2):161-175. DOI:10.1080/10298436.2010.546857.
150. Tarefder R, Kias E, Zaman A Cracking in asphalt concrete under wet and dry conditions. Pavements and Materials 2008: Modeling, Testing, and Performance. Proc. of the Symp. on Pavement Mechanics and Materials at the Inaugural Int. Conf. of the Eng. Mechanics Institute; 2008 p. 37-47.
151. Bhattacharjee S, Mallick RB. Effect of temperature on fatigue performance of hot mix asphalt tested under model mobile load simulator. International Journal of Pavement Engineering. 2012 [cited 2015/08/04]; 13(2):166-180. DOI:10.1080/10298436.2011.653565.
152. Abojaradeh M. Development of Fatigue Failure Criterion for Hot-Mix Asphalt Based on Dissipated Energy and Stiffness Ratio. Jordan Journal of Civil Engineering. 2013; 7(1) Available
153. Kim YR, Lee H-J, Little DN. Fatigue characterization of asphalt concrete using viscoelasticity and continuum damage theory (with discussion). Journal of the Association of Asphalt Paving Technologists. 1997; 66 Available
154. Guler M. Effect of mix design variables on mechanical properties of hot mix asphalt. Journal of Transportation Engineering 2008; 134(3):128-136. DOI:10.1061//ASCE/0733-947X/2008/134:3/128.
155. Rowe G. Performance of asphalt mixtures in the trapezoidal fatigue test. Asphalt Paving Technology. 1993; 62:344-344. Available
156. Walubita LF. Comparison of fatigue analysis approaches for predicting fatigue lives of hot-mix asphalt concrete (HMAC) mixtures: Texas A&M University; 2006.
157. Shukla PK, Das A. A re-visit to the development of fatigue and rutting equations used for asphalt pavement design. International Journal of Pavement Engineering. 2008; 9(5):355-364. DOI:10.1080/10298430701690462.
158. Pereira PAA, Oliveira JRM, Picado-Santos LG. Mechanical Characterisation of Hot Mix Recycled Materials. International Journal of Pavement Engineering. 2004; 5(4):211-220. DOI:10.1080/10298430412331333668.
159. Monismith CL, J.A. Epps, and F.N. Finn. Improved asphlt mix design. Journal of Association of Asphalt Paving Technology. 1985; 55:347-406. Available

160. Ghuzlan KA, Carpenter SH. Traditional fatigue analysis of asphalt concrete mixtures. Urbana. 2002; 51:61801. Available
161. Carpenter S, Shen S. Dissipated energy approach to study hot-mix asphalt healing in fatigue. Transportation Research Record: Journal of the Transportation Research Board. 2006; (1970):178-185. Available
162. Lytton RL, J. Uzan, E.G. Fernando, R. Roque, D. Hiltunen, and S.M. Stoffels. Development and validation of performance prediction models and specifications for asphalt binders and paving mixes. Strategic Highway Research Program; 1993.
163. Hopman P, Kunst P, Pronk A A renewed interpretation method for fatigue measurements, verification of miner's rule. 4th Eurobitume Symposium in Madrid; 1989 p. 557-561.
164. Cho Y-H, Park D-W, Hwang S-D. A predictive equation for dynamic modulus of asphalt mixtures used in Korea. Construction and Building Materials. 2010; 24(4):513-519. Available
165. Shu X, Huang B. Micromechanics-based dynamic modulus prediction of polymeric asphalt concrete mixtures. Composites Part B: Engineering. 2008; 39(4):704-713. Available
166. Witczak M, Bonaquist R, Von Quintus H, Kaloush K Specimen geometry and aggregate size effects in uniaxial compression and constant height shear tests. Association of Asphalt Paving Technologists Proc; 2000.
167. Zhou F, Chen D-H, Scullion T, Bilyeu J. Case study: Evaluation of laboratory test methods to characterize permanent deformation properties of asphalt mixes. International Journal of Pavement Engineering. 2003; 4(3):155-164. Available
168. Zhao Y, Tang J, Liu H. Construction of triaxial dynamic modulus master curve for asphalt mixtures. Construction and Building Materials. 2012; 37:21-26. DOI:http://dx.doi.org/10.1016/j.conbuildmat.2012.06.067.
169. Zhou F, Scullion T Case study: preliminary field validation of simple performance tests for permanent deformation. Transportation Research Board, Annual Meeting CD printing, Washington, DC; 2003.
170. Sias Daniel J, Gibson N, Tarbox S, Copeland A, Andriescu A. Effect of long-term ageing on RAP mixtures: laboratory evaluation of plant-produced mixtures. Road Materials and Pavement Design. 2013; 14(sup2):173-192. Available
171. Birgisson B, Roque R, Kim J, Pham LV. The use of complex modulus to characterize the performance of asphalt mixtures and pavements in Florida. 2004.
172. Ping WV, Xiao Y. Empirical Correlation of Indirect Tension Resilient Modulus and Complex Modulus Test Results for Asphalt Concrete Mixtures. Road Materials and Pavement Design. 2008; 9(sup1):177-200. DOI:10.1080/14680629.2008.9690165.

"Every reasonable effort has been made to acknowledge the owners of copyright material. I would be pleased to hear from any copyright owner who has been omitted or incorrectly acknowledge"

Appendix A. Properties of Materials

Appendix A1. Los Angeles abrasion test (AS 1141.23-1995)

Los Angeles value	Sample Number		
	1	2	3
Before abrasion			
• Total mass of washed and dried material, m_T (g)	5002.3	5003.3	5002.7
After abrasion			
• Mass passing 1.70 mm sieve, m_P (g)	1078.51	1067.39	1087.88
• Mass of material retained on 1.70 mm sieve, m_R (g)	3921.75	3931.32	3910.61
• Check $m_P + m_R = m_T \pm 25$ g (g)	5000.26	4998.71	4998.49
After washing			
• Net mas of material retained on 1.7 mm sieve, m_W, (g)	3912.16	3924.16	3900.04
• Total mass passing 1.70 mm sieve m_T-m_W, (g)	1090.14	1079.14	1102.66
Los Angeles value (%)	21.8	21.6	22.0
• Average (%)	21.8		
• Standard deviation (%)	0.24		
• Coefficient of variation (%)	1.1		

Appendix A2. Flakiness index test (AS 1141.15-1999)

Sieve size	Sample-1			Sample-2			Sample 3		
	Retained the slotted		Passing the slotted	Retained the slotted		Passing the slotted	Retained the slotted		Passing the slotted
(mm)	(gr)	(%)	(gr)	(gr)	(%)	(gr)	(gr)	(%)	(gr)
63.00									
53.00									
37.50									
26.50									
19.00	329.33	7.69	51.01	264.50	5.29	36.70	345.40	6.91	41.40
13.20	2330.34	54.41	332.33	3449.00	68.98	452.70	3024.00	60.48	479.30
9.50	1335.18	31.18	182.73	1015.40	20.31	148.90	1314.90	26.30	139.90
6.30	287.95	6.72	72.68	271.30	5.43	33.90	341.80	6.84	45.79
Total	4282.80		638.75	5000.20		672.20	5026.10		706.39
Flakiness index (%)			14.91			13.44			14.05
• Average (%)			14.14						
• Standard deviation (%)			0.74						
• Coefficient of variation (%)			5.2						

Appendix A3. Particle density and water absorption of coarse aggregate: weighing-in-water method (AS 1141.5-2000)

	Sample number		
	1	2	3
Mass of dry aggregate, m_1 (g)	5003.1	5,000.00	5,001.79
Mass of the saturated surface-dry condition, m_2 (g)	5043.7	5,032.20	5,023.70
Weight of basket and material under water, w_1 (g)	3074	3,120.20	3,113.20
Weight of basket under water, w_2 (g)	0	0	0
1. The apparent particle density, ρ_A (t/m^3)	2.59	2.65	2.64
• Average (t/m^3)	2.63		
• Standard deviation (t/m^3)	0.04		
• Coefficient of variation (%)	1.35		
2. The particle density on a dry basis, ρ_D (t/m^3)	2.53	2.61	2.61
• Average (t/m^3)	2.58		
• Standard deviation (t/m^3)	0.04		
• Coefficient of variation (%)	1.71		
3. The particle density on saturated surface-dry density, ρ_S (t/m^3)	2.55	2.62	2.62
• Average (t/m^3)	2.60		
• Standard deviation (t/m^3)	0.04		
• Coefficient of variation (%)	1.55		
4. Water absorption of the aggretgate, W_A (%)	0.81	0.64	0.44
• Average (%)	0.63		
• Standard deviation (%)	0.19		
• Coefficient of variation (%)	29.64		

Appendix A4. Particle density and water absorption of fine aggregate (AS 1141.5-2000)

	Sample number		
	1	2	3
The mass of dry aggregate, m_1 (g)	489.9	482.1	485.51
The mass of the saturated surface-dry condition, m_2 (g)	500	500	500
The mass of pycnometer plus aggregate plus water, m_3 (g)	1028.6	997.9	1020.29
The mass of pycnometer plus water, m_4 (g)	724.5	699	725.02
1. The apparent particle density, ρ_a (t/m^3)	2.63	2.62	2.54
• Average (%)	2.60		
• Standard deviation (%)	0.05		
• Coefficient of variation (%)	1.82		
2. The particle density on a dry basis, ρ_{bd} (t/m^3)	2.49	2.39	2.36
• Average (%)	2.42		
• Standard deviation (%)	0.07		
• Coefficient of variation (%)	2.82		
3. The particle density on saturated surface-dry density, ρ_{bs} (t/m3)	2.54	2.48	2.44
• Average (%)	2.49		
• Standard deviation (%)	0.06		
• Coefficient of variation (%)	2.22		
4. Water absorption of the aggretgate, W_a (%)	2.06	3.71	2.98
• Average (%)	2.92		
• Standard deviation (%)	0.83		
• Coefficient of variation (%)	28.34		

Appendix A5. Bitumen content test for granular BRA modifier binder (WA 730.1 – 2011)

	Number of sample		
	1	2	3
a. The mass of matter on the filter ring			
Mass of filter ring in grams, m_2	44.58	52.44	47.34
Mass of filter ring and matter in grams, m_3	66.89	62.83	55.55
Mass of matter on filter ring in grams, m_{FR}	22.31	10.39	8.21
b. The mass of matter in extraction fluid			
Mass of centrifuge tubes in grams, m_6	9.37	9.39	9.45
Mass of centrifuge tubes in grams, m_7	9.41	9.51	9.35
Mass of centrifuge tubes and sediment in grams, m_8	12.94	11.29	12.48
Mass of centrifuge tubes and sediment in grams, m_9	13.15	11.42	12.57
Volume of extraction fluid in mL, V_1	1720	1760	1580
Volume of aliquot in mL, V_2	89.5	84	76
Mass of matter in extraction fluid in grams, m_{EF}	140.48	79.83	129.93
c. The Percentage bitumen			
Mass of test portion in grams, m_1	758.19	762.41	768.04
mass of oven dish in grams, m_4	1909.63	1909.66	1909.36
Mass of oven dish and contents in grams, m_5	2275.68	2348.67	2310.04
Bitumen content as a percentage, B_{it}	30.25	30.58	29.84
Bitumen content in average as a percentage	30		
Standard deviation (%)	0.37		
Coefficient of variation (%)	1.2		

Appendix A6. Particle size distribution of granular BRA mineral

Sieve size (mm)	Sample 1			Sample 2			Sample 3			Average
	Retained (gram)	Retained (%)	Passing (%)	Retained (gram)	Retained (%)	Passing (%)	Retained (gram)	Retained (%)	Passing (%)	Passing (%)
2.36	0.0	0.0	100.0	0.0	0.0	100.0	0.0	0.0	100.0	100
1.18	16.5	3.0	97.0	7.6	1.3	98.7	22.1	3.9	96.0	97
0.600	28.2	5.1	92.0	27.2	4.6	94.1	36.0	6.4	89.6	92
0.300	61.0	11.0	81.0	71.6	12.2	81.8	51.5	9.2	80.4	81
0.150	113.1	20.3	60.7	117.6	20.0	61.8	104.6	18.7	61.8	61
0.075	138.3	24.9	35.8	147.6	25.1	36.7	141.3	25.2	36.5	36
Pan	199.0	35.8	0.0	215.4	36.7	0.00	204.9	36.5	0.00	
Total	556.1	100.0		587.0	100		560.4	100.00		

Appendix B. Mix Design Data

Appendix B1. Maximum density of asphalt mixtures test (Test method WA 732.2 – 2011)

	5.0% binder content			5.5% binder content			6.0% binder content		
	1	2	3	4	5	6	7	8	9
Density of water at 25°C in t/m^3, ρ_w	0.997	0.997	0.997	0.997	0.997	0.997	0.997	0.997	0.997
Mass of Buchner flask in water in grams, m_1	741.38	741.38	741.38	743.18	743.18	743.18	743.15	743.15	743.15
Mass of test portion in air in grams, m_2	1198.05	1034.25	1077.52	1181.43	1075.36	1055.34	1061.60	1144.54	1051.52
Mass of flask plus contents in water in grams, m_3	1456.75	1359.06	1384.72	1443.73	1380.85	1368.55	1371.15	1420.63	1365.58
Maximum density of the asphalt in t/m^3, ρ_{max}	2.475	2.475	2.474	2.449	2.450	2.447	2.441	2.443	2.443
Average maximum density of the asphalt in t/m^3	2.475			2.449			2.442		
Standard deviation (t/m^3)	0.001			0.002			0.001		
Coefficient of variation (%)	0.02			0.06			0.05		

Appendix B2. Bulk density and void content of asphalt mixtures test (Test method WA 733.1 – 2011)

	5.0% binder content			5.5% binder content			6.0% binder content		
	1	2	3	4	5	6	7	8	9
m_1, mass of test specimen in grams	1194.40	1205.19	1205.05	1200.43	1198.8	1203.41	1135.72	1215.68	1206.22
m_2, mass of suspension device immersed in water in grams	0	0	0	0	0	0	0	0	0
m_3, mass of test specimen and suspension device immersed in water	686.01	689.02	689.86	687.38	685.69	687.94	649.54	694.95	689.16
ρ_w, density of water at 25°C in g/cm^3	0.997	0.997	0.997	0.997	0.997	0.997	0.997	0.997	0.997
V_{sample}, volume of test specimen in cm^3	509.92	517.72	516.74	514.59	514.65	517.02	487.64	522.30	518.62
ρ_{bulk}, bulk density of the test specimen in t/m^3	2.342	2.328	2.332	2.333	2.329	2.328	2.329	2.328	2.326
ρ_{max}, maximum density of the test specimen determined by Test Method WA 732.2-2011 in t/m^3	2.475	2.475	2.475	2.449	2.449	2.449	2.442	2.442	2.442
VIM, percentage air voids in %	5.4	5.9	5.8	4.8	4.9	5.0	4.6	4.7	4.8
BIT %,percentage bitumen as determined by Test Method WA 730.1	5.0	5.0	5.0	5.5	5.5	5.5	6.0	6.0	6.0
ρ_{BIT},density of bitumen at 25°C in t/m^3	1.03	1.03	1.03	1.03	1.03	1.03	1.03	1.03	1.03
VMA, percentage voids in mineral aggregates	16.7	17.2	17.1	17.2	17.4	17.4	18.2	18.2	18.3
VFB, percentage voids filled with bitumen	68.0	65.5	66.2	72.4	71.8	71.5	74.6	74.3	74.0
VIM in average (%)	5.7			4.9			4.7		
• Standard deviation (%)	0.30			0.10			0.06		
• Coefficient of variation (%)	5.3			2.2			1.4		
VMA in Average (%)	17.0			17.3			18.2		
• Standard deviation (%)	0.26			0.09			0.06		
• Coefficient of variation (%)	1.6			0.5			0.3		
VFB in Average(%)	66.6			71.9			74.3		
• Standard deviation (%)	1.25			0.47			0.28		
• Coefficient of variation (%)	1.9			0.7			0.4		

Appendix B3. Stability and flow of asphalt mixtures test (Test method WA 731.1-2010)

Sample Number	Bitumen Content (%)	Height (mm)					Height of Correction Factor	Maximum Load (kN)	Stability (kN)	Flow (mm)
		1	2	3	4	Average				
1	5.0	66.60	66.34	66.38	66.74	67	0.92	13.16	12.11	3.15
2	5.0	67.35	67.53	67.43	67.23	67	0.92	13.02	11.98	3.42
3	5.0	63.89	63.73	63.54	63.75	64	0.99	12.15	12.03	3.44
4	5.5	65.87	66.13	65.95	66.22	66	0.94	10.81	10.16	3.73
5	5.5	66.55	66.99	66.58	66.68	67	0.92	10.78	9.92	3.65
6	5.5	65.91	66.13	65.87	66.10	66	0.94	10.69	10.05	3.70
7	6.0	64.65	64.22	64.27	64.33	64	0.99	9.06	8.97	4.55
8	6.0	68.31	68.36	68.28	68.19	68	0.90	9.51	8.56	5.50
9	6.0	63.45	63.38	64.40	63.80	64	0.99	8.80	8.71	5.05

Appendix B4. The results of design parameter test with optimum bitumen content of 5.4%

Appendix B4-1. Stability and flow of asphalt mixtures test (5.4% bitumen content) (Test method WA 731.1-2010)

Sample number	Bitumen content (%)	Height (mm)					Height of correction factor	Maximum load (kN)	Stability (kN)	Flow (mm)
		1	2	3	4	Average				
1	5.4	66.13	66.10	66.25	66.22	66	0.94	10.91	10.26	3.53
2	5.4	66.25	66.21	66.15	66.26	66	0.94	11.08	10.42	3.45
3	5.4	66.18	66.65	66.10	66.31	66	0.94	10.71	10.07	3.37
Average									10.25	3.45
Standard deviation									0.17	0.08
Coefficient of variation (%)									1.70	2.32

Appendix B4-2. Maximum density of asphalt mixtures test (5.4% bitumen content) (Test method WA 732.2-2011)

	Sample number		
	1	2	3
Density of water at 25°C in t/m^3, ρ_w	0.997	0.997	0.997
Mass of Buchner flask in water in grams, m_1	742.08	742.08	742.08
Mass of test portion in air in grams, m_2	1013.68	1033.38	1016.36
Mass of flask plus contents in water in grams, m_3	1344.40	1356.23	1346.5
Maximum density of the asphalt in t/m^3, ρ_{max}	2.457	2.458	2.460
Maximum density of the asphalt (average) in t/m^3	2.458		
• Standard deviation	0.002		
• Coefficient of variation (%)	0.07		

Appendix B4-3. Bulk density and void content of asphalt mixtures test (5.4% bitumen content) (Test method WA 733.1 – 2011)

	Sample number		
	1	2	3
m_1, mass of test specimen in grams	1199.51	1199.8	1207.45
m_2, mass of suspension device immersed in water in grams	0	0	0
m_3, mass of test specimen and suspension device immersed in water	686.38	686.03	690.45
ρ_w, density of water at 25°C in g/cm^3	0.997	0.997	0.997
V_{sample}, volume of test specimen in cm^3	514.67	515.32	518.56
ρ_{bulk}, bulk density of the test specimen in t/m^3	2.331	2.328	2.328
ρ_{max}, maximum density of the test specimen determined by Test Method WA 732.2-2011 in t/m^3	2.458		
VIM, percentage air voids in %	5.18	5.28	5.27
BIT %,percentage bitumen as determined by Test Method WA 730.1	5.4	5.4	5.4
ρ_{BIT},density of bitumen at 25°C in t/m^3	1.04	1.04	1.04
VMA, percentage voids in mineral aggregates	17.3	17.4	17.4
VFB, percentage voids filled with bitumen	70.0	69.6	69.6
VIM in average (%)	5.2		
VMA in Average (%)	17.3		
VFB in Average(%)	69.8		

Appendix B5. Maximum density for BRA modified asphalt mixtures (Test method WA 732.2 – 2011)

	10% BRA Modified			20% BRA modified			30% BRA modified		
	4	4	6	7	8	9	10	11	12
ρ_w, Density of water at 25°C in t/m^3	0.997	0.997	0.997	0.997	0.997	0.997	0.997	0.997	0.997
m_1, Mass of Buchner flask in water in grams	742	741.91	741.91	740.86	740.86	740.86	741.35	741.35	741.35
m_2, Mass of test portion in air in grams	1013.14	1017.70	1024.15	1008.26	1041.20	1023.55	1023.63	1073.26	1199.77
m_3, Mass of flask plus contents in water in grams	1343.91	1346.26	1349.65	1340.00	1359.19	1349.10	1350.38	1380.33	1456.15
ρ_{max}, Maximum density of the asphalt in t/m^3	2.456	2.455	2.452	2.457	2.455	2.457	2.462	2.464	2.466
Average of maximum density in t/m^3	2.454			2.456			2.464		
• Standard deviation (t/m^3)	0.003			0.002			0.003		
• Coefficient of variation (%)	0.09			0.06			0.10		

Appendix C. Indirect Tensile Stiffness Modulus Test Data

Appendix C1. Bulk density of compacted asphalt (AS 2891.9.2-2005) and air voids content tests (AS 2891.8-2005) - First Stage

	Unmodified (0%)			BRA Modified (10%)			BRA Modified (20%)			BRA Modified (30%)		
	1	2	3	4	5	6	7	8	9	10	11	12
m_1, mass in air of the sample, in grams	1154.36	1150.63	1151.14	1158.04	1157.13	1155.8	1155.68	1152.48	1159.12	1156.05	1154.77	1144.54
m_2, mass in water of the saturated sample, in grams	664.92	663.08	663.75	666.62	666.16	665.35	665.57	664.59	668.54	668.54	666.27	660.29
m_3, mass in air of the saturated sample, in grams	1157.63	1154.73	1154.81	1162.11	1161.8	1159.15	1159.01	1157.79	1163.12	1160.21	1158.7	1148.25
ρ_w, density of water at the test temperature, in t/m^3	0.997	0.997	0.997	0.997	0.997	0.997	0.997	0.997	0.997	0.997	0.997	0.997
ρ_{bulk}, bulk density of the sample, in t/m^3	2.336	2.333	2.337	2.330	2.328	2.334	2.335	2.330	2.337	2.344	2.338	2.339
ρ_{max}, maximum density of the mix, in t/m^3	2.458	2.458	2.458	2.454	2.454	2.454	2.456	2.456	2.456	2.464	2.464	2.464
AV, air voids in compacted mix (%)	5.0	5.1	4.9	5.0	5.2	4.9	4.9	5.1	4.9	4.9	5.1	5.1
AV, in average (%)	5.0			5.1				5.0		5.1		
• Standard deviation (%)	0.08			0.13				0.15		0.14		
• Coefficient of variation (%)	1.6			2.5				3.00		2.8		

Appendix C2. Indirect Tensile Stiffness Modulus Test Results (AS 2891.13.1 – 1995) - First Stage

	Unmodified (0%)			BRA Modified (10%)			BRA Modified (20%)			BRA Modified (30%)		
	1	2	3	1	2	3	1	2	3	1	2	3
1. Resilient modulus (MPa) - Mean	4325	4413	4360	5208	5431	5000	7218	7316	7114	7854	7588	7337
- Standard deviation	53.9	130.7	116.3	90.17	88.55	53.5	77.26	152.58	88.68	112.3	69.57	136.16
- Coefficient of variation (%)	1.25	2.96	2.67	1.73	1.63	1.07	1.07	2.09	1.25	1.43	0.92	1.86
2. Rise time (ms) - Mean	39.8	38.2	39.4	36.0	36.5	35.9	36.7	37.6	36.0	36.5	36.7	35.9
- Standard deviation	0.61	0.48	0.29	0.38	0.70	0.45	1.22	0.61	0.93	0.96	0.45	0.24
- Coefficient of variation (%)	1.54	1.26	0.75	1.05	1.92	1.25	3.33	1.63	2.58	2.63	1.22	0.67
3. Test temperature (°C): - Skin	24.5	24.6	24.5	24.7	24.6	24.5	24.6	24.6	24.6	24.5	24.7	24.6
- Core	24.4	24.3	24.3	24.5	24.4	24.3	24.6	24.6	24.6	24.2	24.5	24.4

Appendix C3. Bulk density (AS 2891.9.2-2005) and air void tests (AS 2891.8-2005) for unmodified mixtures - Second Stage

	Testing temperature – Sample number														
	5°C			15°C			25°C			40°C			60°C		
	1	2	3	4	5	6	7	8	9	10	11	12	13	14	15
m_1, mass in air of the sample (gr)	1203.58	1208.51	1202.51	1201.69	1206.9	1198.59	1183.55	1182.15	1184.52	1187.93	1186.6	1184.19	1186.73	1188.3	1206.1
m_2, mass in water of the saturated sample (gr)	695.31	697.18	694.36	691.44	696.19	691.83	683.48	682.53	683.75	684.83	684.98	683.43	684.87	685.22	695.51
m_3, mass in air of the saturated sample (gr)	1208.93	1212.62	1207.26	1205.16	1211.91	1203.63	1188.37	1187.3	1190.76	1192.62	1192.76	1189.1	1191.81	1193.79	1211.09
ρ_w, density of water at the test temperature (t/m^3)	0.997	0.997	0.997	0.997	0.997	0.997	0.997	0.997	0.997	0.997	0.997	0.997	0.997	0.997	0.997
ρ_{bulk}, bulk density of the sample (t/m^3)	2.336	2.338	2.337	2.332	2.333	2.335	2.337	2.335	2.329	2.332	2.330	2.335	2.334	2.330	2.332
ρ_{max}, maximum density of the mix (t/m^3)	2.458	2.458	2.458	2.458	2.458	2.458	2.458	2.458	2.458	2.458	2.458	2.458	2.458	2.458	2.458
AV, air voids in compacted mix (%)	5.0	4.9	4.9	5.1	5.1	5.0	4.9	5.0	5.2	5.1	5.2	5.0	5.0	5.2	5.1
AV, in average (%)	5.0			5.1			5.1			5.1			5.1		

Appendix C4. Bulk density (AS 2891.9.2-2005) and air void tests (AS 2891.8-2005) for BRA modified asphalt mixtures - Second Stage

	Testing temperature – Sample number														
	5°C			15°C			25°C			40			60		
	1	2	3	4	5	6	7	8	9	10	11	12	13	14	15
m_1, mass in air of the sample (gr)	1202.81	1201.13	1202.4	1197.76	1206.26	1206.1	1196.76	1206.26	1204.82	1202.81	1153.79	1194.06	1206.07	1202.7	1196.41
m_2, mass in water of the saturated sample (gr)	692.29	691.74	692.4	690.22	695.92	694.51	688.22	694.92	694.41	692.3	664.84	687.37	694.66	692.71	688.79
m_3, mass in air of the saturated sample (gr)	1206.78	1205.22	1206.05	1201.9	1210.99	1210.37	1200.17	1210.38	1209.74	1207.91	1158.48	1198.12	1210.62	1207.44	1201.55
ρ_w, density of water at the test temperature (t/m^3)	0.997	0.997	0.997	0.997	0.997	0.997	0.997	0.997	0.997	0.997	0.997	0.997	0.997	0.997	0.997
ρ_{bulk}, bulk density of the sample (t/m^3)	2.331	2.332	2.334	2.334	2.335	2.331	2.331	2.333	2.331	2.326	2.330	2.331	2.331	2.330	2.326
ρ_{max}, maximum density of the mix (t/m^3)	2.456	2.456	2.456	2.456	2.456	2.456	2.456	2.456	2.456	2.456	2.456	2.456	2.456	2.456	2.456
AV, air voids in compacted mix (%)	5.1	5.0	5.0	5.0	4.9	5.1	5.1	5.0	5.1	5.3	5.1	5.1	5.1	5.1	5.3
AV, in average (%)	5.1			5.0			5.1			5.2			5.2		

Appendix C5. Equation of each individual specimen for unmodified asphalt mixtures - Second Stage)

Triplicate samples	Pulse repetition period (ms)	Test temperature									
		5°C (sample 1 - 3)		15°C (sample 4-6)		25°C (sample 7-9)		40°C (sample 10 -12)		60°C (sample 13-15)	
		Equation	R^2	Equation	R^2	Equation	R^2	Equation	R^2	Equation	R^2
1	1000	$y = 27785.382x^{-0.159}$	0.982	$y = 21725.341x^{-0.210}$	0.995	$y = 18037.920x^{-0.394}$	0.989	$y = 3641.624x^{-0.465}$	0.968	$y = 335.703x^{-0.227}$	0.950
1	2000	$y = 26930.682x^{-0.149}$	0.988	$y = 23032.387x^{-0.236}$	0.999	$y = 15065.596x^{-0.380}$	0.995	$y = 2825.163x^{-0.414}$	0.969	$y = 347.121x^{-0.252}$	0.988
1	3000	$y = 23941.545x^{-0.108}$	0.985	$y = 23331.290x^{-0.243}$	0.998	$y = 14746.090x^{-0.386}$	0.986	$y = 2446.640x^{-0.383}$	0.998	$y = 311.577x^{-0.239}$	0.988
2	1000	$y = 27396.909x^{-0.153}$	0.982	$y = 20565.153x^{-0.222}$	0.994	$y = 17458.032x^{-0.417}$	0.991	$y = 4166.256x^{-0.510}$	0.989	$y = 458.458x^{-0.270}$	0.980
2	2000	$y = 24547.431x^{-0.122}$	0.971	$y = 20312.883x^{-0.229}$	0.998	$y = 13216.321x^{-0.381}$	0.999	$y = 2646.707x^{-0.428}$	0.992	$y = 397.220x^{-0.244}$	0.989
2	3000	$y = 21751.530x^{-0.078}$	0.970	$y = 21257.903x^{-0.243}$	0.999	$y = 12505.327x^{-0.378}$	0.997	$y = 2315.536x^{-0.402}$	1.000	$y = 607.105x^{-0.367}$	0.934
3	1000	$y = 28880.879x^{-0.161}$	0.943	$y = 21330.896x^{-0.222}$	0.998	$y = 17212.980x^{-0.394}$	0.996	$y = 4774.301x^{-0.551}$	0.987	$y = 297.327x^{-0.187}$	0.897
3	2000	$y = 25226.077x^{-0.124}$	0.991	$y = 21187.294x^{-0.233}$	0.995	$y = 13186.563x^{-0.358}$	0.994	$y = 2299.887x^{-0.396}$	0.995	$y = 302.845x^{-0.200}$	0.981
3	3000	$y = 23880.484x^{-0.097}$	0.948	$y = 21186.306x^{-0.235}$	0.999	$y = 15999.522x^{-0.412}$	0.996	$y = 2210.813x^{-0.393}$	0.996	$y = 334.296x^{-0.234}$	0.940

Appendix C6. Equation of each individual specimen for 20% BRA modified asphalt mixtures - Second Stage)

Triplicate samples	Pulse repetition period (ms)	Test temperature									
		5°C (sample 1 - 3)		15°C (sample 4-6)		25°C (sample 7-9)		40°C (sample 10 -12)		60°C (sample 13-15)	
		Equation	R^2	Equation	R^2	Equation	R^2	Equation	R^2	Equation	R^2
1	1000	$y = 35539.136x^{-0.139}$	0.929	$y = 26862.268x^{-0.197}$	0.993	$y = 16006.005x^{-0.249}$	0.999	$y = 5338.460x^{-0.382}$	0.953	$y = 946.113x^{-0.295}$	0.989
1	2000	$y = 29514.125x^{-0.084}$	0.978	$y = 24569.065x^{-0.181}$	0.998	$y = 22314.351x^{-0.339}$	0.998	$y = 6000.386x^{-0.438}$	0.994	$y = 726.499x^{-0.244}$	0.980
1	3000	$y = 29690.724x^{-0.074}$	0.959	$y = 25515.661x^{-0.189}$	0.996	$y = 23930.820x^{-0.363}$	0.985	$y = 4555.450x^{-0.377}$	0.999	$y = 705.464x^{-0.243}$	0.987
2	1000	$y = 34105.364x^{-0.126}$	0.945	$y = 24478.870x^{-0.174}$	0.993	$y = 22210.018x^{-0.328}$	0.975	$y = 8012.826x^{-0.464}$	0.995	$y = 657.052x^{-0.210}$	0.988
2	2000	$y = 31777.213x^{-0.105}$	0.981	$y = 25854.603x^{-0.192}$	0.995	$y = 19941.144x^{-0.325}$	0.987	$y = 6246.397x^{-0.435}$	1.000	$y = 643.461x^{-0.211}$	0.993
2	3000	$y = 28178.571x^{-0.063}$	0.916	$y = 26729.407x^{-0.199}$	0.998	$y = 17600.860x^{-0.308}$	1.000	$y = 6266.442x^{-0.448}$	0.999	$y = 652.761x^{-0.218}$	0.998
3	1000	$y = 34368.643x^{-0.122}$	0.981	$y = 26361.399x^{-0.179}$	0.991	$y = 19441.004x^{-0.287}$	0.994	$y = 7313.293x^{-0.457}$	0.996	$y = 868.060x^{-0.260}$	0.991
3	2000	$y = 32337.845x^{-0.103}$	0.982	$y = 26484.699x^{-0.186}$	0.996	$y = 19764.196x^{-0.312}$	0.999	$y = 4760.660x^{-0.369}$	0.999	$y = 805.999x^{-0.251}$	0.986
3	3000	$y = 32971.991x^{-0.099}$	0.988	$y = 26345.712x^{-0.182}$	0.997	$y = 19324.621x^{-0.313}$	0.998	$y = 5238.498x^{-0.396}$	0.999	$y = 703.411x^{-0.248}$	0.957

Appendix C7. The change in resilient modulus (%) due to the increase in repetition period Second stage)

Asphalt mixtures	Rise time (ms)	Pulse repetition period (ms)	Temperature (°C)				
			5	15	25	40	60
Unmodified	40	1000 to 2000	0.6	-4.2	-12.7	-11.6	-4.0
Unmodified	40	2000 to 3000	4.1	-0.9	-3.1	-3.4	-3.6
Unmodified	60	1000 to 2000	1.7	-4.6	-11.6	-8.0	-5.1
Unmodified	60	2000 to 3000	5.6	-1.3	-3.8	-2.5	-5.2
Unmodified	80	1000 to 2000	2.5	-4.9	-10.8	-5.4	-5.9
Unmodified	80	2000 to 3000	6.7	-1.6	-4.3	-1.9	-6.3
BRA Modified	40	1000 to 2000	1.2	-2.1	-6.3	-11.0	-4.8
BRA Modified	40	2000 to 3000	3.6	0.7	-2.7	-3.1	-5.3
BRA Modified	60	1000 to 2000	2.4	-2.1	-7.4	-10.0	-4.0
BRA Modified	60	2000 to 3000	4.4	0.5	-3.2	-2.8	-5.1
BRA Modified	80	1000 to 2000	3.2	-2.2	-8.1	-9.3	-3.4
BRA Modified	80	2000 to 3000	5.0	0.3	-3.5	-2.6	-5.0

Appendix C8. Results of analysis of covariance (ANCOVA)

Appendix C8(a). Results of Levene's test of equality of error variances[a]

F	df1	df2	Significant
3.295	1	178	0.071

Tests the null hypothesis that the error variance of the dependent variable is equal across groups.

[a] : Design: Intercept + Temperature + Risetime + Pulse + Asphalt

Appendix C8(b). Test of between – subject effects

Source	Type III sum of squares	df	Mean square	F	Significant	Partial Eta squared
Corrected Model	6944873521[a]	4	1736218380	161.050	0.000	0.786
Intercept	2551620719	1	2551620719	236.686	0.000	0.575
Temperature	6627107821	1	6627107821	614.724	0.000	0.778
Rise time	21393718.53	1	21393718.53	1.984	0.161	0.011
Pulse repetition period	63131.339	1	63131.339	0.006	0.939	0.000
Asphalt mixtures	296308850.1	1	296308850.1	27.485	.000	0.136
Error	1886607926	175	10780616.72			
Total	17208583635	180				
Corrected Total	8831481447	179				

Dependent Variable: Modulus

[a]: R Squared = 0.786 (Adjusted R Squared = 0.781)

Appendix C8(c). Estimated marginal means asphalt

Asphalt mixtures	Mean	Standard error	95% confidence interval	
			Lower bound	Upper bound
Unmodified	5538.956a	346.099	4855.890	6222.021
BRA modified	8105.011a	346.099	7421.945	8788.077

Appendix C8(d): Pairwise comparison

Asphalt mixtures		Mean difference (I-J)	Standard error	Significant [b]	95% confidence interval for difference [b]	
Unmodified (I)	BRA modified (J)				Lower bound	Upper bound
1.00	2.00	-2566.056*	489.458	0.000	-3532.056	-1600.055
2.00	1.00	2566.056*	489.458	0.000	1600.055	3532.056

Based on estimated marginal means

** : The mean difference is significant at the 0.05 level.*

b : Adjustment for multiple comparisons: Bonferroni.

Appendix C8(e). Univariates test

	Sum of squares	df	Mean square	F	Significant	Partial Eta Squared
Contrast	296308850.1	1	296308850.1	27.485	0.000	0.136
Error	1886607926	175	10780616.72			

The F tests the effect of Asphalt. This test is based on the linearly independent pairwise comparisons among the estimated marginal means.

Appendix D. Dynamic Creep Test Data

Appendix D1. Bulk density of compacted asphalt (AS 2891.9.2-2005) and air voids (AS 2891.8-2005) - Dynamic Creep Test

	Unmodified (0%)			BRA modified (10%)			BRA modified (20%)			BRA modified (30%)	
	1	2	3	4	5	6	7	8	9	10	11
m_1, mass in air of the sample, in grams	853.95	915.68	904.14	884.92	931.25	939.06	916.96	915.58	919.75	868.11	894.05
m_2, mass in water of the saturated sample, in grams	490.52	529.18	521.36	508.34	536.52	540.26	527.32	527.57	528.72	501.25	517.15
m_3, mass in air of the saturated sample, in grams	855.66	919.89	908.12	887.66	934.89	942.12	919.66	918.89	922.12	871.66	897.89
ρ_w, density of water at the test temperature, in t/m^3	0.997	0.997	0.997	0.997	0.997	0.997	0.997	0.997	0.997	0.997	0.997
ρ_{bulk}, bulk density of the sample, in t/m^3	2.332	2.337	2.331	2.326	2.331	2.330	2.330	2.333	2.331	2.337	2.341
ρ_{max}, maximum density of the mix, in t/m^3	2.458	2.458	2.458	2.454	2.454	2.454	2.456	2.456	2.456	2.464	2.464
AV, air voids in compacted mix (%)	5.1	4.9	5.2	5.2	5.0	5.1	5.1	5.0	5.1	5.2	5.0
AV, in average (%)	5.1			5.1			5.1			5.1	
• Standard deviation (%)	0.15			0.10			0.06			0.14	
• Coefficient of variation (%)	3			2			1			3	

Appendix D2. The results obtained from the dynamic creep test

	Unmodified (0%)			BRA modified (10%)			BRA modified (20%)			BRA modified (30%)	
	1	2	3	4	5	6	7	8	9	10	11
Total permanent strain (ε_p) (%)	2.974	2.988	2.956	2.884	2.967	3.039	3.008	3.038	2.994	2.058	2.225
Number of cycle[1]	1919	1856	1483	6869	6703	5474	15803	13415	14649	30000	27906
Minimum strain rate (μ€/cycle)	5.74	6.06	7.92	1.805	1.915	2.515	0.698	0.723	0.645	0.155	0.398
Cycles at minimum strain rate	1584	1692	1298	3840	3376	3640	6992	12784	13344	29248	24448
Strain at minimum strain rate (%)	2.758	2.877	2.800	2.232	2.279	2.52	2.29	2.99	2.899	2.044	2.101

[1]*Number of cycles to obtain the total permanent strain (ε_p)*

Appendix D3: The results of creep modulus calculated at 1800 cycles (3600 seconds)

	Unmodified			BRA Modified (10%)			BRA Modified (20%)			BRA Modified (30%)	
	1	2	3	4	5	6	7	8	9	10	11
Cyclic stress[1] (kPa)	199.9	199.6	199.6	199.4	199.6	199.3	199.4	199.3	199.4	199.4	199.1
Total permanent strain[1] (%)	2.768	2.818	2.956	1.807	1.933	2.024	1.785	1.868	1.731	1.165	1.299
Creep modulus (MPa)	7.2	7.1	6.8	11.0	10.3	9.8	11.2	10.7	11.5	17.1	15.3
Average creep modulus (MPa)	7.0			10.4			11.1			16.2	
Total permanent strain[2] (%)	2.971			1.981			1.841			1.222	
Creep modulus[3] (MPa)	6.7			10.1			10.9			16.4	

[1]*: The results obtained from the dynamic creep test*

[2]*: The results based on the equation obtained by using regression analysis*

[3]*:The calculation used the total permanent strain obtained from the regression analysis and cyclic stress of 200 kPa*

Appendix D4: Results obtained by using the stepwise concept

	Unmodified (0%)			Modified (10%)			Modified 20%			Modified 30%	
	1	2	3	4	5	6	7	8	9	10	11
Flow Number, FN (cycle)	1681	1473	1363	4143	5321	4529	7777	8289	10561	27457	23585
-Average FN	1506			4664			8876			25521	
-Standard Deviation	161			601			1482			2738	
-Coefficient of Variation (%)	10.7			12.9			16.7			10.7	
Flow Point (%)	2.847	2.711	2.900	2.382	2.709	2.731	2.341	2.595	2.703	2.024	2.821
-Average Flow point	2.819			2.607			2.546			2.423	
-Standard Deviation	0.097			0.195			0.186			0.398	
-Coefficient of Variation (%)	3.5			7.5			7.3			16.4	
Minimum strain rate (με/cycle)	6.272	6.771	8.232	1.954	2.029	2.749	0.757	0.832	0.77	0.186	0.418
-Average rate of strain	7.092			2.244			0.786			0.302	
-Standard Deviation	1.019			0.439			0.040			0.116	
-Coefficient of Variation (%)	14.4			19.6			5.1			38.4	
Sloop at steady state	0.07	0.08	0.09	0.02	0.02	0.03	0.008	0.009	0.009	0.002	0.005

Appendix E. Wheel Tracking Test Data

Appendix E1. Bulk density of compacted asphalt (AS 2891.9.2-2005) and air voids content tests (AS 2891.8-2005)

	Unmodified (0%)			BRA Modified (10%)			BRA Modified (20%)			BRA Modified (30%)		
	1	2	3	4	5	6	7	8	9	10	11	12
m_1, mass in air of the sample, in grams	10458	10690	10414	10600	10675	10605	10302	10341	10435	10669	10697	10688
m_2, mass in water of the saturated sample, in grams	6010	6204	5974	6165	6189	6169	5965	6019	5967	6175	6212	6202
m_3, mass in air of the saturated sample, in grams	10479	10769	10430	10697	10750	10710	10369	10427	10424	10729	10770	10754
ρ_w, density of water at the test temperature, in t/m^3	0.997	0.997	0.997	0.997	0.997	0.997	0.997	0.997	0.997	0.997	0.997	0.997
ρ_{bulk}, bulk density of the sample, in t/m^3	2.333	2.335	2.330	2.332	2.333	2.328	2.332	2.339	2.334	2.336	2.340	2.341
ρ_{max}, maximum density of the mix, in t/m^3	2.458	2.458	2.458	2.454	2.454	2.454	2.456	2.456	2.456	2.464	2.464	2.464
AV, air voids in compacted mix (%)	5.1	5.0	5.2	5.0	4.9	5.1	5.0	4.8	5.0	5.2	5.0	5.0
AV, in average (%)	5.1			5.0			4.9			5.1		
• Standard deviation (%)	0.10			0.11			0.14			0.11		
• Coefficient of variation (%)	1.9			2.1			2.8			2.2		

Appendix E2. Rut progression curve of wheel tracking test for each specimen

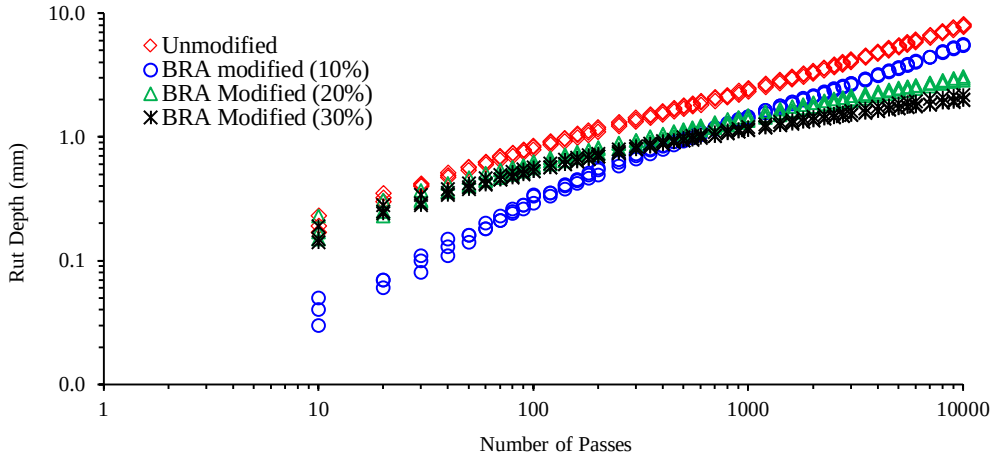

Appendix E3. Tracking rate for each specimen

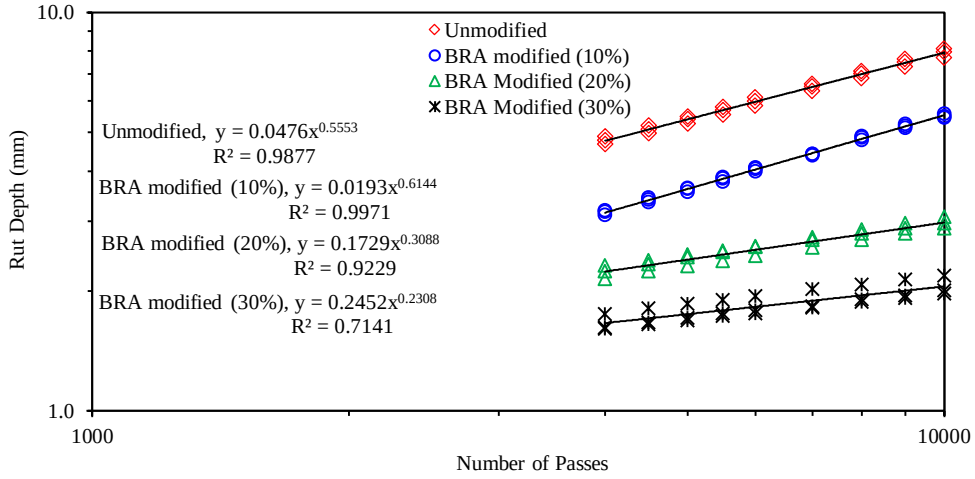

Appendix E4. Average tracking rate for asphalt mixtures based on average rut depth obtained in Appendix E3

Asphalt mixtures	For 4,000 passes		For 10,000 passes		Tracking rate (mm/k passes)
	x (passes)	y (Depth-mm)	x (passes)	y (Depth-mm)	
Unmodified	4,000	4.77	10,000	7.93	0.53
BRA modified (10%)	4,000	3.15	10,000	5.52	0.40
BRA modified (20%)	4,000	2.24	10,000	2.97	0.12
BRA modified (30%)	4,000	1.66	10,000	2.05	0.07

Appendix E5. Velocity values for each specimen

Sample No	Velocity (mm/minute)			
	Unmodified	BRA modified (10%)	BRA modified (20%)	BRA modified (30%)
1	0.02230	0.01659	0.00573	0.00303
2	0.02148	0.01675	0.00508	0.00250
3	0.02254	0.01652	0.00444	0.00263
Average	0.02211	0.01662	0.00508	0.00272
SD	0.00056	0.00012	0.00065	0.00028
CV (%)	2.5	0.7	12.7	10.2

Appendix E6. Dynamic stability values for each specimen

Sample No	Dynamic stability (passes/mm)			
	Unmodified	BRA modified (10%)	BRA modified (20%)	BRA modified (30%)
1	1207	1750	3684	5833
2	1207	1750	3684	5833
3	1186	1842	3333	5833
Average	1200	1781	3567	5833
SD	12	53	203	0
CV (%)	1.0	3.0	5.7	1.08E-13

Appendix F. Repeated Flexural Bending Test Data

Appendix F1. Bulk density of compacted asphalt (AS 2891.9.2-2005) and air voids content (AS 2891.8-2005) for unmodified asphalt mixtures

	400 με			600 με			800 με		
	1	2	3	4	5	6	7	8	9
m_1, mass in air of the sample, in grams	2793.25	2792.43	2783.02	2862.69	2877.82	2864.32	2887	2878.99	2893.08
m_2, mass in water of the saturated sample, in grams	1606.33	1602.06	1600.14	1645.67	1654.28	1644.79	1658.02	1653.67	1663.44
m_3, mass in air of the saturated sample, in grams	2800.22	2797.32	2789.24	2868.41	2882.96	2869.44	2892.66	2884.65	2898.18
ρ_w, density of water at the test temperature, in t/m^3	0.997	0.997	0.997	0.997	0.997	0.997	0.997	0.997	0.997
ρ_{bulk}, bulk density of the sample, in t/m^3	2.333	2.329	2.333	2.334	2.335	2.332	2.331	2.332	2.336
ρ_{max}, maximum density of the mix, in t/m^3	2.458	2.458	2.458	2.458	2.458	2.458	2.458	2.458	2.458
AV, air voids in compacted mix (%)	5.1	5.2	5.1	5.0	5.0	5.1	5.2	5.1	5.0
AV, in average (%)	5.1			5.0				5.1	
• Standard deviation (%)	0.06			0.06				0.10	
• Coefficient of variation (%)	1.1			1.1				2.0	

Appendix F2. Bulk density of compacted asphalt (AS 2891.9.2-2005) and air voids content (AS 2891.8-2005) for BRA modified asphalt mixtures

	400 με			600 με			800 με		
	1	2	3	4	5	6	7	8	9
m_1, mass in air of the sample, in grams	2865.14	2869.4	2857.24	2885.59	2879.86	2874.16	2912.39	2910	2888.25
m_2, mass in water of the saturated sample, in grams	1645.18	1647.05	1641.99	1656.82	1654.25	1649.59	1672.62	1673.26	1658.96
m_3, mass in air of the saturated sample, in grams	2869.66	2872.34	2861.55	2889.65	2884.83	2878.19	2918.09	2915.97	2893.18
ρ_w, density of water at the test temperature, in t/m^3	0.997	0.997	0.997	0.997	0.997	0.997	0.997	0.997	0.997
ρ_{bulk}, bulk density of the sample, in t/m^3	2.333	2.335	2.336	2.334	2.333	2.332	2.331	2.335	2.333
ρ_{max}, maximum density of the mix, in t/m^3	2.456	2.456	2.456	2.456	2.456	2.456	2.456	2.456	2.456
AV, air voids in compacted mix (%)	5.0	4.9	4.9	5.0	5.0	5.0	5.1	4.9	5.0
AV, in average (%)	4.9			5.0				5.0	
• Standard deviation (%)	0.06			0.00				0.10	
• Coefficient of variation (%)	1.2			0.0				2.0	

Appendix F3. Initial flexural stiffness and phase angle for unmodified and BRA modified asphalt mixtures

Sample Number	Initial flexural stiffness (MPa)						Phase angle (Degree)					
	Unmodified			BRA modified			Unmodified			BRA modified		
	400 με	600 με	800 με	400 με	600 με	800 με	400 με	600 με	800 με	400 με	600 με	800 με
	4457	5230	5015	8867	8244	9032	36.6	34.2	34.8	23.1	28.9	22.32
	5324	5279	5484	8518	9005	9121	32.5	33.8	32.5	21.2	24.2	24.12
	5352	4957	5597	8533	8436	8855	32.4	34.3	33.6	21.5	24.6	22.06
Average	5044	5155	5365	8639	8562	9003	33.8	34.1	33.7	21.9	25.9	22.83
SD	509	174	309	197	396	135	2.4	0.3	1.1	1.0	2.6	1.12
CV (%)	10.0	3.4	5.7	2.3	4.6	1.5	7	1	3	4	10	5

Appendix F4. Determination of fatigue life for unmodified asphalt mixtures

Sample number	Dimension (mm)			Initial tensile strain (με)	Initial flexural stiffness, S_0 (MPa)	Classical method		Energy stiffness ratio method			Ratio (S_f/S_0)
	Width	Height	Length			N_f (Cycle)	Stiffness at N_f (MPa)	N_f (Cycle)	Energy ratio	Stiffness at N_f, S_f (MPa)	
1	62.27	48.69	400	400	4457	122,550	2228	149,040	65870	1956	0.44
2	62.33	48.98	400	400	5324	142,880	2665	168,520	76143	2404	0.45
3	62.38	48.70	400	400	5352	138,030	2677	171,780	75828	2356	0.44
Average					5044	134,487	2523	163,113	72613	2238	0.44
SD					509	10,618	255	12,296	5842	246	0.006
CV (%)					10.0	7.9	10.1	7.5	8.0	11.0	1.3
4	62.08	49.26	400	600	5230	39,000	2610	61,030	23491	1994	0.38
5	62.31	49.40	400	600	5279	35,570	2639	47,610	20027	2209	0.42
6	62.04	49.24	400	600	4957	53,420	2476	60,100	27795	2277	0.46
Average					5155	42,663	2,575	56,247	23771	2160	0.42
SD					174	9,472	86	7494	3891	148	0.04
CV (%)					3.4	22.2	3.4	13.3	16.4	6.8	9.5
7	62.15	49.59	400	800	5015	11,420	2510	13,200	5571	2240	0.45
8	62.43	49.30	400	800	5484	8,770	2749	11,920	4655	2098	0.38
9	62.57	49.21	400	800	5597	8,660	2800	10,850	4604	2389	0.43
Average					5365	9,617	2,686	11,990	4943	2242	0.42
SD					309	1562	154	1176	544		0.04
CV (%)					5.7	16.2	5.8	9.8	11.0		8.6

Appendix F5. Determination of fatigue life for unmodified BRA modified asphalt mixtures

Sample number	Dimension (mm)			Initial tensile strain (με)	Initial flexural stiffness, S_0 (MPa)	Classical method		Energy stiffness ratio method			Ratio (S_f/S_0)
	Width	Height	Length			N_f (Cycle)	Stiffness at N_f (MPa)	N_f (Cycle)	Energy ratio	Stiffness at N_f, S_f (MPa)	
1	62.26	48.82	400	400	8867	324,830	4458	348,060	167,427	4208	0.47
2	62.18	49.02	400	400	8518	293,980	4309	332,400	153,637	3944	0.46
3	61.43	48.97	400	400	8533	301,990	4264	345,400	170,103	4208	0.49
Average					8639	306,933	4,344	341,953	163,722	4120	0.48
SD					197	16008	101	8,380	8,836	152	0.02
CV (%)					2.3	5.2	2.3	2.5	5.4	3.7	3.2
4	62.43	48.81	400	600	8244	95,400	4122	98,050	48,408	4014	0.49
5	62.53	49.31	400	600	9005	72,450	4511	75,150	36,691	4355	0.48
6	62.56	49.13	400	600	8436	88,000	4229	91,650	44,853	4089	0.48
Average					8562	85,283	4,287	88,283	43,317	4153	0.48
SD					396	11713	200	11815	6007	179	0.006
CV (%)					4.6	13.7	4.7	13.4	13.9	4.3	1.2
7	62.36	49.46	400	600	9032	23,250	4523	24,300	11,714	4292	0.48
8	62.61	49.31	400	600	9121	21,550	4568	22,650	10,740	4360	0.48
9	62.51	48.94	400	600	8855	24,000	4482	25,200	12,191	4360	0.49
Average					9002	22,933	4,524	24,050	11,548	4337	0.48
SD					135	1255	43	1293	739	39	0.006
CV (%)					1.5	5.4	0.9	5.4	6.4	0.9	1.2

Appendix F6. The value of k_1 and k_2 for Unmodified and BRA modified asphalt mixtures

Asphalt mixtures	No	Classical approach				Energy stiffness ratio approach			
		k_1	Log k_1	k_2	R^2	k_1	Log k_1	k_2	R^2
Unmodified	1	8.386E+13	13.924	3.384	0.986	1.302E+14	14.115	3.412	0.939
	2	3.614E+15	15.558	3.987	0.990	1.214E+15	15.084	3.775	0.985
	3	2.144E+15	15.331	3.886	0.925	2.709E+15	15.433	3.893	0.946
BRA modified	1	2.065E+15	15.315	3.753	0.981	2.797E+15	15.447	3.793	0.984
	2	1.735E+15	15.239	3.749	0.997	3.802E+15	15.580	3.862	0.999
	3	8.153E+14	14.911	3.613	0.987	2.013E+15	15.304	3.744	0.992

Appendix F7. Damage parameter for unmodified and BRA modified asphalt mixtures based on the flexural stiffness

Initial tensile strain (με)	Sample number	Unmodified			BRA modified		
		dE/dN*	E_{00}	*dD/dN*	*dE*/dN*	E_{00}	*dD/dN*
400	1	0.00863	3292	2.621E-06	0.00712	6830	1.042E-06
	2	0.00677	3854	1.756E-06	0.00835	6740	1.239E-06
	3	0.00786	3776	2.082E-06	0.00757	7086	1.068E-06
Average		0.00775	3641	2.153E-06	0.00768	6885	1.116E-06
SD		9.3E-04	304	4.4E-07	6.2E-04	180	1.1E-07
CV		12.1	8.4	20.3	8.1	2.6	9.6
600	4	0.0276	3699	7.461E-06	0.0171	6020	2.840E-06
	5	0.0299	3716	8.046E-06	0.0196	6137	3.193E-06
	6	0.0225	3674	6.123E-06	0.0111	5360	2.071E-06
Average		0.0267	3696	7.210E-06	0.0159	5839	2.701E-06
SD		3.8E-03	21	9.9E-07	4.4E-03	419	5.7E-07
CV		14.2	0.6	13.7	27.4	7.2	21.2
800	7	0.1341	4034	3.324E-05	0.0456	5727	7.962E-06
	8	0.1814	4328	4.191E-05	0.0974	6616	1.472E-05
	9	0.1587	4162	3.812E-05	0.0388	5542	7.001E-06
Average		0.1581	4175	3.776E-05	0.0606	5962	9.894E-06
SD		2.4E-02	147	4.3E-06	3.2E-02	574	4.2E-06
CV		15.0	3.5	11.5	52.9	9.6	42.5

Appendix F8. Damage parameter values for unmodified and BRA modified asphalt mixtures based on the cumulative dissipated energy

Initial tensile strain (με)	Sample number	Unmodified			BRA modified		
		dE/dN*	E_{00}	*dD/dN*	*dE*/dN*	E_{00}	*dD/dN*
400	1	1.620E-06	1.250	1.296E-06	1.440E-06	2.203	5.193E-07
	2	2.068E-06	1.424	1.452E-06	1.235E-06	2.066	5.978E-07
	3	1.894E-06	1.398	1.355E-06	1.235E-06	2.175	5.678E-07
Average		1.861E-06	1.357	1.368E-06	1.303E-06	2.148	5.616E-07
SD		2.3E-07	0.094	7.9E-08	1.2E-07	0.072	4.0E-08
CV		12.1	6.9	5.8	9.1	3.4	7.1
600	4	0.0009	38.924	2.312E-05	0.0005	141.76	5.270E-06
	5	0.0014	60.644	2.309E-05	0.0008	94.839	8.435E-06
	6	0.0014	78.378	1.786E-05	0.00061	132	4.621E-06
Average		0.0012	59	2.136E-05	0.0006	123	6.109E-06
SD		2.9E-04	20	3.0E-06	1.5E-04	25	2.0E-06
CV		23.4	33.3	14.2	23.8	20.2	33.4
800	7	0.0029	26.589	1.091E-04	0.0015	69.26	2.166E-05
	8	0.0029	23.349	1.241E-04	0.0017	60.724	2.800E-05
	9	0.0038	12.952	2.934E-04	0.0015	79.91	1.877E-05
Average		0.0032	21	1.755E-04	0.0016	70	2.281E-05
SD		5.2E-04	7	1.0E-04	1.2E-04	10	4.7E-06
CV		16.2	34.0	58.3	7.4	13.7	20.7

Appendix G. Asphalt Mixtures Performance Test Data

Appendix G1: Bulk density of compacted asphalt (AS 2891.9.2-2005) and air voids content tests (AS 2891.8-2005) of dynamic modulus specimens

	Unmodified (0%)			BRA Modified (10%)			BRA Modified (20%)			BRA Modified (30%)		
	1	2	3	4	5	6	7	8	9	10	11	12
Average height (mm)	149.53	149.40	149.09	149.78	149.44	149.59	151.84	151.48	151.58	149.46	149.37	149.37
• Standard deviation (mm)	0.092	0.120	0.161	0.061	0.107	0.195	0.079	0.109	0.074	0.132	0.145	0.136
• Coefficient of variation (%)	0.061	0.080	0.108	0.040	0.072	0.130	0.052	0.072	0.049	0.088	0.097	0.091
Average diameter (mm)	100.40	100.39	100.75	100.40	100.04	100.07	102.30	102.31	102.35	100.51	100.18	100.18
• Standard deviation (mm)	0.06	0.10	0.37	0.23	0.03	0.04	0.06	0.09	0.04	0.43	0.03	0.05
• Coefficient of variation (%)	0.064	0.095	0.366	0.225	0.032	0.041	0.061	0.090	0.036	0.431	0.030	0.052
m_1, mass in air of the sample, in grams	2915.11	2917.32	2914.31	2914.89	2947.49	2949.34	2923.35	2940.59	2939.25	2893.26	2887.17	2888.21
m_2, mass in water of the saturated sample, in grams	1677.71	1675.43	1677.16	1674.45	1697.73	1699.66	1687.46	1702.62	1696.53	1667.58	1666.20	1668.71
m_3, mass in air of the saturated sample, in grams	2921.85	2921.19	2920.82	2921.83	2960.46	2960.26	2936.27	2957.52	2953.45	2900.97	2898.56	2900.25
ρ_w, density of water at the test temperature, in t/m^3	0.997	0.997	0.997	0.997	0.997	0.997	0.997	0.997	0.997	0.997	0.997	0.997
ρ_{bulk}, bulk density of the sample, in t/m^3	2.336	2.335	2.336	2.330	2.327	2.333	2.334	2.336	2.331	2.339	2.336	2.338
ρ_{max}, maximum density of the mix, in t/m^3	2.458	2.458	2.458	2.454	2.454	2.454	2.456	2.456	2.456	2.464	2.464	2.464
AV, air voids in compacted mix (%)	4.96	5.01	4.95	5.06	5.17	4.95	5.0	4.9	5.1	5.08	5.20	5.11
AV, in average (%)	4.98			5.06			5.0			5.1		
• Standard deviation (%)	0.03			0.11			0.10			0.06		
• Coefficient of variation (%)	0.67			2.17			2.0			1.25		

Appendix G2. Measured dynamic modulus values ($|E^*|_{Lab}$) of asphalt mixtures, MPa

Asphalt mixtures	Sample No.	Temp. (°C)	Frequencies(Hz)									
			25	20	10	5	2	1	0.5	0.2	0.1	0.01
Unmodified	1	4.4	16729	16383	15153	13910	12205	10904	9637	8018	6871	3609
	2	4.4	17943	17368	15903	14547	12732	11368	10052	8391	7228	3880
	3	4.4	17110	16742	15561	14357	12733	11524	10311	8736	7598	4229
	Average		17261	16831	15539	14271	12557	11265	10000	8382	7232	3906
	Std Deviation		621	498	375	327	305	322	340	359	364	311
	CV (%)		3.6	3.0	2.4	2.3	2.4	2.9	3.4	4.3	5.0	8.0
	1	21.1	6872	6530	5425	4412	3217	2437	1794	1141	790.7	237.3
	2	21.1	7461	7063	5900	4837	3569	2726	2013	1283	888.8	269.4
	3	21.1	7750	7414	6248	5155	3844	2962	2215	1431	997.4	296.7
	Average		7361	7002	5858	4801	3543	2708	2007	1285	892	268
	Std Deviation		447	445	413	373	314	263	211	145	103	30
	CV (%)		6.1	6.4	7.1	7.8	8.9	9.7	10.5	11.3	11.6	11.1
	1	37.8	1527	1362	926.1	611.1	342.3	229.7	159.2	102.7	77.6	42.9
	2	37.8	1693	1517	1027	677.5	376.6	245.5	164.7	101.1	73.2	37.6
	3	37.8	1872	1674	1143	758.5	424.2	274.2	184.4	113.5	80.9	40.1
	Average		1697	1518	1032	682	381	250	169	106	77	40
	Std Deviation		173	156	109	74	41	23	13	7	4	3
	CV (%)		10.2	10.3	10.5	10.8	10.8	9.0	7.8	6.4	5.0	6.6
	1	54	318.2	297.6	199.2	131.2	73.1	57	47.8	39.5	35.1	26.1
	2	54	378.3	323.5	213.5	136.2	72.6	52.2	41.4	33.2	29.4	18.9
	3	54	385.7	331.6	216.8	139	73.3	54.5	43.2	35	30.9	24.6
	Average		361	318	210	135	73	55	44	36	32	23
	Std Deviation		37	18	9	4	0	2	3	3	3	4
	CV (%)		10.3	5.6	4.5	2.9	0.5	4.4	7.5	9.0	9.3	16.4
BRA modified (10%)	4	4.4	18984	18659	17528	16372	14804	13585	12343	10731	9536	5929
	5	4.4	19060	18697	17565	16383	14780	13576	12353	10760	9580	5954
	6	4.4	19197	18862	17717	16536	14924	13667	12423	10788	9564	5926
	Average		19080	18739	17603	16430	14836	13609	12373	10760	9560	5936
	Std Deviation		108	108	100	92	77	50	44	29	22	15
	CV (%)		0.6	0.6	0.6	0.6	0.5	0.4	0.4	0.3	0.2	0.3
	4	21.1	8860	8473	7307	6216	4898	4006	3214	2298	1728	584.5
	5	21.1	9031	8652	7463	6345	4988	4068	3244	2298	1712	578.6
	6	21.1	8934	8527	7332	6232	4901	4004	3193	2266	1692	579
	Average		8942	8551	7367	6264	4929	4026	3217	2287	1711	581
	Std Deviation		86	92	84	70	51	36	26	18	18	3
	CV (%)		1.0	1.1	1.1	1.1	1.0	0.9	0.8	0.8	1.1	0.6
	4	37.8	2740	2558	1907	1373	837.4	566.6	387	234.9	162.6	60.7
	5	37.8	2609	2416	1768	1248	751.3	504.8	344.3	210.2	147.4	60.9
	6	37.8	2589	2400	1766	1251	757.9	511.7	349.5	214.9	151.7	62.4
	Average		2646	2458	1814	1291	782	528	360	220	154	61
	Std Deviation		82	87	81	71	48	34	23	13	8	1
	CV (%)		3.1	3.5	4.5	5.5	6.1	6.4	6.5	6.0	5.1	1.5
	4	54	672.3	587.9	389.4	254	136.6	94.5	70.4	50	44.6	36.3
	5	54	694.7	603.7	397.3	257.6	139	96.5	70.6	50.1	41.1	37.4
	6	54	611	543.9	364.5	239.6	135.4	97.3	76.7	59.4	50.5	37.8
	Average		659	579	384	250	137	96	73	53	45	37
	Std Deviation		43	31	17	10	2	1	4	5	5	1
	CV (%)		6.6	5.4	4.5	3.8	1.3	1.5	4.9	10.2	10.5	2.1

Appendix G2. Measured dynamic modulus values ($|E^*|_{Lab}$) of asphalt mixtures, MPa (Continued)

Asphalt mixtures	Sample No.	Temp. (°C)	Frequencies(Hz) 25	20	10	5	2	1	0.5	0.2	0.1	0.01
BRA modified (20%)	7	4.4	21676	21328	20257	19080	17461	16179	14870	13127	11814	7616
	8	4.4	21292	21036	19878	18689	17063	15794	14525	12836	11556	7553
	9	4.4	21665	21358	20336	19257	17777	16592	15384	13734	12509	8506
	Average		21544	21241	20157	19009	17434	16188	14926	13232	11960	7892
	Std Deviation		219	178	245	291	358	399	432	458	493	533
	CV (%)		1.0	0.8	1.2	1.5	2.1	2.5	2.9	3.5	4.1	6.8
	7	21.1	10929	10527	9202	7938	6375	5291	4294	3120	2371	827
	8	21.1	10848	10496	9211	7990	6470	5419	4463	3325	2591	966
	9	21.1	11612	11196	9871	8609	7045	5968	4970	3778	2990	1130
	Average		11130	10740	9428	8179	6630	5559	4576	3408	2651	974
	Std Deviation		420	396	384	373	363	360	352	337	314	152
	CV (%)		3.8	3.7	4.1	4.6	5.5	6.5	7.7	9.9	11.8	15.6
	7	37.8	3573	3361	2545	1856	1160	795.5	548.1	341.5	244.1	103
	8	37.8	3721	3561	2760	2075	1349	944.6	659.1	411.1	290.3	113
	9	37.8	4585	4359	3466	2675	1805	1280	904.8	558.2	380.1	122
	Average		3960	3760	2924	2202	1438	1007	704	437	305	113
	Std Deviation		547	528	482	424	332	248	183	111	69	9
	CV (%)		13.8	14.0	16.5	19.3	23.1	24.6	25.9	25.3	22.7	8.1
	7	54	951.7	833.6	554.9	370.8	210.8	149.7	111.2	79.1	63.3	37.6
	8	54	866.6	763.6	519	357.1	210.6	157	122.4	92.8	79	55.4
	9	54	1041	927.2	628.6	420.3	238.2	163.2	116.7	79.8	61.8	36.2
	Average		953	841	568	383	220	157	117	84	68	36
	Std Deviation		87	82	56	33	16	7	6	8	10	1
	CV (%)		9.1	9.8	9.8	8.7	7.2	4.3	4.8	9.2	14.0	3.1
BRA modified (30%)	10	4.4	21658	21415	20476	19489	18118	17051	15930	14419	13260	9421
	11	4.4	23172	22868	21829	20731	19207	18015	16804	15147	13871	9653
	12	4.4	22831	22615	21607	20541	19026	17850	16619	14969	13701	9468
	Average		22554	22299	21304	20254	18784	17639	16451	14845	13611	9514
	Std Deviation		794	776	726	669	584	516	461	380	315	123
	CV (%)		3.5	3.5	3.4	3.3	3.1	2.9	2.8	2.6	2.3	1.3
	10	21.1	12223	11859	10596	9365	7801	6703	5665	4412	3568	1452
	11	21.1	12870	12450	11093	9771	8098	6928	5829	4496	3601	1439
	12	21.1	12649	12239	10881	9573	7921	6764	5680	4363	3479	1382
	Average		12581	12183	10857	9570	7940	6798	5725	4424	3549	1424
	Std Deviation		329	300	249	203	149	116	91	67	63	37
	CV (%)		2.6	2.5	2.3	2.1	1.9	1.7	1.6	1.5	1.8	2.6
	10	37.8	4613	4387	3491	2697	1826	1310	933.1	589.3	416.1	156
	11	37.8	4651	4399	3475	2655	1771	1258	888.6	562.6	402	155.3
	12	37.8	4702	4461	3532	2706	1803	1280	904.4	568.2	399.9	148.2
	Average		4655	4416	3499	2686	1800	1283	909	573	406	153
	Std Deviation		45	40	29	27	28	26	23	14	9	4
	CV (%)		1.0	0.9	0.8	1.0	1.5	2.0	2.5	2.5	2.2	2.8
	10	54	1545	1403	977.3	666.7	389.9	267.1	190.4	125.6	94.3	59.5
	11	54	1432	1321	909.3	613.6	358.6	248.9	178.8	120.4	91.9	59.4
	12	54	1415	1272	870.1	585.8	339.1	232.8	166.5	110.5	83.6	57.9
	Average		1464	1332	919	622	363	250	179	119	90	59
	Std Deviation		71	66	54	41	26	17	12	8	6	1
	CV (%)		4.8	5.0	5.9	6.6	7.1	6.9	6.7	6.5	6.2	1.5

Appendix G3. Average dynamic modulus values ($|E^*|_{master\ curve}$) of asphalt mixtures, MPa

Asphalt mixtures	Sample No.	Temp. (°C)	Frequencies (Hz) 25	20	10	5	2	1	0.5	0.2	0.1	0.01
Unmodified	1-3	4.4	15244	15075	14489	13797	12710	11753	10687	9136	7894	3936
	1-3	21.1	7890	7485	6234	5034	3606	2695	1949	1216	830.2	224
	1-3	37.8	1636	1458	1005	680.3	401.7	270.7	184.8	115.5	83.63	36.3
	1-3	54	318.5	280.7	191.4	133.2	86.07	64.19	49.51	36.97	30.74	20.1
BRA modified (10%)	4-6	4.4	16888	16735	16204	15581	14603	13737	12763	11319	10127	5962
	4-6	21.1	9865	9464	8198	6931	5328	4225	3254	2206	1595	483
	4-6	37.8	2640	2397	1745	1242	773	534	369	229	163	62
	4-6	54	572	507	351	244	155	113	85	60	48	28
BRA modified (20%)	7-9	4.4	20178	19962	19229	18399	17149	16085	14925	13261	11926	7386
	7-9	21.1	12141	11703	10325	8944	7173	5919	4775	3470	2654	950
	7-9	37.8	3873	3573	2740	2057	1368	986.9	704.5	447.5	317.6	109
	7-9	54	843.4	756.3	537.2	380.8	243.1	175.1	127.9	86.79	66.32	32
BRA modified (30%)	10-12	4.4	20618	20468	19950	19349	18410	17583	16648	15248	14070	9640
	10-12	21.1	13444	13031	11705	10331	8500	7151	5879	4373	3398	1260
	10-12	37.8	4787	4439	3455	2627	1770	1287	923	589	419	145
	10-12	54	1313	1182	846	602	384	275	200	135	102	49

Appendix G4. Normalized error values for asphalt mixtures, %

Asphalt mixtures	Temp. (°C)	Frequencies (Hz) 25	20	10	5	2	1	0.5	0.2	0.1	0.01
Unmodified	4.4	11.7	10.4	6.8	3.3	1.2	4.3	6.9	9.0	9.2	0.8
	21.1	7.2	6.9	6.4	4.9	1.8	0.5	2.9	5.3	6.9	16.5
	37.8	3.6	4.0	2.7	0.3	5.4	8.3	9.4	8.9	8.6	9.3
	54	11.8	11.7	8.9	1.3	17.9	16.7	12.5	2.7	3.9	12.8
BRA modified (10%)	4.4	11.5	10.7	7.9	5.2	1.6	0.9	3.2	5.2	5.9	0.4
	21.1	10.3	10.7	11.3	10.6	8.1	4.9	1.1	3.6	6.7	16.8
	37.8	0.2	2.5	3.8	3.8	1.2	1.2	2.4	4.1	5.7	1.6
	54	13.3	12.3	8.6	2.4	13.5	17.8	16.6	13.2	6.1	25.3
BRA modified (20%)	4.4	6.3	6.0	4.6	3.2	1.6	0.6	0.0	0.2	0.3	6.4
	21.1	9.1	9.0	9.5	9.4	8.2	6.5	4.4	1.8	0.1	2.5
	37.8	2.2	5.0	6.3	6.6	4.9	2.0	0.1	2.4	4.1	3.5
	54	11.5	10.1	5.4	0.6	10.5	11.5	9.3	3.3	2.5	11.2
BRA modified (30%)	4.4	8.6	8.2	6.4	4.5	2.0	0.3	1.2	2.7	3.4	1.3
	21.1	6.9	7.0	7.8	8.0	7.0	5.2	2.7	1.2	4.3	11.5
	37.8	2.8	0.5	1.3	2.2	1.7	0.3	1.6	2.7	3.2	5.4
	54	10.3	11.3	7.9	3.2	5.9	10.3	12.0	13.2	13.6	17.6

Appendix G5. Measured phase angle values of asphalt mixtures, Degree

Asphalt mixtures	Sample No.	Temp. (°C)	Frequencies(Hz)									
			25	20	10	5	2	1	0.5	0.2	0.1	0.01
Unmodified	1	4.4	10.05	10.35	11.39	12.59	14.44	16.06	17.84	20.56	22.66	30.61
	2	4.4	10.07	10.36	11.42	12.58	14.4	15.98	17.72	20.33	22.37	30.4
	3	4.4	9.45	9.77	10.7	11.79	13.52	14.98	16.68	19.21	21.22	29.01
	Average		9.86	10.16	11.17	12.32	14.12	15.67	17.41	20.03	22.08	30.01
	Std Deviation		0.35	0.34	0.41	0.46	0.52	0.60	0.64	0.72	0.76	0.87
	CV (%)		3.6	3.3	3.6	3.7	3.7	3.8	3.7	3.6	3.4	2.9
	1	21.1	24.71	25.01	27.3	29.64	32.86	35.21	37.09	39.06	39.77	41.69
	2	21.1	23.95	24.47	26.67	29.05	32.2	34.53	36.51	38.64	39.64	40.7
	3	21.1	23.26	23.56	25.66	27.91	31.07	33.39	35.46	37.73	38.9	38.3
	Average		23.97	24.35	26.54	28.87	32.04	34.38	36.35	38.48	39.44	40.22
	Std Deviation		0.73	0.73	0.83	0.88	0.91	0.92	0.83	0.68	0.47	1.75
	CV (%)		3.0	3.0	3.1	3.0	2.8	2.7	2.3	1.8	1.2	4.3
	1	37.8	41.75	41.29	42.44	43.16	43.56	42.82	42.21	39.92	37.35	29.69
	2	37.8	41.8	41.23	42.36	43.21	43.67	42.63	42.45	39.75	37.22	29.1
	3	37.8	40.6	40.14	41.48	42.5	43.38	43.02	42.01	39.56	37.49	29.5
	Average		41.38	40.89	42.09	42.96	43.54	42.82	42.22	39.74	37.35	29.41
	Std Deviation		0.68	0.65	0.53	0.40	0.15	0.20	0.22	0.18	0.14	0.32
	CV (%)		1.6	1.6	1.3	0.9	0.3	0.5	0.5	0.5	0.4	1.1
	1	54	47.35	43.35	41.61	40.83	39.33	36.55	33.85	29.75	25.55	17.27
	2	54	42.58	42.46	41.36	39.84	38.64	36.14	32.32	27.88	24.9	18
	3	54	43.13	42.48	41.79	39.94	38.7	36.03	32.07	28.88	25.09	15
	Average		44.35	42.76	41.59	40.20	38.89	36.24	32.75	28.84	25.18	16.76
	Std Deviation		2.61	0.51	0.22	0.55	0.38	0.27	0.96	0.94	0.33	1.56
	CV (%)		5.9	1.2	0.5	1.4	1.0	0.8	2.9	3.2	1.3	9.3
BRA modified (10%)	4	4.4	7.97	8.14	8.92	9.75	11.06	12.18	13.46	15.49	17.05	23.7
	5	4.4	7.98	8.16	8.89	9.71	10.98	12.09	13.34	15.26	16.91	23.57
	6	4.4	7.97	8.2	8.89	9.73	11.01	12.11	13.41	15.34	17.07	23.52
	Average		7.97	8.17	8.90	9.73	11.02	12.13	13.40	15.36	17.01	23.60
	Std Deviation		0.01	0.03	0.02	0.02	0.04	0.05	0.06	0.12	0.09	0.09
	CV (%)		0.1	0.4	0.2	0.2	0.4	0.4	0.4	0.8	0.5	0.4
	4	21.1	19.88	20.28	22.14	24.14	27	29.15	31.15	33.76	35.27	37.89
	5	21.1	19.54	19.99	21.92	23.96	26.79	28.9	30.86	33.46	35.14	37.45
	6	21.1	19.67	20.07	22.02	24.04	26.89	28.96	30.96	33.51	35.07	37.35
	Average		19.70	20.11	22.03	24.05	26.89	29.00	30.99	33.58	35.16	37.56
	Std Deviation		0.17	0.15	0.11	0.09	0.11	0.13	0.15	0.16	0.10	0.29
	CV (%)		0.9	0.7	0.5	0.4	0.4	0.4	0.5	0.5	0.3	0.8
	4	37.8	36.76	36.08	37.7	39.09	40.6	40.83	40.36	39	37.38	29.16
	5	37.8	37.12	36.51	38.2	39.7	41.2	41.42	40.67	38.74	36.87	28.41
	6	37.8	36.82	36.23	37.87	39.35	40.77	41.04	40.28	38.46	36.32	27.66
	Average		36.90	36.27	37.92	39.38	40.86	41.10	40.44	38.73	36.86	28.41
	Std Deviation		0.19	0.22	0.25	0.31	0.31	0.30	0.21	0.27	0.53	0.75
	CV (%)		0.5	0.6	0.7	0.8	0.8	0.7	0.5	0.7	1.4	2.6
	4	54	44.41	42.57	41.77	40.67	40.15	36.88	32.81	28.21	26.96	14.87
	5	54	43.52	42.28	41.75	41.09	40.26	37	33.01	27.92	23.27	15.04
	6	54	43.33	40.41	38.79	37.55	36.37	33.2	28.86	24.25	21.28	13.97
	Average		43.75	41.75	40.77	39.77	38.93	35.69	31.56	26.79	23.84	14.63
	Std Deviation		0.58	1.17	1.71	1.93	2.21	2.16	2.34	2.21	2.88	0.58
	CV (%)		1.3	2.8	4.2	4.9	5.7	6.1	7.4	8.2	12.1	3.9

Appendix G5. Measured phase angle values of asphalt mixtures, Degree (Continued)

Asphalt mixtures	Sample No.	Temp. (°C)	Frequencies(Hz) 25	20	10	5	2	1	0.5	0.2	0.1	0.01
BRA modified (20%)	7	4.4	6.97	7.3	7.91	8.68	9.86	10.89	12.06	13.85	15.43	21.71
	8	4.4	6.74	7.04	7.67	8.42	9.61	10.64	11.8	13.6	15.1	21.23
	9	4.4	6.54	6.66	7.19	7.84	8.85	9.74	10.73	12.34	13.65	19.35
	Average		6.75	7.00	7.59	8.31	9.44	10.42	11.53	13.26	14.73	20.76
	Std Deviation		0.22	0.32	0.37	0.43	0.53	0.60	0.70	0.81	0.95	1.25
	CV (%)		3.2	4.6	4.8	5.2	5.6	5.8	6.1	6.1	6.4	6.0
	7	21.1	18.28	18.63	20.49	22.4	25.2	27.29	29.4	32.15	33.91	36.69
	8	21.1	17.43	17.92	19.74	21.6	24.4	26.35	28.32	30.9	32.55	35.67
	9	21.1	16.2	16.68	18.39	20.2	22.8	24.74	26.71	29.41	31.2	36.25
	Average		17.30	17.74	19.54	21.41	24.11	26.13	28.14	30.82	32.55	36.20
	Std Deviation		1.05	0.99	1.06	1.14	1.23	1.29	1.35	1.37	1.36	0.51
	CV (%)		6.0	5.6	5.4	5.3	5.1	4.9	4.8	4.5	4.2	1.4
	7	37.8	35.57	34.79	36.48	38	39.4	39.72	39.23	37.72	35.97	27.43
	8	37.8	34.39	33.57	35.1	36.4	37.8	38.33	38.16	37.25	36.19	29.26
	9	37.8	31.15	30.57	32.26	34	36	37.34	37.67	37.58	37.08	30.86
	Average		33.70	32.98	34.61	36.12	37.75	38.46	38.35	37.52	36.41	29.18
	Std Deviation		2.29	2.17	2.15	1.99	1.70	1.20	0.80	0.24	0.59	1.72
	CV (%)		6.8	6.6	6.2	5.5	4.5	3.1	2.1	0.6	1.6	5.9
	7	54	43.33	42.12	41.29	40.3	39.2	36.18	32.86	28.91	25.22	8.69
	8	54	41.47	40.11	39.14	37.8	36.6	33.24	29.91	25.77	23.33	17.37
	9	54	41.92	40.81	40.4	39.9	39.3	37.19	34.26	29.93	26.46	17.27
	Average		42.24	41.01	40.28	39.32	38.34	35.54	32.34	28.20	25.00	14.44
	Std Deviation		0.97	1.02	1.08	1.30	1.52	2.05	2.22	2.17	1.58	4.98
	CV (%)		2.3	2.5	2.7	3.3	4.0	5.8	6.9	7.7	6.3	34.5
BRA modified (30%)	10	4.4	6.03	6.22	6.73	7.35	8.23	9.01	9.89	11.22	12.47	17.41
	11	4.4	6.05	6.23	6.74	7.36	8.3	9.12	10.02	11.43	12.69	17.93
	12	4.4	6.15	6.28	6.79	7.39	8.33	9.15	10.04	11.45	12.65	17.94
	Average		6.08	6.24	6.75	7.37	8.29	9.09	9.98	11.37	12.60	17.76
	Std Deviation		0.06	0.03	0.03	0.02	0.05	0.07	0.08	0.13	0.12	0.30
	CV (%)		1.1	0.5	0.5	0.3	0.6	0.8	0.8	1.1	0.9	1.7
	10	21.1	15.01	15.39	16.96	18.65	21.09	22.98	24.94	27.69	29.51	35.19
	11	21.1	14.95	15.38	16.98	18.69	21.16	23.09	25.04	27.79	29.62	34.81
	12	21.1	15.26	15.64	17.25	18.97	21.46	23.37	25.28	27.94	29.8	34.65
	Average		15.07	15.47	17.06	18.77	21.24	23.15	25.09	27.81	29.64	34.88
	Std Deviation		0.16	0.15	0.16	0.17	0.20	0.20	0.17	0.13	0.15	0.28
	CV (%)		1.1	1.0	0.9	0.9	0.9	0.9	0.7	0.5	0.5	0.8
	10	37.8	31.06	30.68	32.47	34.24	36.25	37.28	37.56	37.32	35.54	26.1
	11	37.8	30.95	30.52	32.37	34.14	36.19	37.24	37.47	37.02	35.06	26.42
	12	37.8	30.96	30.4	32.2	33.99	36.14	37.26	37.6	37.23	36.49	27.16
	Average		30.99	30.53	32.35	34.12	36.19	37.26	37.54	37.19	35.70	26.56
	Std Deviation		0.06	0.14	0.14	0.13	0.06	0.02	0.07	0.15	0.73	0.54
	CV (%)		0.2	0.5	0.4	0.4	0.2	0.1	0.2	0.4	2.0	2.0
	10	54	40.69	39.71	39.93	38.86	36.65	34.2	30.79	26.4	22.21	12.66
	11	54	41.39	39.56	39.74	38.65	36.23	33.34	29.93	25.37	21.39	12.4
	12	54	40.71	39.48	39.76	38.71	36.53	33.97	30.5	25.97	22.21	12.41
	Average		40.93	39.58	39.81	38.74	36.47	33.84	30.41	25.91	21.94	12.49
	Std Deviation		0.40	0.12	0.10	0.11	0.22	0.45	0.44	0.52	0.47	0.15
	CV (%)		1.0	0.3	0.3	0.3	0.6	1.3	1.4	2.0	2.2	1.2